APTD-0734 271

PB 202 666

STATE OF THE ART: 1971
INSTRUMENTATION FOR MEASUREMENT OF PARTICULATE EMISSIONS FROM COMBUSTION SOURCES
VOLUME II: PARTICULATE MASS - DETAIL REPORT

by

Gilmore J. Sem
John A. Borgos
John G. Olin
John P. Pilney
Benjamin Y. H. Liu
Nicholas Barsic
Kenneth T. Whitby
Frank D. Dorman

Thermo-Systems Inc.
2500 North Cleveland Avenue
St. Paul, Minnesota 55113

This report was prepared under Contract No. CPA 70-23
with the Division of Process Control Engineering,
Air Pollution Control Office, Environmental Protection Agency.

Reproduced by
NATIONAL TECHNICAL
INFORMATION SERVICE
Springfield, Va. 22151

225

PB-202 666

BIBLIOGRAPHIC DATA SHEET

1. Report No. APTD-0734

2.

3. Recipient's Accession No.

4. Title and Subtitle
State of the Art: 1971 Instrumentation for Measurement of Particulate Emissions From Combustion Sources Volume II: Particulate Mass-Detail Report

5. Report Date
April 1971

6.

7. Author(s) Gilmore J. Sem, John A. Borgos, John G. Olin, John P. Pilney, Benjamin Y. H. Liu, Nicholas Barsic, Kenneth T. Whitby, and Frank D. Dorman

8. Performing Organization Rept. No.

9. Performing Organization Name and Address
Thermo-Systems Inc.,
2500 North Cleveland Avenue
St. Paul, Minnesota 55113

10. Project/Task/Work Unit No.

11. Contract/Grant No.
CPA 70-23

12. Sponsoring Organization Name and Address
Environmental Protection Agency
Air Pollution Control Office
Division of Process Control Engineering
Research Triangle Park, North Carolina 27711

13. Type of Report & Period Covered

14.

15. Supplementary Notes DISCLAIMER - This report was furnished to the Office of Air Programs by Thermo-Systems Inc., 2500 North Cleveland Avenue, St. Paul, Minnesota 55113 in fulfillment of Contract No. CPA 70-23

16. Abstracts
All known sensing techniques available for application to automatic, continuous measurement of the rate of particulate mass emissions from large fossil-fuel combustion facilities are discussed. The measurement of particle mass rather than other particle parameters is emphasized. Although the report emphasizes permanently-installed effluent monitoring systems, much of the information is also applicable to portable and research instruments. Detailed discussions of particle sensing techniques as applied to emissions monitoring are presented. Each discussion analyzes possible problems and their solutions, in using the technique for emission monitoring, and includes an analysis of what particulate parameter the technique sees, how closely the measurement correlates with particulate mass, inherent measurement errors, practical design problems and possible solutions, the potential sensitivity and response of each technique, the complexity of the potential instrument, the present state of development of the technique, and recommendations for further development. Each discussion includes a complete bibliography. A separate chapter describes typical conditions found in large fossil-fuel effluent gases in greater detail than found in Volume I. Another separate chapter summarizes many of the problems encountered in the design of sampling probes required by most of the particle sensing techniques.

17. Key Words and Document Analysis. 17a. Descriptors
Air pollution
Measuring instruments
Particles
Exhaust emissions
Combustion products
Continuous sampling
Flue gases

17b. Identifiers/Open-Ended Terms

17c. COSATI Field/Group 13B

18. Availability Statement Unlimited

19. Security Class (This Report) UNCLASSIFIED

20. Security Class (This Page UNCLASSIFIED

21. No. of Pages ~~223~~ 225

22. Price 3.00 - .95

FORM NTIS-35 (10-70)

USCOMM-DC 40329-P71

BLANK PAGE

STATE OF THE ART: 1971
INSTRUMENTATION FOR
MEASUREMENT OF PARTICULATE EMISSIONS
FROM COMBUSTION SOURCES
VOLUME II: PARTICULATE MASS - DETAIL REPORT

by

Gilmore J. Sem
John A. Borgos
John G. Olin
John P. Pilney
Benjamin Y. H. Liu
Nicholas Barsic
Kenneth T. Whitby
Frank D. Dorman

Thermo-Systems Inc.
2500 North Cleveland Avenue
St. Paul, Minnesota 55113

This report was prepared under Contract No. CPA 70-23 with the Division of Process Control Engineering, Air Pollution Control Office, Environmental Protection Agency.

When U. S. Government drawings specifications, or other data are used for any purpose other than a definitely related Government procurement operation, the Government thereby incurs no responsibility nor any obligation whatsoever, and the fact that the Government may have formulated, furnished, or in any way supplied the said drawings, specifications, or other data, is not to be regarded by implication or otherwise, or in any manner licensing the holder or any other person or corporation, or conveying any rights or permission to manufacture, use, or sell any patented invention that may in any way be related thereto.

References to named commercial products in this report are not to be considered in any sense as an endorsement of the product by the Government.

TABLE OF CONTENTS

VOLUME I

Page

FOREWORD 5

ABSTRACT 6

INTRODUCTION 8

SUMMARY OF STACK EMISSIONS PROPERTIES AND INSTRUMENT SPECIFICATIONS 11

SUMMARY OF PARTICLE SENSING TECHNIQUES 15

INDEX OF PARTICLE SENSING TECHNIQUES 17

REFERENCES 87

VOLUME II

FOREWORD 5

ABSTRACT 6

SAMPLING PROBE DESIGN 7

DISCUSSION OF MEASUREMENT TECHNIQUES

MASS SENSING TECHNIQUES:

BETA RADIATION ATTENUATION 29

PIEZOELECTRIC MICROBALANCE 43

RESONANT FREQUENCY 57

GRAVIMETRIC WEIGHING 67

ELECTROSTATIC MEASUREMENT METHODS 73

OPTICAL SENSING TECHNIQUES:

LIGHT TRANSMISSION 98

MULTI-WAVELENGTH LIGHT TRANSMISSION 115

LIGHT SCATTERING: POLARIZATION RATIO METHODS . . . 126

ANGULAR LIGHT SCATTERING 134

TABLE OF CONTENTS (continued)

Page

SOILING POTENTIAL 145

OPTICAL COUNTERS AND PHOTOMETERS 148

LIDAR 158

HOLOGRAPHY 163

MISCELLANEOUS SENSING TECHNIQUES:

ACOUSTICAL ATTENUATION AND DISPERSION 172

HOT-WIRE ANEMOMETRY 177

PRESSURE DROP IN NOZZLES 179

STACK EMISSIONS PROPERTIES AND INSTRUMENT SPECIFICATIONS . . 181

FOREWORD

The compilation of the information contained in this publication was performed pursuant to Contract 70-23 with the Air Pollution Control Office, Environmental Protection Agency.

The information was compiled by Thermo-Systems Inc., and their subcontractor, North Star Research and Development, during the period 12 February 1970 to April 1971.

Volume I of this report is written for the engineer or planner who needs to know a few basic facts about a particulate mass measurement technique and wishes to minimize the time required to obtain this information. Volume I is intended for use as a quick reference guide.

Volume II of this report is designed as a detailed in-depth report on operating principles, techniques, historical data, and discussion of the more viable techniques for particulate mass monitoring. Volume II is designed for the plant engineer, abatement and control officials, and others who may not be familiar with the detailed technology of these areas. Included are sections on power plant emissions properties and extraction sampling probes.

Volume III of this report is a comprehensive survey of particle sizing techniques which may be used by the plant engineer, abatement and control officials, and others as a quick reference guide or as a source of more detailed information, including references to original work.

Volume IV of this report describes an experimental evaluation of the beta radiation attenuation and piezoelectric microbalance techniques for mass concentration measurements on a coal-fired power generating plant. Problem areas requiring further development are identified for personnel concerned with improving the techniques.

This report is reviewed and approved.

F. C. Jaye
Project Officer
Environmental Protection Agency

ABSTRACT AND CONCLUSION

Volumes I and II of this report discuss all known sensing techniques available for application to automatic, continuous measurement of the rate of particulate mass emissions from large fossil-fuel combustion facilities. Volume III discusses techniques for automatic, continuous measurement of particle size in the same environment. Volume I and II emphasize the measurement of particle mass rather than other particle parameters, and all volumes emphasize emissions downstream rather than upstream of any control equipment. Although the report emphasizes permanently-installed effluent monitoring systems, much of the information is also applicable to portable and research instruments.

Volume I contains brief surveys of all known particle sensing techniques. A brief discussion of the principle of operation is followed by a list of inherent and practical strengths and weaknesses of each technique. A list of commercial manufacturers of related equipment and a list of references helps the reader who needs more information on a specific technique. Recommendations for further development outline areas of needed improvement for techniques which offer some promise for stack monitoring. The introduction includes general comments which apply to all sensing techniques, and ranks all techniques in order of present apparent potential. A separate chapter summarizes typical conditions found in large fossil-fuel effluent gases and sets the necessary specifications for a particulate monitoring instrument which operates in an effluent gas atmosphere.

Volume II (this volume) contains detailed discussions of particle sensing techniques as applied to emissions monitoring. Each discussion analyzes possible problems, and their solutions, in using the technique for emissions monitoring, and includes an analysis of what particulate parameter the technique senes, how closely the measurement correlates with particulate mass, inherent measurement errors, practical design problems and possible solutions, the potential sensitivity and response of each technique, the complexity of the potential instrument, the present state of development of the technique, and recommendations for further development. Each discussion includes a complete bibliography. A separate chapter describes typical conditions found in large fossil-fuel effluent gases in greater detail than found in Volume I. Another separate chapter summarizes many of the problems encountered in the design of sampling probes required by most of the particle sensing techniques.

Accurate measurement of the particulate mass emissions rate requires an instrument which directly senses the true mass of the particles. Sensors that are not sensitive to particulate mass, even though they may be calibrated against a mass sensor, do not and cannot yield satisfactory correlation with particle mass emissions during periods of changing and/or abnormal plant operating conditions. Effluent characteristics, such as particle size and density, change often in stacks. This may be a result of changes in combustion efficiency, fuel composition, collector performance, or other system variables.

All existing mass sensors require at least partial extraction of a representative effluent sample from the stack. No present commercial mass sensors meet the requirements for accurate, long-term, continuous monitoring. Two techniques could probably be developed into next-generation commercial stack monitors within 1 - 3 years: beta radiation attenuation and piezoelectric microbalance. Beta radiation attenuation has been partially developed for stacks with several first-generation commercial instruments available. These instruments appear to need design improvements. First-generation piezoelectric microbalance instruments exist for ambient air monitoring, but no stack monitoring development has been done.

Optical, or light, transmission is presently the most commonly used particulate monitoring technique. It measures the optical density of stack effluents very accurately if the instrument is carefully designed. Unfortunately, few of the presently available transmissometers are well-designed for accurate long-term optical density measurements. Although light transmission offers several significant instrument design advantages, the measurement does not correlate well with particulate mass measurement, especially during changing effluent conditions.

Volume III contains discussions of automatic or semi-automatic particle size measuring techniques as applied to emissions monitoring. The discussions emphasize the particulate parameter (mass, number, surface area, etc.) which each technique senses as well as the method of classifying particles into size ranges (aerodynamically, electrostatically, optically, etc.). Included are major features of each technique, including practical problems which may be encountered when applying the technique to effluent streams. Also included is a brief, but comprehensive, survey of the many methods of expressing particle size, and an evaluation of which are most useful for effluent particles.

Volume IV is the final report containing preliminary results of an experimental evaluation of the beta radiation attenuation technique and the piezoelectric microbalance technique. Most of the experimental work was performed on an effluent duct of a larger coal-fired power generating plant. The experimental sampling system and the method of evaluation are described.

STACK EMISSIONS PROPERTIES AND INSTRUMENT SPECIFICATIONS

by: John Pilney

INTRODUCTION

The objective of this study is to characterize the effluent properties and particulate emissions of large, stationary, fossil-fuel-fired power plants.* The information presented in this report was sought through a comprehensive survey of the published literature and other sources. This information is needed to provide a guide for judging the merit of various techniques to continuously monitor the mass concentration of particulate matter emitted by power plants. It is also used to define the instrument specifications that a continuous stack monitor should have.

The purpose of this section of the report is to characterize emissions from coal- and oil-fired power plants only. Gas-fired plants were found to produce so little particulate matter that they are not considered a source of particulate pollution of any consequence. Discussed in the following sections are:

- The amount of particulate matter emitted by power plants
- Variables affecting the emissions
- Particulate loading
- Size-distribution of particulate emissions
- Control of particulate emissions
- Physical properties and the composition of emissions
- Characteristics and properties of the stack gases

Following this, a set of nominal effluent characteristics for both coal and oil-fired power plants, and a set of instrument specifications, are presented.

TECHNICAL BACKGROUND

The burning of fossil fuels generates pollutants in the form of aerosols and gases, both organic and inorganic. The aerosols include all liquid and solid particles including ash, carbon, and sulfur trioxide. The gases include oxides of nitrogen, sulfur dioxide, hydrocarbons, and carbon monoxide. The particulate emission resulting from the combustion of coal in power plants is formed from coal ash and is referred to as fly ash. In oil combustion, however, the particulate emissions may contain a relatively large fraction of sulfates, mineral ash, carbon, and carbonaceous matter in addition to ash. Emissions from oil combustion are also commonly referred to as fly ash.

---

*Large stationary power plants are those having at least: an electrical output of 10 megawatts, a steam output of 8×10^4 pounds/hr, or a heat input of 10^8 Btu/hr.

An estimate of the annual fuel consumption in a stationary sources in the U.S. in 1965 [365,407] show that equal heat equivalents of coal and fuel oil were consumed. The estimated particulate emissions in thousands of tons per year from stationary sources in the U.S. in 1965 was 7,000 for coal-firing (92 percent of the total), 540 (7 percent) for oil-firing and 100 (1 percent) for natural gas-firing. A summary of a recent estimate of emissions from coal-fired electric and industrial power plants[727] is shown in Table 1. The figures shown for the efficiency, amount, and extent of control for pulverized coal firing in electrical power plants are based on several interesting estimates. These estimate are that 54.6 percent of stack gas volume is controlled with electrostatic precipitators with an overall efficiency of 93 percent, and that 91 percent of the remaining 45.4 percent of the stack gas volume is controlled with cyclones having an average efficiency of 70 percent. In comparison, newly built, large coal-fired power plants are being equipped with electrostatic precipitators with an overall efficiency of 98 percent[727], and a few with precipitators having efficiencies of greater than 99 percent. This information, including that in Table 1, illustrates that in order of particulate pollution potential based upon mass, coal burning is utmost, oil burning is second, and gas burning is third and of little importance. The information in Table 1 also shows that pulverized coal-fired furnaces are presently the largest source of particulate pollutants emitted by power plants.

Total particulate emissions from power production will probably continue to increase in the future, if the present trend in population growth and the standard of living continues. A look at the past, present, and future consumption of coal and oil illustrates this assumption. For example, in 1958, electric utilities consumed approximately 156 million tons of coal[526]; in 1965 an estimated 300 million tons[365]; and, it has been estimated that by 1980, 440 million tons will be consumed annually[401]. Likewise, for fuel oil, the consumptions were 78 million barrels in 1958 [526] and 1300 million barrels in 1965 [365]; it is estimated that 1900 million barrels will be consumed in 1980 [749].

EMISSIONS FROM COAL FIRING

1. Variables Affecting Emissions From Coal-Fired Power Plants

The amount of fly ash emitted from coal-burning furnaces is related to many factors. Some of the more important factors are gas velocity, particle size, particle density, fuel-burning rate, combustion efficiency, furnace configuration, and coal composition and size. An indication of how these variables affect the emission rate is shown in Table 2 [946]. In addition, such practices as soot blowing and fly ash reinjection increase particulate emissions. In fly ash reinjection, fly ash captured in control devices is injected back into the furnace.

TABLE 1. Particulate Pollutants[727]

Source	Yearly Production Tons P	Emission Factor Lb/Ton e_f	Eff'y.[d] of Control C_c	Amount[c] of Control C_t	Extent[e] of Control	Emissions Tons/Yr E
1. Coal-Fired Boilers						
a. Electric Utilities						
1) Pulverized	265,200,000	16A[a] = 190	0.83	0.96	0.80	5,049,000
2) Stoker	0					
3) Cyclone	29,500,000	3A = 36	0.90	0.99	0.89	58,000
			Total from Electric Utilities			5,107,000
b. Industrial Power Generation						
1) Pulverized	19,300,000	16A[b] = 128	0.75	0.99	0.74	321,000
2) Stoker	68,600,000	14A = 112	0.70	0.80	0.56	1,690,000
3) Cyclone	9,800,000	3A = 24	0.90	0.80	0.72	33,000
			Total from Industrial Power			2,044,000
			Total from Coal-Fired Boilers			7,151,000

---

[a] Average percent ash in coal to electric utilities has been calculated to be 11.9%.

[b] Average percent ash in coal to industrial power generation has been assumed to be 8.0%, which is the average of all coal produced in the U.S.

[c] Amount of Control is defined as that fraction of the total production which has controls.

[d] Efficiency of Control is defined as the average fractional efficiency of the control equipment, prorated on the basis of production capacity.

[e] Extent of Control is defined as the overall level of control, and is the product of amount of control multiplied by the efficiency of control.

TABLE 2. Some Variables Affecting Particulate Emission Rates[946]

Variable Increasing	Mass Emissions Rate Increasing	Mass Emissions Rate Decreasing
Gas Velocity	X	
Particle Size		X
Particle Density		X
Coal Ash	X	
Coal Size		X
Coal Fired in Suspension	X	
Coal-Burning Rate	X	
Coal Heat Value		X
Combustion Efficiency		X
Boiler Efficiency		X

The majority of reinjected fly ash is slagged in the furnace, and is then removed and hauled away. However, a certain portion of the reinjected fly ash escapes with the stack gases. Thus, the amount of fly ash both challenging and penetrating the control devices is larger when fly ash reinjection is practiced. In soot blowing, steam jets are used to remove ash from heat transfer surfaces. Soot blowing practices vary from plant to plant, and in some cases may occur as much as 50% of the time.

Generalization concerning particulate emissions from the combustion of coal is not appropriate because each coal burning power plant is strongly affected by the type of furnace and amount and type of ash in the coal. Typically, coal used in power plants contains 5 to 25 percent ash with an average value of around 8 to 15 percent. A rather comprehensive discussion of the properties, composition, and distribution of coals can be found in reference[946]. A discussion of the dependence of the type of furnace used on the characteristics of the coal is found in reference[1163].

Basically there are three types of coal-firing furnaces: pulverized, cyclone, and stoker fired. In pulverized firing, finely-divided coal is thrown or blown into the furnace and combustion takes place in suspension. As the coal particles burn and become smaller, many become suspended in the stack gases. In dry-bottom furnaces of this type, as much as 80 percent of the ash in the coal is emitted from the furnace[857,1240]; in wet-bottom furnaces, as much as 50 percent of the ash is trapped in the furnace[1240]. The size and amount of the ash emitted from pulverized-fired furnaces is primarily influenced by the fineness to which coal is pulverized.

In stoker firing, coal is pushed or pulled into the furnace to form a burning bed of coal. A whole family of methods of firing stoker furnaces are used. These are referred to as the traveling-grate, vibrating-grate, single-retort underfeed, multi-retort underfeed and the spreader stoker. Some 5 to 40 percent of the ash from the coal is emitted from stoker-fired furnaces with the flue gases[857]. The amount of small particles in the coal, degree of agitation of the burning bed, and the combustion rate are the major factors influencing emission rates from stocker-fired furnaces.

In cyclone-fired furnaces, crushed coal is burned in a water-cooled, cylindrically-shaped furnace. Because air is blown tangentially into the furnace, the strong swirling motion of the air throws most of the coal to the wall of the furnace, where the combustion rate is so high that the melting temperature of fly ash is exceeded. This produces a molten layer of slagged ash on the furnace wall that is continuously tapped off. From 80 to 90 percent of the ash in the coal is trapped in the slag layer[857,1240]. However, ash that does escape from the furnace is extremely fine. Because cyclone furnaces operate with a minimum of excess air, the concentration of ash in stack gases can be as high as 2 1/2 pounds per 1000 pounds of gas[1240].

More detailed discussions on methods of coal firing are found in references 946 and 1240.

2. Particulate Loading From Coal Combustion

Particulate emissions information found in the literature is reported in several different units: grains per cubic foot of stack gas, grams per cubic meter of stack gas, percentage of the ash in the coal, pounds of particulate per 1000 pounds of dry flue gas, and pounds per million Btu input. For the purpose of this study, emissions in terms of concentration in the stack gas (either in grains/ft^3 or grams/m^3)* are the most appropriate. Converting to units of concentration from one of the other units requires a knowledge of the fuel composition and the amount of excess air used in firing the fuel. Frequently, the concentration is corrected to some basis such as 12% CO_2 dry volume basis and 60°F and 30 inches Hg.

---

*2.29 gm/m^3 = 1 gr/ft^3

Table 3[946] presents uncontrolled particulate emission per ton of coal burned for various types of coal firing units. Figure 1[946] is a nomograph of the same information but with particulate emission expressed in lb/10^6 Btu or lb/10^3 lb flue gas at 50% excess air. Figure 2 shows the relationship between type of fuel burned, excess air, and resulting volume of combustion products. Using Figures 1 and 2, particulate emissions for coal combustion by six firing methods can be estimated for 50 percent excess air and for a known heating value, ash content, and type of coal. For example, using a typical heating value of 13,000 Btu/lb and an ash content of 10 percent, Figure 1 gives the particulate emissions for all stokers other than spreader stokers (case B) as 1.9 pounds particles per 10^6 Btu.

TABLE 3. Particulate Emission Factors For Coal Combustion Without Control Equipment[946]

Type of Unit	Particulate Per Ton of Coal Burned,[a] lb
Pulverized	
General	16A
Dry bottom	17A
Wet bottom without fly-ash reinjection	13A
Wet bottom with fly-ash reinjection[b]	24A
Cyclone	2A
Spreader stoker	
Without fly-ash reinjection	13A
With fly-ash reinjection[b]	20A
All other stokers	5A
Hand-fired equipment	20

[a] The letter A on all units other than hand-fired equipment indicates that the percent ash in the coal should be multiplied by the value given. Example: If the factor is 17 and the ash content is 10 percent, the particulate emission before the control equipment would be 10 times 17 or 170 pounds of particulate per ton of coal.

[b] Values should not be used as emission factors. Values represent the loading reaching the control equipment always used on this type of furnace.

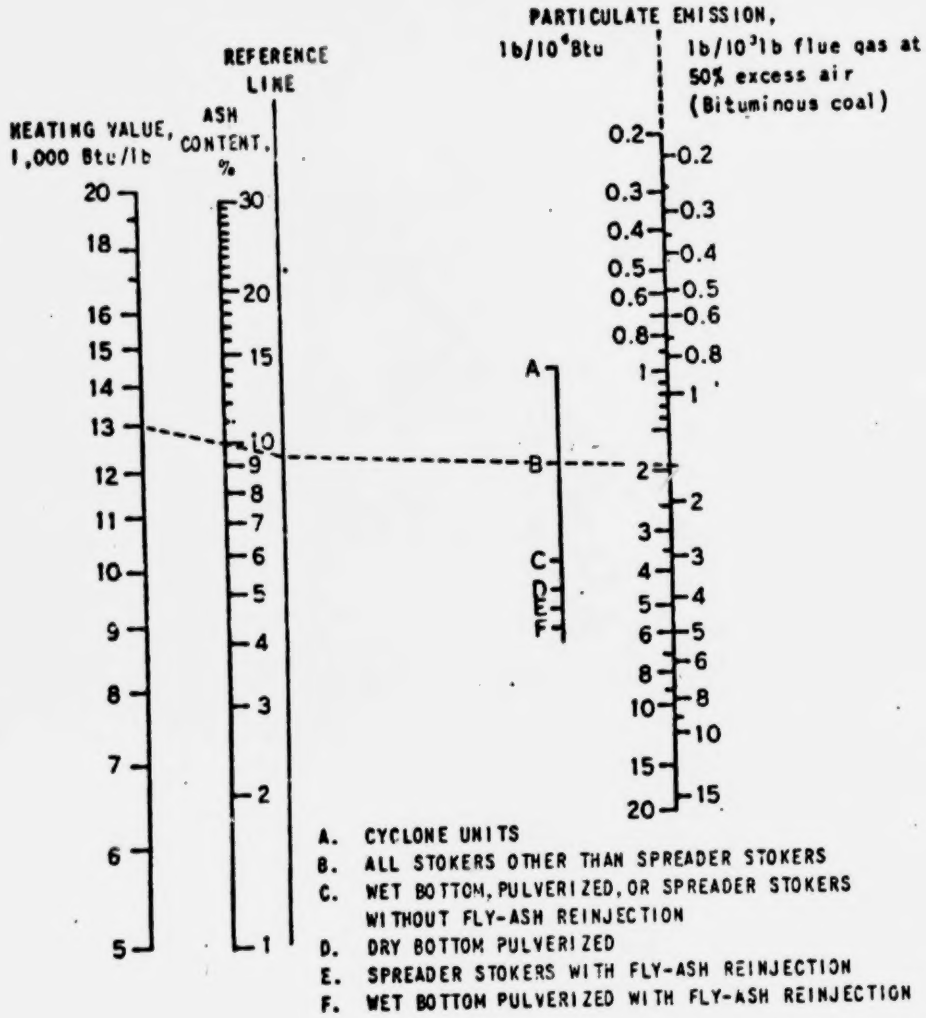
PARTICULATE EMISSION,
lb/10⁶Btu
lb/10³lb flue gas at 50% excess air (Bituminous coal)
REFERENCE LINE
HEATING VALUE, 1,000 Btu/lb
ASH CONTENT, %
20
18
16
15
14
13
12
11
10
9
8
7
6
5
30
20
15
10
9
8
7
6
5
4
3
2
1
A
B
C
D
E
F
0.2
0.3
0.4
0.5
0.6
0.8
1
2
3
4
5
6
8
10
15
20
A. CYCLONE UNITS
B. ALL STOKERS OTHER THAN SPREADER STOKERS
C. WET BOTTOM, PULVERIZED, OR SPREADER STOKERS WITHOUT FLY-ASH REINJECTION
D. DRY BOTTOM PULVERIZED
E. SPREADER STOKERS WITH FLY-ASH REINJECTION
F. WET BOTTOM PULVERIZED WITH FLY-ASH REINJECTION

Fig. 1. Nomograph for estimating particulate emissions from coal combustion (without air pollution control equipment).[946]

From Figure 2, the volume of dry flue gas per 10^4 Btu fired is about 150 ft^3 for a typical bituminous coal. Hence the estimated gas concentration of particles for this case is about 0.9 gr/ft^3. Similarily for the other firing methods (see notation in Figure 1), the estimated loadings in gr/ft^3 are: 0.37 for A, 2.3 for C, 3.0 for D, 3.5 for E, and 4.2 for F.

Figures 3 and 4[189] show the range and typical particulate emissions (gr/scf) for pulverized- and cyclone-firing in relation to the percent ash in the coal. The data contained in these figures agree quite well with those loadings estimated from reference[946].

Mass loading before and after electrostatic precipitators in three electrical power stations operating under normal conditions and burning various coals are presented in Table 4.[334] Note that the loadings before the precipitator for cyclone firing with fly ash reinjection are considerably greater than the value estimated above for cyclone firing without fly ash reinjection.

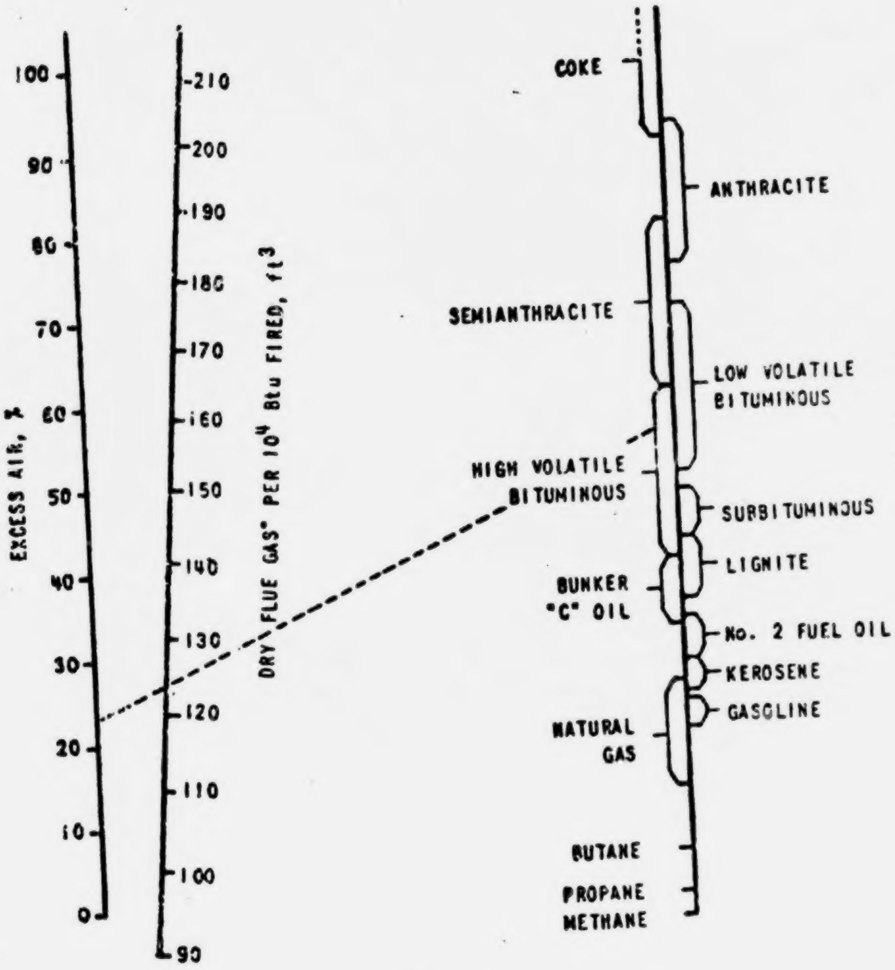
EXCESS AIR, %
0
10
20
30
40
50
60
70
80
90
100
DRY FLUE GAS* PER 10⁶ Btu FIRED, ft³
90
100
110
120
130
140
150
160
170
180
190
200
210
COKE
ANTHRACITE
SEMIANTHRACITE
LOW VOLATILE BITUMINOUS
HIGH VOLATILE BITUMINOUS
SUBBITUMINOUS
LIGNITE
BUNKER "C" OIL
No. 2 FUEL OIL
KEROSENE
GASOLINE
NATURAL GAS
BUTANE
PROPANE
METHANE

* Volume corrected 60 °F and 30 in. Hg dry

Fig. 2. Relationship between type of fuel burned, excess air, and resulting volume of combustion products.[946]

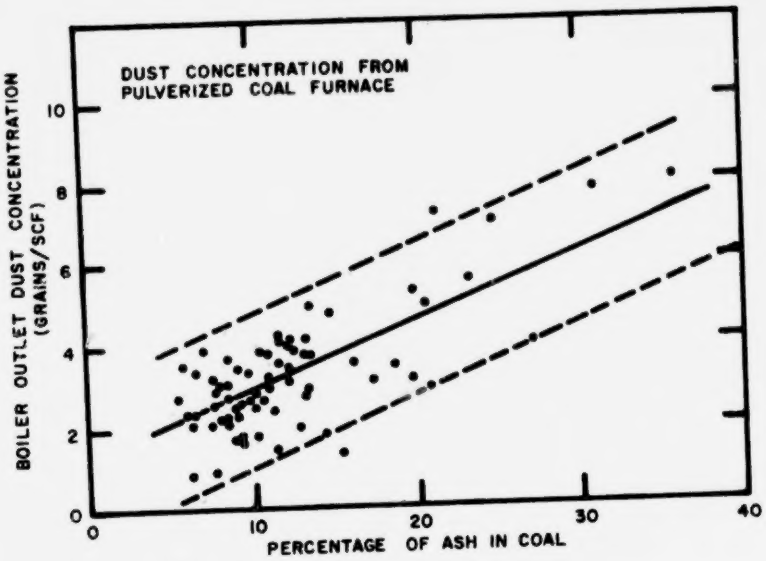

Fig. 3. Dust concentration from pulverized coal firing.[189]

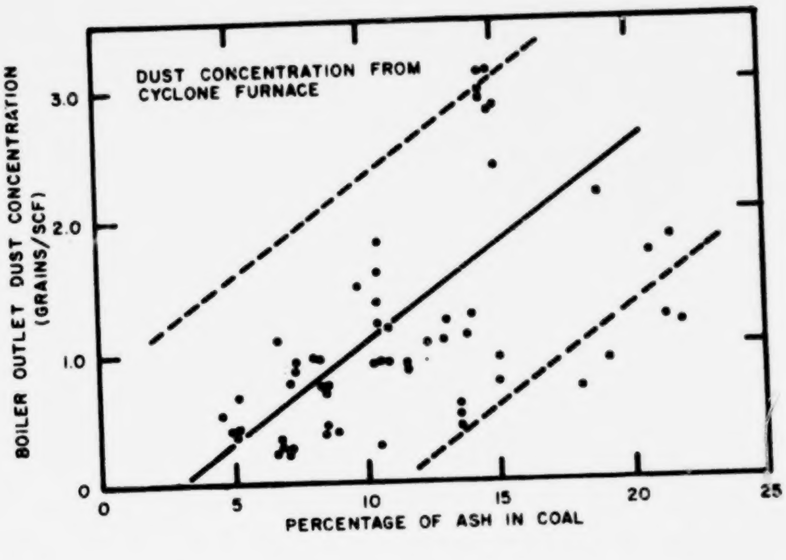

Fig. 4. Dust concentration from cyclone coal firing.[189]

TABLE 4. Particle Mass Loading Before and After Electrostatic Precipitator[334]

Unit Capacity* (MW)	Fuel	Burning Rate (Tons/Hr.)	Particle Mass Loading (gr/ft^3) Before Precipitator**		After Precipitator**		Overall Removal Efficiency, (%)
			Unit 1	Unit 2	Unit 1	Unit 2	
223	Illinois Coal & Coke	90	0.58	0.50	0.086	0.085	84.1
223	Illinois Coal	90	1.84	1.97	0.20	0.16	90.4
223	Montana Coal	90	0.85	0.61	0.29	0.14	71.4
135.6	Illinois Coal & Coke	60	2.16	2.54	0.069	0.074	96.9
135.6	50% Illinois & 50% Montana Coal	60	0.88	1.03	0.049	0.043	95.2
135.6	Montana Coal	60	0.78	0.90	0.063	0.11	89.7
580	Illinois Coal	240	1.80-2.16***	1.57-1.82***	0.017-0.040***	0.0154-0.028***	98.3-99.2

*The 135.6 MW station is a pulverized-coal feed forced-air furnace; the 223MW and 580 MW stations are crushed-coal feed cyclone furnaces. All three stations practice fly ash reinjection.

**The precipitator in each station consists of two parallel units; unit 1 and unit 2.

***At 29.92" Hg and 32°F.

Tables 5 - 8 present emissions information from two pulverized coal-firing power plants.[415] Unit C is a corner-fired dry bottom unit and Unit D is a horizontally-opposed-firing, wet-bottom unit designed for fly ash reinjection. Particulate emissions from Unit C before fly ash collection are seen to vary in accordance with the percent ash in the coal for constant load. Fly ash reinjection in Unit D is seen to result in a very pronounced increase in the loadings, up to a factor of about 3.7.

TABLE 5. Test Conditions and Major Pollutant Emissions - Unit C[415]

Test No.	Load, %	Coal Source	Coal Sulfur,[b] %	Coal Ash,[c] %	Sampling Point (Fig. 2)	Emissions: Fly-Ash, grs/scf[d]	Emissions, ppm by volume, dry basis: Nitrogen Oxides[e]	Emissions, ppm by volume, dry basis: Sulfur Dioxide	Emissions, ppm by volume, dry basis: Sulfur Trioxide
1	100	Ohio	2.2	15.1	B	3.7	509	1610	8
					A	0.19	397	1470	11
2	75	Ohio	2.2	15.8	B	3.5	381	1480	14
					A	0.08	304	1390	13
3[a]	100	Ohio	2.0	17.0	B	4.1	514	1250	7
					A	0.24	430	1310	12
4	100	W. Va.	1.0	12.7	B	3.4	555	590	8
					A	0.25	—	620	13
5	75	W. Va.	1.1	11.2	B	2.4	404	760	5
					A	0.15	346	600	10
Average					B	3.4	473	1138	8
					A	0.18	370	1078	12

B: before fly-ash collector.
A: after fly-ash collector.
[a] Low level heat economizer in operation.
[b] Moisture and ash-free basis.
[c] Moisture free basis.
[d] Corrected to 12% CO_2, dry basis.
[e] Reported as NO_2.

TABLE 6. Summary of Boiler and Flue Gas Data - Unit C[415]

Test No.	Boiler Conditions: Steam Rate, lbs/hr	Boiler Conditions: Coal Rate, tons/hr	Sampling Point (Fig. 2)	Flue-Gas Volume, scfm	Average Flue-Gas Temp., °F.	Moisture, %	CO_2,[a] %	O_2, %	Excess Air,[b] %
1	900,000	55	B	326,500	289	8.0	14.4	4.7	28.3
			A	336,000	279	9.5	14.4	4.6	27.4
2	693,000	42.7	B	285,700	243	8.75	15.2	3.8	21.6
			A	256,500	241	8.0	14.8	4.2	24.4
3	960,000	59	B	387,100	286	6.3	14.1	5.0	30.7
			A	362,000	261	8.05	14.2	4.9	29.9
4	960,000	54.2	B	375,100	283	6.6	14.7	4.5	26.8
			A	355,000	284	6.7	14.3	4.9	29.9
5	700,000	39	B	282,000	263	7.3	14.6	4.5	26.8
			A	272,000	264	6.85	14.6	4.5	26.8
Average			B		271	7.4	14.6	4.5	26.8
			A		266	7.8	14.5	4.6	27.7

B: before fly-ash collector.
A: after fly-ash collector.
[a] Calculated values, based on oxygen values, and fuel analyses.
[b] Measured at fly-ash collectors; average excess air at boiler outlet was 16.3%.
Standard Conditions—70°F and 29.9 in Hg.

NOT REPRODUCIBLE

TABLE 7. Test Conditions and Major Pollutant Emissions - Unit D[415]

Test No.	Load, %	Coal Source	Coal Sulfur,[c] %	Coal Ash,[d] %	Sampling Point (Fig. 3)	Fly-Ash, grs/scf[e]	Nitrogen Oxides[f] (ppm by volume, dry basis)	Sulfur Dioxide (ppm by volume, dry basis)	Sulfur Trioxide (ppm by volume, dry basis)
1[a]	100	Ill.	2.3	8.8	B	7.4	347	1580	13
					A	0.79	348	—	—
2	100	Ill.	2.6	8.1	B	2.0	429	—	—
					A	0.50	331	—	—
3[a]	100	Ill.	2.8	8.1	B	6.1	453	1670	12
					A	0.77	393	1500	9
4	75	Ill.	3.1	7.9	B	3.7	421	1880	6
					A	0.71	308	1840	6
5[a]	75	Ill.	2.7	7.7	B	2.0	369	1680	7
					A	0.51	347	1530	10
6[b]	100	Ill.	2.1	7.9	B	4.0	341	1430	5
					A	0.65	329	1260	—
Average					B	4.2	393	1650	9
					A	0.65	343	1530	8

B: before fly-ash collector.
A: after fly-ash collector.
[a] With fly-ash reinjection.
[b] With fly-ash reinjection and below normal excess air.
[c] Moisture and ash free basis.
[d] Moisture free basis.
[e] Corrected to 12% CO_2, dry volume basis.
[f] Expressed as nitrogen dioxide.

NOT REPRODUCIBLE

TABLE 8. Summary of Boiler and Flue Gas Data - Unit D[415]

Test No.	Boiler Conditions Steam Rate, lbs/hr	Boiler Conditions Coal Rate, tons/hr	Sampling Point (Fig. 3)	Flue-Gas Volume, scfm	Average Flue-Gas Temp., °F.	Moisture, %	CO_2, %	O_2, %	Excess Air[a]
1	149,000	8.8	B	56,600	310	6.5	12.7	6.7	45.6
			A	60,300	305	6.7	12.8	6.6	45.1
2	152,000	10.8	B	68,000	312	6.1	13.8	5.7	36.8
			A	65,600	305	6.3	13.4	6.2	41.4
3	149,000	0.1	B	66,500	311	5.8	11.7	7.0	48.5
			A	65,000	310	6.5	11.8	7.1	40.8
4	105,000	6.4	B	43,600	318	6.7	12.5	6.3	41.7
			A	44,900	316	7.2	12.2	6.7	45.7
5	111,000	6.7	B	44,000	310	6.5	13.1	5.6	35.2
			A	44,300	301	6.0	12.5	6.3	41.7
6	147,000	9.5	B	57,500	326	9.0	14.6	4.1	23.7
			A	57,700	315	—	14.1	4.5	26.5
Average			B		315	6.8	13.1	5.9	38.6
			A		309	6.5	12.8	6.2	41.7

B: before fly-ash collector.
A: after fly-ash collector.
[a] Measured at fly-ash collectors: Average excess air at furnace outlet was 37.4%.
Standard Conditions--70°F and 29.9 in. Hg.

Table 9 presents particulate loadings before and after collectors for vertically fired (Unit A) and a front wall fired (Unit B), dry bottom, pulverized-coal units.[413] Note in Table 9 the high loadings for Unit A, the vertically-fired unit. The loadings of about 5 grains/scf for Unit A are about the upper limit of emissions from pulverized-fired furnaces.

TABLE 9. Fly-Ash Collection Efficiency[413]

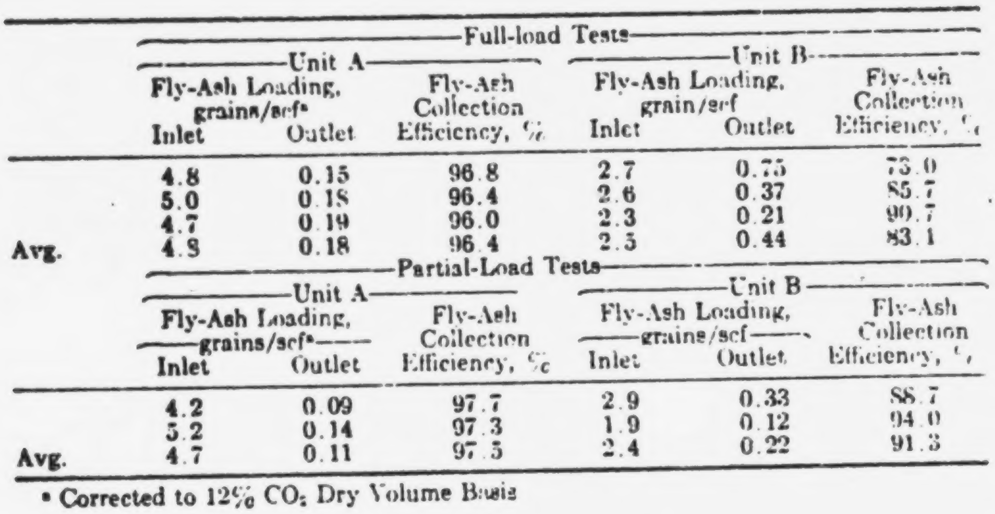

	Full-load Tests					
	Unit A			Unit B		
	Fly-Ash Loading, grains/scf* Inlet	Fly-Ash Loading, grains/scf* Outlet	Fly-Ash Collection Efficiency, %	Fly-Ash Loading, grain/scf Inlet	Fly-Ash Loading, grain/scf Outlet	Fly-Ash Collection Efficiency, %
	4.8	0.15	96.8	2.7	0.75	73.0
	5.0	0.18	96.4	2.6	0.37	85.7
	4.7	0.19	96.0	2.3	0.21	90.7
Avg.	4.8	0.18	96.4	2.5	0.44	83.1
	Partial-Load Tests					
	Unit A			Unit B		
	Fly-Ash Loading, grains/scf* Inlet	Fly-Ash Loading, grains/scf* Outlet	Fly-Ash Collection Efficiency, %	Fly-Ash Loading, grains/scf Inlet	Fly-Ash Loading, grains/scf Outlet	Fly-Ash Collection Efficiency, %
	4.2	0.09	97.7	2.9	0.33	88.7
	5.2	0.14	97.3	1.9	0.12	94.0
Avg.	4.7	0.11	97.5	2.4	0.22	91.3

* Corrected to 12% CO_2 Dry Volume Basis

NOT REPRODUCIBLE

Compared in Table 10[414] are findings from the units described above from references 413 and 415 with those from a cyclone fired wet-bottom unit and a traveling-grate spreader-stoker. Concentrations under partial and full-load tests of each unit are presented. The concentrations all seem to decrease with a decrease in load except for cyclone firing. The concentration from a cyclone furnace could, however, be expected to increase with decreased load because of a corresponding decrease in the centrifugal-force effect on the particles in the furnace. The data also shows that pulverized-fired units produce higher particulate concentrations than cyclone or spreader-stoker firing, even though the spreader stoker and the cyclone utilized fly ash reinjection and the pulverized units did not.

Table 11 shows the particle loadings before and after mechanical collectors for a spreader stoker (Boiler No. 1) and a pulverized-coal stoker (Boiler No. 2), all without fly ash reinjection.[744] These data shows that using pulverized coal in a stoker increases emissions.

Tables 12 and 13[368] summarize the design and operational conditions, and emissions from coal, oil, and gas heat generation sources. For the coal units listed, the emissions in gr/ft^3 at 60°F can be estimated by multiplying the values in pounds per 1000 pounds of gas by 0.6. For example, the uncontrolled emissions from the chain-grate stoker are, therefore, estimated to be about 0.6 gr/scf for 50 percent excess air. This value compares well with the value estimated from Figure 1[946] for a heating value of 13,000 Btu/lb and ash content of 7 percent.

TABLE 10. Fly-Ash Concentrations and Collection Efficiencies[414]

	Type of Boiler Firing	Ash in Coal,[a] %	Concentrations gr/scf[b] B	Concentrations gr/scf[b] A	Concentrations lbs/1000 lb[c] dry flue gas B	Concentrations lbs/1000 lb[c] dry flue gas A	Type of Fly-ash Collector[d]	Collector Efficiency, %
Full-Load Tests[e]	**Vertical** (Pulverized)	20.2	4.8	0.18	8.8	0.27	C, E	96.4
	Corner (Pulverized)	14.9	3.7	0.23	6.9	0.42	C, E	93.9
	Front-wall (Pulverized)	10.3	2.5	0.44	4.6	0.82	E	83.1
	Spreader-stoker	8.4	2.3	0.38	4.2	0.66	C	83.9
	Cyclone	7.7	1.5	0.39	2.8	0.62	E	74.5
	Horizontally opposed (Pulverized)	8.2	4.9	0.68	8.9	1.27	C	83.9
Partial-Load Tests[f]	**Vertical** (Pulverized)	19.0	4.7	0.11	8.7	0.21	C, E	97.5
	Corner (Pulverized)	13.5	2.9	0.13	5.5	0.21	C, E	95.7
	Front-wall (Pulverized)	9.2	2.4	0.22	4.4	0.41	E	91.3
	Spreader-stoker	8.7	1.5	0.19	2.8	0.35	C	87.3
	Cyclone	7.4	1.8	0.22	3.1	0.36	E	86.3
	Horizontally opposed (Pulverized)	7.8	2.9	0.61	5.1	1.1	C	77.7

[a] Moisture-free basis.

[b] Corrected to 12 percent CO_2, dry volume basis.

[c] 1000 pounds of dry flue gas corrected to 50 percent excess air.

[d] C designates cyclone; E designates electrostatic precipitator.

[e] Average values for either three or four tests at each unit.

[f] Average values for two tests at each unit.

B: Before fly-ash collector. A: After fly-ash collector

TABLE 11. Flow and Grain Loading Results[744]

Boiler #	ACFM	SCFM*	Temp.°F	Grain Loading (gr/SCF)
1 -Inlet	167,000	111,000	340	0.91
Outlet	176,000	117,000	340	**
2 -Inlet-East	110,000	73,000	340	1.99
Outlet-East	132,000	87,500	340	1.67
Inlet-West	105,000	69,500	340	1.99
Outlet-West	115,000	76,100	340	1.31

* Standard conditions 70°F, 30"Hg.

** Boiler leaking, could not test

Variation of particle concentration across a duct is a factor that can strongly affect the reliability of emission rates estimated from manual sampling information. One investigation[590] experimentally determined the distribution of particle loading in a vertical duct. The results are presented in Figure 5. These results show the loading lowest in the center of the duct and highest near the four corners. However, because a cyclone was used for sampling, the data may be baised towards the larger particles. Unfortunately, no mention is made of the size and type of firing equipment, and no velocity distribution is given.

TABLE 12. Design and Operational Summary--Heat Generation Sources[368]

	Design Data				Rated Capacity per hr			Fuel Data as-received basis			Operating Conditions During Test				
Source No.	Fuel Used	Firing Method	Type of Unit	Utilization	10^3 Lb Steam	Million Btu*	Dust Collector	Volatile, %	Ash, %	S, %	Fuel Rate Per Hr, Lbs	Gross Btu Input Per Hr, Million Btu	Steam Rate Per Hr, 10^3 Lb	Steam Pressure Psig	Smoke, Opacity, %
1	Coal	Pulverized (dry bottom furnaces)	Water-tube boiler	Electric generation	1060		Mechanical electrical	31	20.2	2.3	132,000	1560	1120	2000	30–40
2				Process heating	200		Multiple cyclone	36	4.3	0.9	9,420	130	106	307	60
3		Chain grate stoker	Water-tube boiler	Electric generation	125		None	44	7.0	3.8	12,400	147	111	450	20–40
4		Spreader stoker (with reinjector)		Process heating	70.5		Multiple cyclone	37	4.7	0.8	4,280	59.2	49	160	0–20
5		Underfeed stokers	Fire-tube boiler	Process heating		7.2	None	36	4.7	0.7	317	4.4		110	20–40
6				School heating		3.8	"	19	5	0.8	214	3.0		37	0–20
7			Cast-iron sectional boiler	Home heating		0.26		38	3.9	1.0	4.8	0.066		9	0–20
8		Hand-stoked	Hot-air furnace	Home heating		0.20		38	2.7	0.5	8	0.115			40–80
9	Oil	Steam-atomized	Water-tube boiler	Process heating	22	23	None	No. 2 Fuel Oil (28.5° API)		3.2	1,110	21	17.9	250	5
10					30	30		No. 6 Fuel Oil (13.5° API)		0.7	769	14.4	10.3	125	5
11		Low-pressure air-atomized	Scotch-marine boiler	Hospital heating		4.2		No. 1 Fuel Oil (43.5° API)			35	0.70		95	0
12		Centrifugal-atomized	Cast-iron sectional boiler	Home heating		0.25		No. 2 Fuel Oil (31.5° API)			8.8	0.17			0
13			Hot-air furnace			0.14		No. 2 Fuel Oil (31.5° API)			4.4	0.085			0
14		Vaporized	Hot-air furnace	Home heating		0.09		No. 1 Fuel Oil (43° API)		0.05	1.2	0.025			0
15	Gas	Premix burners	Fire-tube boiler	Process heating		7.2	None	Natural gas (94.2% methane 3.6% ethane)			402	9.3		108	0
16			Scotch-marine boiler	Hospital heating		4.2					42	0.98		96	0–20
17			Double-shell boiler	Home heating		0.18					7.9	0.18			0
18			Hot air furnace			0.21					7.4	0.17			0
19			Wall space heater			0.025					0.52	0.012			0

* Gross heat input.

TABLE 13. Pollutant Emission Summary - Heat Generation Sources[368]

Source No.	Fuel Used	Firing Method	Flue Gas Conditions in Stack: Flow, scfm	Flue Gas Conditions in Stack: Temp. °F	Flue Gas Conditions in Stack: H_2O, %	Flue Gas Conditions in Stack — Dry Basis: CO_2 %	Flue Gas Conditions in Stack — Dry Basis: O_2 %	Total Particulates: 1000 Lb[b]	Total Particulates: Lb Per Million Btu	Total Particulates: Ton of fuel[c]	% Benzene-Soluble Organics	Carbon Monoxide Lb Per: Million Btu	Carbon Monoxide Lb Per: Ton of fuel[c]	Hydrocarbons (as Methane) Lb Per: Million Btu	Hydrocarbons (as Methane) Lb Per: Ton of fuel[c]	Oxides of Nitrogen (as NO_2) Lb Per: Million Btu	Oxides of Nitrogen (as NO_2) Lb Per: Ton of fuel[c]	Oxides of Sulfur (as SO_2): Ppm by Vol.	Oxides of Sulfur (as SO_2) — Lb Per: Million Btu	Oxides of Sulfur (as SO_2) — Lb Per: Ton of fuel[c]	Formaldehyde — Lb Per: Million Btu	Formaldehyde — Lb Per: Ton of fuel[c]
1	Coal	Pulverized	415,000	260	5.4	12.3	6.9	0.50	0.59	14.0	0.7	0.004	0.1	0.007	0.16	0.47	11	1490	3.72	88	1.3×10^{-4}	30×10^{-4}
2			32,300	235	6.2	12.3	6.1	1.90	2.23	61.6	0.3	0.10	2.8	0.094	0.11			405	1.00	28	0.9×10^{-4}	26×10^{-4}
3		Chain grate stoker	45,000	430	6.7	12.1	7.7	0.99	1.31	31.0	0.3	0.51	12	0.005	0.11			2030	6.14	146	1.4×10^{-4}	33×10^{-4}
4		Spreader stoker	18,100	405	6.9	10.6	8.5	0.66	0.82	22.6	1.4	<0.1	<3	0.006	0.16						2.2×10^{-4}	60×10^{-4}
5		Underfeed stokers	3,340	380	2.1	3.0	17.2	0.68	0.62	17.0	1.1	0.16	1.5	0.116	3.2						21×10^{-4}	590×10^{-4}
6			3,290	235	2.1	2.5	18.1	0.24	0.25	7.0	3.6	0.14	3.9	0.036	1.0	0.30	8.3	205	2.3	62	3.8×10^{-4}	100×10^{-4}
7			43	345	2.2	2.6	17.1	0.52	0.44	12	1.2	1.1	31	0.12	3.3	0.36	~9.8	178	1.2	32		
8		Hand-stoked	78	220	2.1	2.8	17.7	1.80	1.29	37	17	3.5	99	0.73	21	0.11	3.2	80	0.54	15		
												<0.1	<4	0.013	0.51			1250	3.0	116	0.63×10^{-4}	24×10^{-4}
9	oil	Steam-atomized	5,200	530	8.5	9.0	8.2	0.32	0.306	11.7	1.0					0.31	12	188	1.3	48	2.4×10^{-4}	89×10^{-4}
10			10,000	340	5.4				0.267	10.0	2.7	0.055	2.2	0.001	0.17			125	0.35	14	1.6×10^{-4}	62×10^{-4}
11		Low-pressure air-atomized	195	230	7.4	8.8	9.0	0.049	0.051	2.0	69											
12		Centrifugal-atomized	145	170	3.0	2.9	16.9	0.041	0.046	1.8	39	0.038	1.5			0.44	17	14	0.12	4.5		
13			115	175	2.6	1.8	18.3	0.070	0.080	3.1	9.4	0.075	2.9	0.021	0.82			35	0.46	18	6.4×10^{-4}	250×10^{-4}
14		Vaporized	49	185	1.9	1.2	19.3	0.067	0.071	2.8	11	0.25	9.8	0.030	1.2	0.03	1.3	4	0.08	3	5.8×10^{-4}	230×10^{-4}
15	Gas	Premix burners	3,640	380	8.4	3.6	14.3	0.026	0.021	1.0	11	0.013	0.6	0.003	0.14	0.14	6.4				0.89×10^{-4}	41×10^{-4}
16			325	210	11.4	5.9	10.0	0.030	0.032	1.5	8.0	3.00	110	0.082	3.8	0.16	7.3				2.2×10^{-4}	$100 \quad 10^{-4}$
17			92	170	4.8	2.4	16.9	0.010	0.006	0.3	33	0.02	0.9			0.35	16	0	0	0	2.4×10^{-4}	110×10^{-4}
18			82	140	4.1	2.2	17.3	0.011	0.007	0.3	23	0.626	1.2	0.022	1.0	0.09	4.1	0	0	0	1.1×10^{-4}	53×10^{-4}
19			11	295	4.4	2.0	17.5	0.027	0.026	1.2	19	0.030	1.4	0.016	0.74	0.06	2.8				26×10^{-4}	1200×10^{-4}

[a] Blanks in the table indicate that no test was made.

[b] Pounds of particulate per 1000 pounds of dry flue gas adjusted to 50% excess air.

[c] API gravities of the fuel oils are given in Table 1; the density of natural gas = 0.0443 lb per cu ft (60°F, 1 atm).

NOT REPRODUCIBLE

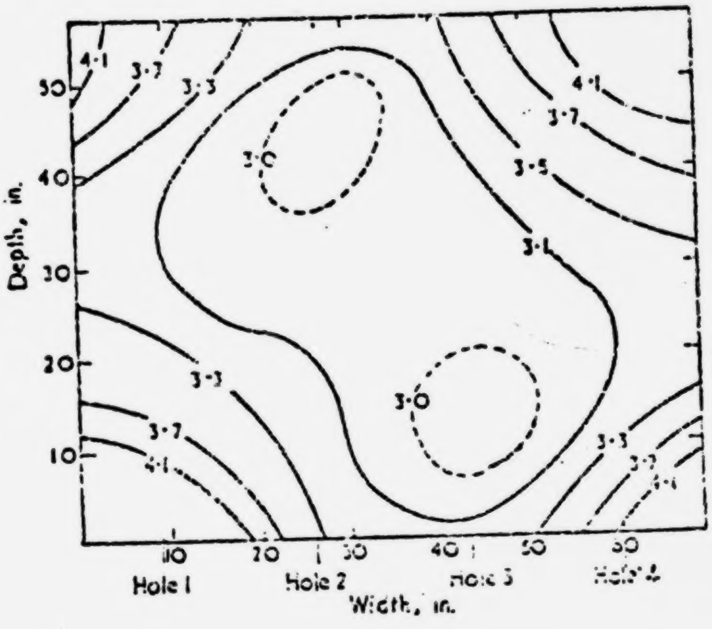

Fig. 5. Dust concentration patterns at constant load (gr/ft^3).[590]

3. Particle Size of Emissions From Coal Combustion

Particle size of fly ash from coal combustion ranges from less than 0.1 micron to several hundred microns.[1019] For most uncontrolled fly ashes, over 90 percent of the particles by weight are in the range of 1 to 100 microns, with the mass median diameter commonly in the range of 20 to 50 microns. Particle size results obtained independently by different laboratories on samples of the same ash may show substantial differences.[1019] Particle-size distribution for many fly ash samples closely follow the log-probability law. It should be noted that most particle size data was obtained by the Bahco sizing technique, which has a lower size cutoff of about 1 micron.

Typical sizes and ranges of size distribution of particulate emissions before collectors are shown in Figures 6 - 9 for pulverized-, cyclone-, spreader-stoker-, and stoker-fired furnaces.[946] The data from which these curves were compiled were obtained in the literature.

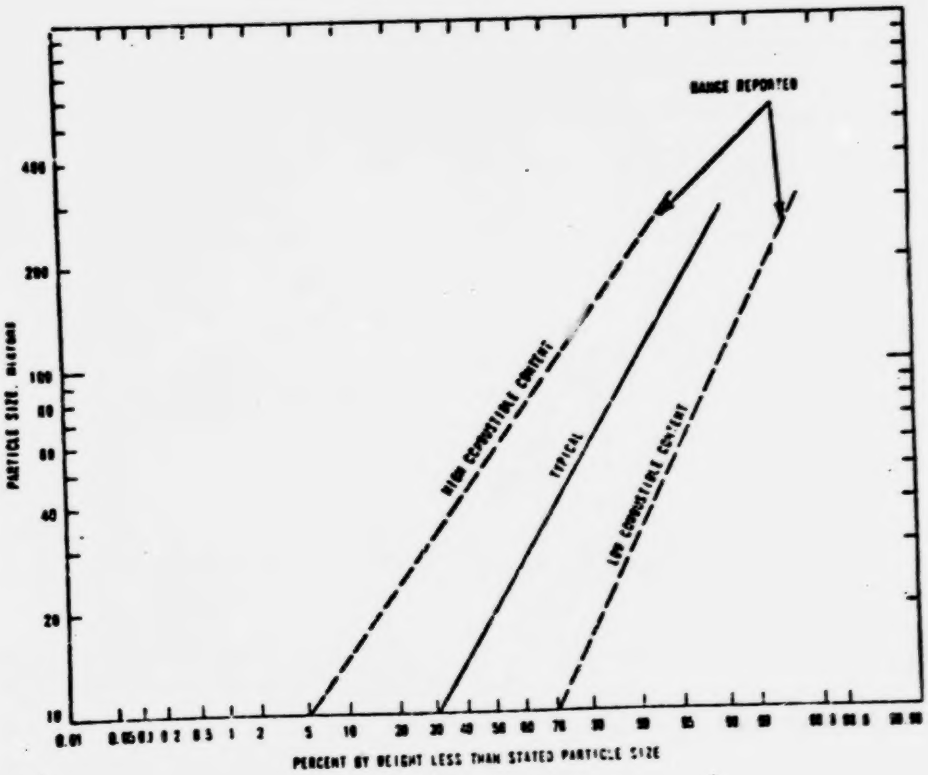

.Fig. 6. Estimated Size Distribution for Particles from Pulverized-Coal-Fired Furances (Before Collectors).946

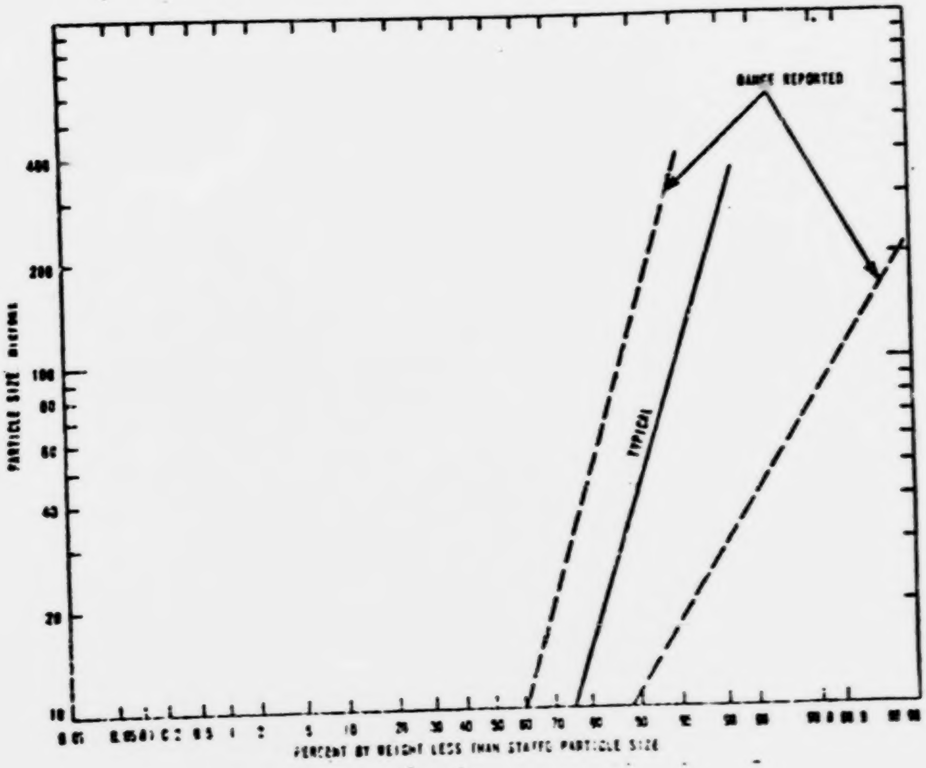

Fig. 7. Estimated Size Distribution for Particles Emitted from Cyclone Furnaces (Before Collectors).946

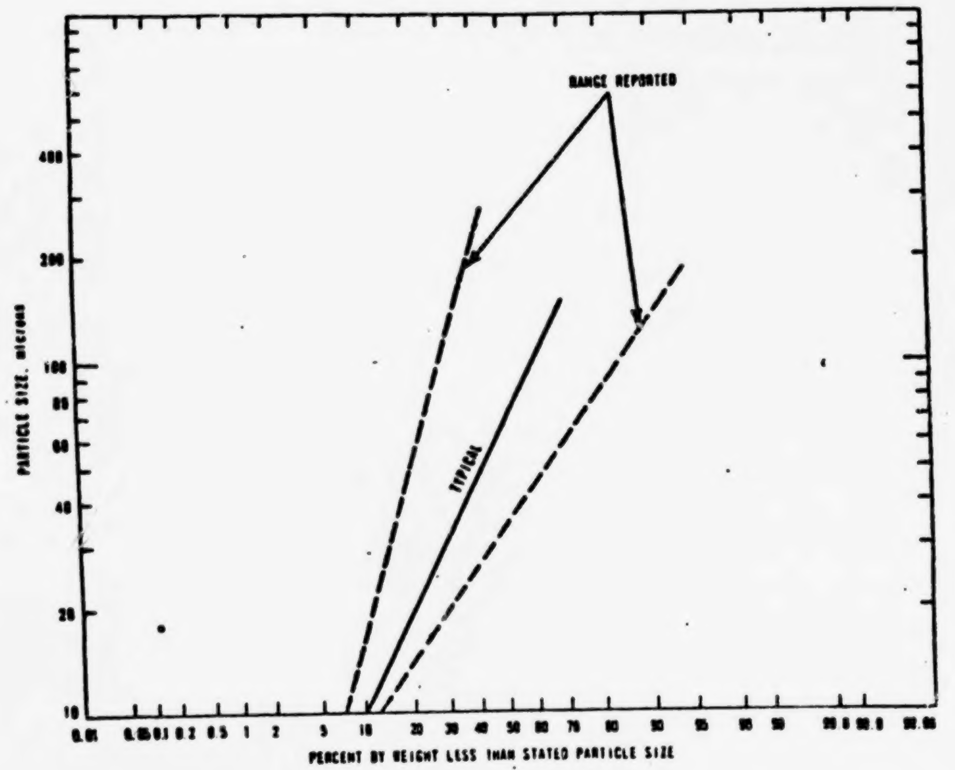

Fig. 8. Estimated Size Distribution for Particles Emitted from Spreader-Stoker-Fired Furnaces (Before Collectors).946

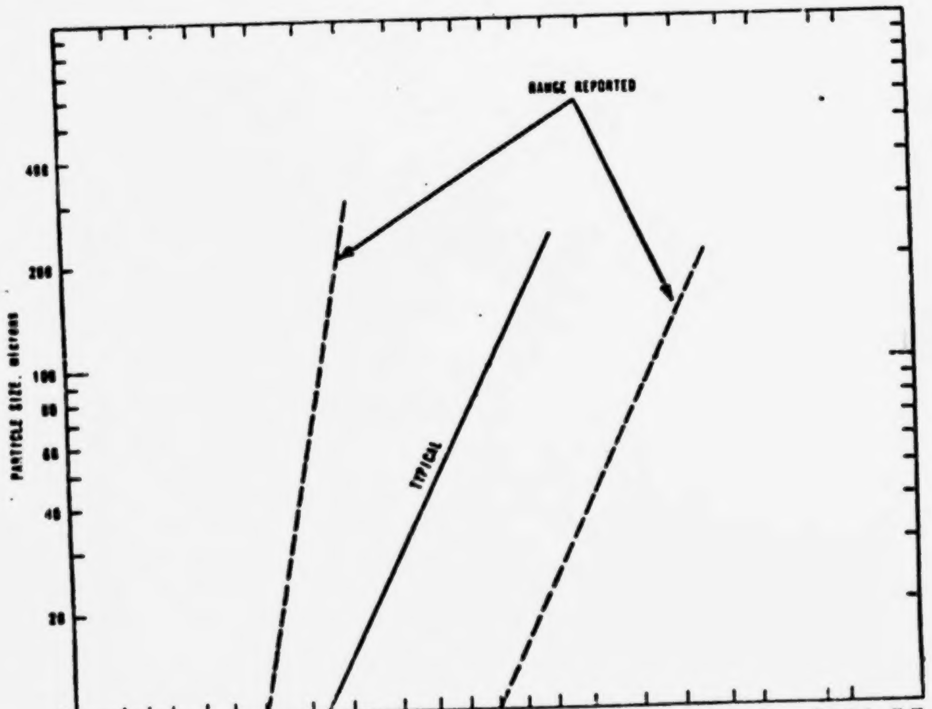

Fig. 9. Estimated Size Distribution for Particles Emitted from Stoker-Fired (Other than Spreaders) Furnaces (Before Collectors).946

Figures 10 - 12 show particle size distributions of emissions for pulverized-fired, cyclone-fired, and stoker-fired furnaces.[189] The size distributions were all determined by the ASME PTC 28 method of analysis (Bahco).[239] The dashed curves bracket the size range and the solid curves indicate the most probable size distribution. These size distributions and their ranges do agree fairly well with those in Figures 6 - 9.

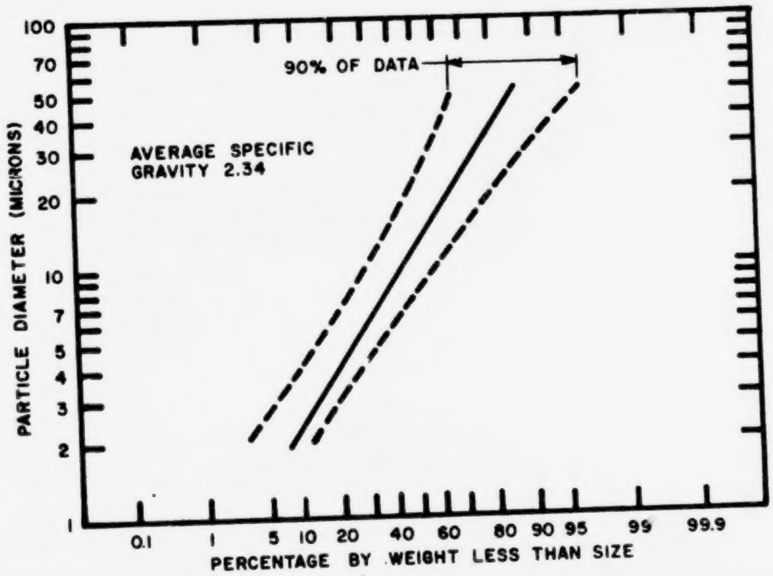

Fig. 10. Particle size distribution for pulverizer-coal-fired furnaces.[189]

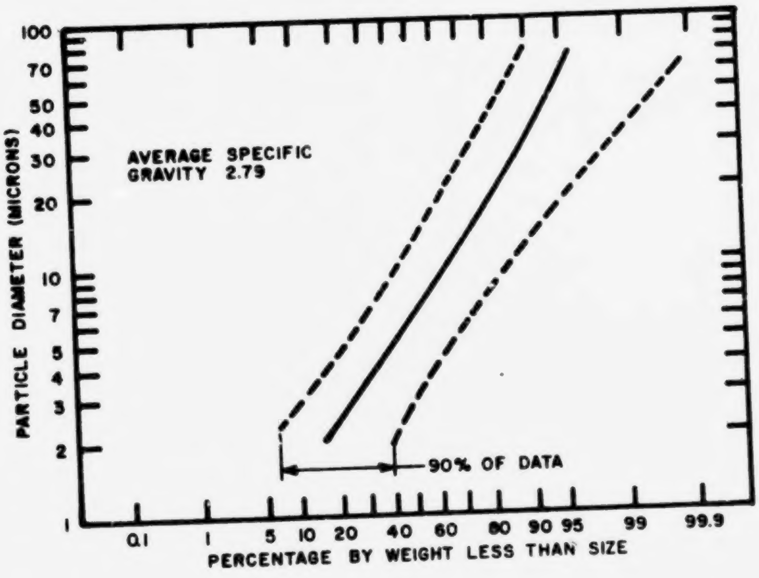

Fig. 11. Particle size distribution for cyclone-coal-fired furnaces.[189]

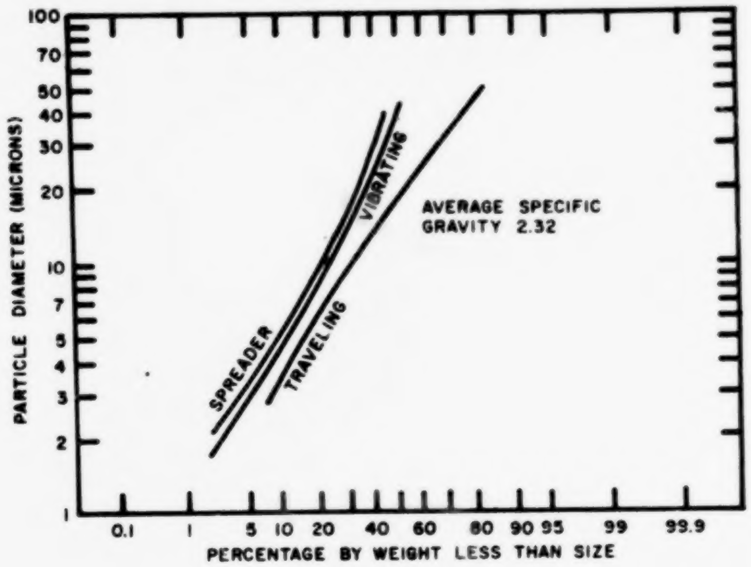

Fig. 12. Particle size distribution for stoker-coal-fired furnaces.[189]

Figures 13 and 14 show size distribution of emissions for pulverized-fired furnaces and stoker-fired furnaces other than spreader stokers. The data reported in these figures were recently obtained from several power plants. For comparison, the corresponding range of size distributions and typical size distribution reported in reference 946 are included and given by the dashed lines. Even though the size analysis methods used were not all the same, there is reasonably good agreement among the data. Also, although most of the curves do lie within the corresponding range reported in reference 946, the most recent data gathered during this study indicates a narrower size range and smaller particles.

Number-size distributions of fly ash before and after electrostatic precipitators for a cyclone-fired furnace and a pulverized-fired furnace are shown in Figures 15 and 16.[334] These curves show that the size distribution of fly ash after a precipitator is smaller than it is before a precipitator. The electrostatic precipitators were the only control devices on the furnaces, and a portion of the precipitators were being cleaned by rapping when the samples were being collected. The sizing was done with an optical microscope on a filter sample.

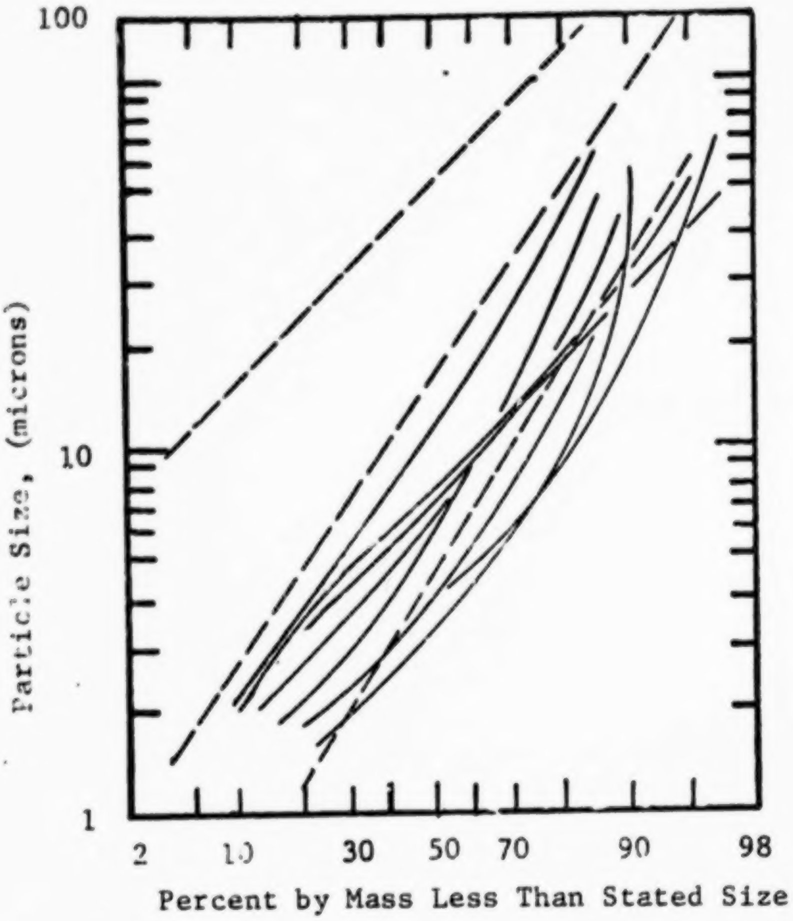

Fig. 13. Particle Size Distributions for Pulverized Coal-Fired Furnaces.

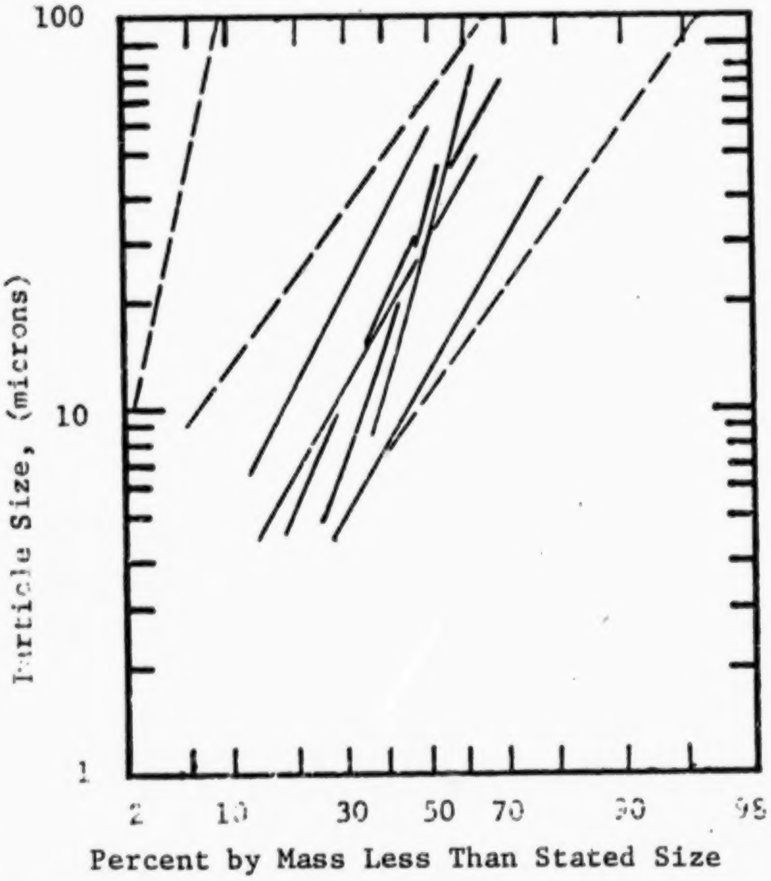

Fig. 14. Particle Size Distributions for Stoker Coal-Fired Furnaces.

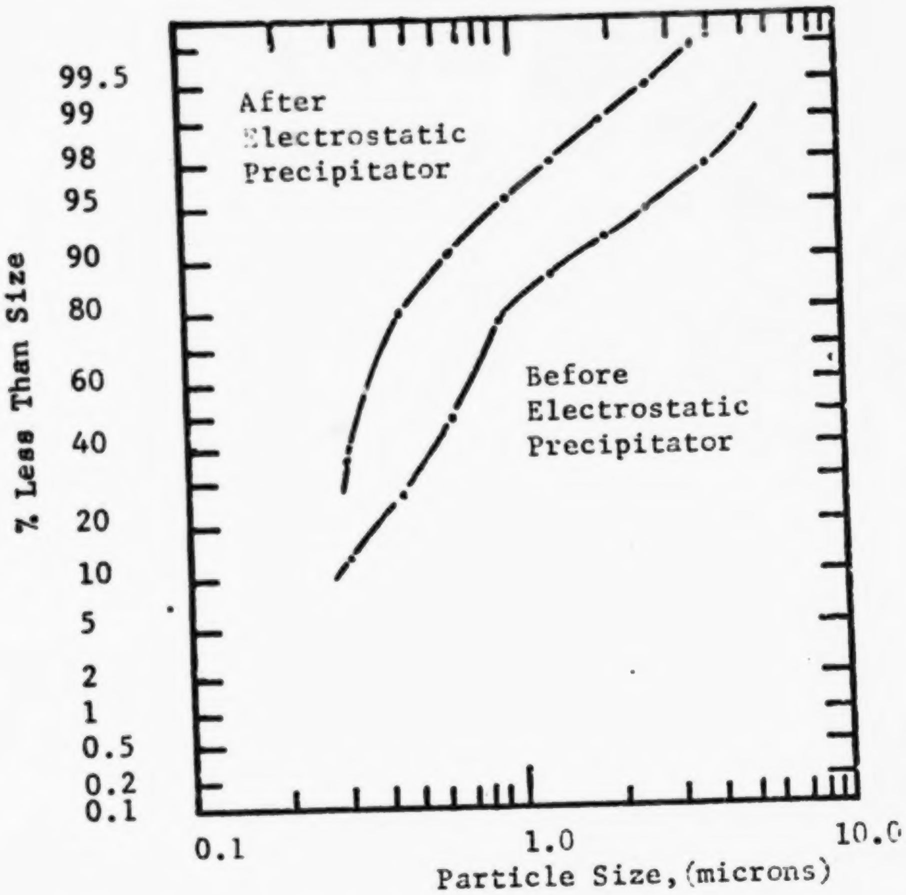

Fig. 15. Particle Number-Size Distribution for Cyclone-Fired Furnace.334

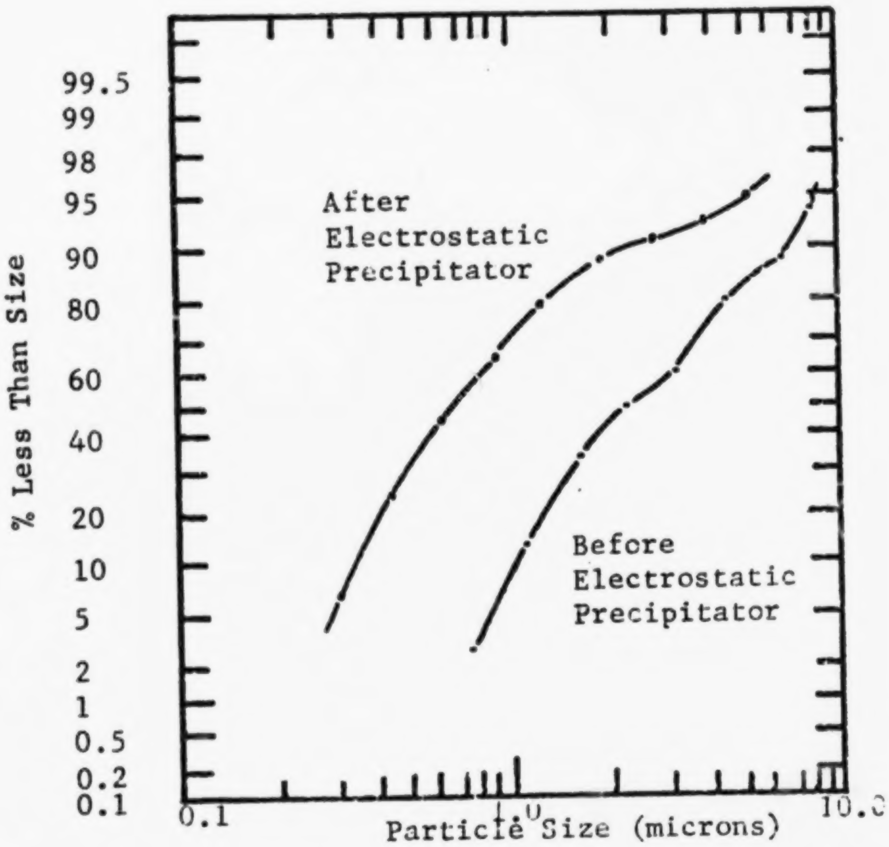

Fig. 16. Particle Number-Size Distribution for Pulverized-Fired Furnace.334

4. Control of Particulate Emissions From Coal-Fired Power Plants

The amount and efficiency of control of particulate emissions from coal-fired power plants are shown in Table 1.[727] This table shows the extent of control to be higher for electric utilities than industrial power generation, although the emissions from utilities are still about 70 percent of the total. It also shows that most coal-burning power plants have some type of control equipment.

The control equipment used is the settling chamber effects of large breeches and chimney bases, mechanical collectors such as cyclones, electrical precipitators, or combination mechanical-electrical precipitators.[788] Efficiency ranges generally achieved by these collectors on various units are given in Table 14.[946] Thus, if the uncontrolled emissions are known or can be estimated, the controlled emissions of particles can be estimated from a knowledge of the type of controls.

Table 14 USUAL EXPECTED EFFICIENCY RANGES FOR COMMONLY USED CONTROL EQUIPMENT (percent) [946]

Type of firing or furnace	Type of control equipment			
	Electrostatic precipitator	High-efficiency cyclone	Low-resistance cyclone	Settling chamber, expanded chimney bases
Cyclone	65-99[a]	30-40	20-30	-
Pulverized	80-99.9[a]	65-75	40-60	-
Spreader stoker	-	85-90	70-80	20-30
Other stokers	-	90-95	75-85	25-50

[a] The higher efficiencies can only be attained with high-efficiency cyclones in series with electrostatic precipitators.

NOT REPRODUCIBLE

5. Physical Properties and Composition of Particulate Emissions From Coal-Fired Power Plants

In general, the physical properties and chemical composition of particulate emissions vary considerably, probably because of the large number of variables affecting them. This undoubtedly is the reason why no information was found in the literature relating the physical properties and chemical composition of the emissions to the coal composition.

a. Particle Density. Density of particulate emissions depends primarily on particle size, structure and composition. In general, the relatively large, coarse, lace-like particles containing a high percentage of carbon have a low density of the order of 0.6 to 1.0 gm/cm^3. The finer particles of ash, which tend to be low in carbon, have a much higher density, usually in the range of 1.5 to 3.0 gm/cm^3.[1019] The average density of fly ash is 2.0 to 2.7 gm/cm^3.[946,442] The density variation among constituents of fly ash is quite large; the magnetite-hematite particles have a value of about 5 gm/cm^3, hollow glass spheres of less than one, and dense glass spheres between 2.0 and 3.0 gm/cm^3.[442]

The average particle density of fly ash can therefore be expected to decrease as the carbon content of the ash increases. A decrease in combustion or boiler efficiency, or an increase in the burning rate or gas velocity will most likely result in an increase in the carbon content of the ash. An increase in the silica content of the fuel could either increase or decrease the average particle density of fly depending upon whether a predominance of hollow or solid glass spheres results from firing the coal.

b. Bulk Density. Dry, uncompacted fly ash weighs about 55 pounds per cubic foot and, when completely compacted, 70 to 80 pounds per cubic foot.[1241] The bulk density can be expected to vary in accordance with the particle density.

c. Particle Shape. Glass, the abundant constituent of fly ash, is present in the shape of spheres, broken hollow spheres, ellipsoids, teardrop, and irregularly shaped particles. Magnetite-hematite particles, the second most abundant constituent, is present in the shape of spheres. Carbon particles vary widely in shape, but most of them are present as highly irregularly-shaped cellular particles that increase in abundance with increasing particle size.[442] The size of carbon particles generally range from 10 μm to 300 μm.[1019]

d. Electrical Properties. Much information exists on the electrical resistivity of fly ash.[422,434,496,608,744,1019] Resistivity normally varies from 10^8 to 10^{10} ohm-cm. Electrical conductivity of fly ash particles is increased by absorbed SO_3 and by increasing carbon content. Resistivity of fly ash greater than 2 x 10^{10} ohm-cm hampers collection in electrostatic precipitators.

e. Chemical Composition. The major constituents of most fly ashes are silica, alumina and iron oxide.[323,442,1019] Typical coal ash analysis limits are:[1019]

Constituent	Percent by Weight
Silica	30-60
Aluminum oxide	10-40
Ferric oxide	5-30
Calcium oxide	5-20
Magnesium oxide	0.5-4
Titanium oxide	0.5-3
Alkalies	1-4

Table 15 shows the concentration of seventeen trace metals before and after collectors.[414]

Table 15. **Metals Analysis for Full-Load Tests** 414

(grains/scf x 10^{-4})[a]

Type of Boiler Firing	Avg. Coll. Eff., %	Samp. Point	Cd	Ba	Be	Fe	Pb	Cr	Cu	Sn	Sb	Mn	Ni	Mo	V	Ti	Zn	Co	As
Vertical	89	B	T	9.5	0.24	480	3.6	0.95	9.5	T	T	7.2	4.0	0.95	9.5	95	T	0.48	
		A	T	0.34	0.02	17	1.1	0.08	0.87	0.04	T	0.26	1.1	0.17	0.88	3.4	0.34	0.06	
Corner	94	B	<.42	20.8	0.42	1900	4.2	8.3	25	<.42	<4.2	4.2	8.8	<1.22	24.8	420	12.2	1.22	1.4
		A	<.024	1.4	0.024	102	0.24	0.58	1.1	<0.22	<.24	0.44	0.58	0.10	1.4	22	<.72	.082	0.11
Front-Wall	86	B	0.73	20.4	0.60	480	12.5	4.8	3.6	<.26	<0.8	17.0	12.5	3.8	24	460	<24	2.0	
		A	0.26	3.4	0.11	58	1.2	0.68	0.88	0.26	<0.8	1.6	0.76	0.58	2.4	48	<2.8	0.37	
Spreader-Stoker	47	B	T	3.65	0.20	1100	4.8	1.95	1.9	T	<2.4	6.1	3.6	0.73	6.1	48	<7.3	<0.73	2.6
		A	T	0.94	0.06	380	7.4	1.52	1.1	0.17	<0.4	1.3	1.5	0.37	1.5	17	3.0	0.21	1.6
Cyclone	69	B	0.30	27.2	0.28	1360	11.4	8.2	3.2	0.65	<1.4	5.7	10.3	1.14	13.6	136	<4.2	2.2	0.66
		A	0.12	7.5	0.08	380	3.8	2.2	0.8	0.26	<0.4	1.2	2.2	0.38	4.7	38	<1.2	0.8	0.30
Horizontally Opposed	84	B	<.97	6.8	0.94	6800	68	9.7	20	<.68	<6.7	10.6	20	10.6	42	540	42	5.1	4.0
		A	0.58	1.1	0.14	730	14	1.8	4.4	0.32	<0.8	0.73	3.0	2.2	6.6	73	14	0.66	0.54

[a] Based on particulate grain loading. Each value is the average of at least two tests.

B: Before fly-ash collector

A: After fly-ash collector

T: Trace; blank indicates no data.

Carbon content of fly ash ranges from virtually zero to 55 percent. Representative figures are about 2 to 20 percent, with an average of about 10 percent.[1019] Factors which influence the degree of carbon in ash include character of the coal, fineness of pulverization, burner design, location and adjustment, furnace temperature, coal-feed rate, and amount of excess air.

f. Solubility. Fly ash contains water-soluble sulfates whose content varies from less than 0.1 percent to several percent.[1019] The average water solubility is about 7 percent.[744] Some values of percent benzene-soluble organics are listed in Table 13.

g. Toxicity. In past practice, fly ash has been considered to be non-toxic, and overall acidic in nature.

h. Wetability. Fly ash is usually difficult to wet and is believed to become more difficult to wet as the combustible content of the ash increases.

i. Bulk Characteristics. Fine fly ash of less than about 20 to 40 μm has a pronounced tendency to form stable agglomerates or masses and also to adhere to surfaces. Coarse fly ash acts more like sand and does not exhibit these cohesive and adhesive tendencies. Some kinds of fly ash will cement and form semi-hard accretions on surfaces if allowed to become moist or slightly wet. Fume particles, which typically are less than 1 μm,show a high degree of cohesion. The specific surface area for fly ash is usually between about 2,000 and 15,000 cm^2/gm.[442,1019]

j. Optical. Some glass particles in fly ash are light green or amber in color while others contain inclusions of iron oxide, a birefringent material. The index of refraction for glass ranges from about 1.50 to about 1.64. The lower index particles are generally clear or semiopaque due to bubbles; the higher index particles are green or amber. The magnetite-hematite particles are opaque in transmitted light and have a gray metallic luster in reflected light.[442,1019]

EMISSIONS FROM OIL FIRING

1. Variables Affecting Emissions From Oil-Fired Power Plants

Although particulate loadings from large oil-fired furnaces are usually considerably lower than for coal, oil-fired loadings vary over a much broader range. The major factors influencing particulate emissions in oil combustion are efficiency of combustion and atomization. Combustion efficiency is lowered by poor mixing, turbulence of the air and oil, low flame temperature and short residence time in the combustion zone.[620] This results in larger particles, higher combustible content and higher particle loadings.

The extent of atomization is strongly affected by the oil pressure. Low pressure atomization of oil promotes larger fly ash particles and greater particle concentrations; high pressure atomization yields smaller fly ash particles, fewer cenospheres (hollow carbon skeletons) and lower particulate emissions.

The extent of atomization is also affected by the temperature of the fuel oil. Increasing the oil temperature decreases its viscosity. In a 186-megawatt plant, an increase in the oil temperature of 35°F above the usual range of 230 to 240°F halved the emission rate and reduced the combustible content of the emissions by 15 to 17 percent.[1251]

Other factors and circumstances influencing emissions are: windbox air admittance, burner tilt, excess air, flue gas recirculation, and soot blowing.[620]

Varying the settings on the main and auxiliary air dampers, which effects the windbox air admittance, caused pronounced effects on ash emissions in two series of tests on a 186-megawatt plant.[1251] In the first series of tests, the main dampers were not completely opened, but the auxiliary controls were opened quickly. This produced large increases in the fly ash loading and combustible content.[1251] In the second series of tests, a much wider range of damper setting was used. The fly ash loading did not rise as sharply as under conditions of the first series of tests. The combustible content stayed essentially constant in the second series of tests.

Increasing the amount of excess air usually decreases the fly ash loading and the combustible content since more complete combustion results. In a series of four tests,[1251] an increase in the oxygen content of the stack gases from 2 to 4 percent resulted in a seven-fold decrease in particulate loading.

Recirculation of flue gases into the firebox increases fly ash emissions because of cooling of the flame. One investigator[1251] reported that an increase in flue gas recirculation from 0 to 15 percent increased the fly ash emissions 100 percent in a 186-megawatt plant. The same investigation found that when some flue gas was recirculated, the burner tilt affected emissions. With the burner tilted zero degrees from the horizontal, fly ash emissions reached a maximum. Hence, a burner tilted either up or down should be the best position from a particulate emissions standpoint.

Sootblowing obviously increases the particulate emissions. For example, this same investigator[1251] reported a 2.3X increase in normal emissions of 0.028 gr/scf during sootblowing.

Table 16[620] shows the affects on total emissions due to an increase in these variables.

TABLE 16. Effects On Emissions Of Increasing Operating Variables[a,620]

Increasing Operating Variables	NO_x	SO_2	SO_3	Particulates
Percent Load	I	-	I	-
Fuel Temperature	D	-	I	D
Fuel Pressure	D	-	I	D
Excess Air	I	-	I	D
Percent CO_2 in Stack	D	-	D	I
Dirt in Firebox	I	-	I	I
Flue Gas Recirculation	D	-	-	I
Flame Temperature	I	-	I	D
Stack Temperature	-	-	I	D
Percent Sulfur in Oil	-	I	I	I
Percent Ash in Oil	-	-	D	I

[a] I means increase; D means decrease; - means no change.

2. Particulate Loadings From Oil Combustion

Unlike coal combustion, the particulate emissions from oil firing do not follow any trend when correlated with the ash content of the oil. When oil containing one pound of ash is introduced into a larger boiler, as little as one-half pound or as much as 10 pounds of particles could be emitted.[620] The emissions may result from a build-up or detachment of boiler deposits, carbon and carbonaceous matter in the fly ash, sulfuric acid reacting with the boiler stack, or from a combination of these factors.

Most fuel oils contain less than 0.2 percent incombustible ash[526] which appears in the stack gases as particles. Since 1 gallon of oil when fired equals about 1760 scf of stack gas at 12 percent CO_2, 0.2 percent ash content of the oil corresponds to a stack gas loading of 0.065 gr/scf. Emissions cited in the literature, however, range from 0.008 to 0.49 gr/scf.[218,367,368,465,1055] More typical reported values are between 0.03 to 0.08 gr/scf. Most of the values reported in the literature are for small combustion units, but these values are believed to be typical of large units as well.

3. Particle Size of Emissions From Oil Combustion

Particle size of ash in stack gases resulting from oil combustion usually varies from less than 0.01 micron up to 40 microns in size.[526] The extremely small particles are carbon produced by cracking of vapor distilled from fuel oil. The larger particles, composed of carbon and ash and often in the form of hollow spheres of lattice construction (cenospheres), are produced by cracking of fuel in the liquid droplet state.[591] Under proper combustion conditions the carbon can usually be consumed.

Sulfur trioxide gases condense on fine, free carbon particles causing them to agglomerate to large flakes which may vary in size up to 1/8 or 1/4 inch diameter.[451] Electron photomicrographs have shown that liquid fuels produced sulfated ash particles predominantly in the 0.2 to 1.2 micron range.[1071]

It is believed that the time-temperature relationship of the products of combustion determine the size distribution of submicron particles discharged from the stack.

4. Control of Particulate Emissions From Oil-Fired Power Plants

The only pollution control devices used to any extent on oil-fired units are cyclone collectors limited for use during sootblowing. Cyclones are highly efficient for particles greater than 10 microns in size but are quite inefficient for particles 2 microns or smaller in size. The use of electrostatic precipitators is presently very limited. However,when electrostatic collectors are used, they not only reduce solid particle emissions by as much as 90 percent, but also SO_3 emissions by as much as 50 percent.[620]

5. Physical Properties and Composition of Particulate Emissions From Oil-Fired Power Plants

A paucity of information on the physical properties and composition of particulate emissions from oil-fired plants exists in the literature. Consequently, this section contains far less information than the corresponding section for coal-fired power plants.

a. Particle Density. Density is normally about 2.5 gm/cm^3.[620] Insufficient information is available to determine a range for particle density.

b. Bulk Density. No information available.

c. Particle Shape. Shape is extremely variable.[1349] Generally, the smaller particles tend to be spherical while the large ones form hollow spheres of lattice construction.

d. Electrical Properties. No quantitative data available. However, the resistivity of fly ash from oil firing is probably less than for fly ash from coal combustion because of its higher carbon and sulfate content.

e. Chemical Composition. Fly ash is mainly carbon and ash.[1241] Depending upon the source of the fuel oil burned, the ash will contain varying amounts of silica, sulfate, and oxides of iron, aluminum, titanium, calcium, magnesium, vanadium, nickel, and sodium.[620]

f. Solubility. Solubility varies from 30-60 percent. Some values of percent benzene-soluble organics are listed in Table 13.[620]

g. Toxicity. Fly ash is considered to be nontoxic but acidic, having an initial pH of about 3.0.[425,620]

h. Wetability. Fly ash is difficult to wet and becomes more so as the combustible content increases.

i. Bulk Characteristics. No information available.

j. Optical. No information available.

Characteristics and Properties of Stack Gases From Coal-Fired and Oil-Fired Power Plants

Particulate emissions from power plants are measured in the ducting before and after collectors or in the stack. The choice of station for measuring emissions is governed by its accessibility and the expected flow conditions. The vertical stack is usually the preferred location for sampling if it is accessible.

The flow conditions at any sampling station can be adversely affected by bends, turning vanes, distributor plates, and expansions or contractions in the ducting ahead of the sampling station. In most power plants, there are no sampling stations where the flow conditions are nearly ideal (i.e., low mechanical turbulence and a well defined flow profile). Figure 17 [334] shows that the velocity profile at the entrance to an electrostatic precipitator can be nonuniform, in spite of careful design to ensure good flow conditions through the collector equipment, a requirement for efficient collector operation. The velocity profile downstream of the collection equipment is usually even more nonuniform because most ducts are short in length and contain elbows and turning vanes.

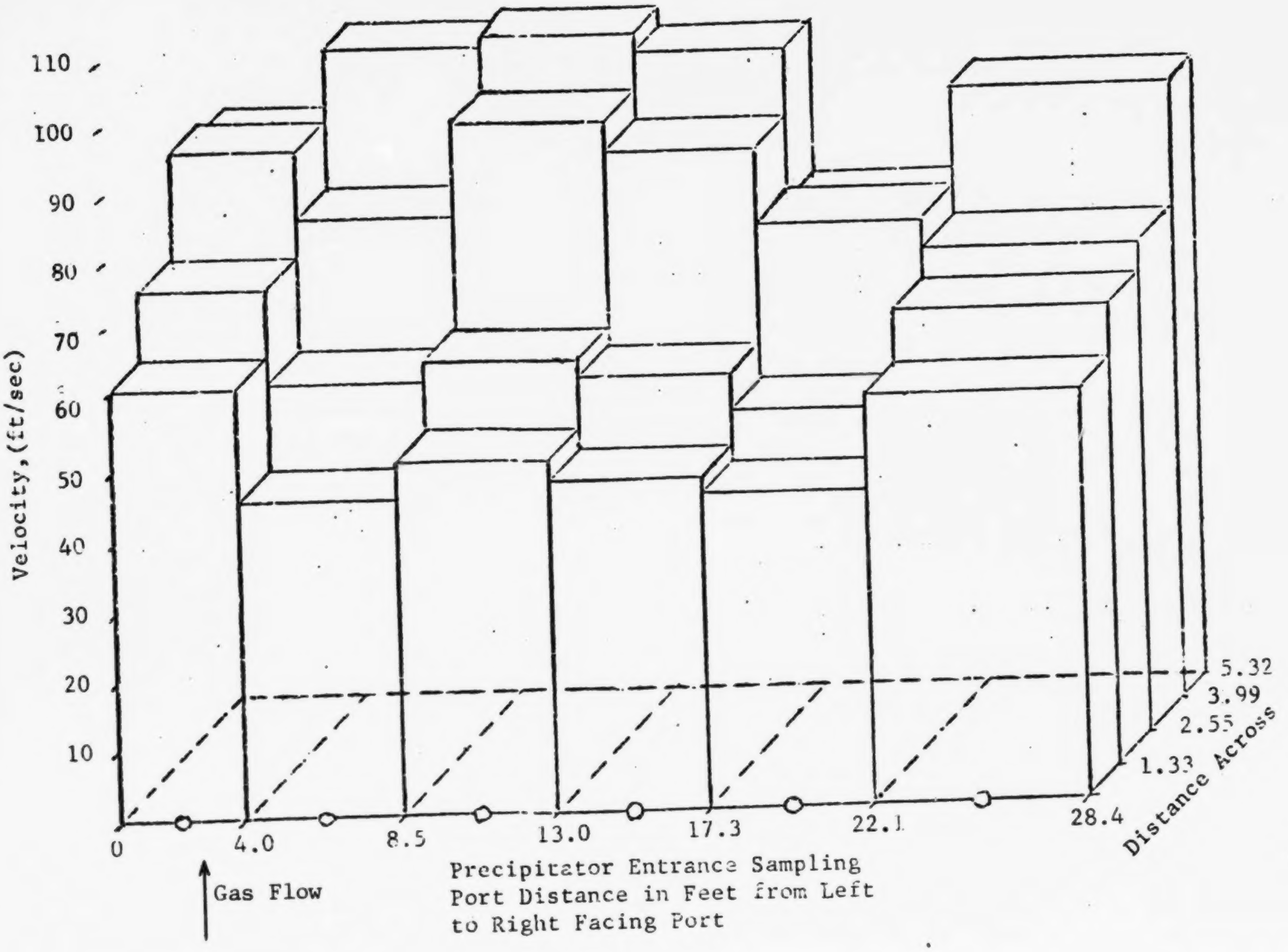

○ Approximate Sampling Port Location

Fig. 17. Velocity Profile in a Flue-Gas Duct Just Upstream of an Electrostatic Precipitator.[334]

From visual observations, the intensity and scale of the turbulence appear to be large. Also, the periodicity of flow fluctuation, judging from the response of monitors installed in power plants and from observed fluctuation at sampling ports, is estimated to be 0.5 to 2 cycles per second. In addition, it is estimated that the flow fluctuations are about 6 percent of the average flow velocity.

The temperature of stack gases from larger power plants varies between 250°F and 400°F. In general, the flue gas temperature of oil-fired plants is slightly higher than for coal-fired plants.

The acid dewpoint of flue gases from coal-fired plants is about 270°F and the water dewpoint is about 140°F. The corrosivity of stack gas becomes a problem when the temperature of an object in contact with the flue gas is below the acid dewpoint. Corrosivity of flue gases from coal combustion reaches a relative maximum at about 220°F. Below the water dewpoint of about 140°F, the corrosivity rises rapidly with decreasing temperature.[428] No information has been found about the dewpoints of vapors in oil-fired plants.

Sulfur trioxide, free or combined, is perhaps the most corrosive agent attacking metal surfaces exposed to flue gases. Sulfur trioxide formation depends on several factors, including flame temperature, rate of effluent cooling and the SO_2 - SO_3 chemical balance, and is normally 10 percent of the sulfur dioxide emission.[398] Some values of the sulfur content of fuels and the sulfur dioxide concentration in flue gases are shown in Tables 5, 7, 12, and 13.

Excess air (or oxygen) and carbon dioxide content of flue gases are important since concentrations of particulate emissions are frequently reported on a basis related to these factors. Some values of carbon dioxide content and excess air are given in Tables 6, 8, and 13.

Typical values of the moisture content lie in the range of 5 - 10 percent. Tables 6, 8, and 13 shows values ranging from 2 - 9.5 percent. The moisture content affects the water dewpoint.

SUMMARY

Table 17 summarizes the effluent characteristics from large coal- and oil-fired combustion facilities. The information presented is based upon information obtained from a search of the literature, from visits to power plants, and from discussions with the operating personnel and engineers in power plants. Obviously, much more information than is presented in Table 17 is needed to define completely the environment in which a continuous mass monitoring instrument must operate. However, to obtain more and better information requires better instrumentation than is now commercially available.

A list of specifications for an acceptable instrument to monitor continuously the mass emissions of particles from the stacks of large coal- and oil-fired power plants is presented following Table 17. The specifications are based upon the information presented in this section, especially that presented in Table 17, plus a knowledge of instruments and techniques that exhibit a potential for measuring mass emissions of particles in stack gases.

TABLE 17 SUMMARY OF EFFLUENT CHARACTERISTICS FOR COAL AND OIL COMBUSTION

<table>
<tr><th></th><th colspan="6">COAL COMBUSTION EMISSIONS
(Controlled and uncontrolled as noted)</th><th>OIL COMBUSTION EMISSIONS
(Uncontrolled)</th></tr>
<tr><td rowspan="4">Particulate Mass Concentration</td><td colspan="2">(units of grams/cubic meter)*</td><td colspan="2">Before Collector</td><td colspan="2">After Collector</td><td rowspan="4">Typical: 0.06 - 0.2
Range: 0.02 - 1.0</td></tr>
<tr><td colspan="2">Pulverized fired</td><td colspan="2">2.0 - 15.0</td><td colspan="2">0.03 - 4.0</td></tr>
<tr><td colspan="2">Stoker fired</td><td colspan="2">0.2 - 10.0</td><td colspan="2">0.06 - 3.0</td></tr>
<tr><td colspan="2">Cyclone fired</td><td colspan="2">0.4 - 4.0</td><td colspan="2">0.03 - 1.0</td></tr>
<tr><td>Mass Concentration Variations:</td><td colspan="6"></td><td></td></tr>
<tr><td>Spatially across duct</td><td colspan="6">Typical: ± 50%</td><td>Typical: ± 50%</td></tr>
<tr><td>With time</td><td colspan="6">No information available</td><td>As much as 10-fold increase over typical</td></tr>
<tr><td>During sootblowing</td><td colspan="6">No information available</td><td>About 4-fold increase over typical</td></tr>
<tr><td rowspan="5">Particle Size</td><td>(units of microns diameter)</td><td colspan="3">Before Collector</td><td colspan="2">After Collector</td><td rowspan="5">Typical: 0.01 - 1.0 microns
Usually uncontrolled</td></tr>
<tr><td></td><td>Rg. of MMD**</td><td>5% of Mass less Than</td><td>95% of Mass Less Than</td><td>Mech. 95% of Mass Less Than</td><td>Elect. 95% of Mass Less Than</td></tr>
<tr><td>Pulverized fired</td><td>7-20</td><td>1.0</td><td>70</td><td>40</td><td>25</td></tr>
<tr><td>Stoker fired</td><td>15-70</td><td>2.0</td><td>100</td><td>40</td><td>25</td></tr>
<tr><td>Cyclone fired</td><td>3-10</td><td>1.0</td><td>50</td><td>40</td><td>25</td></tr>
<tr><td>Extreme particle size range</td><td colspan="6">0.01 - 300 microns diameter</td><td>0.01 - 40 microns diameter</td></tr>
<tr><td>Particle specific density</td><td colspan="6">0.5 - 10.0 gm/cm^3 (variable within each stack)</td><td>0.5 - 5.0 range (variable within each stack)</td></tr>
<tr><td>Flue gas velocity</td><td colspan="6">Range: 30 - 120 fps Average: 50 - 60 fps
Average velocity fluctuates less than ± 3 fps in most stacks</td><td>Range: 30 - 120 fps Average: 50 - 60 fps
Average velocity fluctuates less than ± 3 fps in most stacks</td></tr>
<tr><td>Flow condition</td><td colspan="6">Turbulent and nonuniform</td><td>Turbulent and non-uniform</td></tr>
<tr><td>Periodicity of flow fluctuations</td><td colspan="6">30 - 120 cycles per minute</td><td>30 - 120 cyles per minute</td></tr>
<tr><td>Flue gas temperature</td><td colspan="6">Range: 270 - 400°F Typical 290-330°F (varies less than ± 5°F in most stacks)</td><td>Typical: Slightly higher than coal-fired</td></tr>
<tr><td>Dew point of flue gases</td><td colspan="6">Water: 140°F Acid: 220 - 270°F</td><td>No quantitive information available</td></tr>
<tr><td>Moisture content of flue gas</td><td colspan="6">5 - 10% by volume</td><td>No information available</td></tr>
<tr><td>Existing sampling port size</td><td colspan="6">3 - 8 inch I.D. hole typical</td><td>3 - 8 inch I.D. hole typical</td></tr>
<tr><td>Distance across duct from port</td><td colspan="6">Range: 5 - 30 ft. Typical: 7 - 15 ft.</td><td>Range: 5 - 30 ft. Typical: 7 - 15 ft.</td></tr>
<tr><td>Static pressure at sampling ports</td><td colspan="6">Range: 5" positive to 15" negative water pressure
Typical: 0" to 10" negative water pressure</td><td>No information available</td></tr>
</table>

*1 grain/cubic foot = 2.29 grams/cubic meter

**MMD = mass median diameter of the particle size distribution

INSTRUMENT SPECIFICATIONS

The specifications for an acceptable instrument (permanently installed) to monitor the mass emissions of particles downstream from a control device on a large stationary coal- and oil-combustion facility are as follows:

Performance Characteristics

- Measurement must correlate with total mass emissions of particles into the atmosphere.
- Capability of sensing particle mass concentration in the range of 0.01 - 4.0 grams per cubic meter.
- Must cope with particulate mass concentration profiles which vary by typically ± 50 percent spatially, by a factor of about 10 with time, and by a factor of about 10 during sootblowing.
- Preferably senses the mass of particles from 0.01 to 300 microns. However, it would be acceptable if it senses mass from 0.1 to 50 microns for coal-firing emissions or from 0.05 to 10 microns for oil-firing emissions, which would include over 90 percent of the mass of particles.
- Reproducibility between two identical instruments, including both sampling and sensing error, of ± 20%.
- Calibrated accuracy of ± 30%.
- Should record such items as zero and span every 1 to 6 hours on data recordings.
- Preferably have an instantaneous readout of the total mass of particles emitted into the atmosphere per unit time, or at least one average readout every 15 minutes.
- Outputs compatible with standard strip chart or digital recorders and with computer data inputs.

Environmental Requirements

- Operate with flue gas velocities of 30 to 120 feet per second.
- Operate in a variety of stacks, each having widely different velocity profiles.
- Not adversely affected by turbulent flow with characteristic eddy dimensions of 6 inches to 6 feet.

- Operate with flue gas temperatures ranging from 250 to 400°F and with temperature fluctuations of ± 5°F for short range periods (less than 1 day) and of ± 20°F for long range periods (more than 1 day).
- Operate in corrosive flue gas containing sulfur trioxide, both combined and uncombined.
- Must not restrict the flue gas flow in any significant way.
- Must withstand such environmental conditions as vibrations with amplitudes as high as 1/2 inch and frequencies on the order of 0.1 - 1.0 Hz, all types of meteorological conditions, and direct sunlight. Must withstand environmental temperature variations from +130°F to -30°F on a single installation.
- Must operate with flue gas static pressures from 15" negative to 5" positive water pressure (atmosphere reference) and with fluctuations of ± 3" water pressure.

Maintenance and Operational Considerations

- Rugged enough to last several years without major repair.
- Little or no maintenance except for regular weekly maintenance and for major maintenance only during regular power plant maintenance shutdowns (usually every 6 months).
- Little or no calibration or adjustment while in operation.
- Easily accessible during and after installation for weekly maintenance and for calibration or adjustments.
- Easy for plant operators to understand, operate, and to make minor repairs.
- Operate on 110V or 220V, 60 Hz electrical power and require little power, preferably no more than 1500 watts.
- May use up to 10 scfm of 90 psig compressed air in many facilities.

Economic Factors

- Installs easily within a week by 2 men in present and future stacks with little stack modifications other than holes, flanges, and utilities.
- Preferably cost $10,000 or less but definitely not more than $20,000.
- Power industry personnel must be willing to buy it.

REFERENCES

334 Anon., Power Plant Data (1970).

774 Anon., Stack Emission Reports.

239 Anon., Determining the Properties of Fine Particulate Matter, American Society of Mechanical Engineers, PTC-28-1965, 40 p. (1965).

788 Anon, "Control Techniques for Particulate Air Pollutants", U.S. Public Health Service, Nat. Air Poll. Cont. Admin., Washington, D. C., U.S. Govt. Printing Office (1969).

422 Anon., "Information Required for Selection of Electrostatic and Combination Fly Ash Collectors - Methods of Analysis for Chemical, Physical, and Electrical Properties of Fly Ash", APCA Journal, V. 15, no. 6, p. 256-260.

526 Austin, H. C., "Atmospheric Pollution Problem of the Public Utility Industry. Sources of Potential Air Pollutants", APCA Journal, V. 10, p. 292-294 (1960).

218 Brandon, J. H., "Can A Fuel Treatment Program Control Stack Emissions?", Combustion, p. 20-24 (Oct 1969).

590 Brown, R. L., "Some Coal Research Problem and Their Industrial Implications", Journal Inst. of Fuel, V. 29, p. 218-236 (1956).

465 Bunz, P., Neipenberg, H. P., and Rendle, L. K., "Influence of Fuel Oil Characteristics and Combustion Conditions on Flue Gas Properties in Water-Tube Boilers",Journal Inst. of Fuel, V. 40, no. 320,406-416 (Sep 1967).

434 Busby, H. G. T., and Darby, K., "Efficiency of Electrostatic Precipitators as Affected by the Properties and Combustion of Coal", Journal Inst. of Fuel, V. 36, no. 268, p. 184-197 (May 1963).

413 Cuffe, S. T., Gerstle, R. W., Orning, A. A., and Schwartz, C. H., "Air Pollutant Emissions from Coal-Fired Power Plants - Report No. 1", APCA Journal, V. 14, no. 9, p. 353-362 (Sep 1964).

414 Cuffe, S. T., and Gerstle, R. W., "Emissions from Coal-Fired Power Plants: A Comprehensive Summary", U. S. Public Health Service Pub. No. 999-AP-35, 26 p. (1967).

1055 Duprey, R. L., "Compilation of Air Pollutant Emission Factors", Public Health Service, Raleigh, N. C., Clearinghouse No. PB 190 245 (1968).

1163 Duzy, A. F., "American Coal Characteristics and Their Effects on the Design of Steam Generating Units", Preprint, Am. Soc. of Mech. Engineers, New York, 1959 (Presented at ASME Annual Meeting, Atlantic City, N.J., Paper 59-A242, Nov 29 - Dec 4 1959).

323 Elder, J. L., and Kube, W. R., "Technology and Use of Lignite", Proc., U. S. Bureau of Mines-U. of N. D. Symp., Bismarck, N. D., Apr 29-30, 1965. U. S. Bureau of Mines Information Circular 8304 (1966).

365 George, R. E., and Chass, R. L., "Control of Contaminant Emissions from Fossil Fuel-Fired Boilers", Am. Chem. Soc. Div. Fuel Chemistry, V. 10, no. 1, p. 31-56, papers for meeting March 22-31, 1966.

407 George, R. E., and Chass, R. L., "Control of Contaminant Emissions from Fossil Fuel-Fired Boilers", APCA Journal, V. 17, no. 6, p. 392-395 (1967).

415 Gerstle, R. W., Cuffe, S. T., Orning, A. A., and Schwartz, C. H., "Air Pollutant Emissions from Coal-Fired Power Plants, Report No. 2", APCA Journal, V. 15, no. 2, p. 59-64 (Feb 1965).

1240 Gould, G., "Formation of Air Pollutants", Power, p. 86 (Aug 1960).

857 Grohse, E. S., "Atmospheric Pollution: the Role Played by Combustion Processes", APCA Journal, V. 8, no. 3, p. 255-266 (Nov 1958).

368 Hangebrauck, R. P., Von Lehnden, D. J., and Meeker, J. E., "Emissions of Polynuclear Hydrocarbons and other Pollutants from Heat-Generation and Incineration Processes", APCA Journal, V. 14, no. 7, p. 267-278 (Jul 1964).

398 Hovey, H. H., Risman, A., and Cunnan, J. F., "Development of Air Contaminant Emission Tables for Nonprocess Emissions", APCA Journal, V. 16, 7, p. 362-366 (1966).

1251 Jefferis, G. C., and Sensenbaugh, J. D., "Effect of Operating Variables from a Modern Power Station Boiler", ASME, (Oct 1959).

608 Katz, J., "The Effective Collection of Fly Ash at Pulverized Coal-Fired Plants", APCA Journal, V. 15, no. 11, p. 525-528 (1965).

451 Kirov, N.Y., "Sulfur in Oil Fuels - Its Effects in Combustion", Journal Inst. of Fuel, V. 35, no. 261, p. 426-431 (Oct 1962).

749 McConnel, J. A., "Burner Fuel Oils Market Demand and Quality Requirements", Sun Oil Company, Marcus Hook, Penn., presented at National Fuels & Lubricants Meeting, New York New York, Sep 11-12, 1968.

1349 McCrone, W. C., Draftz, R. G., and Delly, J. G., The Particle Atlas, Ann Arbor Science Publishers, Ann Arbor, Mich. (1967).

442 Nature and Distribution of Particles of Various Sizes in Fly Ash:, U. S. Waterways Experiment Station, Tech. Report 6 - 583, 27 p. (Nov 1961).

1241 Negherbon, W. O., "Sulfur Dioxide, Sulfur Trioxide, Sulfuric Acid and Fly Ash: Their Nature and Their Role in Air Pollution", EEI Research Project RP62, (Jun 1966).

367 Pesterfield, C. H., "Literature and Research Survey to Determine Necessity and Feasibility of Air Pollution Research Project on Combustion of Commercially Available Fuel Oils", AFCA Journal, V. 14, no. 6, p. 203-207 (Jun 1964).

425 Raco, R.J., and Peskin, R. L., "High Voltage, Low Frequency Atomization of Fuel Oil", ASHRAE Trans., V. 75, pt 1, Paper 2099, p. 111-117 (1969).

1071 Salo, E. A., "Visible Exhaust From Fuel Oils", Hydrocarbon Process, V. 49, no. 2, p. 96-98 (Feb 1970).

591 Sambrook, K. H., "Fuel Oils, Their Efficient and Smokeless Combustion", Petroleum, V. 17, p. 56-61, 63 (1954).

401 Shafer, H. E., Jr., and Holland, C. T., "Western States Coal-Associated Mineral Occurences Likely to be Factor in Long Range Air Pollution Considerations", West Virginia University School of Mines-Coal Research Bur. Tech. Report 17, 13 p. (Oct 1965).

496 Shale, C. C., Holden, J. H., and Fasching, G. E., "Electrical Resistability of Fly Ash at Temperatures to 1,500°F", U. S. Bureau of Mines, Publication 7041, 17 p. (1968).

946 Smith, W. S., and Gruber, C. W., "Atmospheric Emissions from Coal Combustion - An Inventory Guide", U. S. Public Health Service, Division of Air Pollution, Cincinnati, Ohio, Clearinghouse No. PB 170 851 (Apr 1966).

620 Smith, W. A., "Atmospheric Emissions from Fuel Oil Combustion", U. S. Public Health Service, Pub. No. 999-AP-2 (Nov 1963).

428 Third, A. D., "The Aim of Chimney Design", Eng. & Boiler House Rev., V. 82, no. 5, p. 124-128 (May 1967).

727 Vandergrift, A. E., "Particulate Pollutant System Study", Midwest Research Institute, Kansas City, Mo., Reports for NAPCA, U. S. Dept. of HEW, Cincinnati, Ohio, Cont. No. CPA 22-69-104 (1970).

189 Walker, A. B., "Emission Characteristics from Industrial Boilers", Air Engineering, V. 9, no. 8, p. 17-19 (Aug 1967).

1019 White, H. J., "Effect of Fly-Ash Characteristics on Collector Performance", APCA Journal, V. 5, p. 37-50 (May 1955).

SAMPLING CONSIDERATIONS

by: John Borgos

INTRODUCTION

The extraction of a sample of particles from a gas stream, such as flue gas in a smokestack, and the delivery of this sample to some sensing instrument for evaluation is a formidable task. The degree to which the sample truly represents the gas stream is always highly dependent on the design of the probe used to remove and transport it. The designer of the probe must have the flow conditions of a particular gas stream in mind to insure that the probe gets an unbiased sample of the stream. He must also have the specific type of particle in mind to insure that, once the aerosol enters the probe, it is not modified in such a manner that it affects the measurement.

A probe must have at least two main parts: a nozzle for sample removal and a tube for sample transport. The nozzle must be sized so that it draws gas at a velocity equal to that in the duct airstream and at a volumetric flow rate compatible with that required by the sensing instrument. It must be shaped so that it obstructs the bulk flow as little as possible. The tube must be sized and fabricated to prevent excessive particle deposition and reentrainment on the tube walls. Bends have to be properly designed to avoid inertial deposition. Heating, cooling, or diluting of the sample may help maintain its integrity. Thus, there are a number of criteria which the probe designer must satisfy to optimize the design of the nozzle and sampling tube.

It must be borne in mind that perfect probes do not exist and, with present information and materials, cannot be made. Therefore, the optimization of the probe design is only half the solution to the problem of getting a sample from the gas stream to the sensing instrument. The other half is an evaluation of the errors which cannot be removed in the probe design. Such evaluations are, at best, intelligent guesses, but they do give the order of magnitude of the errors.

The remainder of this discussion will be limited to the sampling of flue gas from ducts or stacks. A general review of the conditions expected in a typical stack is included. The significant sources of error are discussed in terms of the parameters that govern them. From this, criteria for good probe design develop. Finally, the magnitude and importance of the expected errors are evaluated with specific particle sensing instruments in mind.

STACK GAS PARAMETERS

The authors have conducted an extensive study of the literature on the properties of flue gas from coal- and oil-fired combustion sources. The assimilation and condensation of all this information, which is presented in a previous section of this report, has provided a comprehensive picture of what is now known about the gas flow and particle properties of flue gas. One of the first lessons learned from this study is that each of the variables has a wide range of values. Therefore, any instrumentation has to be designed for use over a wide range of conditions.

Before going into a detailed discussion on probe design features, a more general presentation of the relevant gas flow and particle properties will be given. Although data is available for conditions both upstream and downstream of particle collectors (e.g., cyclones and electrostatic precipitators), attention will be focused primarily on conditions downstream of the collectors. The reason for this is that a measurement of particles here defines what is actually going out of the stack, and thus what may become air pollution.

There are a couple of disadvantages in monitoring conditions downstream, as opposed to upstream, of the particle collectors. First, the gas flow is usually more turbulent downstream of collectors than upstream. This is due perhaps mainly to the fact that particle collectors require a fairly stable flow condition, and therefore an effort is made, either with a straight section of breeching or a series of guide vanes, to provide uniform, stable flow in the collector. This is not done downstream, however, because the chimney follows quite closely behind the collector; thus uniform flow conditions do not have time to develop between the collector and the chimney. Second, the particles downstream of an electrostatic precipitator are often electrically charged. This affects their behavior somewhat in a sampling probe and significantly in most sensing instruments. The magnitude and distribution of the charge are unpredictable. Therefore, a well designed instrument should not be affected by this residual charge possessed by the sampled particles.

The level of turbulence in flue gas ducts and the resulting sampling problems have not really been assessed. If the particles are not all flowing in the same direction, or if they are not moving in the same direction as the local gas, the orientation of a probe nozzle is critical. Indeed, if the velocity vectors of the particles in the duct are not unidirectional, a severe sampling bias may occur regardless of the nozzle orientation. The mean velocity of flue gas in ducts is usually about 15 - 20 m/sec, which means the Reynolds number varies from 10^6 - 10^7 for typical ducts (based on the duct diameter). The normal frequency range of flow fluctuations appears to be around 0.5 - 2 Hz. Thus, large scale (about a meter in diameter) turbulent eddies are likely to be present. These eddies help distort the distribution of the particulate mass loading across the duct, which probably varies by as much as ± 50% from one position to another.

A second factor contributing to the skewed distribution of particulate mass loading across a duct is the duct configuration, which contributes also to the formation of turbulent eddies. Right-angle bends, for instance, cause large particles (i.e.,$>5\mu m$) to be hurled toward the outside of the bend because the aerodynamic drag forces are not great enough to overcome inertial forces. It is usually recommended that about ten diameters should be allowed downstream of a bend for the gas flow to become uniform. Unfortunately, few effluent ducts have any straight sections which are this long. Worse yet, since the particle eddy diffusivities are always smaller than those of the gas, the particles will not become uniformly distributed as quickly as the gas flow. Therefore, bends in the duct configuration are likely to contribute a great deal to the distortion of the particulate mass loading distribution as well as the distortion of the velocity profile across a dust cross-section.

A third contribution to nonuniform particulate mass concentration across a duct can be made by the malfunction of various parts of the electrostatic precipitator. Suppose several electrodes in a localized region of the precipitator are not functioning. The result is a heavier concentration of particles in that part of the flue gas stream. The difference between this concentration and the average concentration may be as much as one order of magnitude immediately downstream from the precipitator.

INTEGRATED VS. POINT MEASUREMENT

Before comparing the virtues of so-called "integrated" and "point" measurements, the definitions of each must be clear. Measurements made by all techniques which require extraction of a sample from the duct are called "point measurements". Point measurements are not made at a point in the true sense of the word, but are averages over a small area defined by the sampling nozzle. The measurements are nearly always the average concentration of particles at the nozzle entrance. Use of this measurement as an estimate of the average concentration across the entire duct requires knowledge of the particle concentration profile. On the other hand, to estimate the flux of particles passing through the duct, one must also know the velocity profile within the duct. Mathematically, the total particulate flux F passing through the duct can be expressed as:

$$F = \int C(A)V(A)dA. \qquad (1)$$

Note that particle concentration C(A) and velocity V(A) are both functions of the specific location within the cross-sectional area A of the duct.

In practice, concentration and velocity profiles can be handled in two ways: 1) by measuring the concentration and velocity continuously at a number of points within the duct cross-section; or 2) by measuring the concentration and velocity profiles once, locating the sample extraction nozzle at a representative location within the duct cross-section, and assuming that the concentration and velocity profiles remain constant. With the first method, Eq. 1 is approximated by:

$$F = \Sigma_i C_i V_i A_i \tag{2}$$

where the subscript i denotes each of the measured points and A_i is the portion of the duct cross-section represented by measurement i. With the second method, Eq. 1 is approximated by:

$$F = K C \overline{V} A \tag{3}$$

where:

C is the measured particulate concentration,

$\overline{V}$ is the average velocity across the duct cross-sectional area A, and

K is a proportionality constant relating the average duct concentration to the concentration at the sampling point.

The value of K is determined for any sampling point from initial concentration and velocity profile measurements.

The most commonly-used particulate monitoring technique for stacks at the present time (light transmission) does not require sample extraction, but simply measures the attenuation of a light beam shining through the duct. Measurements made by transmissometers are often called "integrated" measurements. The term "integrated" measurement, however, can be confusing since these measurements give simply the average concentration (actually optical density) of particles within the light beam. Use of this measurement as an estimate of the average concentration within the entire duct cross-section requires knowledge of the particle concentration profile, just as with extracted sampling. To estimate the flux of particles passing through the duct, one must also know the velocity profile within the duct, again just as with extracted sampling. The second method outlined above for locating the sampling nozzle of a "point" sampler must also be used for locating the path of a transmissometer light beam. If this procedure is used, Eq. 3 approximates the total particulate flux passing through the entire duct. Locating of the measuring beam of a transmissometer is just as important as locating the sampling point of a point extraction sampler.

The ideal situation would be to measure the total mass flux of particles passing through the entire cross-section of the stack. However, there is no way to do this in practice. The only practical methods of measuring the particulate flux are to 1) measure the average concentration across a diameter of the stack (so-called "integrated" measurement) or 2) measure the concentration at a point within the stack (so-called "point" measurement). In addition to the concentration measurement, both methods require additional knowledge of the velocity and concentration profiles within the cross-section of the stack at the measuring location. Thus, neither method has an obvious advantage from this standpoint.

The advantage that an optical transmissometer measurement does have over a point measurement is that the transmissometer does not require sample extraction. As will be explained in the section on "Light Transmission", however, transmissometers do not sense the mass of particles, a severe handicap if mass is the parameter of interest.

The transmissometer can measure the average particle concentration across a stack diameter. However, the object in stack monitoring is not to measure the average particle concentration across a stack diameter, but to measure the flux of particles across a stack cross-section. Both "integrated" and "point" concentration measurements require similar information about velocity and concentration profiles to relate the actual measurements to the desired particle flux. Thus, it is not clear at this time whether one or the other offers significant advantages for measurement of particle flux. The question may be academic for this study because all mass sensing instruments require extracted, point samples.

EXTRACTIVE SAMPLING

The aim of this discussion is to develop guidelines for good probe design and to apply these guidelines as specifically as possible to the most typical stack sampling situations. The guidelines are based on the parameters of the flue gas and particulate matter that were discussed above, since it is these parameters which affect the removal and transport of the particles in the flue gas. The removal of the sample from the gas stream will be considered first (i.e., the nozzle). Following this the transport of the particles out of the stack (i.e., the tube) will be discussed.

It is commonly stated that in order for an extracted aerosol sample to represent what is actually in the flue gas stream, the gas must be withdrawn isokinetically. In other words, the velocity of the gas inside the sampling nozzle must be equal to the velocity of the gas outside the nozzle. Unfortunately, this is a practical impossibility in stack sampling because of the random fluctuations of the bulk velocity of the flue gas. In addition, turbulent eddies cause the local velocity to change, not only in magnitude, but in direction as well. Even if it were possible for the nozzle to follow the eddy fluctuations, the sample would not be representative because particles in the gas do not precisely follow the eddies. Thus, the term "isokinetic" becomes rather meaningless.

The problem of getting a good sample is now twofold: first, to get the "best" possible sample; and second, to find out how representative that sample is.

NOZZLE DESIGN

The nozzle diameter that is chosen for a particular situation depends on several variables. If the probe is sampling for an instrument that requires a certain volumetric flow rate, the nozzle size is defined by the required flow rate and the flue gas velocity. Such is the case with most particle sensors. For ordinary filter sampling, the flow rate through the filter may not be nearly as critical. In such cases the nozzle diameter can be more arbitrary, and may be limited only by the capacity of the suction pump.

The probe nozzle diameter should always be made as large as the other constraints permit, within reasonable limitation. Badzioch[829] has shown that the effect of increasing the nozzle diameter is a decrease in the disturbance of the free gas stream. The result of this is a more representative sample. The magnitude of the improvement in changing from one nozzle to another cannot be determined without additional data on the turbulence characteristics in flue gas streams.

Whiteley and Reed[868] have studied various nozzle shapes. A sketch of each nozzle they tested is shown in Figure 1. The results of some data taken in a wind tunnel under controlled conditions showed that, for both fine and coarse dust, nozzle 1 gave the most accurate results. Neither the length of the nozzle nor the chamfer angle seemed to cause any error, so for their particulate situation nozzles 2, 3, 4, and 5 were nearly as accurate. Probe 7 gave slightly higher errors, while probe 6 was very much in error. Lundgren and Calvert[508] have also experimented with side port probes. Their results show that only limited accuracy (approximately 20% error for 5 μm particles) can be achieved with such probes.

It is felt that the nozzle should be kept fairly long (at least two diameters) so that particles enter the nozzle parallel to its axis. This will reduce losses by inertial deposition within the nozzle and by the nonrepresentative entrance of the particles into the nozzle. In addition, small chamfer angles (approximately 12° - 15°) are desirable because they limit the accumulation of dust.

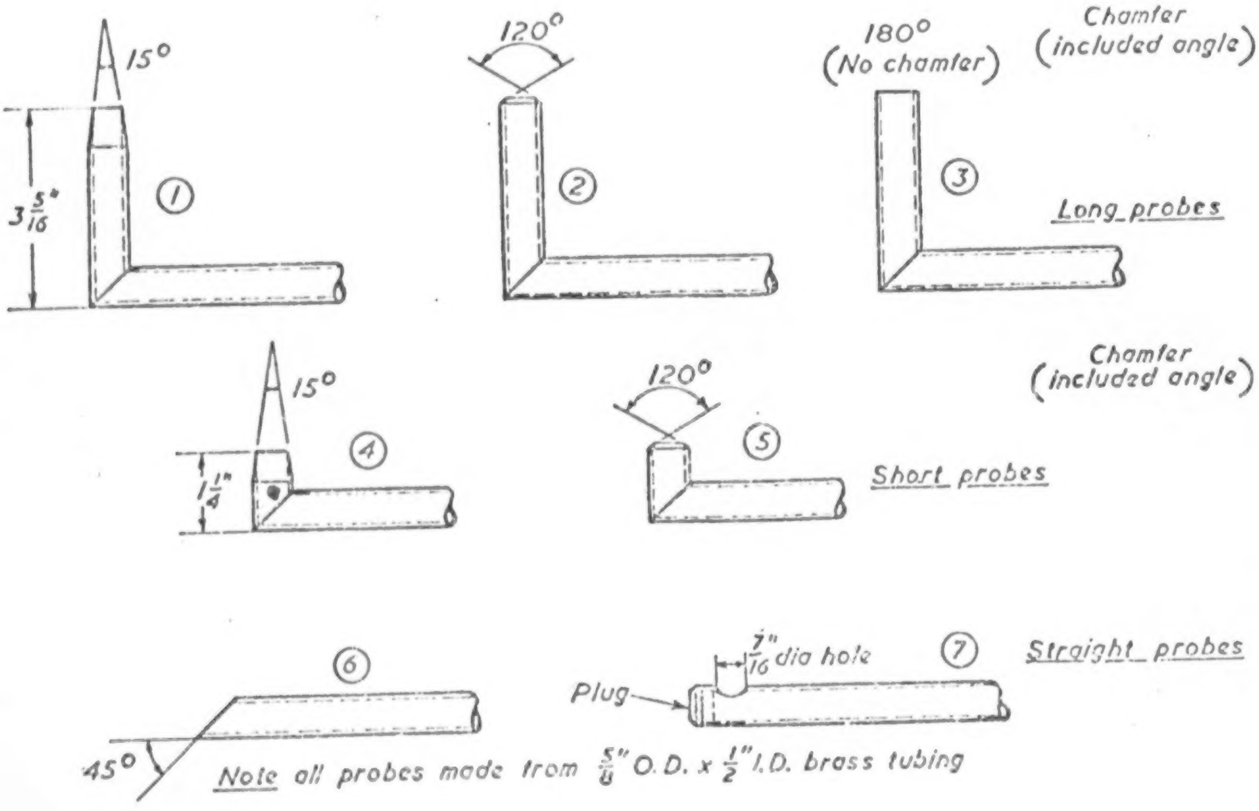
15°
3 5/16"
①
120°
②
180°
(No chamfer)
③
Chamfer
(included angle)
Long probes
15°
1 1/4"
④
120°
⑤
Chamfer
(included angle)
Short probes
⑥
7/16" dia hole
⑦
Straight probes
Plug
45°
Note all probes made from 5/8" O.D. x 1/2" I.D. brass tubing

Fig. 1. Various configurations of sampling nozzles tested with coal-combustion particles.[868]

Although the turbulence in flue gas streams does not permit truly isokinetic sampling, it is important that the velocity of the gas in the probe nozzle be kept as close as possible to the mean velocity of the flue gas. The flue gas velocity need not be monitored continuously, but it should be checked frequently to avoid errors due to low-frequency fluctuations. Several methods can be used for this.

Perhaps the most convenient means of keeping the velocity adjusted properly is the use of "zero-pressure" or "null-balance" probes.[257,955] These are probe nozzles that are constructed such that the static pressures of the main and sampled streams can be monitored (Figure 2). They are usually operated such that the pressures are equalized and it is assumed that under these conditions the two velocities must be equal also. Unfortunately, these conditions do not in fact assure that the velocities are equal. Dennis et al[955] have shown that errors in the order of 5% should be expected due to the interference caused by the tip of the nozzle, and that this accuracy is possible only after a calibration. If such a probe is used in flue gas, the accumulation of particles on the nozzle over a period of time will no doubt change the calibration. Furthermore, the turbulence in flue gas ducts, which is characterized by changes in the direction of the gas velocity, would certainly make the error significantly greater because the static pressure measurements are directionally sensitive. Such nozzles are therefore not acceptable for use in stack gas.

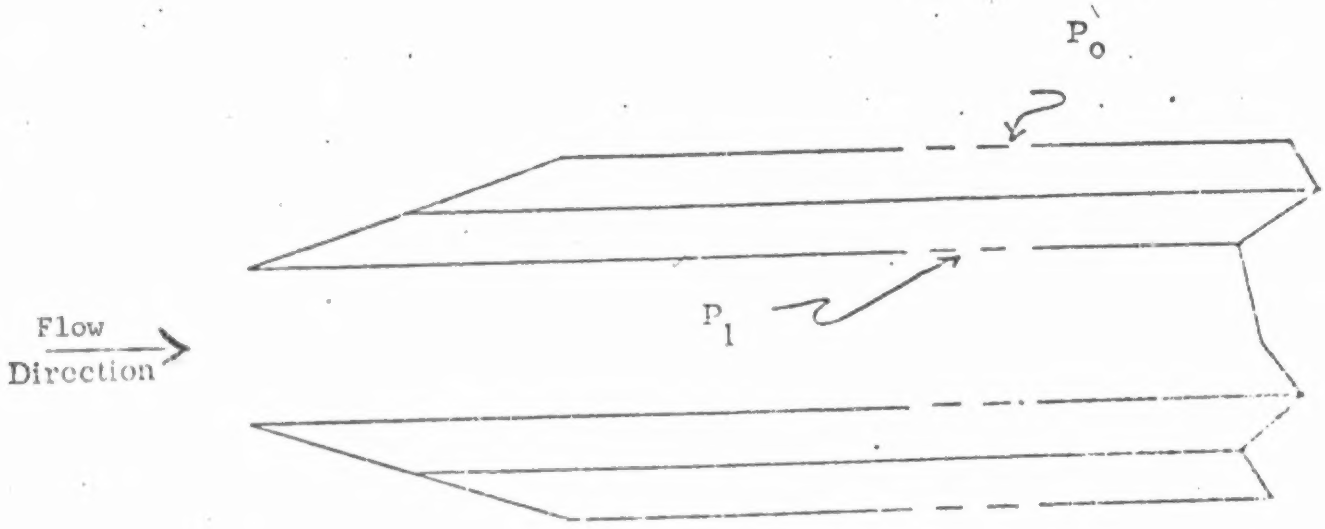

Fig. 2. Schematic diagram of a "null-balance" sampling nozzle.

Groutsch[1060] has built a zero-pressure device that has two nozzles. One of the nozzles is the sampling nozzle. The other is a short section of pipe which is open at both ends. It has a venturi throat which is designed such that the differential pressure between the venturi throat and ambient is equal to the differential pressure between the interior of the sampling nozzle and ambient when the sampling flow rate is isokinetic. Unfortunately, this technique is not feasible for stack monitoring becuase it would have the same directional sensitivity and particle accumulation problems as conventional "null-balance" probes.

Boothroyd[256] has satisfactorily used a hot-wire anemometer to monitor the flue gas velocity. This technique involved placing the hot-wire sensor in the flue gas stream and noting the voltage. Then the probe nozzle was quickly placed just downstream from the sensor and the aspiration rate was adjusted so that the voltage on the hot-wire sensor equalled the previously measured voltage. The velocity-voltage relationship of the hot-wire anemomter does not remain constant for a long period of time because of contamination by particles in the gas. Therefore, measurements cannot be made for longer than a few minutes. Furthermore, the fact that the probe must be removed and then replaced for every measurement makes this technique undesirable for continuous stack gas monitoring.

Another interesting technique has been tested by Grindell[122]. A sketch of the apparatus is shown in Figure 3. It operates on the principle that the exit

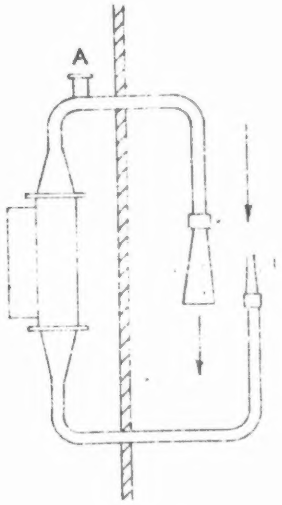

Fig. 3. Schematic diagram of an aspirating probe using a suction cone to replace the vacuum pump.[122]

cone will produce enough suction to overcome frictional pressure losses in the system and small pressure drops in the sensing instrument. The suction is created by the flow of the flue gas around the cone, which is designed such that the nozzle samples essentially isokinetically. The results reported from tests in a wind tunnel showed that the instrument did indeed sample nearly isokinetically. However, it did not operate as well in a stack, probably because of the increased level of turbulence. These tests were not conclusive, and therefore this technique should be investigated further. If it works, it would eliminate the need for an aspirating pump. This is a major advantage because most pumps do not last long in flue gas. In addition, such a probe would respond automatically to changes in the flue gas velocity, eliminating the need for elaborate pressure sensors or flow controllers.

The use of a pitot tube which is separate from the sampling probe is the most reliable technique for monitoring the flue gas velocity. These have been covered in detail by Falgout.[123] In particular, "S" type pitot tubes offer the best combination of sensitivity and reliability (Figure 4). The chief advantage gained by the use of such devices is that they are nearly omnidirectional for small (i.e., less than 10°) angular velocity deviations. They are also less sensitive to contamination by particles because they have much larger sensing areas than, for instance, "null-balance" probes. If it is important to measure small changes in velocity, "S" type pitot tubes offer a gain in sensitivity because they measure the difference between the stagnation pressure and the suction pressure. Pitot-static probes, on the other hand, measure the difference between the stagnation pressure and the static pressure. Since the difference between stagnation pressure and suction pressure always changes more for a given velocity change, "S" type pitot tubes are more sensitive. Unfortunately they require calibration before use, but because of their sensitivity and reliability they should be used when monitoring stack gas velocities over extended periods of time.

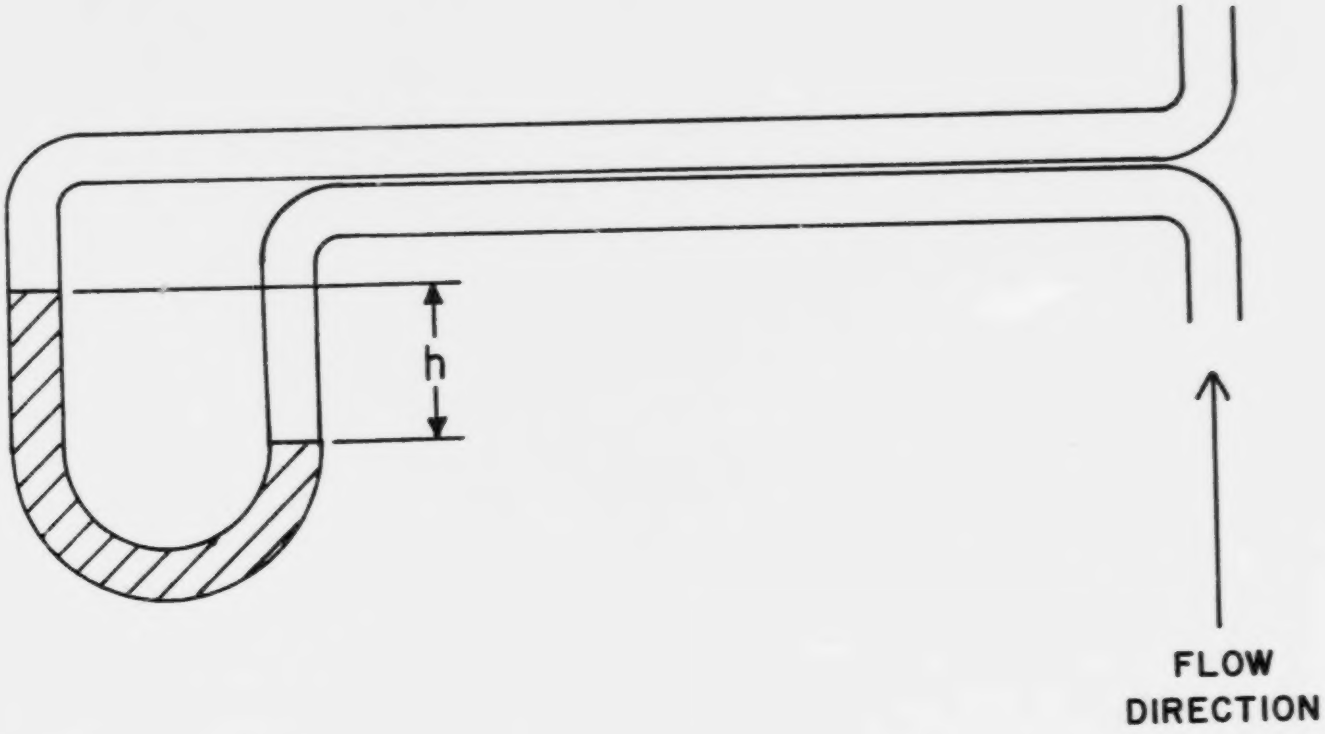

Fig. 4. Schematic diagram of an "S" type pitot tube.

The particle losses caused by anisokinetic sampling flow rates have been studied by several investigators.[719,829,1130,1229] Since the selection of the nozzle inlet diameter is beyond the scope of this discussion (it is based on the choice of the particle sensing instrument), a diameter of 3 cm will be assumed. This size is typical of the majority of sampling probes of interest. Badzioch[719] has calculated the errors from anisokinetic sampling of fly ash with characteristics which are fairly representative. Given the above nozzle size, one finds that the error in the particulate mass concentration measurement is roughly 60% of the error in the velocity measurement. Since average velocity measurements in stacks are only accurate to within ± 5% at best, an error of at least ± 3% has to be expected in the concentration measurement. In addition, although little is known about flow conditions in stacks, a great deal of turbulence is expected. This has not been taken into account in the error estimates. Therefore, a more realistic estimate of the error caused by anisokinetic sampling and losses in the nozzle would be 5 - 10%.

SAMPLING TUBE DESIGN

The design of the sampling tube and the estimation of the errors due to particle deposition are considerably more complicated. The tube characteristics, flow characteristics, and particle characteristics are all important. Particles can be lost by inertial impaction (this normally occurs around bends in the tube), electrical charge effects, thermophoresis, gravitational settling, Brownian diffusion, and turbulent eddy diffusion. The loss of particles by electrical charge effects and thermophoresis is assumed to be negligible for purposes of this discussion, assuming metal tubes are used that are at the same temperature as the particles. The other effects are all significant in most situations.

Gravitational settling provides the smallest contribution to particle losses because of the particle sizes and flow ranges involved. Most of the mass of particles in flue gas is contained in particles smaller than 25 μm. For typical flue gas particles in a horizontal tube with a length of 3 m, a diameter of 2 cm, and an average velocity of 9 m/sec, only about 6% of the mass of the particles will be lost by gravitational settling. The error due to gravitational settling is proportional to

$$E_s \propto LD_p^2/UD,$$

where

L = tube length,

D_p = particle diameter,

U = average gas velocity in the tube,

D = tube diameter, and

E_s = error due to gravitational settling.

For a given particle size, volumetric flow rate, and tube length, the error varies directly as the tube diameter; i.e.,

$$E_s \propto L D_p^2 D/Q,$$

where

Q = volumetric flow rate.

Inertial impaction causes severe particle losses if the flow has to change direction or if the fluid rotates about the axis of the tube. The deposition of particles in curved sampling lines has been studied by Sehmel and Schwendiman (Ref. 801, p. 88). These tests show that for both laminar and turbulent flow, deposition increases with fluid velocity, decreases with probe diameter, and is highly dependent on particle accommodation to the probe surface. Re-entrainment of the particles depends on the stickiness of the particles and the smoothness and stickiness of the tube wall. These effects are very difficult to assess because little data is available on them and that which is available does not apply to the particles in flue gas. It is a reasonable assumption that particle re-entrainment will be significant for the larger particles in flue gas (typically >15μm), which may make up as much as half the total particulate mass. Therefore, any error estimate that ignores re-entrainment may istelf be in error by as much as 50%. By making the probe diameter as large as possible, thereby decreasing the fluid velocity, it is felt that the sampling error due to inertial impaction around bends can be reduced to about 10%.

The impaction of particles by fluid rotation is usually not serious. For example, in a 3 cm diameter tube with the gas rotating at one revolution per second and moving with a mean velocity of 6 m/sec, the velocity of deposition of particles due to centrifugal action is nearly an order of magnitude less than the gravitational settling velocity. Guide vanes would eliminate this error altogether, and should be used if they can be conveniently installed.

The deposition of particles in tubes by Brownian and turbulent eddy diffusion has received a good deal of attention[133,134,774,801,1173,1175] The error caused by eddy diffusion can be affected greatly by the re-entrainment of particles once they deposit on the wall. Thus, there is a strong dependence on tube wall and particle surface properties. Both brownian diffusion and eddy diffusion are very dependent on particle size. Brownian diffusion is important only for particles smaller than about 1 - 3 μm, whereas eddy diffusion is important only for particles larger than this size.

The deposition of particles by eddy and Brownian diffusion is usually described by a deposition velocity. This can be thought of as the average velocity of particles toward the wall of the tube. It is equal to the mass (or number) of particles deposited per unit area per second per unit particle concentration in the air over the surface, and has the dimensions length per unit time.

Davies[133,134] has derived expressions that can be used to calculate the deposition of particles due to the combined effects of Brownian and eddy diffusion. These equations predict a strong dependence on particle size with somewhat less dependence on the friction velocity, defined as the square root of the ratio of the local shear stress to the fluid density. The friction velocity affects only eddy diffusion and is a measure of the turbulence intensity. As the friction velocity increases, the deposition due to eddy diffusion increases. Wells and Chamberlain[1175] have compared this theory with some experimental data (Figure 5). While this does not show clearly the dependence on the friction velocity (denoted by u_*), the dependence on particle size is made quite clear. A minimum deposition velocity is seen to occur at a particle size of about 1 - 4 µm. A similar behavior should be expected in sampling lines containing flue gas. The particles sizes and tube diameter used by Wells and Chamberlain[1175] are fairly representative of sampling lines. These tests also revealed a strong dependence on the surface roughness of the tube wall. The roughness may be on a very small scale such that it does not affect the turbulence level of the airflow. In fact, it was found that the deposition velocity could be increased by more than an order of magnitude by simply lining the tube with a fibrous filter material. It appears that if particles begin to accumulate on the surface of a "smooth" tube, the deposition characteristics of the tube may change over a period of time. This is quite serious if one is trying to correct for losses in the sampling tube during a long test or a continuous monitoring operation, since the correction would be a function of time. No theory has been suggested that takes into account the minute roughness characteristics of the walls of the tube.

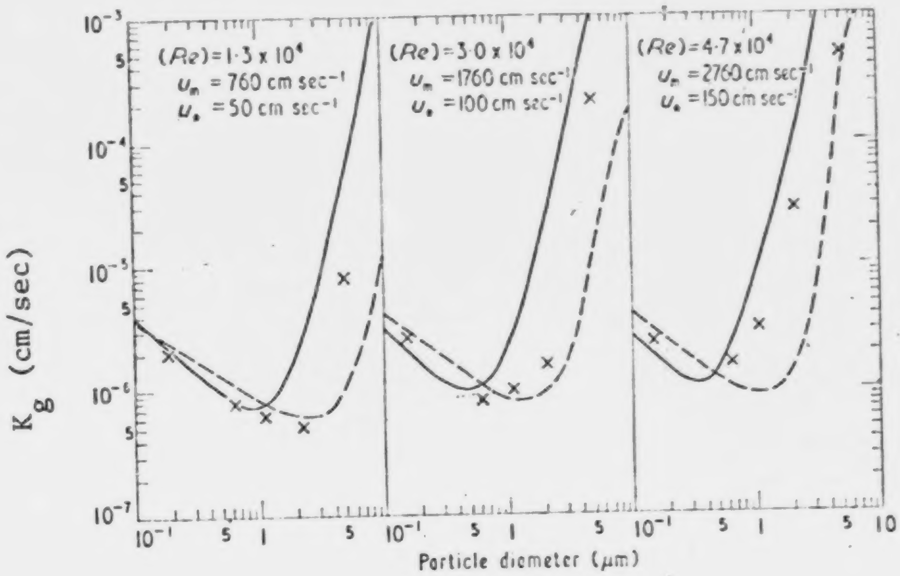

Fig. 5. Deposition velocity as a function of particle size showing the particle-size dependence of Brownian and turbulent eddy diffusion.[1175]

Brownian diffusion will cause significant particle deposition only for particles less than about 0.1 μm. Thus, the importance of Brownian diffusion depends on the particle sizes found in flue gas. The majority of emissions data leads to the conclusion that most of the particulate mass from coal-fired sources is contained in particles larger than 0.1 μm, and hence to the conclusion that Brownian diffusion makes only a small contribution to the loss of particle mass.

On the other hand, turbulent eddy diffusion becomes significant for particles larger than about 3 μm under typical sampling conditions. Since it causes the particle deposition velocity to increase rapidly with particle size (it appears to vary with something between $D_p^2 - D_p^3$), its effect is important.

The prediction of particle losses is greatly complicated by the re-entrainment of particles once they have come in contact with the wall of the tube. This phenomena has been observed by Sehmel[774], who measured radial concentration profiles in a tube for various degrees of wall stickiness and particle sizes. As shown in Figure 6, for 12 μm particles the concentration was a minimum near the tube wall

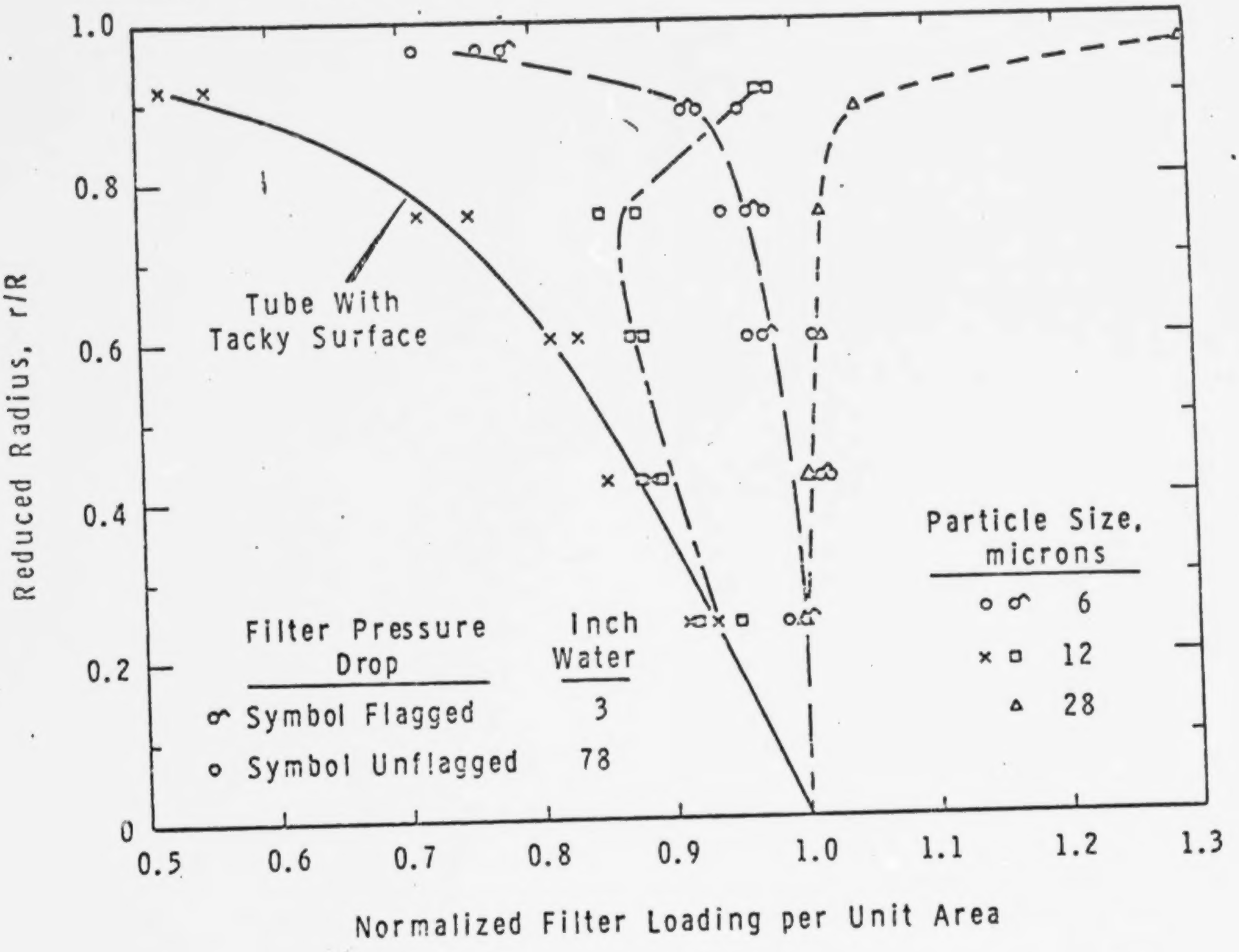

Fig. 6. Particle concentration as a function of tube radius for smooth and tacky tube surface.[774]

when the surface was coated with a sticky substance, whereas it increased close to the wall when the surface was smooth. Also, for 28 μm particles, the concentration was 30% greater near the wall than at the tube center for a smooth tube. Such concentration profiles can only be explained by the proposition that the particles tend to stick well to the coated tube wall while many are re-entrained into the gas stream from a smooth wall.

The re-entrainment of particles from tube surfaces does not lend itself to theoretical treatment. Sehmel and Schwendiman[801](p. 106) have performed experiments with a variety of particle sizes, tube sizes, and air velocities. From these studies of radial concentration profiles and deposition velocities along the length of the deposition surface, it appears that some of the particles that contact the wall do not remain attached to it. They may either bounce off because of their momentum or be swept away by the turbulent eddies that penetrate the laminar sublayer. Since the momentum of particles is proportional to D_p^3 and the adhesive force is probably proportional to D_p, the probability that a particle will bounce is nearly directly related to the square of its diameter. It also depends on the turbulence intensity, for this determines the particle velocity and hence its momentum. However, since the fluid drag force is proportional to D_p^2, the probability of a particle being re-entrained after it is attached to the wall is probably less dependent on particle size than the probability that it will become attached to the wall in the first place. Once the particle is re-entrained, it seems to remain quite close to the surface, as evidenced by the concentration profiles observed. This may be due to the acquisition of a charge by the particles from the tube wall. If all the particles pick up a like charge, the resulting space charge should force the particles outward toward the wall.

Particle re-entrainment is a phenomenon that is difficult to predict even under ideal conditions, let alone in a sampling probe aspirating flue gas. The available data attests to this, as it shows considerable scatter. Figure 7 shows the relationship of the particle diameter to the deposition velocity for mean gas velocities of approximately 2 and 12 m/sec. The significantly lower deposition velocity for the lower Reynolds number verifies the dependence on the turbulence intensity. The initial positive slope of the curves is caused by the rapid increase in deposition with particle size in a regime where re-entrainment is not allowed to take place. Eventually, a size is reached where the particles possess enough momentum to bounce off the walls of the tube, and further increase of the particle size causes a reduction in the net deposition velocity. Figure 8[111] shows more clearly the dependence of re-entrainment on particle size. Notice that the deposition velocity may vary over several orders of magnitude.

For a given volumetric flow rate of air, the turbulent deposition velocity always decreases with increasing tube diameter. This is because the Reynolds number varies inversely as the tube diameter, and turbulent deposition is a strong function of the Reynolds number. Therefore, the tube diameter should be increased as much as possible to minimize turbulent deposition. However, it was shown that the sedimentation deposition rate was directly related to the tube diameter. This places an upper limit on the tube size, which must be chosen such that the total deposition is a minimum.

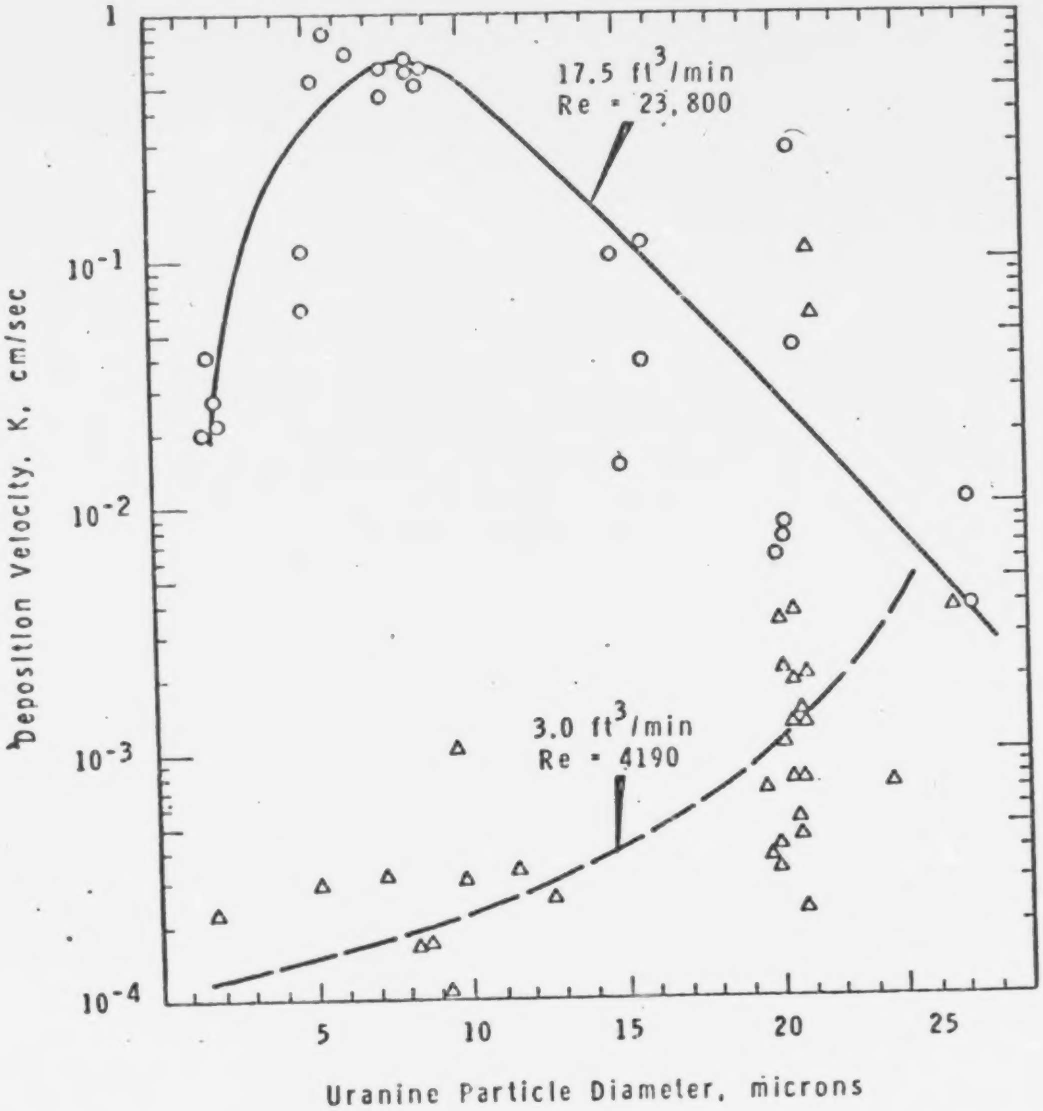

Fig. 7. Deposition velocity versus particle diameter showing the effect of re-entrainment.801

As an example, assume a sampling nozzle with 2 cm diameter is used to aspirate the flue gas, and that the mean gas velocity in the duct is 20 m/sec. This fixes the volumetric flow rate through the tube. If the tube diameter is 2 cm (which is typical of aspirating probes), the mean velocity in the tube is also 20 m/sec, corresponding to a Reynolds number of about 13,000. Taking the particle size to be around 10 μm (which is the particle size above which re-entrainment will occur at this Reynolds number, as seen in Figure 8), one can estimate the deposition velocity to be 0.2 cm/sec. Then, for a tube length of 3 m, one can calculate the diffusion loss by the following equation:

$$\ln \frac{C}{C_o} = -4 \left(\frac{V}{U_m}\right) \left(\frac{L}{D}\right),$$

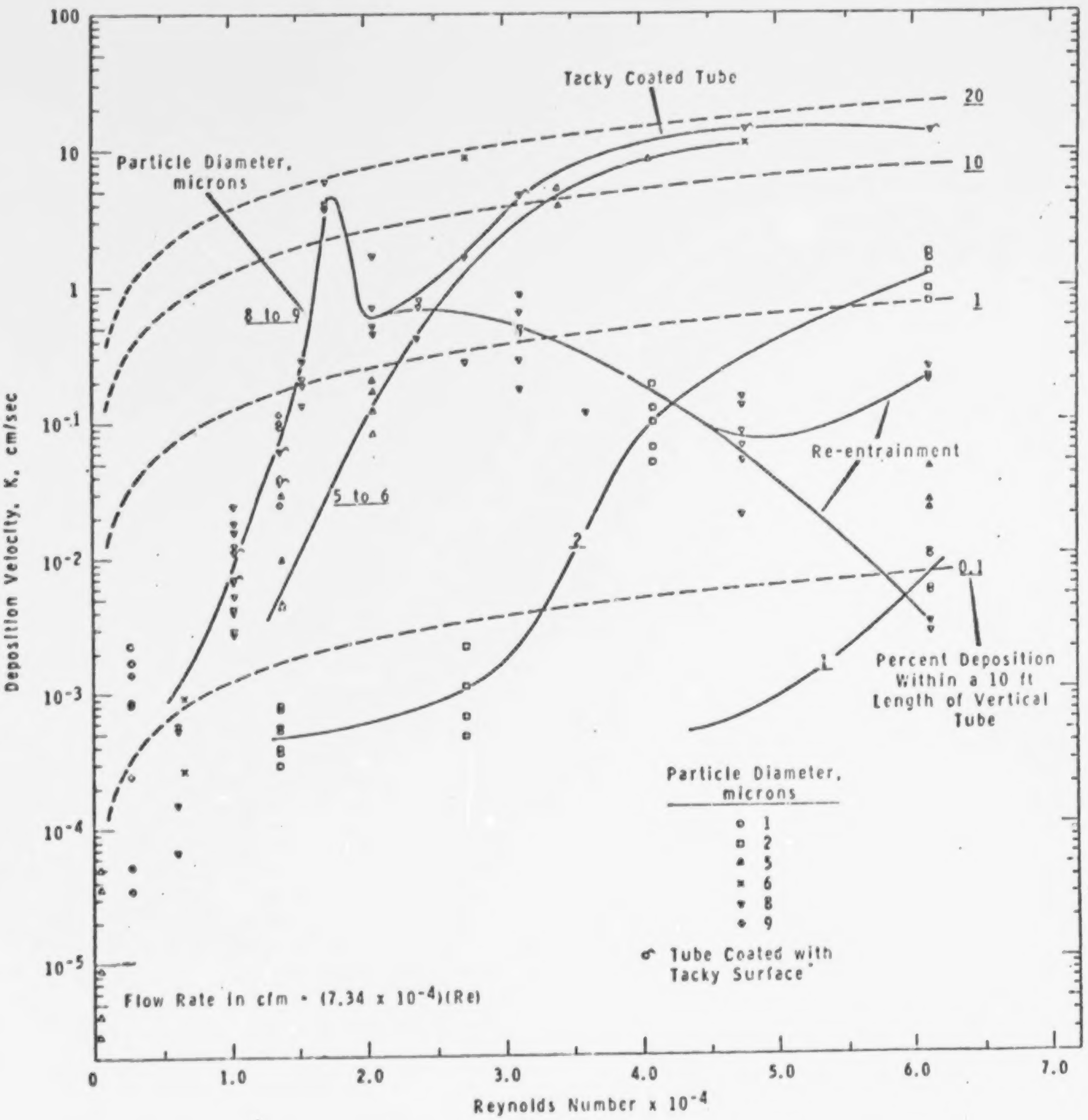

Fig. 8. Deposition velocity as a function of Reynolds number and particle size.[1111]

where:

C = the particle concentration at the tube exit, gm/m^3,

C_o = the particle concentration at the tube entrance, gm/m^3,

V = turbulent deposition velocity, cm/sec,

U_m = mean gas velocity in the tube, cm/sec,

L = tube length, cm, and

D = tube diameter, cm.

With the numbers given above, the concentration ratio, C/C is 0.94, so the error is 6%. The error due to gravitational settling was calculated previously for these conditions and found to be about 6%. Thus, under these sampling conditions, 2 cm is probably the optimum probe diameter. A significant reduction in size would increase the inertial losses around bends, and an increase in size would make sedimentation losses too great.

It is quite apparent by now that the losses in sampling probes, including the tube and the nozzle, will have to be taken into account in the interpretation of any data. By simply adding the contribution made by the various loss mechanism, one finds that the expected error lies somewhere around 30%. This error will almost always be negative because particles are always lost, not gained, with the exception that a low aspiration flow rate may increase the concentration of large particles somewhat. Thus, if the various parameters were somehow known the measurement error could be greatly reduced, probably as low as ± 15%.

As stated earlier, particle losses caused by thermophoresis effects have not been determined because no reliable evidence has shown it to be significant. Electrical charge effects may be a major factor since the sampling probe is usually downstream of an electrostatic precipitator. However, almost no information exists regarding the electrostatic charge level on the particles. Several investigators have reported losses apparently caused by electrical effects.

Since particle deposition on sampling tube walls has been a serious problem in so many aerosol measurements, a probe has been invented that is designed to eliminate it. This is known as the boundary layer diluter probe.[1156] Although a number of variations exist, they all operate on essentially the same principle (see Figure 9). A boundary layer of clean air is introduced, either at the entrance to the tube or all the way along the tube, which serves to keep the particle-laden air away from the wall. The particles must therefore get through this layer of clean air to be deposited. Their outward radial motion is opposed by the inward motion of the clean air if the diluter has a porous wall. The boundary layer should be kept laminar as much as possible because any turbulent mixing nullifies part of the advantage of the clean air.

There are two problems with boundary layer dilution. The first is that normally the Reynolds number in the sampling tube is too high for a laminar boundary layer to exist. Thus, some turbulent mixing of the boundary layer will occur in the tube, though the deposition of particles will be somewhat decreased.

The second problem arises because the flue gas must eventually be mixed with the clean air, since many sensors require a homogeneous mixture of the aerosol to give an accurate reading of the concentration. A significant percentage of particles may be lost, not only in the turbulent mixing process itself, but also downstream of the mixing, where there is no boundary layer of clean air. Some good data evaluating the effectiveness of these probes would be useful, however.

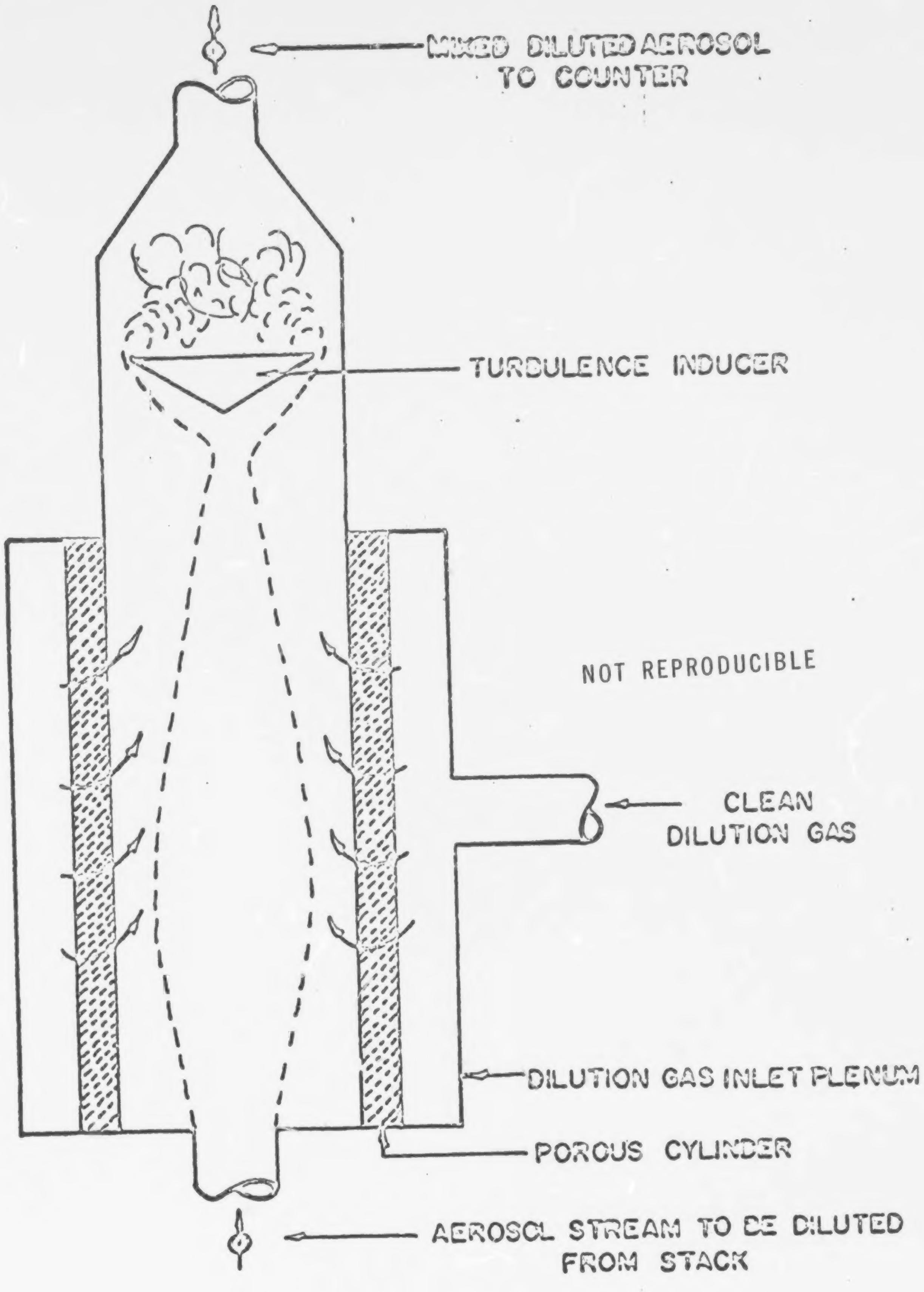
MIXED DILUTED AEROSOL TO COUNTER
TURBULENCE INDUCER
CLEAN DILUTION GAS
DILUTION GAS INLET PLENUM
POROUS CYLINDER
AEROSOL STREAM TO BE DILUTED FROM STACK

NOT REPRODUCIBLE

Fig. 9. Schematic of a tube with boundary layer dilution.

Boundary layer dilution does offer the advantage that the flue gas is cooled without condensation of the water vapor and acid. This may be important in some cases where a sensing instrument cannot be made to operate at elevated temperatures or where the conditions of the flue gas in cooled, diluted form is of interest.

The flow rate capability of the particle-sensing instrument always has to be considered when the sampling probe is designed. Instruments are available that can handle from as little as one liter per minute to as much as several hundred liters per minute. If an instrument can aspirate 300 liters/min or more, a sampling nozzle can be made that will get a fairly representative sample under most conditions. If the flow rate is less than this, or if the sample is diluted, an arrangement such as that shown in Figure 10 should be used. This makes it possible to remove a relatively large amount of flue gas from the stack. Then, once the velocity is reduced by increasing the tube size and the turbulence is somewhat damped out, a smaller sampling probe can be used to aspirate the proper quantity of gas for the particular instrument being used. It is felt that such a configuration will provide a much better sample than a small sampling probe mounted directly in the stack.

This design would not allow the use of a boundary layer diluter in the large tube unless the stream was mixed thoroughly before it got to the small sampling probe. However, the creation of turbulence would defeat the purpose of the system, which is to damp out the turbulence so that a small probe can be effective. Thus, boundary layer diluter probes appear to be of little use in this portion of the sampling system, although they may be useful in the downstream portion just ahead of the particle sensor.

Any continuously operating sampling probe should be heated (unless there is boundary layer dilution) to avoid condensation of the water vapor and acid. Heating should begin as soon as the gas gets outside the duct, and the temperature should be maintained at a temperature above the dew point of the condensable vapors.

SUMMARY

The continuous removal of a representative sample of flue gas from a duct and the transporting of the sample to a particle-sensing instrument involve a great deal of engineering design problems as well as basic scientific problems. The engineering designer faces such problems as the unknown (and perhaps unmeasureable) turbulent flow conditions in the duct, the impaction of particles on the wall of the tube,and the condensation of acid vapors. The scientific aspects include the ability of a particle to stick to a wall and the probability that, once stuck, it will be re-entrained. Agglomeration and fragmentation of particles may also be a cause for concern with particle sizing instruments.

The available data indicates overwhelmingly that the calculation of the magnitude of particle losses in a sampling probe is subject to a variety of random phenomena. For stack particles, where most of the mass is contained by particles smaller than 25 μm, the error has been estimated. Around 5 - 10% error is expected in the removal of the sample from the main flue gas stream, due to the turbulence and to fluctuating mean velocity. As much as 10% will impact on the wall of the tube at bends, and Brownian and turbulent eddy diffusion will cause an additional error of about 6%. This amounts to a total particle loss of about 30%.

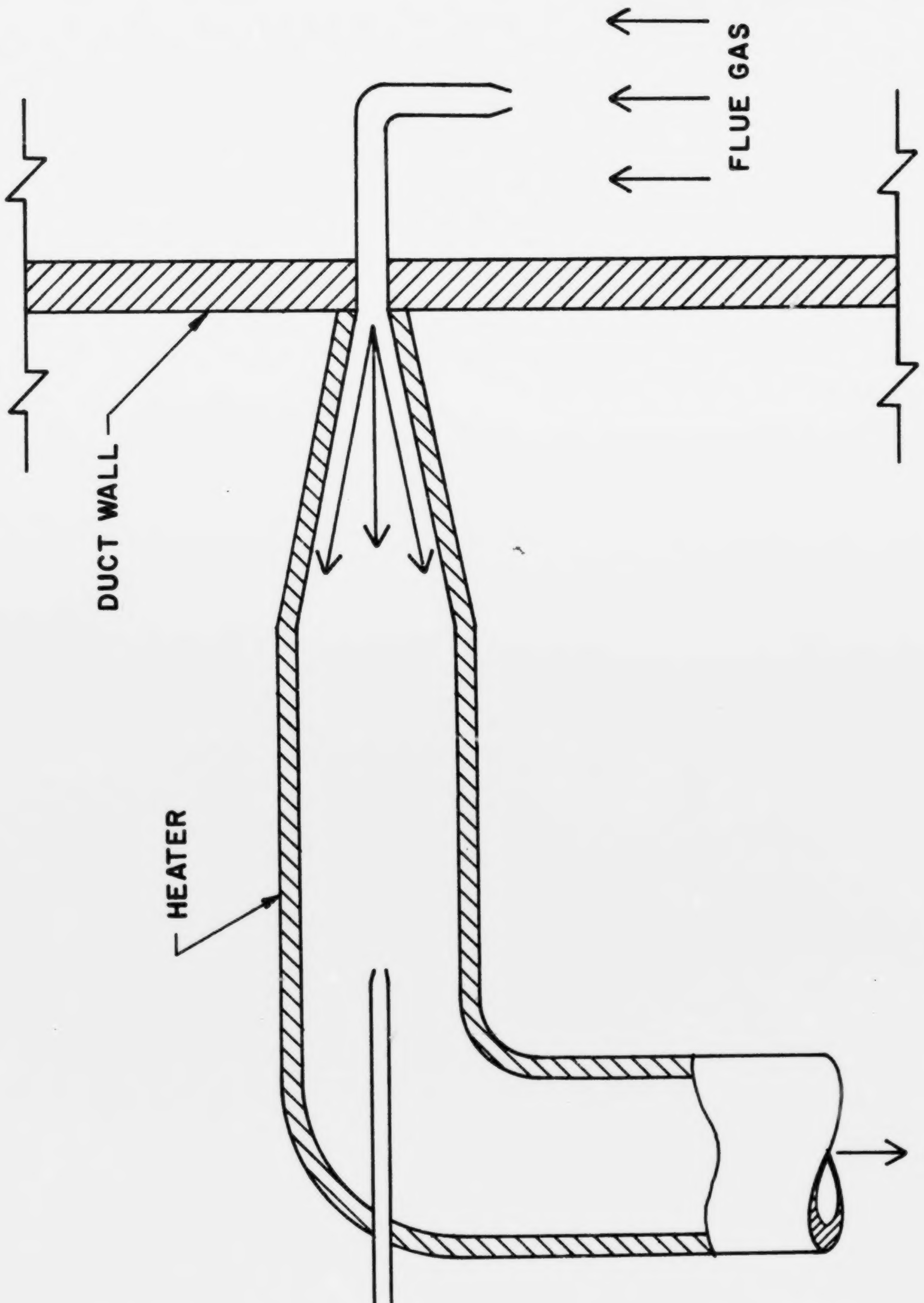
FLUE GAS
DUCT WALL
HEATER
Q_1
Q_2

Fig. 10. High-volume sampling system for instruments with low sample rate capabilities.

Boundary layer diluter probes are designed to reduce the particle losses in the sampling tube and to cool the flue gas without condensing the water and acid vapors. Unfortunately, these probes also have particle losses. More analysis of boundary layer dilution is necessary to completely evaluate the usefulness of the technique.

REFERENCES

719 Badzioch, S., "Correction for Anisokinetic Sampling of Gasborne Dust Particles", Journal Inst. of Fuel, V. 33, p. 106-118 (Mar 1960).

829 Badzioch, S., "Collection of Gas Borne Dust Particles by Means of Aspirated Sampling Nozzle", British Journal of Applied Physics, V. 10, p. 26-32 (Jan 1959).

256 Boothroyd, R. G., "An Anemometric Isokinetic Sampling Probe for Aerosols", Journal of Scientific Instruments, V. 44, no. 4, p. 249-253 (1967).

133 Davies, C. N., "Deposition of Aerosols from Turbulent Flow Through Pipes", Proc. Royal Society, V. A289, p. 235-246 (1966).

134 Davies, C. N., "Brownian Deposition of Aerosol Particles from Turbulent Flow Through Pipes", Proc. Royal Society, V. A290, p. 557-562 (1966).

955 Dennis, R., Samples, W. R., Anderson, D. M., and Silverman, L., "Isokinetic Sampling Probes", Industrial & Engineering Chemistry, V. 49, no. 2, p. 294-302 (Feb 1957).

1231 Falgout, D., Walter C. McCrone Associates, Inc., Chicago, Illinois, unpublished work (1969).

122 Grindell, D. H., "An Electrostatic Dust Monitor", IEE Proc., Series A (34), V. 107, p. 353 (1960).

1060 Groutsch, E. R., "Automatic Dust Sampler", Australasian Institute of Mining and Metallurgy Proc., No. 191, p. 165-189 (Sep 1959).

1130 Hemeon, W. C., and Haines, G. F., Jr., "The Magnitude of Errors in Stack Dust Sampling", Air Repair, V. 4, no. 3, p. 159-164 (1954).

508 Lundgren, D., and Calvert, S., "Aerosols Sampling with a Side Port Probe", American Industrial Hygiene Assoc. Journal, V. 28, no. 3, p. 208-215 (May-Jun 1967).

1156 Mitchell, C. A., and Silverman, L., "The Boundary Layer Diluter - a New Gas and Particulate Calibration Device", Paper presented to New England Section of the Air Pollution Control Association at Providence, Rhode Island (Apr 1963).

257 Narjes, L., "Dust Sampler Equipment for Quasi-Isokinetic Sampling by Means of Novel Zero-Pressure Probes", Chem. Age of India, V. 19, no. 8, p. 595-603 (Aug 1968).

774 Sehmel, G. A., "Validity of Air Samples as Affected by Anisokinetic Sampling and Deposition within the Sampling Line", Battelle Memorial Laboratory, Richland, Wash., Clearinghouse No. BNWL-SA-1045 (Apr 1967).

801 Sehmel, G. A., and Schwendiman, L. C., "The Effect of Sampling Probe Diameter on Sampling Accuracy", in: Pacific Northwest Laboratory Annual Report for 1967 to USAEC Division of Biology and Medicine - V. II: Physical Sciences - Pt. 3: Atmospheric Sciences, Battelle Memorial Inst., Richland, Wash., Clearinghouse No. BNWL-715, Pt. 3, p. 92-95 (Oct 1968).

1111 Sehmel, G. A., "Aerosols Deposition from Turbulent Air-Stream in Vertical Conduits", Battelle Memorial Inst., Richland, Wash., Clearinghouse No. BNWL-578 (Mar 1968).

1173 Sehmel, G. A., "Particle Deposition from Turbulent Air Flow", Journal of Geophysical Research, V. 75, no. 9, p. 1766-1781 (Mar 1970).

1229 Vitol, V., "Theoretical Limits of Errors Due to Anisokinetic Sampling of Particulate Matter", APCA Journal, p. 79-84 (Feb. 1966).

1175 Wells, A. C., and Chamberlain, A. C., "Transport of Small Particles to Vertical Surfaces", British Journal of Applied Physics, V. 18, p. 1793-1799 (1967).

868 Whiteley, A. B., and Reed, L. E., "The Effect of Probe Shape on the Accuracy of Sampling Flue Gases for Dust Content", Journal Inst. of Fuel, V. 32, p. 316-320 (Jul 1959).

BETA RADIATION ATTENUATION

by: John Borgos

INTRODUCTION

When any kind of radiation passes through a medium, its intensity is reduced. The reduction in intensity may be caused by absorption of the radiation by the matter, by absorption of a fraction of its energy by the matter, by its reflection or angular scattering, or by combinations of these phenomena. In the case of absorption of the radiation, the intensity reduction through a layer of matter is quite easily defined by the percent of radiation that gets through. The intensity reduction in the case where some of the energy is lost to the medium is not so easily defined because it is often a function of the energy of the radiation. Angular scattering and reflection are even more complicated because the scattering angle is usually a function of the geometry of the measuring apparatus. In general, absorption of radiation is called attenuation, while reflection and angular scattering are simply referred to as scattering.

Radioactive isotopes emit three types of radiation: alpha particles, beta rays and gamma rays. In general, alpha particles, which are really helium nuclei, are not very energetic; a piece of paper will stop most of them. The energy of a beta ray (which is a high-energy electron) depends on its radioactive source. Many sources emit relatively low energy beta rays (i.e., less than 1 MeV), while others emit beta rays of much higher energies. Likewise, gamma rays can have either high or low energies, depending on the particular source. A gamma ray is an electromagnetic wave with characteristics identical to those of X-rays of the same energy.

The need for instrumentation to accurately measure aerosol properties in both atmospheric and stack gases has led to investigation of the use of these three types of radiation for particle measurements. By passing the radiation through a sample of particulate matter collected on a suitable substrate, the properties of the particles can be evaluated by studying the scattering and attenuation of the radiation.

Since a measure of the particulate mass is of primary interest in most aerosol measurements, a type of radiation that is sensitive only to mass is desired. Alpha radiation is not energetic enough to be useful for this, since it will not penetrate any appreciable distance. The attenuation of gamma radiation, and particularly low energy gamma radiation, is strongly sensitive to the atomic number of the target material. High energy gamma radiation is not appreciably attenuated by thin layers of particles, and would therefore be too insensitive, as well as too dangerous. The attenuation of beta radiation depends only slightly upon the atomic number of the target material, while the scattering of beta radiation is nearly proportional to the atomic number.[1085]

Because of the limitations listed above, alpha and gamma radiation have not been used for monitoring particle mass concentration. Beta radiation, on the other hand, can be made to sense particle mass accurately if a given physical configuration is calibrated properly.

ATTENUATION AND SCATTERING OF BETA RADIATION

A radioactive isotope that emits beta radiation may emit gamma and/or alpha radiation also. The discussion considers only those isotopes that emit beta radiation alone and which decay to a stable element. Otherwise, the alpha or gamma radiation or the radiation from an unstable daughter product would lead to complications that are difficult to deal with. Beta particles emitted from the nuclei of such isotopes possess an energy spectrum of the same general form as that for K^{40} (see Figure 1). Each particular isotope has its own unique maximum energy (E_{max}), which is the maximum energy a beta particle may have if it is radiated from that isotope. The spectrum is continuous, and the mean energy is roughly one-third E_{max} for most known radioisotopes.

The attenuation of beta radiation involves the exchange of energy between the beta particles and the electrons in the target material. A beta particle is surrounded by its electric fields associated with the orbital electrons of the atoms in the matter. Sometimes the interaction results in the exchange of enough energy to release the orbital electron from the atom, a process called ionization. Usually the energy transferred is less than that required for ionization, however. The magnitude of energy transfer is a complicated function of the closeness of the collision and the energy of the beta particle. For the range of beta particle energies of interest, it can be said generally that as the energy possessed by the beta particle decreases, the energy exchange increases. The main reason for this is that as the beta particle energy decreases, its velocity decreases. Thus, the length of time for energy exchange with a particular orbital electron increases, and hence the total energy exchange increases. Lapp[1208] (p. 177) has dealt with this in more detail.

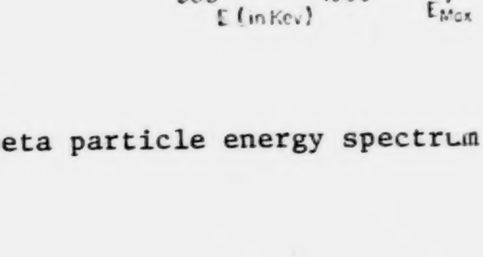

Fig. 1. Beta particle energy spectrum for K^{40}.

Because beta particles are nearly massless compared to atoms, they are deflected by nearly every collision and, therefore, follow extremely crooked paths in passing through matter. The angle of deflection for each collision is random, as is the energy exchanged, so that any estimate of the number of collisions a beta particle may have before being stopped must be found statistically. For this reason, an estimate of the range of a given particle in a given absorber is subject to statistical error. For example, one beta particle may be stopped after traveling 10 cm. through an absorber, while another with the same initial energy may be stopped after traveling only 5 cm. through the same absorber.

The ranges of individual beta particles from a given emitter through a given absorber is even more random because each of the particles has a different initial energy. For this reason, a theory has not been produced that explains all the phenomena observed. Rather, empirical formulas have been developed which predict the range of a particle of known energy in a given absorber. Figures 2 and 3 illustrate the range-energy relationship for beta particles of given energies in an aluminum absorber. For relatively high energy particles (i.e., greater than 1 MeV), the average range of beta particles is linearly proportional to the energy of the particles. For lower energies this is not true, the reason being that ionization losses become significant. It should be noted that the range is expressed in gm/cm^2 rather than number of collisions. This is possible because the energy loss of a beta particle passing through a layer of mass depends on the number of electrons per unit area in this layer. Since the number of electrons is related to the mass per unit area for a given absorber, the range can be expressed in terms of mass per unit area.

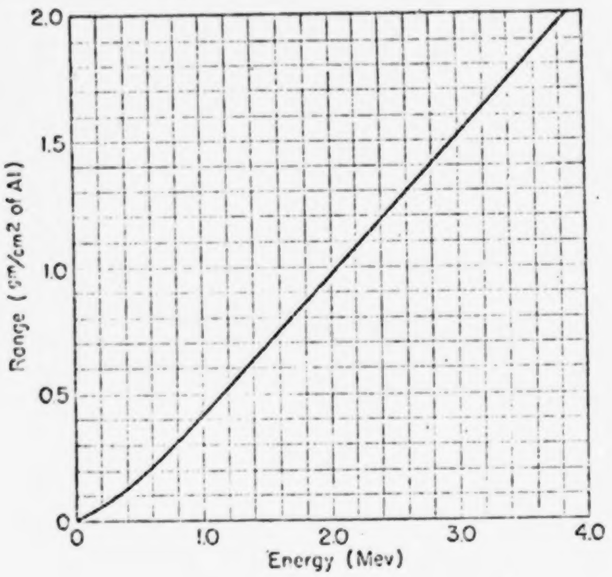

Fig. 2. Range of beta particle in aluminum

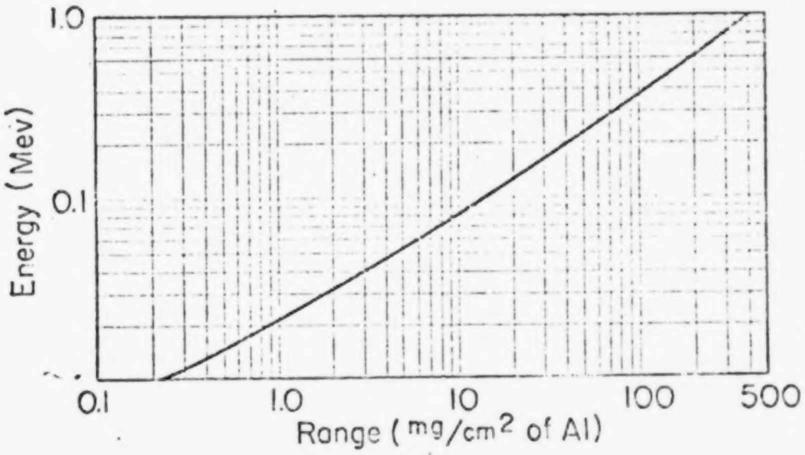

Fig. 3. Range of low-energy beta particles in aluminum

Strictly speaking, these curves are not applicable for any absorber material other than aluminum because there is some dependence on atomic number which can hopefully be neglected in practice with insignificant loss of accuracy. In addition, there is a dependence on the ratio of atomic number to atomic weight (which is between 0.4 and 0.5 for all elements other than hydrogen). This directly affects the conversion from electron density to mass density. Nader and Allen[555] have compared the absorption characteristics of aluminum and membrane tape, and found them to be significantly different as shown in Figure 4. On the other hand, Dresia, et al,[335] give data on a variety of absorbers which are in particle form,

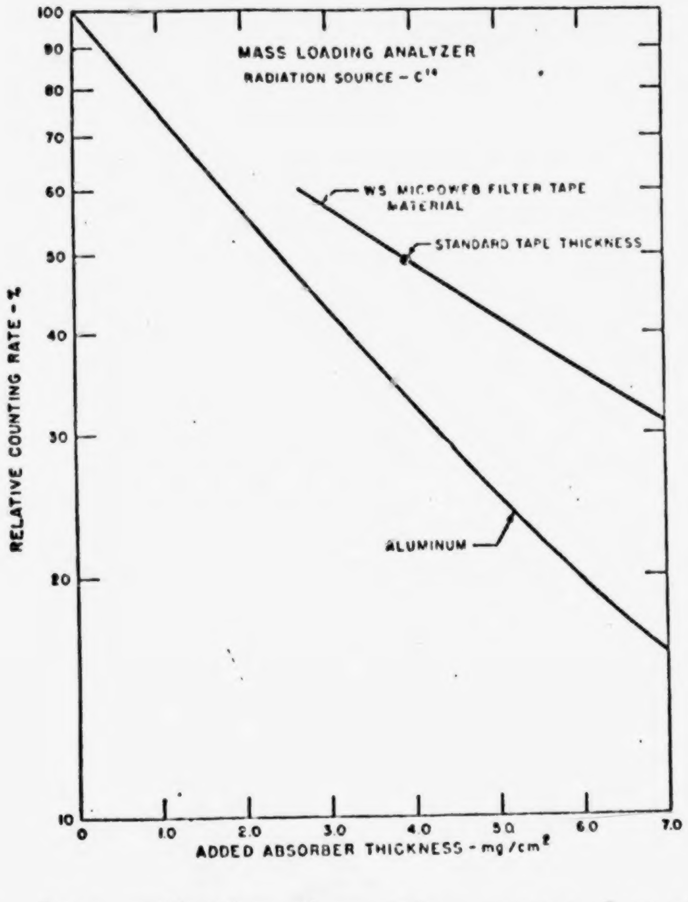

Fig. 4. Beta radiation absorption curves for microweb tape and aluminum.[555]

and the data indicates that these absorbers have very similar absorption characteristics as shown in Figure 5. The error on the data is given as ± 10%. Thus, it appears there is room for more conclusive data for comparison of the absorption characteristics of various materials.

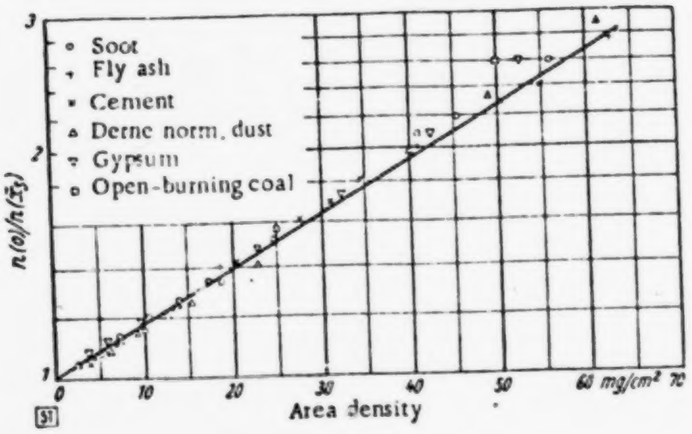

Fig. 5. Calibration curve of the Dresia beta dust meter for different dusts.[335]

One other uncertainty that needs to be considered in practice is the effect of the geometry of the measuring apparatus. Nader and Allen give information that seems to illustrate differences in absorption curves for several variations of the source-absorber distance, the source-detector distance, and the radiation source diameter (Figure 6). The reason for the variation in the curves is that for certain geometries more of the scattered radiation is detected than for other geometries.

The attenuation of beta radiation is used to give a measure of an absorber thickness in terms of mass per unit area (e.g., mg/cm^2) in the following way. A radiation source and a detector are placed opposite each other such that beta particles are emitted from the source in the direction of the detector. After observing the detected count rate (I_o) of beta particles with no absorber present, the absorber material is placed between the source and detector. A new count rate, I, is then detected and recorded. To measure particulate mass, the particles are deposited on a suitable substrate, such as a membrane or fiber filter. The attenuation of the count rate caused by the mass of particles on the substrate, together with the deposition area and air volume from which the particles were extracted, gives a measure of particle mass concentration.

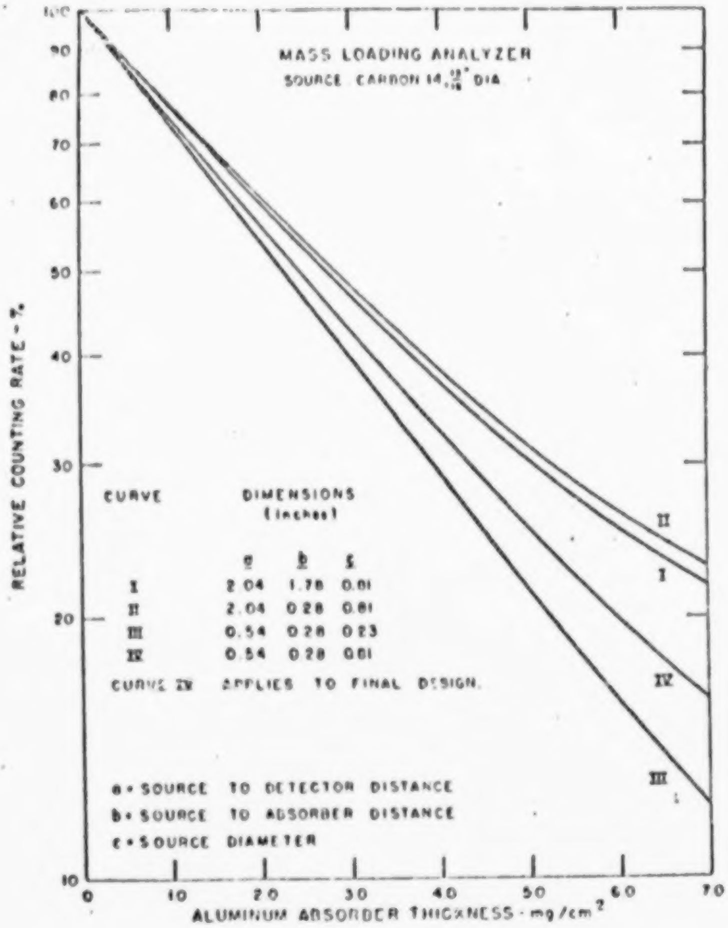

Fig. 6. Relationship of source-detector and source-absorber distance to beta radiation absorption.[555]

If the abscissa of the curve of Figure 7 is expressed in units of range (e.g., mg/cm^2), assuming the range - energy relationship to be linear, and if the coordinate is expressed in terms of relative intensity, then an approximate fit can be made with the relationship

$$I/I_o = \exp\,[-\,\mu_m X], \qquad (1)$$

where I/I_o is the relative intensity, X is the absorber area density in mg/cm^2, and μ_m is a constant with units of cm^2/mg. Thus, if the cumulative energy distribution function is available, the measurement of the relative intensity, I/I_o, will yield the absorber area density with a small error.

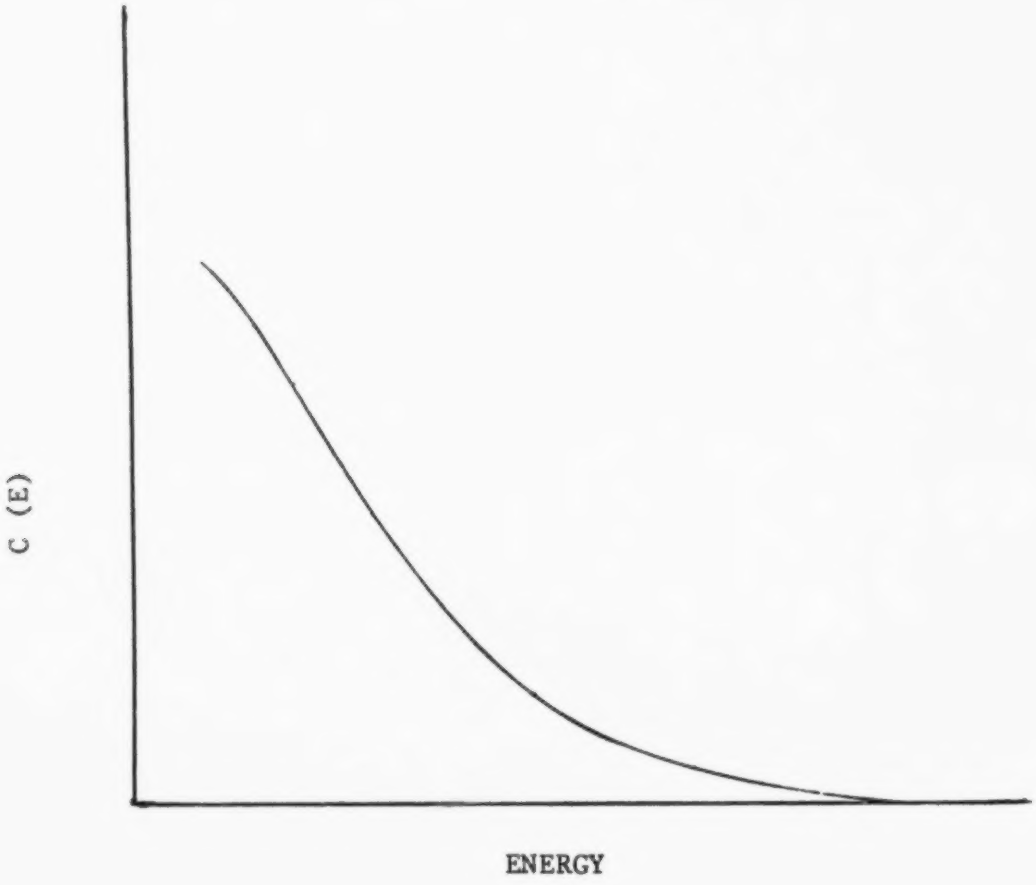

Fig. 7. Typical cumulative energy spectrum of beta particles.

Since the energy distribution function is not generally available, the exact value of μ_m is found experimentally. Equation 1 can then be used to determine the area density of an absorber. The value of μ_m has been found to be a function of E_{max}, the maximum energy of the beta particles. It is practically independent of the properties of the absorber. This function is of the form

$$\mu_m = a\ (E_{max})^{-b}, \tag{2}$$

where μ_m is expressed in mg/cm^2, and E_{max} is expressed in MeV. The values presented by different investigators vary considerably. Table 1 gives a partial list of the values found in the literature.

Table 1. Values of the constants a and b for determining the mass absorption coefficient μ_m, as given by various investigators.

Investigator	a	b
Shumilovskii & Milttsen[1209]	0.022	1.33
Evans[1205]	0.017	1.14
Hart[1206]	0.0151	1.50
Gleason, Taylor, & Tabern[1144]	0.017	1.43

The uncertainty in the values for a and b result from the fact that the cumulative energy distribution curve in Figure 7 is not exactly represented by an exponential function. Thus, the geometry of the experimental apparatus (e.g., the source window thickness, the distance from the source to detector, etc.), which determines the region of the curve that is used, significantly affects the values of these constants.

Calibration of the setup with an absorber of known thickness is the only way to control these uncertainties. With proper calibration, thicknesses of any materials which are fairly similar to the calibration absorber material can be measured.

The scattering of beta radiation is not nearly as straightforward as absorption (or transmission) of beta radiation. The back-scattering of beta radiation has been found by Dresia[1085] to vary roughly as $Z^{0.8}$, where Z is the atomic number of the absorber. Because of this dependence, beta scattering is not suited to measuring absorber area density unless the composition of the absorber is accurately known, which is not the case with a stack aerosol.

If, on the other hand, the area density of an absorber can be gaged (e.g., by beta absorption), the back-scattering or scattering at some angle can be calibrated to give a measure of the composition of the absorber. Dresia[1085] has successfully used the back-scattering of beta radiation to measure the ash content of ground coke. His data shows good sensitivity for two different radioactive sources, RaD and Tl-204 (Figure 8).

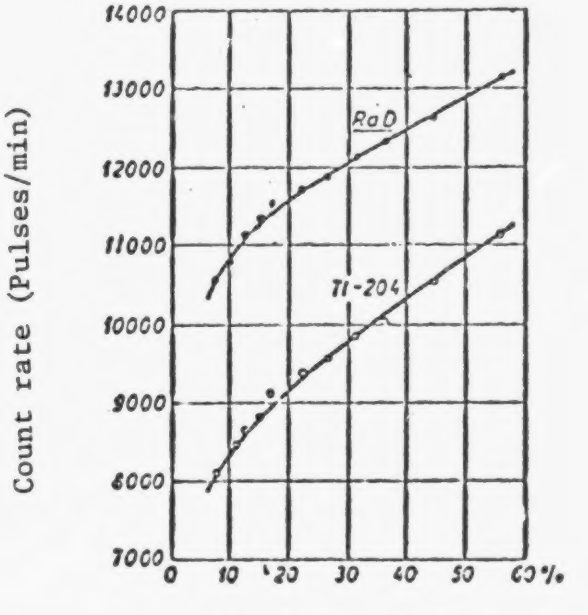

Fig. 8. Count rate for scattered beta radiation as a function of the ash content of the ground coke.[1085]

DUST COLLECTION TECHNIQUES

In order to use the beta radiation attenuation technique to measure particle mass concentration in a stack, it is necessary to concentrate the particles. This is an obvious requirement because the expected relative particle concentration is only about 10^{-5} (i.e., the ratio of mass of particles to mass of air in a given volume is 10^{-5}). Since the attenuation is only dependent on the total mass, which of course includes the mass of air, an instrument would have to be able to be sensitive to changes of 0.001% in order to be useful at all. Such instrumentation does not exist.

Several techniques have been tried which concentrate the particles by depositing them on a tape or similar substrate material. These are the only concentration techniques that hold any merit at this point. A few other ideas have been suggested, including one which prevents the need for depositing the particles by concentration of the particles by passing the carrier gas through a nozzle and keeping the particles in the center of the stream, but it is doubtful that any of these methods can be made to concentrate the particles by the required 4 or 5 orders of magnitude. A review of the four known deposition techniques follows. All four methods appear capable of operating satisfactorily with beta attenuation sensors.

The first and most obvious means of concentrating particles is to collect them on a filter. By varying such parameters as flow rates and sampling time, a wide range of sensitivities can be achieved. A measurement of attenuation of radiation by the filter both before and after particle deposition yields a measure of the particle mass per unit area on the filter, which is a measure of the particle mass concentration in the carrier gas. The advantage of collecting particles on a filter is that the flow rate need not be controlled so precisely, and collection efficiency can be very high for a wide range of particle sizes. A major problem is the periodic movement and replacement of the filter material.

A second method of collecting particles on a substrate is to use a modified electrostatic precipitator in which the particles are given a unipolar charge and deposited electrostatically on a membrane. This generally requires a conducting membrane to drain off the charge from the particles. Aluminum foil has been suggested for this purpose by Horn.[248] Such a system could be made automatic by using a continuously moving membrane whose feed rate could be adjusted to achieve maximum sensitivity under a range of loading conditions. This method would require a significant amount of development before becoming practical.

A third method is to use an impactor, provided nearly all mass of the particles is contained by particles large enough to be collected (i.e., $>0.3\mu$). Lilienfeld[1107] has successfully tested this technique for collection of atmospheric aerosols being measured using beta attenuation. This method provides the greatest sensitivity because the particles can be deposited on such a small spot on the impaction surface. Thus, good time resolution may be attained, on the order of seconds for concentrations found in stacks. Some method of cleaning or replacing the impaction surface is required.

A fourth method is to use a cyclone separator, in which the large particles approach the wall and fall to the bottom. The source and detector are placed such that they detect the mass of particles collected at the bottom of the cyclone. Dresia, et al,[335] and Jackson, et al,[705] have used this technique with some success. The concentration of particles is even greater than with an impactor because of high flow rates. A problem is the low collection efficiency of particles below 1 or 2 microns.

BETA RADIATION SOURCES AND DETECTORS

Several general requirements can be cited for beta radiation sources and detectors. First, the source must be energetic enough (i.e., have a sufficiently high E_{max}) such that some of the beta particles get through the absorber to the detector. At the same time it must have beta particles that are slow enough so that some get absorbed by the absorber. Secondly, enough source material should be present so that a high count rate can be attained in the detector so as to reduce statistical error. However, the count rate must be kept low enough so that dead-time losses in the detector are negligible (further explanation of this type of error is given below in the discussion on detectors). Thirdly, the source should have a fairly long half-life so that changes with time are insignificant over a period of at least several months. Finally, a source should not be so energetic as to endanger the health of the operators.

With any of the particulate collection techniques described above, the thickness of the collection substrate is about 1 mg/cm^2. To reduce errors due to non-uniformity in substrate thickness (it may vary as much as 10% from one location to another) and at the same time maintain good sensitivity and time resolution, the thickness of particles on the substrate must be roughly 1 - 10 mg/cm^2. This requires a beta radiation source with a maximum range of from 20 to 300 mg/cm^2, depending on the thickness of the air gap, source window, and detector window.

Several radioisotopes are available with such maximum ranges. Carbon 14, with a half-life of 5568 yr. and an E_{max} of 0.155 MeV, has been used in most commercial instruments of this type so far. Since it decays to form stable N^{14} and is relatively abundant, it is probably the most attractive candidate. Other radioisotopes that should be considered are thallium 204 (half-life: 2.7 yrs., E_{max}: 0.762 MeV), cesium 137 (half-life: 33 yr., E_{max}: 0.518 MeV), beryllium 10 (half-life: 2.7 x 10^6 yr., E_{max}: 0.56 MeV), and promethium 147 (half-life: 2.26 yr., E_{max}: 0.229 MeV).

Several techniques are available for detecting beta radiation after it has passed through the absorber (i.e., the substrate plus the particulate deposit). All that is required is a count rate of the beta particles; no beta particle energy measurement need be made. The four most attractive counting instruments are the Geiger-Muller counter, the end-window proportional counter, the scintillation counter, and the solid state radiation counter.

The Geiger-Muller (GM) counter has been used almost exclusively in instruments for measurement of particle mass concentration.[335,1107] It has the advantage of being relatively inexpensive ($50 - $100), it can operate in a variety of environments, it is quite simple, it has a long life, and it is relatively small in size. For count rates greater than about 1000 cps, however, the counting efficiency begins to drop off sharply due to dead-time losses. Dead times for GM counters are about 50 - 3000 μsec.[1207]

Proportional counters have also been used for aerosol mass measurement applications.[555] They offer several advantages over GM counters in that they have much shorter dead times - on the order of 1 μsec.[1207] This allows them to measure higher count rates accurately and thus reduce statistical errors. However, they are somewhat temperature sensitive, and often last only about one year. In addition, they are about 5 times as expensive as GM counters. Thus, it seems that the only justification for using a proportional counter instead of a GM counter would be a high count rate that the GM counter cannot measure.

A scintillation counter has been used in a dust measuring instrument in the Soviet Union[1061]. These counters have roughly the same dead time as proportional counters (for sodium iodide crystals), and even shorter dead times are possible. They are extremely temperature sensitive, although this may not be important since pulse height is not important. They are also very fragile, and have lifetimes ranging from months to years, depending on the phototube quality and sealing characteristics. Perhaps the most negative characteristic is the cost, which is about 5 - 10 times that of GM counters. The only real advantage a scintillation counter has over a proportional counter is that it requires less voltage. So far, this has not proven to be sufficient justification for using a scintillation counter.

A solid state radiation detector has been used by Benarie[1117] to sense beta particles in a stack monitoring instrument. The counting rate of these counters is about 100 times greater than GM counters. No window is required. The detectors are very rugged. Solid state detectors cost about 2 - 3 times as much as GM counters. The solid state detector appears to be the most favorable of the four available detectors.

APPLICATION TO MASS CONCENTRATION MEASUREMENT IN STACKS

While the beta attenuation technique does not, strictly speaking, measure particle mass, it does measure something very nearly identical to mass - namely the electron density of the particles. Compared with other techniques which measure different properties of the particles, it offers one of the most direct means of obtaining a measurement in terms of mass. Only analytical balances, vibrating spring-mass systems, and one or two other methods, measure mass more directly.

The required instrumentation can be made relatively simple and reliable, which are important considerations for long range use in stacks. The only moving parts are those which are responsible for transporting the collection substrate from the collection site to the measurement position and from the measurement position to either a cleaning position or disposal. Such machinery can be made to operate for long periods of time without need of repair if proper care is taken. All electronic equipment, from the output of the radiation detector to the readout, can be digital, although analog conversion is possible for strip chart or meter readout.

The technique requires sampling steam aspiration since the low concentration of particles does not allow for enough sensitivity if measurements are made in situ. Thus, it gives essentially a point measurement of particle mass concentration. This may or may not be an advantage, depending on the shapes of the mass concentration and velocity profiles in the stack or duct where measurements are being made. No commercial instrument of this type has been made that will operate at stack temperatures (approx. 350°F), but there appears to be no reason to expect such an instrument could not be made. In either case, the problem of keeping the vapor in the gas from condensing must be dealt with. These are engineering problems that require careful analysis and meaningful testing programs.

Only limited stack sampling data has been taken with instruments using this technique, and much of this data has not yet been made available. Nevertheless, some data has been presented for several different pollutants,[335] and good accuracy and repeatability appear to be possible. Errors in this data are given as ± 10%. It is felt that these errors can be cut in half under well controlled conditions. For an instrument that will run for long periods of time in a stack, however, ± 10% error is the best estimate that can be made without further data. This error does not include the error due to losses in the sampling probe. It only includes errors in the instrument itself, such as varying tape thickness, uncertain flow measurement, particle collection efficiences less than 100%, statistical variation in count rate of beta particles, and the inherent error in the assumption of the Beer-Lambert law (Eq. 1).

A very recent program by Schnitzler, et al[1189], extensively evaluated the Konitest, two light transmission instruments, and two beta attenuation instruments in a modern plant fired by coal. Figure 9 shows the comparative results of the five instruments in terms of manually measured gravimetric concentration as a function of instrument reading. Table 2 indicates the results of these tests. The dark lines in Figure 9 are the calibration curves obtained by drawing lines through the data points. The lighter parallel lines on either side of the calibration line denote extrapolations of the 95% confidence level calculated for the 150 mg/m^3 concentration level.

Even though the beta instruments in these tests were first-generation instruments, they show excellent correlation with gravimetric mass measurements. Second-generation instruments could undoubtedly correlate better.

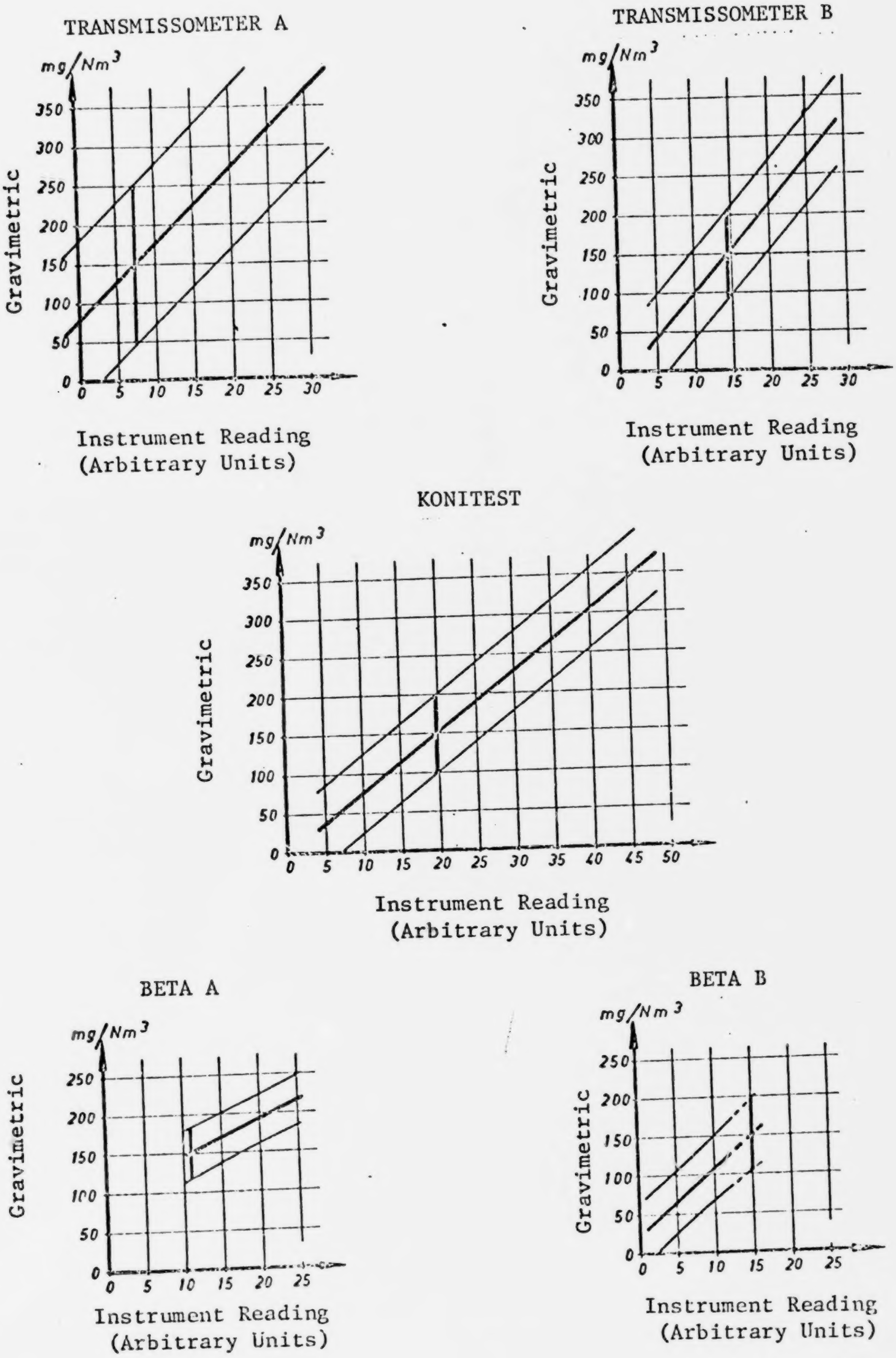

Figure 9. Gravimetric calibration of two light transmissometers, one Konitest, and two beta radiation attenuation instruments in a coal-fired effluent duct from Schnitzler et al[1189].

TABLE 2. Summary of experimental calibration of five instruments by Schnitzler et al[1189].

	Instrument				
	Transmissometer		Contact-Electrostatic Konitest	Beta Radiation Attenuation	
	Durag A	Sick B		A	B
Number of Measurements	312	292	312	29	43
Correlation Coefficient	0.63	0.87	0.92	0.94	0.81
Measurement Tolerance at 150 mg/Nm^3	± 68%	± 39%	± 33%	± 22%	± 31%

Two manufacturers of beta attenuation mass monitors for stack monitoring are known in the U.S.: Gelman Instrument Company and Research Appliance Corporation. Their instruments cost between $8,000 and $10,000. Included are a sampling probe, a sampling unit which includes the beta radiation source, and a digital readout unit. One foreign company manufactures beta instruments for stack monitoring: Verewa, Hans Ugowski & Co. from West Germany. Saphymo Srat from France and a West German company, Frieseke & Hoepfner GMBH, manufacture beta instruments for ambient air monitoring.

CONCLUSIONS

The use of beta attenuation mass monitors for measuring particle mass concentration in stacks appears very promising for the following reasons:

1) The property of the particles that is actually measured is something very close to mass, so that errors involved in correlating the measured property with mass are virtually eliminated,

2) The cost is moderate ($8,000 - $10,000), and can be made lower if large volumes are produced.

3) The instrument can be made quite reliable due to its relative simplicity, and

4) The instrument has had some experience in stacks so that some progress toward its development has already been made.

It has several disadvantages that require further study:

1) It requires a sampling probe, so it is subject to errors due to turbulent flow conditions in a stack and losses within the probe,
2) It gives a point measurement rather than an integrated measurement (this may not be a disadvantage), and
3) It may not have good enough time resolution to detect changes that occur within a few seconds.

In spite of these disadvantages, beta attenuation devices are more accurate than most other particle concentration monitors if a measurement of particle mass is desired, and should be considered for monitoring particle mass concentration in stacks.

REFERENCES

1117 Benarie, M., and Bodin, D., "Mise au Point et Essais d'Utilisation d'un Appareil Continu Pour la Mesure de Poussieres par Absorption de Rayons Beta", *Pollution Atmospherique*, no. 35, p. 147-155 (Jul-Sep 1967).

1085 Dresia, H., "The Determination of the Ash-Content of Coal with Beta and Gamma Rays", *Brennstoff-Chemie*, V. 43, no. 5, p. 149-152 (May 1962).

335 Dresia, H., Fischotter, P., and Felden, G., "Kontinuierliches Messen des Staubegehaltes in Luft und Abgasen mit Betastrahlen", *VDI-Z*, V. 106, no. 24, p. 1191-1195 (Aug 1964).

1205 Evans, R. D., *The Atomic Nucleus*, McGraw-Hill Book Co., Inc., N.Y., p. 628 (1955).

1144 Gleason, G.I., Taylor, J. D., and Tabern, D.L., "Absolute Beta Counting at Defined Geometries", *Nucleonics*, V. 8, no. 5, p. 12-21 (1951).

1206 Hart, H., "Radioactive Isotopes in Industrial Measuring Technology," *VEB Verlag Technik,* Berlin (1962).

248 Horn, W., "Process for Continuous Gravimetric Determination of the Concentration of Dustlike Emissions", *Staub-Reinhalt der Luft (Engl. Trans.)*, V. 28, no. 9, p. 20-25 (Sep 1968).

1061 Izmailov, G. A., "Measuring the Gravimetric Concentration of Dust in the Air using β-Radiation", *Zavodskaya Laboratoriya*, V. 27, no. 1, p. 40-43 (1961). English translation in: *Industrial Laboratory*.

705 Jackson, M. R., Lieberman, A., Townsend, L. B., and Romanek, W., "Prototype Fly Ash Monitor for Municipal Incinerator Stacks", *Proc. 1970 National Incinerator Conf.*, Cincinnati, Ohio, p. 182-188 (May 17-20 1970).

1207 Kaelble, E. F., ed., *Handbook of X-Ray*, McGraw-Hill Book Company (1967).

1208 Lapp, R. E., and Andrews, H. L., *Nuclear Radiation Physics*, Prentice Hall, Inc. (1948).

1107 Lilienfeld, P., "β-Adsorption-Impactor Aerosol Mass Monitor", GCA Technology Division, Bedford, Mass., Presented at American Industrial Hygiene Assoc. Conference, Detroit, Mich. (May 1970).

555 Nader, J. S., and Allen, D. R., "A Mass Loading and Radioactivity Analyzer for Atmospheric Particulates", APCA Annual Meeting No. 52, Los Angeles, Calif. (Jun 1959).

1189 Schnitzler, H., Maier, O., and Jander, K., "Messtand fur die Prufung und Kalibrierung von Registrierenden Staub - und Gasmessgeraten in einem Steinkohlengefeuerten Kraftwerk", *SchrReihe Ver. Wass. - Boden Lufthyg. Berlin-Dahlem*, V. 33, Stuttgart (1970).

1209 Shumilovskii, N. N., and Milttsen, L. V., *Radioactive Isotopes in Instrumentation and Control*, The MacMillan Co. (1964).

PIEZOELECTRIC MICROBALANCE

by: John G. Olin

INTRODUCTION

Piezoelectricity is a property of certain crystals, including quartz, which results in an electrical charge on certain surfaces of the crystal when the crystal becomes mechanically stressed. Conversely, a piezoelectric material becomes mechanically strained if an electrical charge is placed on certain of its crystal faces. A piezoelectric crystal, when placed in an appropriate electronic oscillating circuit, will cause the circuit to oscillate at the natural vibrational frequency of the crystal.

When foreign material adheres to the surface of a vibrating piezoelectric crystal, the natural frequency of vibration of the crystal decreases. The magnitude of the frequency change is directly proportional to the mass of the foreign material. Some piezoelectric materials, such as quartz, vibrate at very precise natural frequencies, so that frequency changes of one part in ten million are significant and easily detectable. This principle has been used recently to measure the mass of aerosol particles deposited onto the sensing surface by an electrostatic precipitator or an impactor.[244,1222,1223] Piezoelectric microbalances also have had wide commercial application for monitoring the thickness of sputtered or evaporated thin films.

Quartz crystals can vibrate in several different modes. Several common vibrational modes for quartz crystals are shown in Figure 1: thickness-shear mode, length-longitudinal mode, free-shear mode, and flexural mode. In all modes, except the flexural mode, the resonant frequency is inversely proportional to the characteristic length L for vibration:

$$f = \frac{N}{L}, \tag{1}$$

where N is a constant depending on the density and elastic properties of the crystal. The change in resonant frequency is:

$$\frac{df}{f} = -\frac{dm}{m}. \tag{2}$$

Eq. (2) is strictly true only for relatively small mass changes (1%, or less)[244].

1. Thickness-Shear Mode

$$f = \frac{N}{L}$$

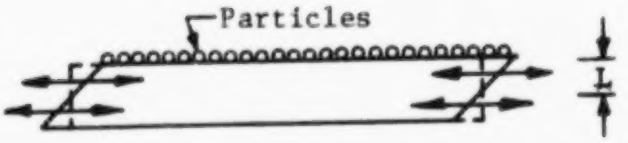

2. Length-Longitudinal Mode

$$f = \frac{N}{L}$$

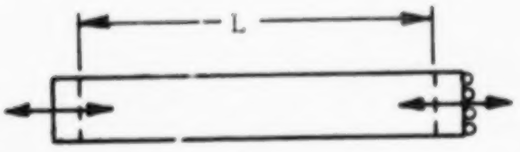

3. Face-Shear Mode

$$f = \frac{N}{L}$$

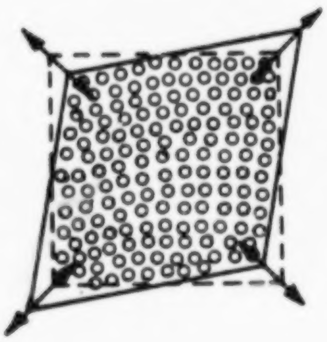

4. Flexural Mode

$$f = \frac{N\ t}{L^2}$$

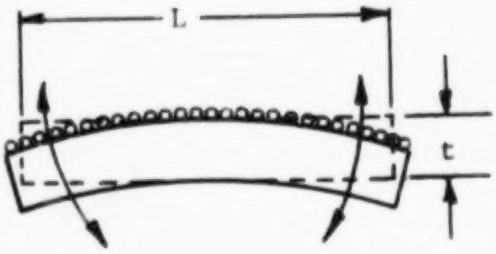

f = Frequency of vibration

N = Frequency constant for fundamental mode

L = Characteristic dimension for vibration

Fig. 1. Several types of quartz crystals.

The type AT crystal, shown in Figure 2, which vibrates in the thickness shear mode, is usually the most useful type for measuring the mass of foreign material, such as small particles, because there are no vibrational nodes on the mass-sensing surface of the crystal. Thus, the mass of all particles is detected equally regardless of their location on the sensing surface. This is not the case with some types of crystals, such as those which vibrate in a flexural mode. Another advantage of the type AT crystals for most mass-sensing applications is the flat, plate-like shape which makes instrument design easier.

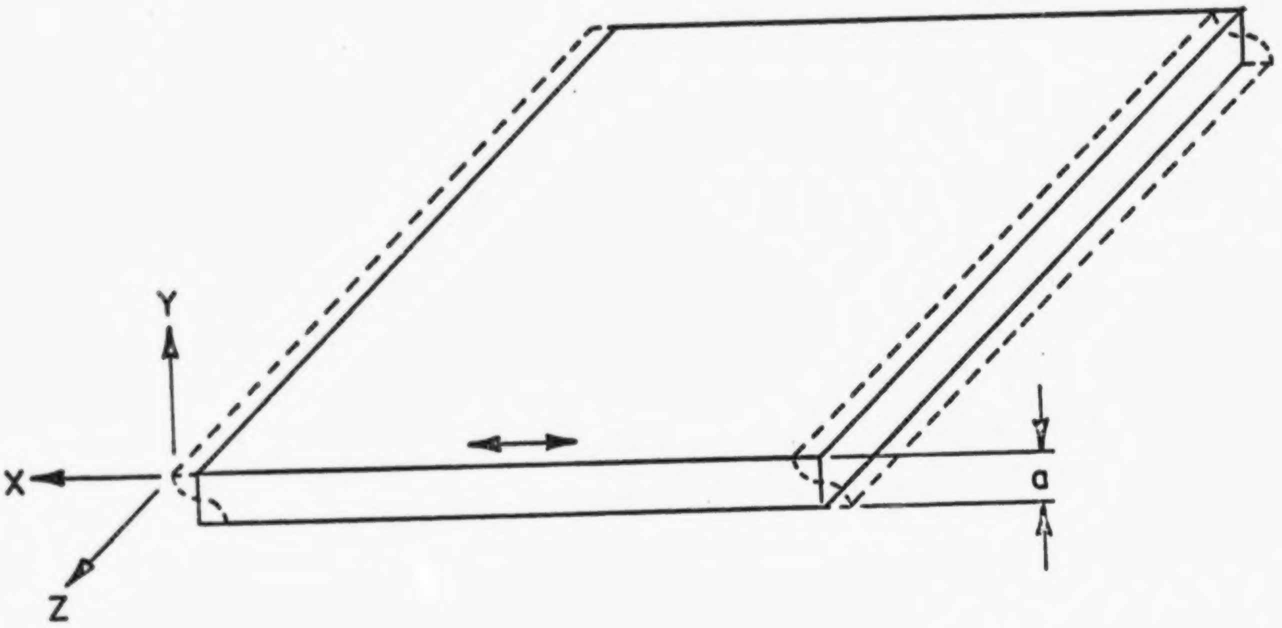

Fig. 2. Type AT quartz crystal in thickness shear mode of vibration.

The use of vibrating piezoelectric crystals for mass measurement (piezoelectric microbalances) was discovered by Sauerbrey in 1959.[1221] Sauerbrey showed theoretically and experimentally that vibrating type AT quartz crystals have a linear frequency decrease in response to the mass of thin metallic films added to the electrode surface of the crystal. The relationship between added mass and the change in natural vibrational frequency for type AT quartz crystals is:

$$\Delta M = -\frac{A}{2.27\ f_o^2}\ \Delta f, \tag{3}$$

where:

Δf = change in natural vibrational frequency, Hz

f_o = natural vibrational frequency of the crystal, MHz

A = electrode area of the crystal, cm^2

ΔM = mass added to the electrode area, μgm

Equation (3) was developed by Sauerbrey[1221] for thin metallic films, but the theory holds for any other material which sticks to the electrode so well that it vibrates with the crystal.

PRINCIPLE OF OPERATION

Recently[244,1222,1223] the piezoelectric microbalance has been used as an effective means of measuring the mass of airborne particles deposited onto the crystal surface. Particles are deposited onto the crystal surface with any collection device, as shown in Figure 3. At the present time, electrostatic precipitators, as shown in Figure 4,[244,1222] and the impactors[244,1223] have been used as particle collectors. In both of these devices, the aerosol to be measured is drawn through the sampling head with a vacuum pump.

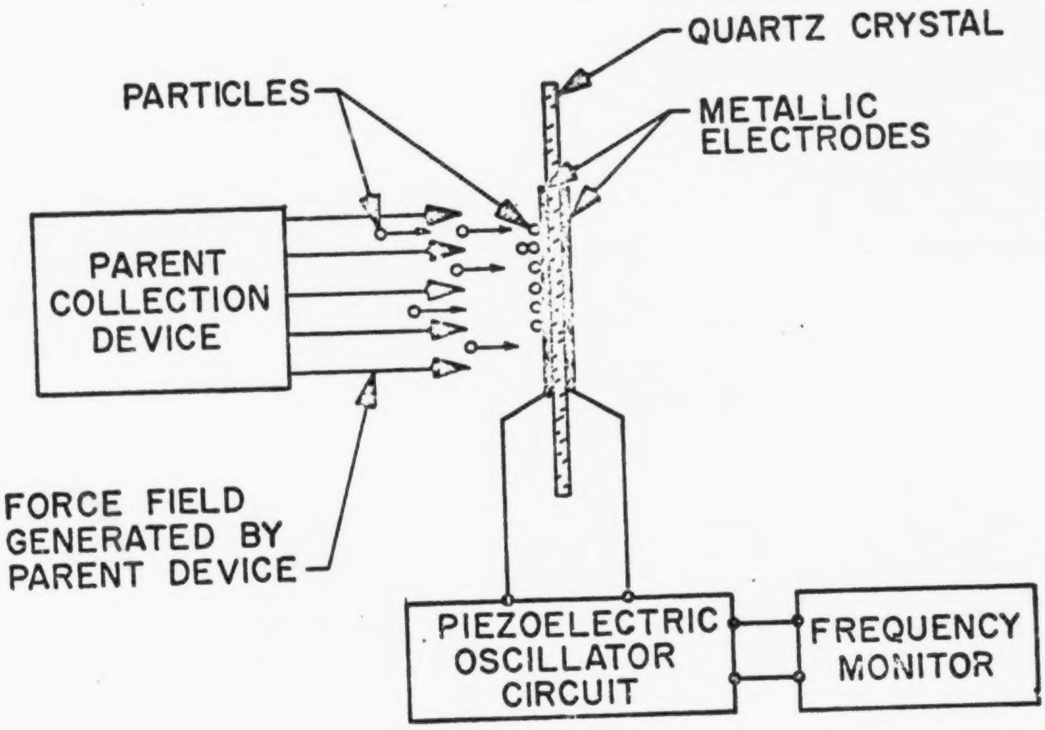
QUARTZ CRYSTAL
PARTICLES
METALLIC ELECTRODES
PARENT COLLECTION DEVICE
FORCE FIELD GENERATED BY PARENT DEVICE
PIEZOELECTRIC OSCILLATOR CIRCUIT
FREQUENCY MONITOR

Fig. 3. Schematic system for tranducing particle mass using quartz crystal oscillator.

A complete instrument system for particle mass concentration measurement consists of the following components:

(1) Primary crystal used to weigh deposited particles.

(2) Particle collector. A vacuum pump draws the aerosol through the collector.

(3) Reference crystal used to subtract out possible frequency changes caused by changes in secondary phenomena, such as operating temperature.

(4) Oscillator circuits for both primary and reference crystals.

(5) Mixer circuit to subtract the signals from the two crystals.

(6) Digital frequency counter to monitor mixer output, f, which is proportional to the integrated mass of the piezoelectric deposition.

(7) (Optional) Direct particle mass concentration computer for calculating particulate mass concentration, which is proportional to df/dt.

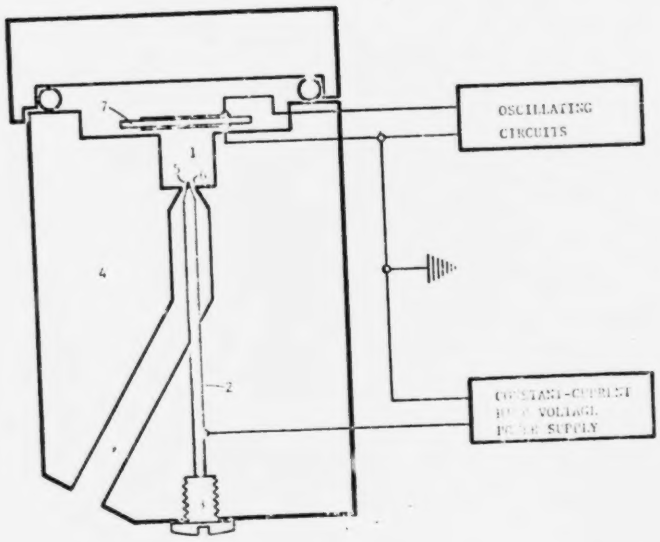

Fig. 4. Side view of electrostatic precipitator and piezoelectric microbalance: 1) precipitating chamber, 1/4 in dia x 1/4 in high, 2) corona needle, 3) needle adjusting screw, 4) teflon precipitating block, 5) high corona region, 6) entrance nozzle to precipitating chamber, 7) piezoelectric crystal sensor.

The entire system, except the collector, is shown in Figure 5.

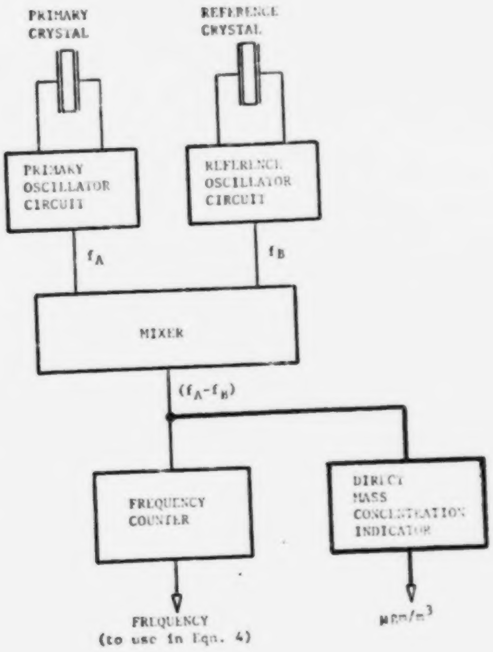
PRIMARY CRYSTAL
REFERENCE CRYSTAL
PRIMARY OSCILLATOR CIRCUIT
REFERENCE OSCILLATOR CIRCUIT
f_A
f_B
MIXER
(f_A-f_B)
FREQUENCY COUNTER
DIRECT MASS CONCENTRATION INDICATOR
FREQUENCY (to use in Eqn. 4)
$\mu gm/m^3$

Fig. 5. Piezoelectric microbalance electronic block diagram. The frequency counter and the direct mass concentration indicator are optional data readout methods.

The piezoelectric particle microbalance is used to measure the mass concentration C (μgm/m^3) of airborne particles:

$$C = \left(\frac{1}{SQ\ E_c\ E_w}\right)\left(\frac{\Delta f}{\Delta t}\right), \tag{4}$$

where:

Δf = change in mixer frequency (Hz),

Δt = sampling time (sec),

Q = sampled aerosol flow rate (m^3/sec.),

S = $\Delta f/\Delta M$ theoretical mass sensitivity, Eq. (1) (Hz/μgm),

E_c = efficiency of particle collection by the collector, and

E_w = efficiency of the piezoelectric microbalance in weighing the deposited particles.

For typical numerical values used with ambient atmospheric aerosols, first assume a 5 MHz type AT quartz crystal with an electrode diameter of 0.635 cm. This yields a mass sensitivity from Eq. (3), of

$$S = -180\ \text{Hz}/\mu\text{gm}. \qquad (5)$$

Further, assuming that E_c and E_w are 100%, and Q is 1 SLPM, then, from Eq. (4) we get,

$$C = 333\ \frac{\Delta f}{\Delta t}. \qquad (6)$$

Piezoelectric microbalances with an impactor collector have been used to measure the impact of individual particles[1223]. The digital mixer output is converted to an analog signal and differentiated. The resulting pulse height is used as a measure of particle size. Particle density must be assumed. The instrument is insensitive to particles with a size less than about one micron. For the dense aerosols found in stacks, coincidence will probably be a problem. For these reasons, this use of the piezoelectric microbalance is not recommended for stack application.

DESIGN CONSIDERATIONS FOR STACK MONITORING

An ideal instrument for measuring total particle mass concentration will have $E_c = 100\%$ and $E_w = 100\%$. Impactor collectors can never have 100% collection efficiency because particles with a size less than the impactor's particle size cut-off will escape the collector. This property of impactor collectors makes them useful for particle size-distribution monitoring. An electrostatic precipitator collector does have the potential for collecting particles of all sizes. Experiments have shown that the collection efficiency E_c of an electrostatic precipitator similar to the one shown in Figure 4 is essentially 100% for several types of particles over a wide mass concentration range (approximately 10 to 10,000 μgm/m^3). Aerosols tested included tobacco smoke, indoor aerosol, and atmospheric aerosol. Figure 6 shows these tests.

A 100% weighing efficiency E_w requires perfect adherence of the particles to the vibrating crystal surface. Particle adhesive force is a complex combination of molecular attraction forces, electrostatic forces, and surface-tension forces[244]. As particle size increases, the ratio of particle adhesive force to inertial force decreases. Hence, the mass of particles above a certain critical size will not be weighed with 100% efficiency by the piezoelectric microbalance. The critical size is maximized by depositing particles uniformly onto the crystal surface and by minimizing crystal drive level. The experimental

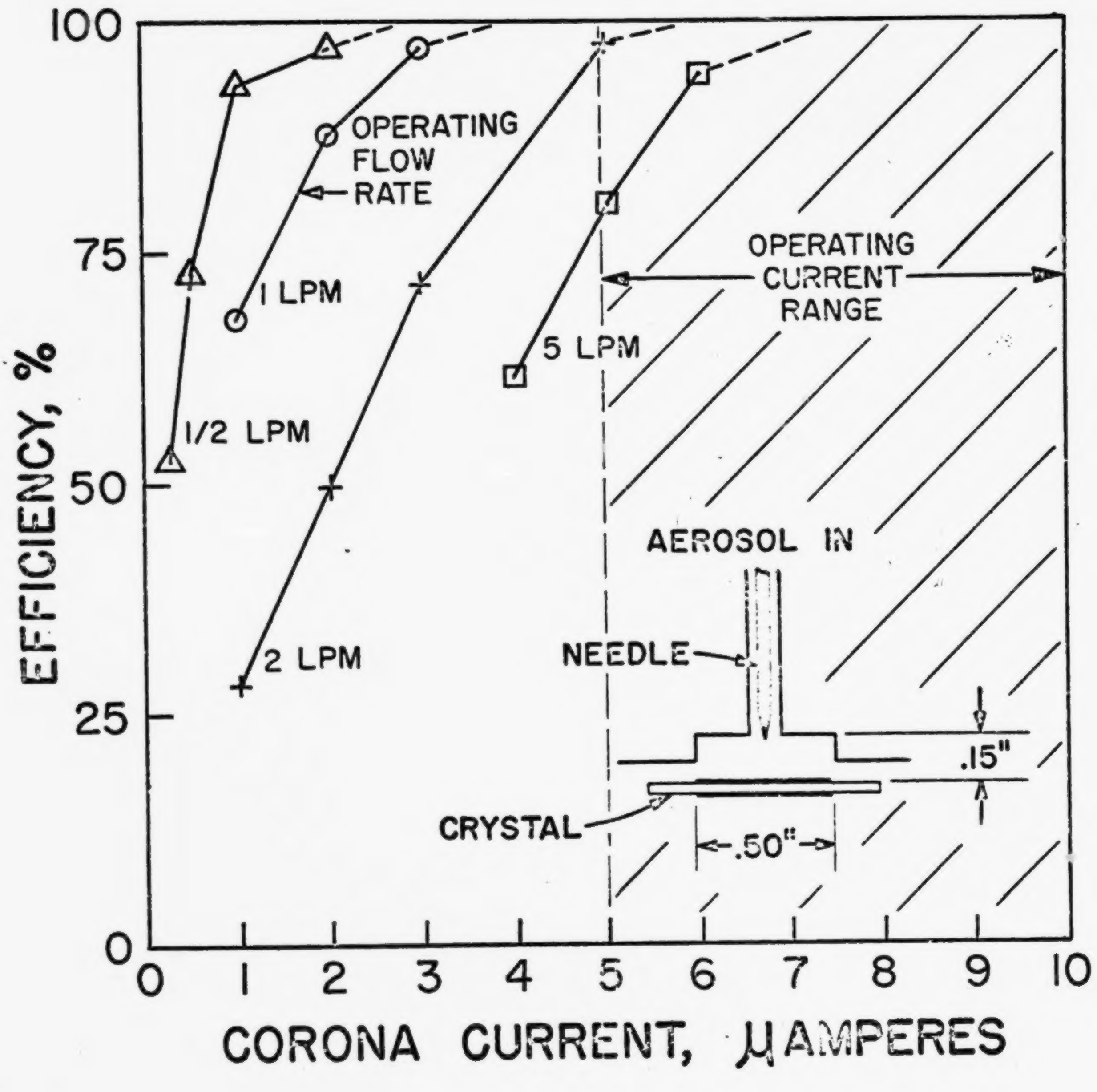

Fig. 6. Results of electrostatic precipitator efficiency tests.

data of Figure 7 shows a weighing efficiency of nearly 100% for tobacco smoke and room aerosol. The tobacco smoke aerosols were diluted by factors of 5 to 20 with relatively clean ambient air, thus stablizing any condensation of vapors. The aerosols used for obtaining data in Figure 7 did not have significant mass above 10 microns.

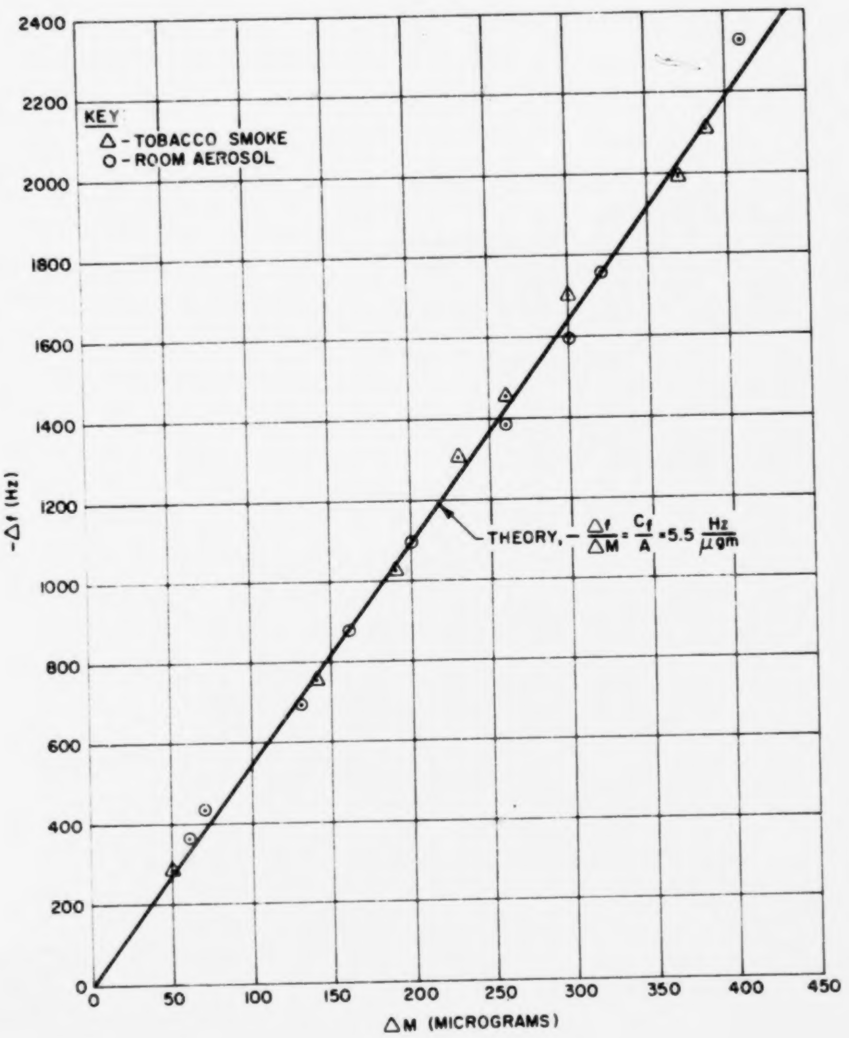

Fig. 7. Experimental mass sensitivity of 1.6 MHz type AT quartz crystal (electrode area = 1.06 cm^2).

The adherence of particles to the crystal surface can be increased by several other methods. The application of a thin coat of sticky material to the crystal surface is one method. This technique has been used for many years to prevent particle bounce and blowoff from the collection plate of aerosol impactors. The application of a thin uniform film of sticky material to the crystal electrode may be a problem. However, various coatings have been applied to crystal surfaces for measurement of trace gases.[1352] In this case, the trace gases are selectively adsorbed by the coating, causing an increase in the mass on the electrode which is detected by a corresponding crystal frequency shift. Thus, thin films of coating material can apparently be applied to the crystal. The film of material must, of course, remain stable during the particulate deposition process. Any mass changes in the film material itself must be insignificant compared to the mass of deposited particles. A sticky film on the crystal surface will not increase the adhesion of more than one layer of particles.

Another way to make particles adhere more strongly to the crystal is to coat the airborne particles with a thin film of sticky material before they are deposited onto the crystal surface. This method has been used with piezoelectric microbalances which sense atmospheric particle mass concentration.[1351] A trace amount of ammonia vapor, or a similar vapor material, can be introduced into the sampling line upstream of the crystal. Approximately one monolayer of material adheres to the particles. This layer, in turn, attracts one or two monolayers of water. The resulting liquid coating contributes insignificantly to the mass of particles, but does increase the surface-tension force causing particles to adhere to the crystal. The water layer also decreases the electrical resistivity of the particle, allowing electrical charge to bleed off the particles in an electrostatic precipitation-piezoelectric instrument. This same principle has been used in the past to improve the performance of large electrostatic collectors used to reduce particulate emissions from smoke stacks.

If the deposited particulate mass becomes excessive, the oscillator circuit can no longer drive the crystal stably. When this occurs, the crystal must be wiped clean either automatically or manually. For cigarette smoke, a mass loading of approximately 250 micrograms is achieved before encountering instability. Since a mass of only 0.5 micrograms is over 100 times greater than the sensor resolution, it is theoretically possible to obtain 500 readings with tobacco smoke before cleaning the crystal. For atmospheric aerosols the total mass loading is probably in the range of 25 - 50 micrograms. Thus, the maximum loading depends on the type of aerosol. For stack emissions, the maximum loading will probably fall between 25 and 50 micrograms. The necessity to clean the crystals is an obvious disadvantage of piezoelectric particle microbalances. However, it appears that several automatic cleaning methods could be developed.

Quartz crystals are sensitive to temperature. Type AT quartz crystals are selected, in part, because they belong to a class of low-temperature coefficient crystals, with values of a fraction of a part per million per °C, as shown in Figure 8. The type AT crystal shown in Figure 8 has a "zero" temperature coefficient at 20°C. By changing the orientation angle of the type AT, the zero temperature coefficient point can be increased to about 60°C. Thus, it will be necessary to cool the gases to that temperature, or to find a different crystal type which has a zero temperature coefficient near 150°C.

Piezoelectric particle microbalances make a point measurement. Hence, they require extracting the sample from the aerosol stream. Like other such instruments, they are possibly subject to sampling errors and to particle loss, vapor condensation, and particle agglomeration in the sampling train. Agglomeration does not affect the total mass concentration measurement, but does affect size-distribution monitoring. If water condenses on the crystal, erroneous results, and even instability, can be encountered. Diluting with clean dry air should eliminate the problem. Alternatively, the entire sampling train and sensing head could be operated at the stack temperature (nominally 150°C) to prevent condensation.

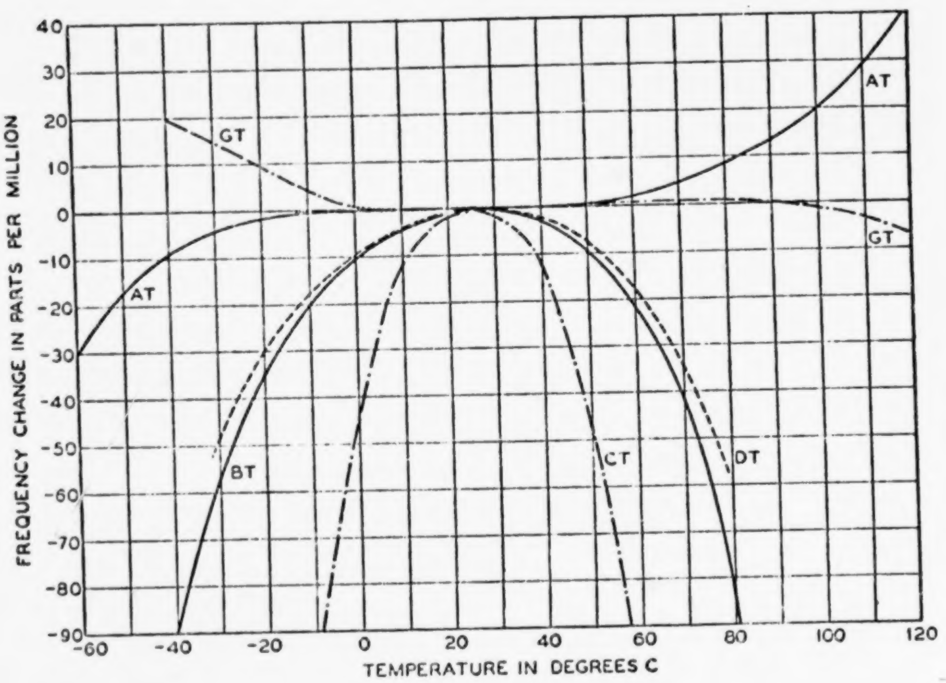

Fig. 8. Temperature frequency characteristics of zero temperature coefficient quartz crystals.

Crystals with a 150°C zero temperature coefficient, for example, type BT, would be used in this case. In any case, the condensation of several vapors in the effluent must be dealt with carefully in the design of a piezoelectric sampler, or in the design of any other extraction sampler.

APPLICATION TO PARTICLE MASS CONCENTRATION MONITORING IN STACKS

Table 1 gives the properties of typical quartz crystals vibrating in the four modes shown in Figure 1. The length-longitudinal and flexural modes have greater damping than the two shear modes: thickness shear and face shear. In face-shear mode, the particle layer is strained, an undesirable feature. For these reasons, the thickness shear mode is most desirable.

Types AT and BT quartz crystals have the best temperature coefficient characteristics of crystal vibrators in the thickness-shear mode:

(a) The temperature coefficient is very low.

(b) The temperature coefficient is relatively flat over a reasonable temperature range.

(c) The range of flat temperature coefficient can be increased (with BT) to cover the high temperature stack environment.

If necessary, low frequency (approx. 500 KHz) type AT crystals can be used for stacks if the sensing of large particles is a problem.

Although types AT and BT crystals appear to be best for stack monitoring, crystals vibrating in the length-longitudinal mode may be used if very low frequencies are necessary to sense large particles.

TABLE 1. PARAMETERS FOR TYPICAL PIEZOELECTRIC CRYSTALS

Mode	Type	Shape	Frequency Range(KHz)	Approx.Frequency Constant N for Fundamental Mode (KHz mm)	Approx. Temperature Coefficient (parts per million per °C)
Thickness-Shear	AT	Plate	500 to 15,000	1,660	0.0 (vary angle of cut to achieve 0.0 from 20°C to 100°C)
	BT	Plate	1,000 to 20,000	2,560	0.0 at 25°C (not as flat as AT)
	Y	Plate	500 to 20,000	1,981	+75 to 125
	AC	Plate	1,000 to 15,000	1,656	+20
	BC	Plate	1,000 to 20,000	2,611	-20
Length-Longitudinal	X	Rod	40 to 350	2,870 (varies with size ratio)	→ 0
	MT	Plate	50 to 500	2,700 (varies with size ratio)	→ 0
Face-Shear	CT	Plate	300 to 1,100	3,070	0.0 at 25°C
	DT	Plate	80 to 300	2,060	→ 0
Flexural	NT	Rod	4 to 70	283 (for width to length ratio=0.05)	→ 0

Thus, the optimum crystal type and frequency for stack application may be different than the crystal used for monitoring atmospheric aerosols. However, to estimate the essential performance of a piezoelectric microbalance for stack application, let us assume that the crystal required is the same as that used for other aerosols. We will impose the further criterion for a good total mass concentration instrument that all of the particles are collected on the crystal surface, i.e., $E_c \approx 100\%$. This implies the use of an electrostatic precipitator to deposit particles onto the crystal surface. However, an impactor may be applicable if the particles are relatively large, e.g., if 90% of the mass is above 1 micron. The weighing efficiency E_w is also taken as 100%. With these assumptions, anticipated instrument performance in stacks is summarized in Table 2.

TABLE 2. TYPICAL PERFORMANCE CHARACTERISTICS

1.	Crystal frequency	5 MHz
2.	Crystal diameter	0.635 cm
3.	Sampled gas flow rate	1 SLPM
4.	Mass Sensitivity S (Eq. 5)	- 180 Hz/μgm
5.	Frequency resolution(a)	± 1 Hz approx.
6.	Mass resolution	± 0.0056 μgm
7.	Time resolution (Eq. 6)	
	a. After collector - high value, C = 3 gms/m^3(b)	0.098 sec.
	b. After collector - low value, C = 0.03 gms/m^3(b)	9.8 sec.
8.	Approximate theoretical number of measurements before cleaning crystal(c)	100
9.	Time before cleaning assuming continuous sampling(c)	
	a. After collector - high value, C = 3 gms/m^3(b)	0.16 min.
	b. After collector - low value, C = 0.03 gms/m^3(b)	16 min.

Notes:

(a) Experiments show that frequency resolution is limited by the frequency counter (± 0.1 Hz), rather than by the piezoelectric microbalance. Nevertheless, we have conservatively chosen a ± 1 Hz frequency resolution.

(b) This time resolution is based on the collector of enough mass so that the specified frequency resolution is 1% of the frequency shift caused by the mass. A pulverized coal boiler is assumed. The mass concentrations assumed represent the typical range expected in coal-fired stacks. The collection and sensing efficiences are assumed to be 100%.

(c) Assuming a total frequency shift of 10 KHz before encountering instability, ± 1 Hz resolution, and 100 Hz per measurement.

A major disadvantage is that the crystal must be cleaned relatively frequently. This disadvantage can be dealt with in several ways:

(1) Operating the electrostatic precipitator only when a measurement is desired - for a few seconds at a time.

(2) Providing a means of automatically cleaning the crystal or indexing another clean one into the precipitator chamber.

(3) Diluting the sampled aerosol to reduce the particle concentration.

(4) Using crystals with a higher total frequency shift, such as lower-frequency, type AT crystals.

All four methods could probably be incorporated into an instrument.

The low sampling rate (about 1 LPM) of piezoelectric monitors may require a special sampling probe system to prevent excessive particle losses. Figure 9 shows one possible system. A separate system removes a convenient, larger flow from the stack and slows it down so that a reasonably-sized probe can remove a sample at the low flow rate necessary for the piezoelectric monitor. The sample may be conditioned by dilution or sample tube heating or cooling, if necessary.

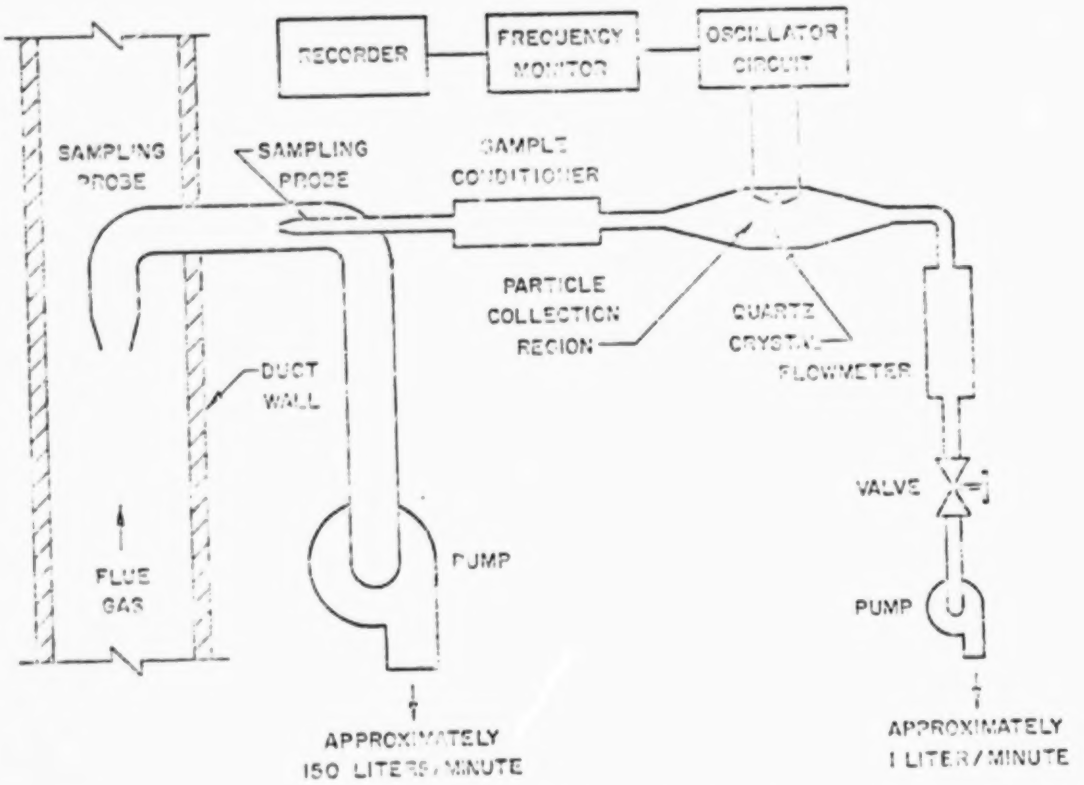
RECORDER
FREQUENCY MONITOR
OSCILLATOR CIRCUIT
SAMPLING PROBE
SAMPLING PROBE
SAMPLE CONDITIONER
PARTICLE COLLECTION REGION
QUARTZ CRYSTAL
FLOWMETER
DUCT WALL
VALVE
FLUE GAS
PUMP
PUMP
APPROXIMATELY 150 LITERS/MINUTE
APPROXIMATELY 1 LITER/MINUTE

Fig. 9. A possible stack sampling system using a piezoelectric microbalance sensor.

Another potential problem is the weighing of larger particles, as discussed earlier. Fortunately, downstream from electrostatic collectors, approximately 95% of the particulate mass is less than 25 microns for all coal-fired facilities.* Experiments with atmospheric aerosols show that the upper size cut-off with the piezoelectric microbalance described in Table 2 is greater than 10 - 15 microns. The exact size cut-off is not known.

If particles in stacks are sticky, they should adhere firmly to the oscillating crystal. This would increase the upper size cut-off. Lower frequency type AT crystals, such as 1.5 MHz, also can be used to increase the upper size cut-off. Several methods discussed earlier can be used to increase the ability of the microbalance to sense large particles. Thus, the piezoelectric microbalance has good promise for weighing particles up to 25 or more microns in coal-fired sources.

Piezoelectric microbalances appear to be quite adaptable to monitoring emissions from oil-fired facilities. Particle sizes are typically small (less than approximately 1 micron). The particles are sticky. Mass concentrations are about 10 times less than coal-fired emissions, resulting in 10 times more instrument operating time before cleaning is required.

As mentioned previously, water or vapor condensation on the crystal can cause erratic operation. This can probably be overcome by diluting the sampled gas and/or heating the crystals.

CONCLUSIONS

The piezoelectric particle microbalance for measuring the total mass concentration of particulate emissions from stationary combustion sources has the following advantages:

(1) It measures particle mass only; it is thus an instrument universally applicable to all stacks without calibration.

(2) It is very sensitive, resulting in high accuracy and time resolution.

(3) It is simple, compact, and rugged, which leads to reliability and moderate cost ($7,000 - $10,000).

(4) It can be easily used with several particle collectors, including impactors and electrostatic precipitators.

It has the following disadvantages:

(1) The crystals require cleaning. If done automatically, this represents an additional system complexity.

---

*See properties of emissions elsewhere in this report.

(2) A potential upper particle size limitation exists.

(3) The instrument makes a point measurement and, with the small sample rate allowable, this may be a disadvantage.

(4) An extracted sample is required. Without dilution or heating this will result in water or other liquids condensing on the crystal and subsequent unstable operation.

(5) The instrument has not yet been used in stacks.

The disadvantages do not seem prohibitive. They can probably be overcome with the appropriate designs discussed in the text.

REFERENCES

1223 Chuan, R. L., "An Instrument for the Direct Measurement of Particulate Mass", Aerosol Science, V. 1, p. 111-114 (1970).

1352 King, W. H., Jr., "Using Quartz Crystals as Sorption Detectors, Parts 1 and 2", Research/Development, V. 20, no. 28, p. 28-34 (Apr 1969), and V. 20, no. 28, p. 28-33 (May 1969).

244 Olin, J. G., and Sem, G. J., "Piezoelectric Aerosol Mass Concentration Monitor", paper presented at Symp. on Advances in Instrumentation for Air Pollution Control, Cincinnati, Ohio, May 26-28, 1969.

1222 Olin, J. G., Sem, G. J., and Christenson, D. L. "Piezoelectric/Electrostatic Aerosol Mass Concentration Monitor", Presented at Amer. Ind. Hyg. Assoc. Annual Conference, Detroit, Mich., (May 11 - 15, 1970).

1351 Olin, J. G., Trautner, R. P., and Sem, G. J. "Air-Quality Monitoring of Particle Mass Concentration with A Piezoelectric Particle Microbalance", Paper No. 71-1, 64th Annual Meeting, Air Pollution Control Association, Atlantic City, N.J. (Jun - Jul 1971).

1221 Sauerbrey, G. A., "Verwendung von Schwing-quarzen sur Wagund dunner Schichten und zur Mikrowagung", Seits. Phys., V. 155, p. 206 (1959).

REFERENCES NOT REFERRED TO IN TEXT

1187 Leemhorst, J. W., "Direct Measurement of Particulate Mass and Humidity", Contamination Control, p. 11-14 (Jul-Aug 1970).

252 Rogallo, V. L., and Newman, F., "A Wide-Range Piezoelectric Momentum Transducer for Measuring Micrometeoroid Impacts", Ames Research Center, Moffett Field, Calif., Clearinghouse No. NASA TN D-2938 (Jul 1965).

RESONANT FREQUENCY

by: J. G. Olin and F. D. Dorman

INTRODUCTION AND PRINCIPLE OF OPERATION

The resonant, or natural, frequency of a vibrating spring-mass system decreases if the mass is increased. The same is true of any mechanical system vibrating at its resonant frequency.

Figure 1 shows some typical vibrating mechanical systems - the spring-mass system, the torsional system, the cantilevered beam system and the vibrating wire. In all cases the resonant frequency f is inversely proportional to the square root of mass m, or

$$f = \frac{C}{\sqrt{m}}, \qquad (1)$$

Where C is a constant depending on the geometry of the vibrating system and its elastic, inertial, and force constants. The change in resonant frequency df is

$$\frac{df}{f} = -1/2 \frac{dm}{m}, \qquad (2)$$

Figure 2 shows one possible mechanical resonant frequency system. The physical configuration is tubular with Figure 2 being an axial cross-section. The filter is made of rigid, porous material while the thin-walled tube can flex to some degree. The oscillator circuit-magnetic coupling causes the filter-tube system to vibrate torsionally at its natural frequency. As particles collect in the filter, the natural frequency decreases in proportion to the mass of added particles. A frequency counter monitors the output. The filter may be sintered metal or porous ceramic. The filter could possibly be cleaned periodically by a reverse blast of air or liquid cleaning solution.

Piezoelectric crystals, such as quartz crystals,constitute a class of resonant frequency devices. They are discussed in detail in the section entitled "Piezoelectric Microbalance".

APPLICATION TO MASS CONCENTRATION MEASUREMENT IN STACKS

Mechanical Vibrators

Since nearly all mechanical resonant frequency devices, including the one described in Figure 2, are only in the conceptual stage, no data or specific working hardware can be discussed. The remainder of this discussion is limited to general concepts.

1. Spring-Mass System

$$f = \frac{1}{2\pi}\sqrt{\frac{k}{m}}$$

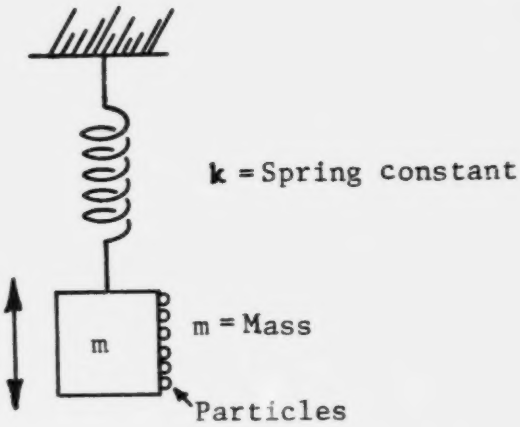
k = Spring constant
m
m = Mass
Particles

2. Torsional System

$$f = \frac{1}{2\pi}\sqrt{\frac{K}{J}}$$

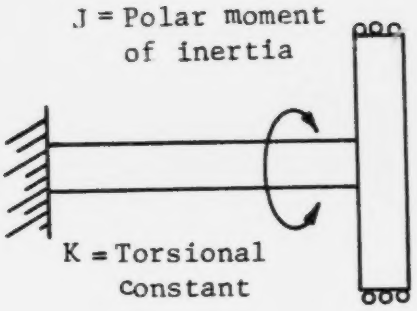
J = Polar moment of inertia
K = Torsional constant

3. Cantilever System

$$f = \frac{1}{2\pi}\sqrt{\frac{3EI}{mL^3}}$$

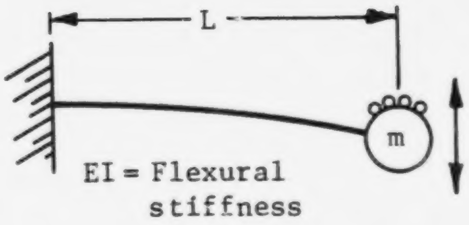
L
m
EI = Flexural stiffness

4. Vibrating Wire

$$f = \frac{1}{2L}\sqrt{\frac{TL}{m}}$$

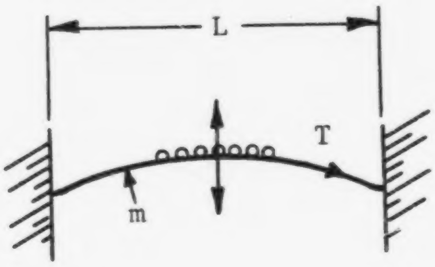

Fig. 1. Typical mechanical vibration systems.

Particles can be deposited onto resonant frequency devices in several ways, including the following common methods:

(a) Impaction,

(b) Electrostatic precipitation, and

(c) Filtration.

In mechanical systems it is advantageous to deposit the particles onto a non-vibrating surface which is unstrained, such as a large "dead" mass. Otherwise, the particulate layer will become strained. Since its elastic properties are undoubtedly different than that of the vibrator, they become additional variables which must be taken into account. This should be avoided. None of the systems shown in Figure 1 have this problem.

The use of resonant mechanical systems for particle mass measurement is a very new field. The work of Gast[1228] with the vibrating wire shown in Figure 1 is the only reported reference known by the authors. Gast uses a relatively complicated feedback control system to maintain the wire at constant tension. The output of the system is the voltage necessary to maintain constant tension. As with piezoelectric particle microbalances, a reference wire which is kept free of particles is used to subtract extraneous changes in temperature, etc., out of the signal. The major problem with the vibrating wire is the difficulty of distributing a representative particulate sample on the wire. Studies of the collection efficiency of fiber filters show that suspending a wire across the stack simply will not have a high or repeatable collection efficiency. Unless a good particle collection mechanism is developed, the vibrating wire is not a good candidate for stack monitoring. It is doubtful that such a collector can be devised.

Shear (e.g., torsional) vibrating systems are generally superior to longitudinal or transverse (spring-mass, centilever, and vibrating wire) vibrating systems. The major energy loss is the viscous loss caused by the shear stress in the hydrodynamic boundary layer. On the other hand, longitudinal or transverse systems alternately compress and expand the adjacent fluid (air) and create sound waves. This requires relatively large amounts of energy to overcome the resulting damping.

In the ideal case of no damping, any vibrating system has zero energy loss. The amplitude of such a vibrating system is constant. This means the system has infinite sensitivity, i.e., it will vibrate at precisely the resonant frequency of the system. As the damping of the system increases, the resonant amplitude decreases with an accompanying broadening of the amplitude-frequency peak, resulting in loss of sensitivity. This phenomenon is shown in Figure 3 for the damped spring-mass system[1239]. In electronics, the parameter Q is a measure of the sharpness of the amplitude-frequency distribution. A very high Q is desirable for generating precise frequencies. For these reasons, shear systems are preferable to other systems. The same conclusion is also true for piezoelectric systems.

Based on these considerations, a torsional system appears to be the best mechanical system. A torsional system with good potential for stack monitoring is shown in Figure 2. Particles are captured with a filter. This permits collecting essentially all particles with 100% efficiency. The filter must be cleaned or replaced periodically. It could be cleaned automatically by flushing with a liquid. An impaction or electrostatic precipitation particle collector could also be used to deposit particles onto the surface of the torsional system. In this case, larger particles may not be sensed with 100% efficiency because they may slide relative to the sensor surface.

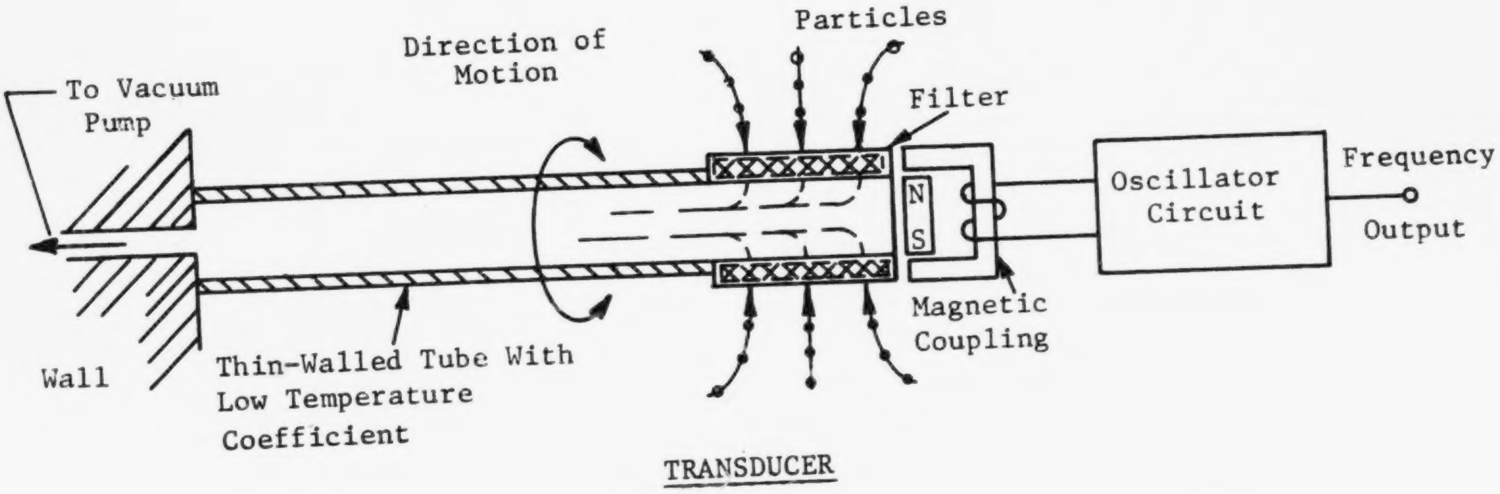

Fig. 2. Torsional filter system transducer.

Mechanical vibrating systems have a major advantage over piezoelectric systems: they have significantly lower resonant frequencies. Therefore, they should be able to sense larger particles because the inertial force acting on the particles is proportional to f^2. Lower frequencies are also associated with reduced mass sensitivity. In stacks, this may not be a problem because particle concentrations are high. Hence, a large mass of particles can be deposited onto the sensor in relatively short time periods.

A reference vibrator, identical to the primary vibrator used to measure particle mass, can be used to subtract out the effects of changes in the temperature of the gas stream. A mixer circuit is used to subtract the frequency signals of the primary and reference vibrators. Furthermore, materials with low sensitivity to temperature can be selected for the vibrating member of the system (e.g., the tube of the torsional system). This is equivalent to the selection of quartz crystals with low temperature coefficients. This means mechanical vibrators can be made relatively insensitive to all environmental and particle parameters except particle mass. This is indeed an important advantage.

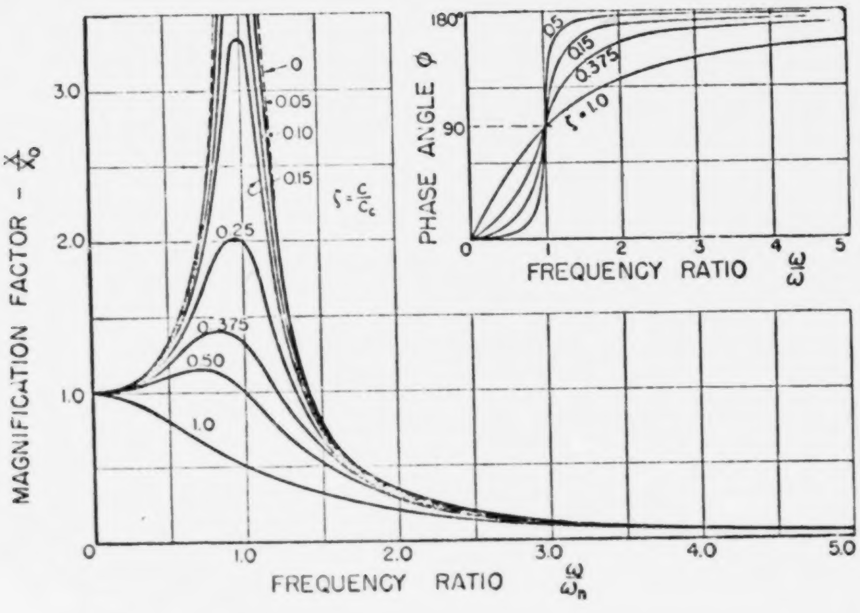

Fig. 3. Resonant amplitude as a function of resonant frequency for a damped spring-mass system from Thomson[3].

CONCLUSIONS

Mechanical resonant frequency systems have the following advantages for monitoring particle mass concentration in stacks:

(a) They measure particle mass. Extraneous effects can be eliminated.

(b) They are inherently simple, rugged devices.

The main disadvantage is their infant state of development. A torsional vibrator with a filter collector has good potential for stack monitoring. The development of mechanical resonant frequency devices should be pursued further.

Piezoelectric vibrators constitute a class of resonant frequency devices. They are discussed in detail in the section entitled "Piezoelectric Microbalance". They have much greater mass sensitivity and resolution than most mechanical vibrators.

REFERENCES

1228 Gast, T., "Akustische Ruckkopplung als Hilfsmittel bei der Bestimmung von Staubkonzentrationen mit Hilfe eines Schwingenden Bandes", Staub-Reinhalt der Luft, V. 30, no. 6, p. 235-238 (Jun 1970).

1239 Thomson, W. T., Mechanical Vibrations, 2nd Ed., Prentice-Hall, Inc., Englewood Cliffs, N.J. (1953).

GRAVIMETRIC WEIGHING

by: John Borgos

INTRODUCTION

Gravimetric weighing devices have been important tools in science and technology for hundreds of years. They are simple to understand, relatively inexpensive to construct, easy to calibrate, and readily applied to a wide variety of situations where a measurement of mass is required. The principle employed is that the force due to gravity acting on an object is proportional to the mass of the object. Since the force of gravity is familiar and fairly constant, it is used often to define standard units of mass or weight.

A gravimetric weighing device can be used to measure the mass concentration of particles in an airstream. The particles must be deposited on a suitable substrate before they can be weighed. This usually involves use of an impactor, filter, or electrostatic precipitator. The measured mass of particles divided by the volume of air sampled gives mass concentration directly.

PRINCIPLES OF OPERATION

A gravimetric weighing device consists basically of a pivot point about which two equal and opposing torques act. One torque is set up by the weight of the particle sample whose mass is to be determined. The other torque is usually controlled, either manually or automatically, such that a "null" position is reached where both torques are equal. Several techniques are possible for measuring and controlling this opposing torque.

The first and most obvious technique is to maintain balance by using opposing weights (Figure 1). This instrument is traditionally known as the analytical balance. Its operation is familiar enough that it need not be discussed further. Such instruments can be made sensitive to mass changes of a few micrograms.

A second technique, described by Gast[243] and shown in Figure 2, uses an electromagnet to produce the restoring torque necessary to maintain zero offset. When weight is applied to the balance beam, it tends to rotate slightly. This rotation is immediately opposed by the electromagnet, which applies a compensating torque around the pivot point. By measuring the current through the electromagnet required to maintain the balance at the null position, the weight on the balance arm can be calculated. This instrument is sensitive to a minimum weight change of about 10 micrograms. Mauer[1096] describes a similar instrument, but his sensitivity is on the order of 10 milligrams.

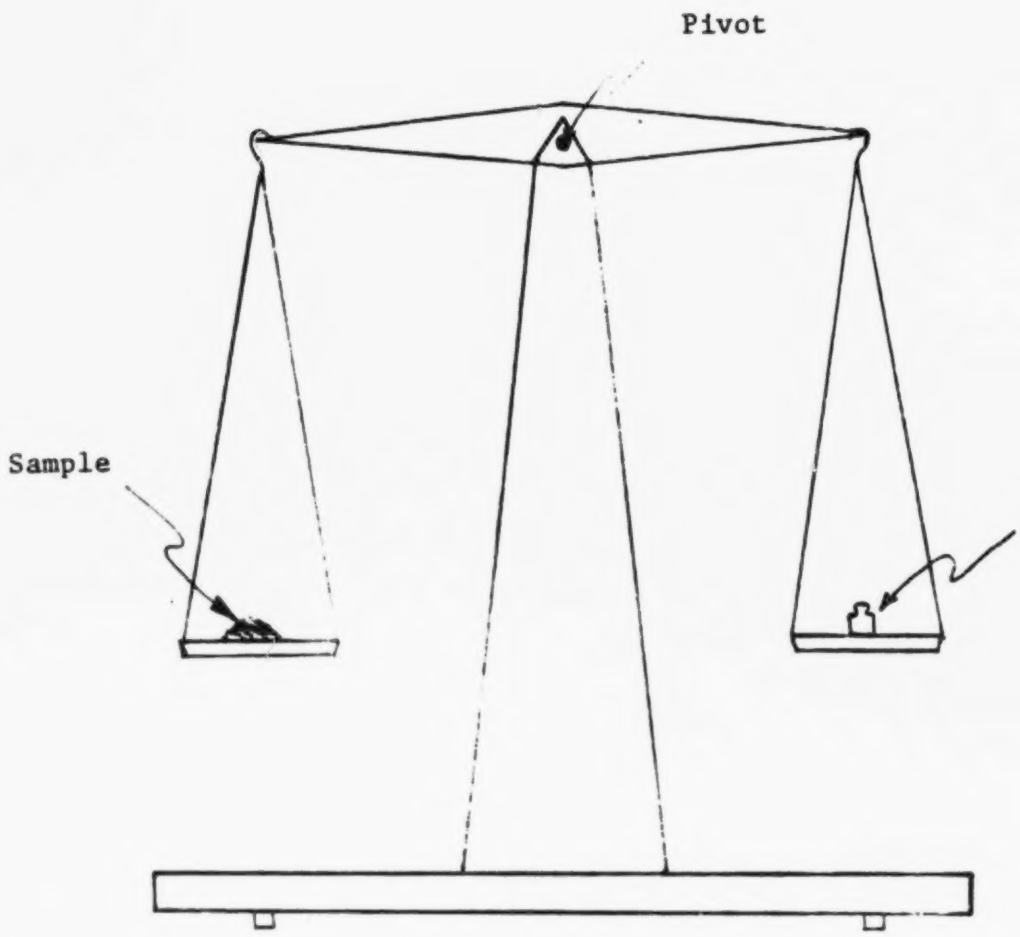
Pivot
Sample
Balance
Mass

Fig. 1. Basic configuration of analytical balance.

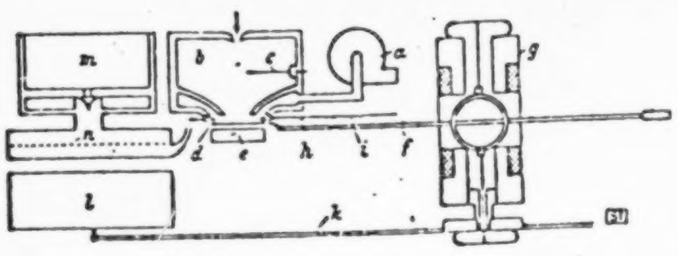
m
b
c
a
g
n
d
e
h
i
f
l
k

Fig. 2. Principle of the recording dust balance: (a) suction pump; (b) separation chamber; (c) discharge wire; (d) electrode: (e) pressure plate; (f) balance beam; (g) microbalance; (h) control disk; (i) velvet strip; (k) scriber; (l) wax paper roll; (m) auxiliary blower; (n) paper filter.[225,243]

A third technique, described by Peterson,[938] is really a modification that can be added to any conventional analytical balance to increase its sensitivity. The operational principle involved is that the induced voltage in the secondary coil of a transformer is linearly related to the position of the core for small (i.e., <.030 inch) displacements of the core. A differential transformer is used, which has three coils: one primary and two secondary coils. The secondary coils are electrically connected such that their output voltages oppose each other. The core is attached to the analytical balance beam and can move freely in the cylindrical space inside the coils. At the null position, the core induces equal voltages in the two secondary coils, and the resultant output voltage is zero. Any displacement of the core causes an increase in one secondary coil voltage and a decrease in the other, resulting in an output voltage. This output voltage can be amplified and interpreted in terms of mass loading. Sensitivities as low as 0.1 microgram can be achieved with this technique.

A fourth technique is described by Caule and McCully[1097] for recording rapid changes in weight (Figure 3). This, too, is really a modification that can be made to an existing balance to increase its sensitivity. Two coils are used. One is fixed in position on the base of the balance and is supplied with A.C. power. The other is hung from the beam of the balance. By Lenz's law, the primary and secondary currents will be repulsive. Thus, by measuring the primary current required to maintain the null position, the weight of a sample can be calculated. Mass sensitivity is on the order of one milligram.

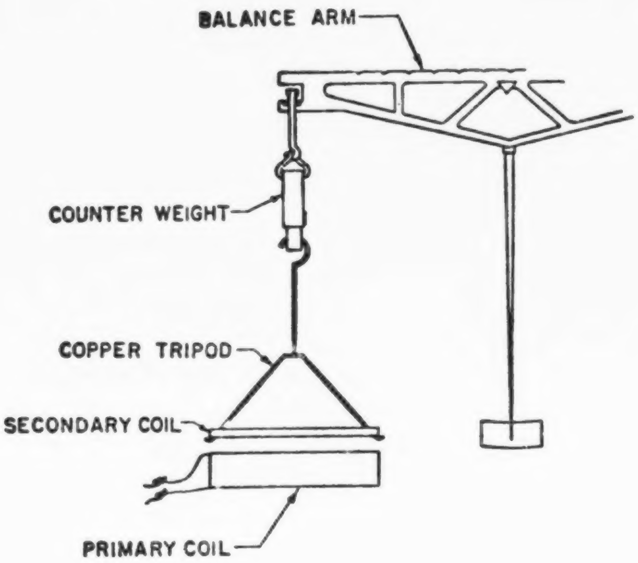

Fig. 3. Sketch showing arrangement of coils and support from balance arm on Caule and McCully sensing technique.[1097]

A fifth technique appears possible which uses a resistor whose resistance value changes as the flux density of a surrounding magnetic field. This phenomena is known as magnetoresistance. Such a resistor might be attached to the balance arm of some device, and a permanent magnet could be attached such that its magnetic field surrounds the resistor. Then any offset of the balance arm would change the position of the resistor in the magnetic field, therefore changing the local flux density and hence the resistance. Sensitivities as low as one microgram might be possible.

When gravimetric weighing devices are used for measuring particle concentrations, a means of collecting the particles is needed. Of the instruments described above, only that of Gast has been used for measuring aerosol mass concentration (Figure 2). This instrument electrostatically deposits the particles on a precipitation plate which is attached to the beam of the electromagnetically controlled balance. The surface on which the particles are actually deposited is a foil section which is automatically cut from a supply roll and discarded after the measurement is completed.[225] An earlier version[243] used a brush to clean the deposition surface, but this did not work for fly ash because the particles were too sticky to be removed. The aspirated gas flow rate is about 60 liters per minute. At a particle concentration of 100 mg/m^3, the instrument need only sample a few minutes to get enough mass accumulated for an accurate reading.

Either an impactor or filter would also be feasible for separation of the particles from the airstream. In any case, the collection surface must be locked while the particles are being collected and freed when weighing is done. The air flow must also be turned off or diverted when weighing is done to avoid disturbing the balance. Thus, any automatic gravimetric device must have a mechanism for cleaning or replacing the collection surface and executing the measurement cycle.

APPLICATION TO MASS CONCENTRATION MEASUREMENT IN STACKS

Only one gravimetric weighing device has been tested in a stack. This is the instrument described by Gast[243] and later revised.[225] This work has shown that the gravimetric weighing technique can be used for stack monitoring, but it has several limitations. It must be maintained at a high enough temperature to avoid condenstaion of vapors. It has a sensitivty limitation because it must be rugged enough to be immune to the vibration around a stack; with this in mind, the best sensitivity that can be achieved is around 1 - 10 mg, which represents a fairly large mass of particles. A sampling train is required in which some particles will inevitably be lost. A sophisticated mechanism would be necessary to clean or replace the particle collecting surface; this reduces the reliability of the instrument and makes it only quasi-continuous. It probably would sell for more than $10,000 when commercially developed.

Nevertheless, the gravimetric weighing technique does possess the enviable advantage that it measures the dust mass and not some other physical quantity. Therefore, since the difficulties are mainly engineering problems that do not make the technique inherently incapable of monitoring stack gases, we place emphasis on the value of such instrumentation. Because it is not now available commercially, development should be postponed until several other sensing methods are tested and proven. Many of the limitations listed above can be eliminated in future development programs.

CONCLUSIONS

The gravimetric weighing technique appears to be a somewhat promising method for monitoring particle mass concentration in stacks because:

1) It has the advantage that it measures the particle mass directly,

2) At least one instrument has been developed, although it is not commercially available, and

3) The technique is well understood, so that the problems are mainly engineering problems.

Several disadvantages limit its immediate usefulness and make it less promising than several other techniques:

1) It requires some sophisticated machinery, so reliability may be poor,

2) It is especially sensitive to mechanical vibrations, which can be severe near stacks,

3) A sampling probe is required, so it is subject to errors due to losses within the probe, and

4) It gives a point rather than an integrated measurement (further study may well indicate this is not a disadvantage for some applications).

Gravimetric weighing devices are inherently quite accurate for measuring particle mass, and development work should be done in the future to fully evaluate the usefullness of automation. Although they are potentially a strong competitor for stack monitoring instrumentation, immediate attention should be given to other more well developed methods which appear simpler and which may be used in stacks with less additional development.

REFERENCES

938 Aronson, M. H., and Peterson, A. H., "A New Recording Microbalance", Instruments & Automation, (Jul 1955).

1097 Caule, E. J., and McCully, G., "An Automatic Recording Analytical Balance", Canadian Journal of Technology, V. 33, p. 1 (1955).

225 Duwel, L., "Latest State of Development of Control Instruments for the Continuous Monitoring of Dust Emissions", Staub-Reinhalt der Luft (Engl. Trans.), V. 28, no. 3, p. 42-53 (Mar 1968).

243 Gast, T., "Staubmessgerate mit massenproportionaler Anzeige oder Registrierung", Staub-Reinhalt der Luft, V. 20, no. 8, p. 266-272 (Aug 1960).

1096 Mauer, F. A., "An Analytical Balance for Recording Rapid Changes in Weight", The Review of Scientific Instruments, V. 25, p. 598-602 (1954).

ELECTROSTATIC MEASUREMENT METHODS

by: Gilmore J. Sem

Three basic electrostatic particle concentration measuring techniques are available for stack monitoring:

1. ION CURRENT ATTENUATION
2. ION CAPTURE
3. CONTACT CHARGE TRANSFER

Each technique is discussed separately below. A conclusion section at the end of this electrostatic report summarizes the potential of such techniques for particle mass emissions measurement from large coal- and oil-fired combustion sources.

ION CURRENT ATTENUATION

As particles pass through a cloud of ions, the particles acquire an electrostatic charge which they carry away, reducing the concentration of ions in the cloud. Assuming a constant particle size distribution, the greater the concentration of particles passing through a cloud, the greater the reduction, or attenuation of the ion concentration. Thus, the decrease in ion concentration is an indication of the concentration of particles. The specific concentration parameter measured by this method will be discussed later.

Hasenclever and Siegmann[242] and Coenen[1040, 245, 284] discuss one instrument design utilizing ion current attenuation. Figure 1, taken from a review article by Schutz[659] describes the instrument. A pump draws dusty air laminarly through the ionization chamber. A radioactive source, 8 microcuries of Cobalt-60, is uniformly distributed around the inner side of the outer tube, creating a low bipolar concentration of ions. Ions of one polarity are drawn across the chamber to the central electrode by a small electric potential. The ion current, collected on the center electrode and measured by an electrometer, decreases with increasing dust concentration.

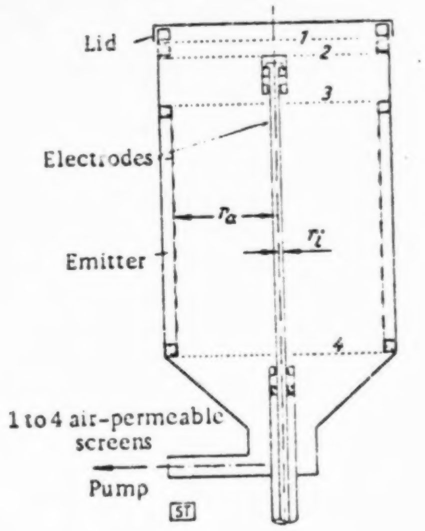

Fig. 1. An ion current attenuation design from Schutz[659].

Mohnen and Holtz[581] describe an instrument which uses two chambers similar to the one in Figure 1. One chamber operates as described above with aerosol passing through. The second chamber operates identically except that the entering air is filtered. This system automatically compares the attenuated current in the aerosol chamber with the reference current in the identical clean-air chamber so that the electrical output signal is directly proportional to ion current attenuation. In the one-chamber design, this comparison must be done manually, a procedure which becomes quite difficult with rapidly fluctuating aerosols. An additional advantage of the two-chamber system is that the clean-air chamber uses the same high voltage power supply so that any voltage fluctuations are nulled out.

The essential components of an ion current attenuation instrument are a constant supply of unipolar ions and a method of measuring the decrease in ion current between the electrodes due to ions carried away by particles. The specific instruments described above use a radioactive ion source because it supplies an essentially constant supply of ions. Since the radioactive source produces ions of both polarities, an electric field across the flow channel is necessary to eliminate one polarity. Fluctuations in the voltage producing the electric field result in similar fluctuations in measured ion current which, in turn, becomes an error in measured particle concentration. Other unipolar ion sources appear to have similar or greater problems. For example, traditional high voltage corona discharge devices are difficult to control such that they produce a constant supply of ions. They also expose the particles to a high electric field, causing many particles to collect on the walls of the device. This results in rapid contamination of the instrument, and an error in the measurement since some particles do not escape the ionizing chamber. The radioactive ion source also utilizes an electric field, but the field is much lower in intensity resulting in considerably less particle collection in the ionizing chamber.

However, since the radioactive sources used in ambient air monitors appear too weak to supply enough ions for stack particle concentrations (see discussion below) alternate designs may be necessary. Sample dilution upstream of the sensor is one possible solution. Another is to find other radioactive materials which result in higher ion production. A third alternative is to use properly designed corona discharge ion sources.

Figure 2 shows schematically a number of possible designs conceived by the authors for an ion current attenuation instrument using corona current ion sources. Designs A - E use primarily field charging while design F uses diffusion charging. Thus, designs A - E would place charge proportional to D^2 (surface area) on the particles if the particles become charge saturated. Design F would place charge proportional to about $D_p^{1.2}$ if the particles became charge saturated.

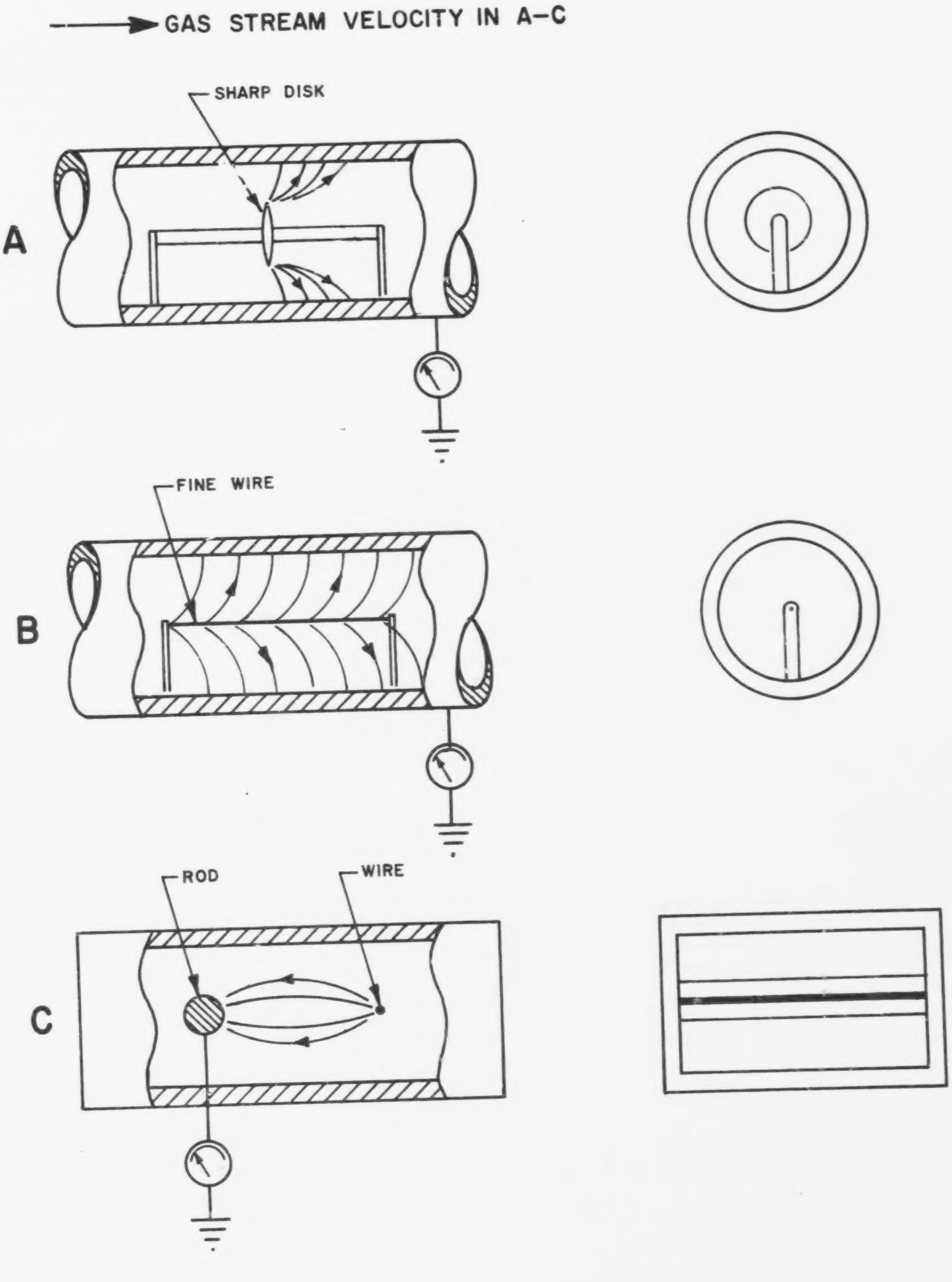
GAS STREAM VELOCITY IN A–C
SHARP DISK
A
FINE WIRE
B
ROD
WIRE
C

Figure 2. A, B, C. Other ion current attenuation designs.

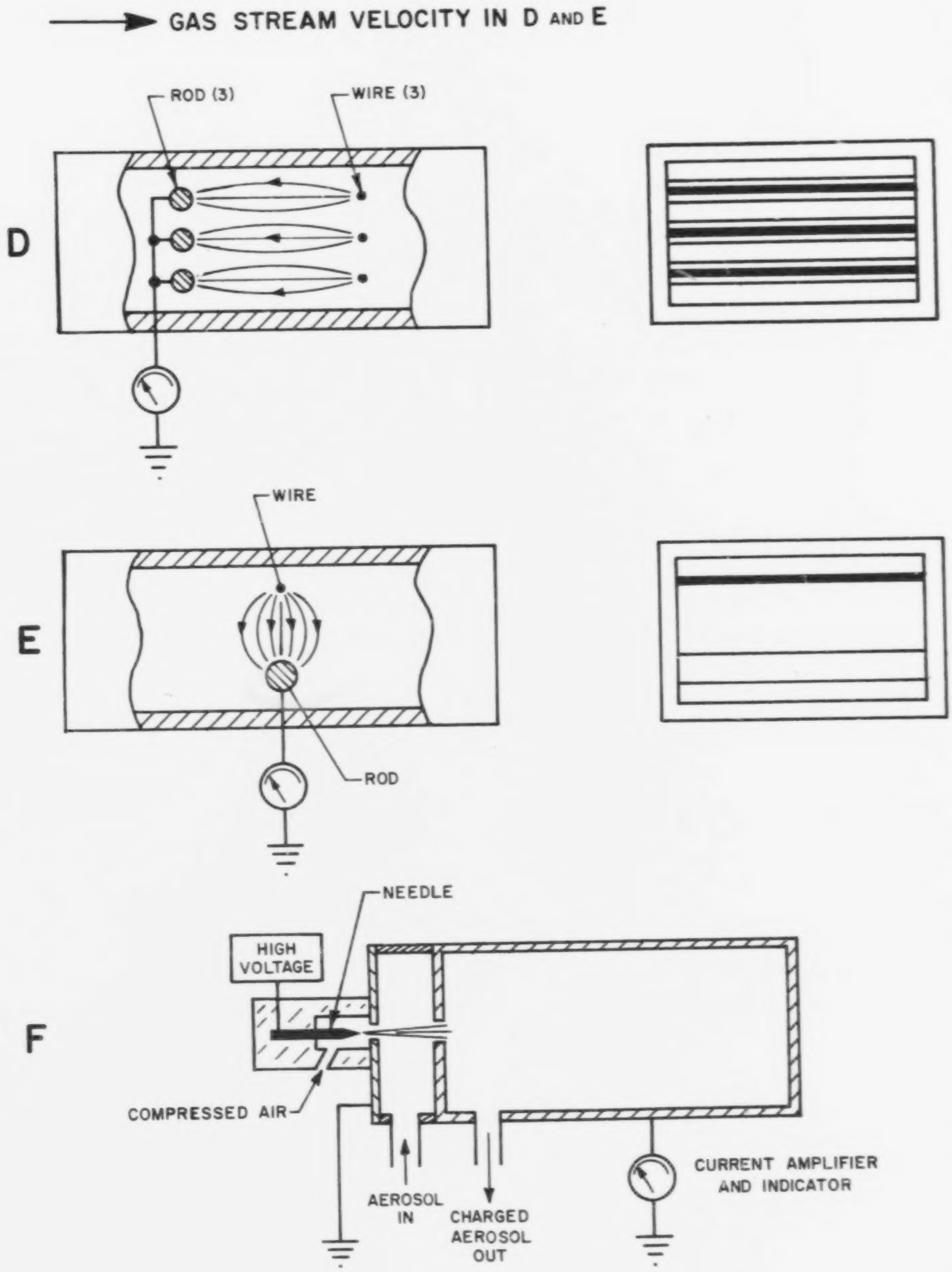
GAS STREAM VELOCITY IN D AND E
D
ROD (3)
WIRE (3)
E
WIRE
ROD
F
NEEDLE
HIGH VOLTAGE
COMPRESSED AIR
AEROSOL IN
CHARGED AEROSOL OUT
CURRENT AMPLIFIER AND INDICATOR

Figure 2. D, E, F. Other ion current attenuation designs.

Designs C and D would minimize particle deposition in the charging area. The mobility of the ions is at least an order of magnitude greater than most of the particles. Thus, the aerosol velocity can be chosen such that ions travel from the corona wire to the current sensing rods while the charged particles pass through. The other designs would definitely require periodic cleaning. Designs C and D may need cleaning, but much less often.

Designs B and F subject nearly all the particles to identical charging conditions while the other designs do not. However, design B will probably have large particle deposition, causing a measurement error and instrument contamination. Design F depends on the particles remaining airborne for the time required to pass completely through the charging chamber. This may be on the order of 10 - 60 seconds, long enough for large particles to settle out due to gravity. Some of the particles will also be lost to the walls because of the mutual repulsion of the charged particles.

Design F closely resembles the particle charger on the Whitby aerosol analyzer (electrical particle counter)[68]. Design A resembles the ion drift anemometer used for measuring the mass flow of a gas.

Designs A - E offer the possibility of easily detecting the ion current attenuation caused by the particles. Figure 3 shows the basic scheme. The ion current attenuation, which is directly proportional to particle concentration, is

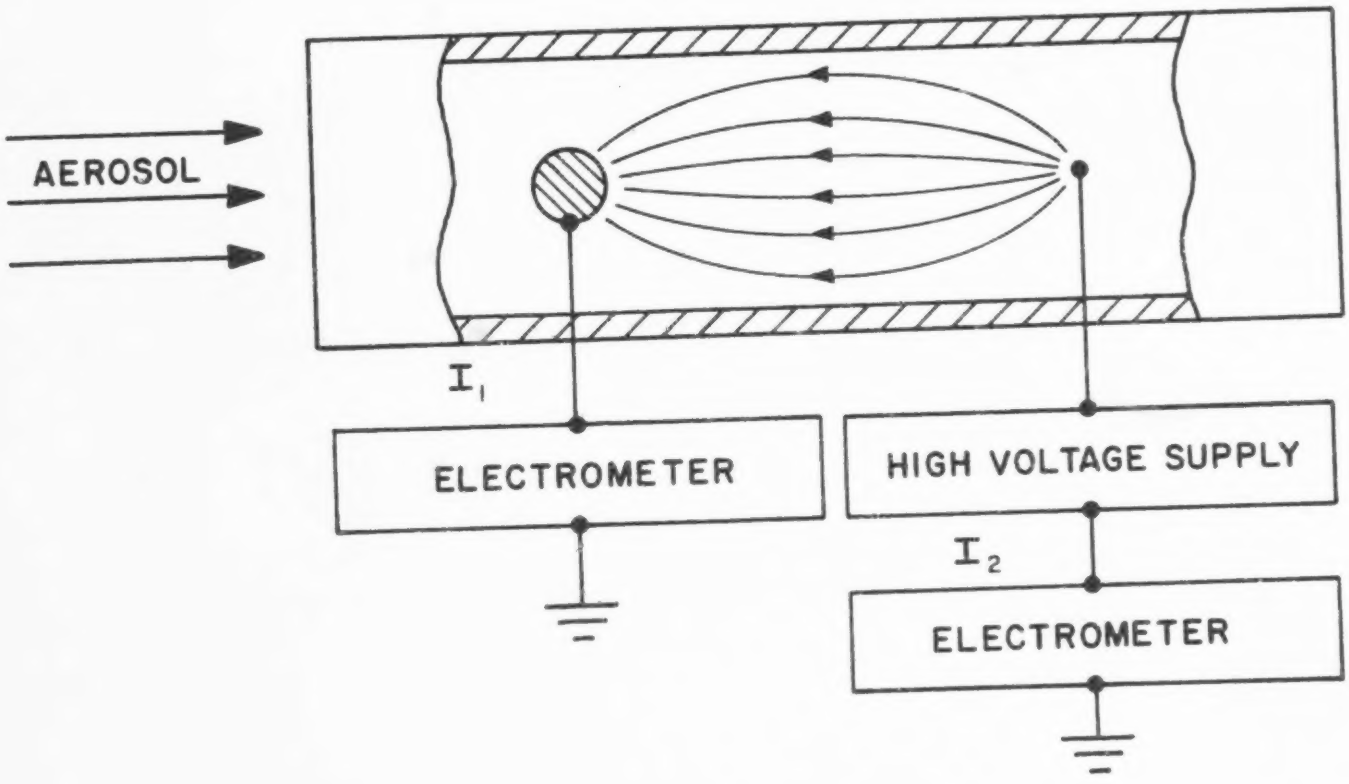

Figure 3. Complete ion current attenuation instrument system for designs shown in Figure 2: A-E.

simply ($I_2 - I_1$). Design F cannot use the same scheme since much of the total ion current is lost in the ionizer orifice area.

Any of these techniques may work. More detailed design and development is needed to fully evaluate each concept. For use as a particle concentration monitor where the mass of particles is not the important parameter, ion current attenuation appears to be one of the best candidates.

Application to Mass Emissions Measurement in Stacks

Figure 4 shows the current ratio of I/I_o compared with gravimetric concentrations for a number of tests using quartz dust with a mean particle size of 0.7 μm in Coenen's[1040] instrument. Notice the nearly linear relationship and good correlation above 1 mg/m^3. In these tests, very small condensation nuclei were eliminated. Apparently, small weights of such nuclei can cause large attenuation of the ion current, resulting in very poor correlation with gravimetric measurements. Since combustion particle sources, such as coal- and oil-fired combustion facilities, probably emit large and varying numbers of such nuclei, somewhat poorer correlation could be expected than that shown in Figure 4.

The high particle concentrations encountered in coal combustion emissions would pose a problem for ion current attenuation instruments which are normally used for measuring cleaner atmospheres such as outdoor city pollution. Figure 4 indicates about 30% attenuation with less than 10 mg/m^3 concentration of quartz dust. At concentrations normally encountered in coal combustion emissions (100 mg/m^3), extrapolation of Figure 4 indicates almost complete attenuation of the ion current. Presumably, good engineering design could improve such an instrument for stack concentrations, but some dilution would probably be necessary. The other proposed designs would presumably operate at higher concentration levels, but further experimental and theoretical work is needed to define the operating range.

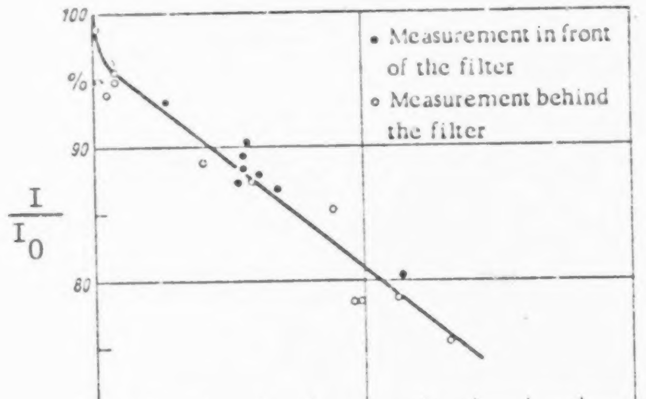

Figure 4. Gravimetric calibration of ion current attenuation instrument on quartz dust according to Coenen[1040].

The difficulties in measuring relatively small current levels with an electrometer may be a problem for stack use. Current levels of 10^{-7} to 10^{-10} amperes could be expected. The insulation of the central electrode in stack environments could probably be done but would require careful design.

Ion current attenuation will probably never yield an output response which correlates well with particle mass concentration. Thus, it cannot be recommended for such measurements. However, the technique appears to offer several important features for other particle concentration measurements, including instantaneous response proportional roughly to particle surface area concentration, another important particle parameter which is more sensitive to submicron particles than is particle mass. The technique offers design simplicity with corresponding low cost. The technique requires point sampling, a necessary feature for many particulate emissions measurements. These features recommend this technique for further research and development to overcome the operational difficulties discussed above.

Application to Particle Size Measurement in Stacks

The ion current attenuation technique does not appear capable of measuring size distribution of particles by itself. However, it could be used as a particle concentration detector downstream from a particle size classifier, such as an impactor or electrical mobility separator.

The ion current attenuation monitor is very sensitive to particles below 0.1 μm and less sensitive to larger particles. Thus, there may be a problem using this technique behind an impactor since impactors operate in the range above 0.3 μm at ambient pressure. In stacks with relatively small numbers of particles below 0.1 μm, such a combination holds some promise. However, if considerable numbers of particles exist below 0.1 μm, particularly if the concentration of such particles fluctuates, they may completely mask out the changes in ion current due to the impactor. Other, more promising, methods exist for measuring particle size distributions in this range.

If an electrical mobility separator (described in the next section) is used to classify particles by size, a simpler, more accurate method exists for measuring particle concentration. The next section on ion capture discusses the better method.

ION CAPTURE

Another way of using the charging of particles passing through an ion cloud for measuring aerosol particle concentration is to measure the ion current carried away by the particles. This can be done, as shown in Figure 5, by collecting the particles, either by filtration or by electrostatic precipitation, and measuring the current draining from the particles to ground with an electrometer. Several such instruments have been developed.

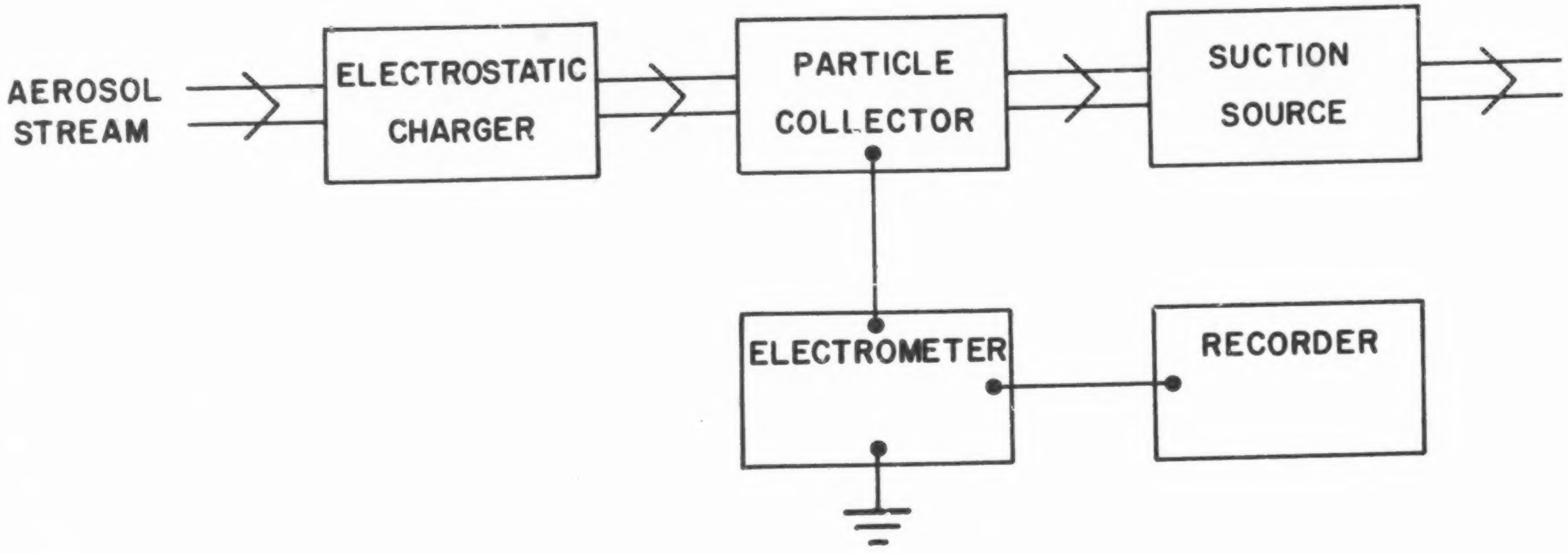
AEROSOL
STREAM
ELECTROSTATIC
CHARGER
PARTICLE
COLLECTOR
SUCTION
SOURCE
ELECTROMETER
RECORDER

Figure 5. Basic requirements for ion capture measurements.

Grindell[554,122,552] reported on the electrostatic dust monitor shown in Figure 6. The sensing portion of the monitor is located outside the stack. As flue gas passes through the monitor, particles first become charged by a corona discharge. The particles then pass into the collecting section where an electric field precipitates them onto the tube wall. The charge carried by the particles then passes through an electrometer to ground. The measured current, a direct indication of particle surface area passing through the monitor per unit time, can be amplified and recorded.

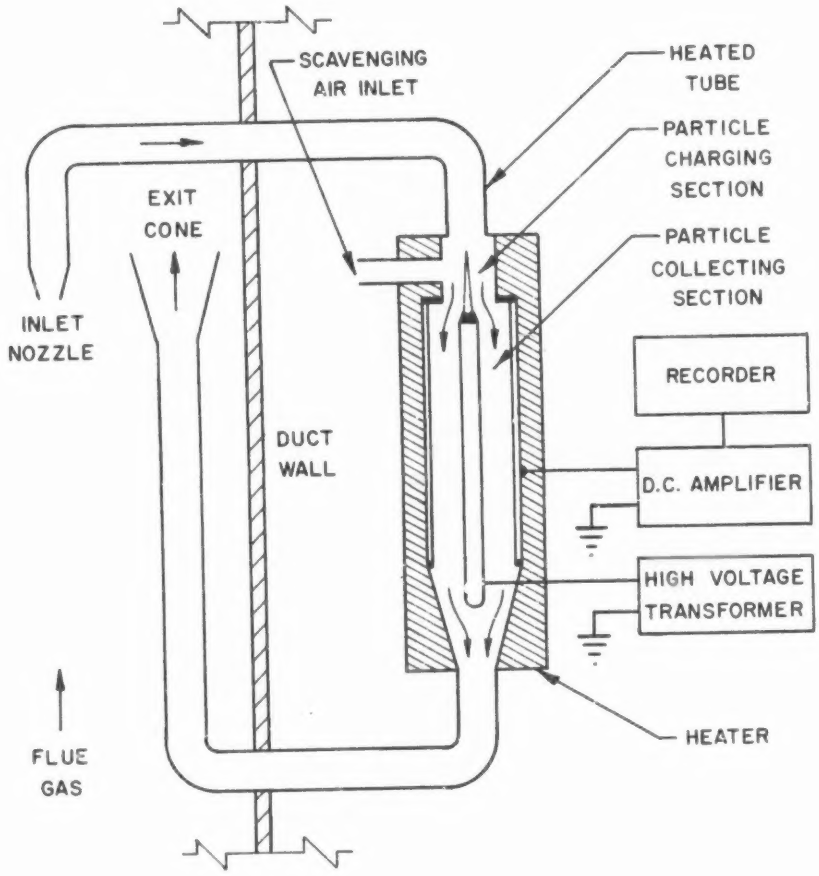
SCAVENGING AIR INLET
HEATED TUBE
PARTICLE CHARGING SECTION
PARTICLE COLLECTING SECTION
EXIT CONE
INLET NOZZLE
RECORDER
DUCT WALL
D.C. AMPLIFIER
HIGH VOLTAGE TRANSFORMER
FLUE GAS
HEATER

Fig. 6. An ion capture design from Grindell.[544]

The monitor responds automatically to changes in stack gas velocity because of the unique suction system. Flue gas passing the exit cone causes a suction inside the cone. Since the electrostatic system causes very little resistance to gas flow, little suction is needed. By correct design of the exit cone and the inlet nozzle, nearly isokinetic sampling can be automatically obtained over a reasonable range of stack gas flow conditions, a very desirable feature.

This suction system has the additional feature of making the measurement proportional to particulate emissions per unit time rather than just particle concentration such as most monitors measure. As the velocity of gas past the exit cone increases, the rate of suction automatically increases. Thus, the instrument responds to the product of particle concentration and volumetric gas flow rate, yielding a direct measurement of the particulate emissions rate. This would simplify interpretation of data from stacks with changing flow conditions.

Since the charging mechanism here is primarily field charging, the monitor is sensitive to particle surface area.[1211] Grindell[122,554] points out several advantages to surface area measurements, and discusses, in some detail, the theoretical basis for the monitor.

The Grindell monitor cleans itself periodically by rapping the collector electrode and purging the monitor with a blast of relatively clean, outside air. The purge air enters the monitor through a wide mesh which also forms the ground electrode from the corona discharge. Grindell reports little particle loss in the charging region during the measuring operation. However, what does collect in the charging region as well as what deposits elsewhere, including the precipitating region, is cleaned out well by rapping and purging for about 30 sec every 20 min.

The monitor must be heated above the dew point of the vapors in the stacks. An earlier Grindell monitor was designed for mounting inside the the stack, eliminating the need for external heating. However, because of installation difficulties, he mounted models outside the stack and supplied 700 watts to the outside casing of the body and the exterior pipes to raise the temperature to about 100°C. Reasons for heating the monitor are:

a) To prevent excessive corrosion of metal parts,

b) Damp fly ash contaminates the monitor and will not come off with an air blast,

c) Moisture interferes with the electrical insulators, and

d) Electrolytes in contact with dissimilar metals cause a battery effect giving unwanted signals to the amplifier.

The monitor has been tested in a stack with coal combustion emissions. It can operate for weeks without human attention. The largest operational problem appears to be long term deterioration and contamination of the apparatus.

Slone, et al,[302] describes the construction and testing of a similar instrument on a coal-fired boiler stack. Although the prototype instrument had several minor design weaknesses, they report positive results. The report stresses that the instrument measures particulate surface area and does not make a strong attempt to correlate the measurement with particulate mass.

Any of the alternate design concepts shown in Figure 2 may be modified so that the charge placed on the particles is monitored. The same problem and features discussed for ion current attenuation would be present in an ion capture instrument.

Whitby and McFarland[8] suggest a modification of this technique to measure the mass concentration of particles in ambient air. If the particles are charged by diffusion and the high mobility, small particles are separated out of the main aerosol stream, the resulting ion current carried by the remaining particles will theoretically correlate better with mass concentration. The principle requires the shape of the particle size distribution to remain constant, which is the reason for removing the small particles which have rapidly fluctuating concentration. Figure 7 shows a schematic of the monitor with a mobility separator. Whitby and McFarland found a significant improvement in the correlation of the measured parameter with volume concentration for atmospheric aerosols sampled with an instrument using diffusion charging. The charge per particle placed on the particles by this instrument is proportional to $D_p^{1.2}$ which makes the measurement quite sensitive to large numbers of small particles, even with the smallest of them removed.

The fluctuations in particle size distribution within stacks is not experimentally known. However, relatively large fluctuations can be expected on a short-term (10 sec) basis, even in the particle size range above 0.1 μm. Thus, little improvement in the correlation with mass could be expected with the addition of a mobility separator to the monitor.

Whitby and Clark[68] have successfully used the mobility separation technique described in Figure 7 to measure the size distribution of submicron aerosol particles. In their system shown in Figure 8, the mobility separator can be adjusted manually or automatically to separate out particles with mobilities above preset values. The mobility of a particle is, in turn, inversely proportional to particle diameter for particles below 1 μm. The commercial version of the electrical particle counter can measure number concentration as a function of particle diameter for 14 size ranges from 0.006 to 1 μm. No other instrument is known which can automatically measure size distributions in this size range.

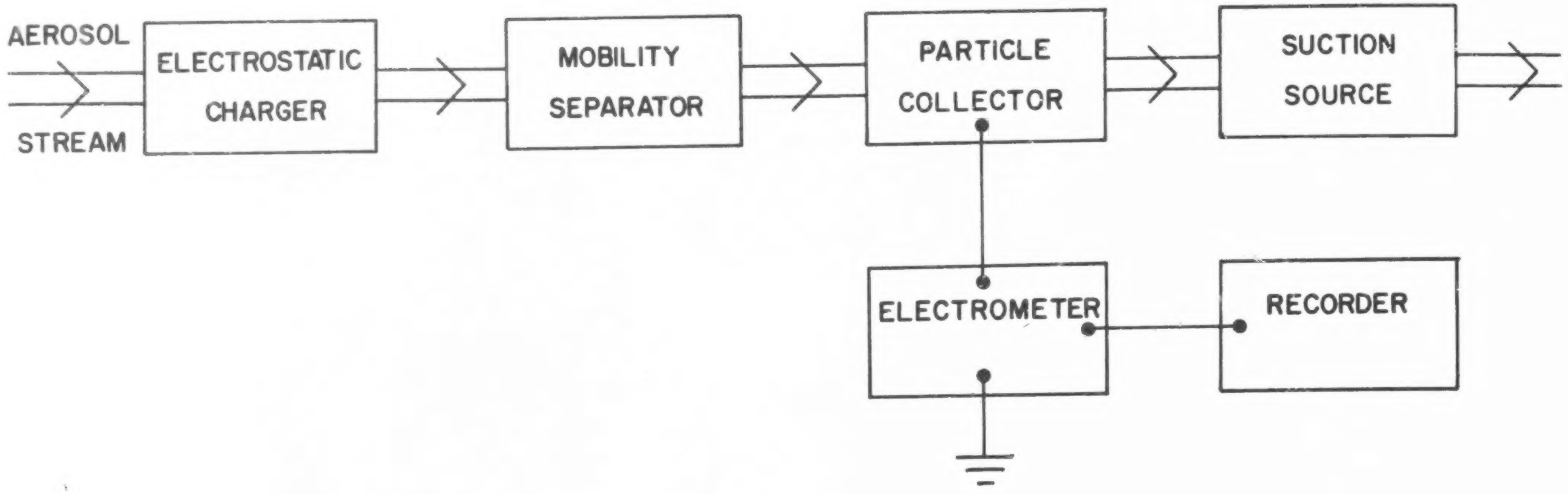
AEROSOL
STREAM
ELECTROSTATIC CHARGER
MOBILITY SEPARATOR
PARTICLE COLLECTOR
SUCTION SOURCE
ELECTROMETER
RECORDER

Figure 7. Modified ion capture design using a mobility separator from Whitby and McFarland[8].

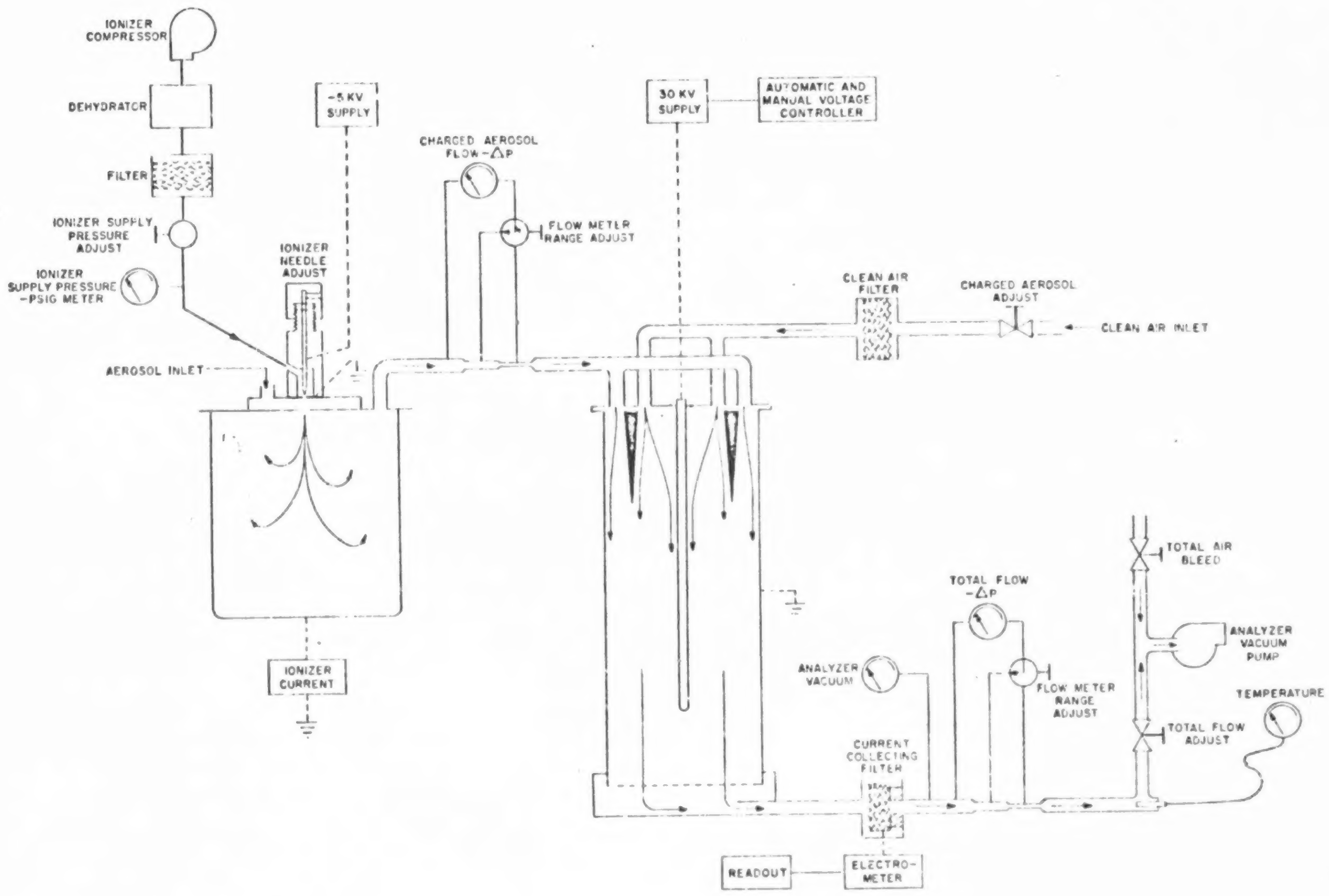
IONIZER COMPRESSOR
DEHYDRATOR
FILTER
IONIZER SUPPLY PRESSURE ADJUST
IONIZER SUPPLY PRESSURE -PSIG METER
-5 KV SUPPLY
IONIZER NEEDLE ADJUST
AEROSOL INLET
CHARGED AEROSOL FLOW-ΔP
FLOW METER RANGE ADJUST
30 KV SUPPLY
AUTOMATIC AND MANUAL VOLTAGE CONTROLLER
CLEAN AIR FILTER
CHARGED AEROSOL ADJUST
CLEAN AIR INLET
IONIZER CURRENT
TOTAL AIR BLEED
TOTAL FLOW -ΔP
ANALYZER VACUUM PUMP
ANALYZER VACUUM
FLOW METER RANGE ADJUST
TEMPERATURE
TOTAL FLOW ADJUST
CURRENT COLLECTING FILTER
READOUT
ELECTRO-METER

Figure 8. Modified ion capture design used to measure submicron particle size distribution.

Application to Mass Emissions Measurement in Stacks

The correlation of the measurement made with Grindell's monitor with mass emissions is not expected to be very good. The monitor is sensitive roughly to particle surface area and directly to the gas flow rate if it has the automatic suction system.

The monitor appears to have a number of positive features, however. It gives a continuous-measurement of emissions rate rather than quasi-continuous measurement of mass concentration as most instruments do. It appears possible to design a monitor to operate inside a stack, eliminating the need for dilution or heating systems. Even with sample extraction, the heating system is very simple. The monitor can be made rugged and can clean itself easily. The monitor should be relatively inexpensive, perhaps in the $5,000 range. At least 2 monitors have been built and operated within coal-fired boiler stacks with no apparent major problems. They were operated for weeks without human attention. Output data is analog and continuous, making recording or other data manipulations, simple. The monitor measures particle surface area which is more sensitive to small particle number concentration measurement. Thus, particle area is a compromise parameter which responds somewhat to all particle sizes rather than just the large or the small ones.

This technique will not measure particle mass very well. However, if particle surface area is of interest, this technique is one of the most promising for continuous monitoring.

CONTACT CHARGE TRANSFER

When particles hit or slide along a surface, they usually transfer electrical charge to the surface. This principle has been used in the design of several dust concentration measuring instruments. Three such instruments are discussed below:

a. the Konitest,

b. the Probe-in-Nozzle Technique, and

c. the Particle Bounce Technique.

Konitest

The Konitest uses the electrical charge transfer caused by particles sliding along a wall as a measure of aerosol particle concentrations. Figure 9 shows the complete measuring system as it samples from a duct. Figure 10 schematically shows the details of the Konitest sensor. As the aerosol stream is sucked into the sensing exciter tube, the stream is given a whirling motion by the tangential inlet duct. Centrifugal force throws particles against the exciter tube wall where they slide through the sensor in a helical path. Electrical charge generated at the exciter tube wall leaks to ground through a measuring amplifier. The amplified signal can then be recorded, e.g., by a strip-chart recorder.

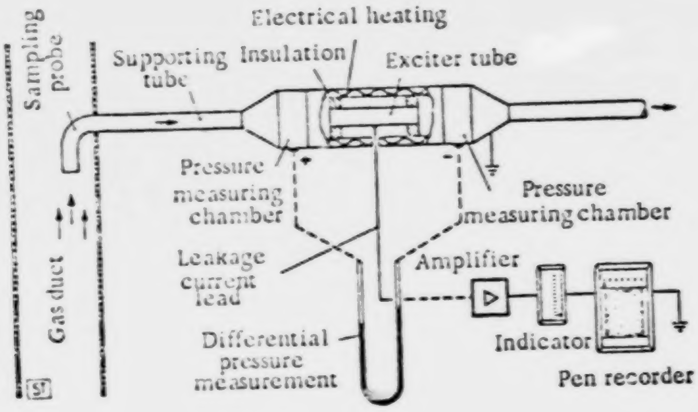
Sampling probe
Electrical heating
Supporting tube
Insulation
Exciter tube
Pressure measuring chamber
Pressure measuring chamber
Leakage current lead
Amplifier
Differential pressure measurement
Indicator
Pen recorder
Gas duct
ST

Fig. 9. Complete Konitest stack monitoring system from Schutz[659] and Prochazka.[923]

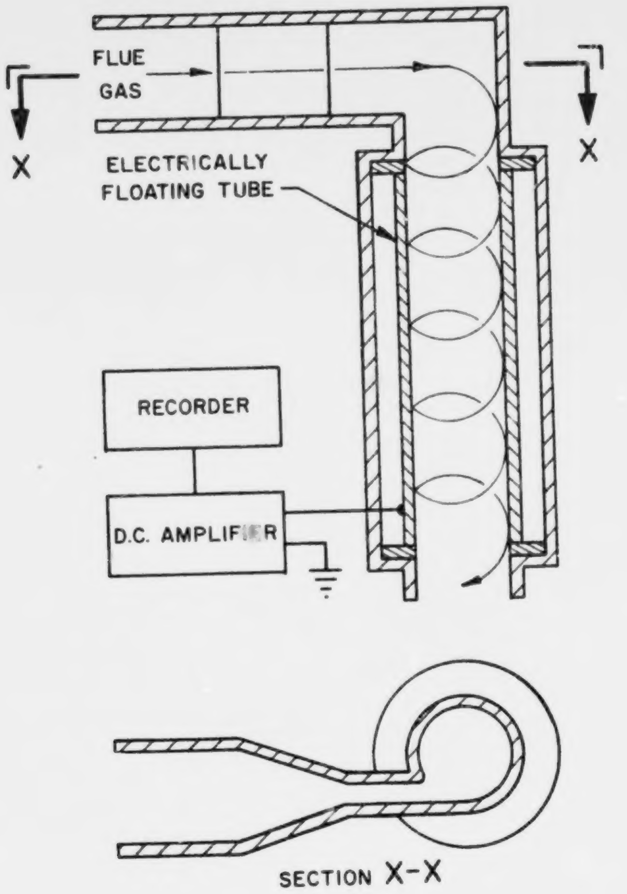

Fig. 10. Detail of Konitest sensing head showing particle trajectories from Prochazka[923]

A later version of the Konitest, shown in Figure 11, uses a venturi nozzle as the sensing exciter tube. With equal dust concentrations, the nozzle yields lower current levels than the centrifugal device. However, the current levels are still high enough to amplify and record with most dusts.

Both versions use the Konitest sensor as a gas flow measuring instrument simultaneous with the dust concentration measurement. This is done with the differential pressure measuring systems shown in Figure 9 and 11. The exciter tube material is steatite, a semiconductor substance, also known as magnesium hydrosilicate. The exciter tube must be electrically insulated from the outer housing so that leakage currents can be detected by the amplifier.

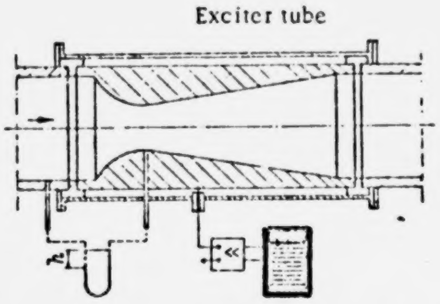

Fig. 11. Alternate Konitest design using an electrically floating venturi as the exciter tube rather than the cyclone from Prochazka.[923]

Both the inlet tube and sensor itself are electrically heated to prevent vapor condensation. The dust passing through the instrument must be dry or it will stick to the exciter tube. Schutz[659] reports that very thin coatings of particles, just a few microns thick, cause severe changes in measured values, at times even reversing the current polarity. Duwel[225] and Konig and Rock[241] report that the Konitest calibration changes with temperature. Thus, not only is it important to heat the device to reduce contamination but the temperature must also be kept constant. With thermostatically-controlled electric heaters, temperature control should not be a major problem. However, Schutz suggests that long term operation in dusts containing many small particles is difficult because of contamination of the exciter tube.

The electrical charge generated by the particle-surface contact depends on both the surface material and the particle composition. Some materials yield positive polarity currents while others yield currents of negative polarity. Certain combinations of dusts may yield no current. Thus, each different type of particle requires individual calibration. The composition of coal combustion emissions is probably constant enough so that this problem would not become overwhelming, but this certainly must be checked experimentally.

The particle size distribution and the air flow rate through the instrument may affect the contact of particles with the exciter tube, and, thus, affect the calibration of the instrument.

In spite of the many factors affecting the measured value of the Konitest, several investigators[225,241,659,923] report excellent correlation with particle mass concentration if the instrument is calibrated for each new condition. Figure 12, from Prochazka[923], shows the indicated current versus gravimetric particle concentration for flue gas from a power station with concentrations of 0.1 to 2.2 gm/m^3. The data was obtained by determining an average Konitest current during the time necessary to collect enough material on a filter so that it can be weighed. The filter was immediately downstream from the Konitest, eliminating any error due to spatial variation in dust concentration in the duct. The data shows very little scatter.

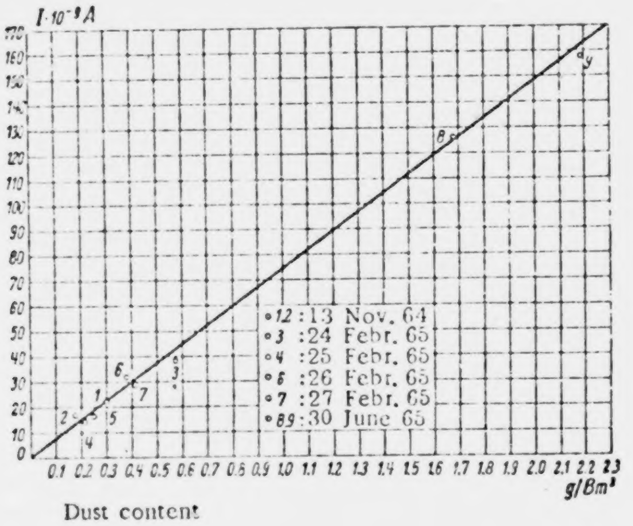

Fig. 12. Gravimetric calibration of Konitest for flue gas from Prochazka.[923]

A very recent program by Schnitzler, et al[1189], extensively evaluated the Konitest, two light transmission instruments, and two beta attenuation instruments in a modern plant fired by coal. Figure 13 shows the comparative results of the five instruments in terms of manually measured gravimetric concentration as a function of instrument reading. Table 1 indicates the results of these tests. The dark lines in Figure 13 are the calibration curves obtained by drawing lines through the data points. The lighter parallel lines on either side of the calibration line denote extrapolations of the 95% confidence level calculated for the 150 mg/m^3 concentration level.

Each of the calibration curves shown in Figure 14 were obtained from one instrument operating in one effluent duct. The data is the average of measurements made with three significantly different plant operating conditions: 1) with soot-blowing, 2) without soot-blowing, and 3) with 45% of plant operating capacity. A look at the calibration curves for each of these conditions can show how well the measured parameter correlates with mass, i.e., how much error can be expected if the effluent conditions change from what they were during calibrations.

The beta attenuation instruments, which sense a parameter closely related to particle mass, show excellent correlation with gravimetric mass measurements. However, notice the surprisingly good mass correlation of the Konitest and the second light transmission instrument which was manufactured by Sick in Germany.

TABLE 1. Summary of experimental calibration of five instruments by Schnitzler et al[1189].

	Instrument				
	Transmissometer		Contact-Electrostatic Konitest	Beta Radiation Attenuation	
	Durag A	Sick B		A	B
Number of Measurements	312	292	312	29	43
Correlation Coefficient	0.63	0.87	0.92	0.94	0.81
Measurement Tolerance at 150 mg/Nm^3	±68%	±39%	±33%	±22%	±31%

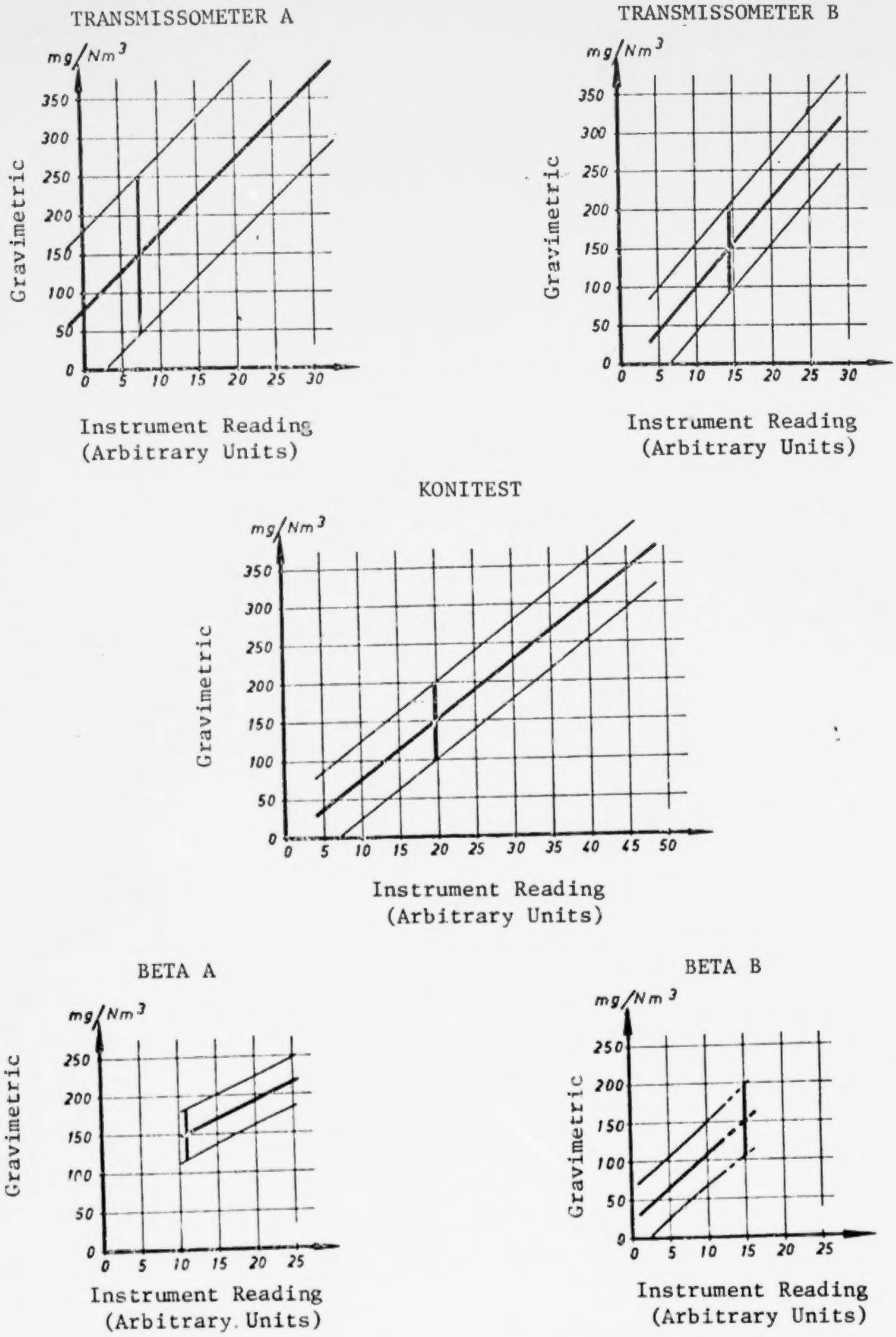

Figure 13. Gravimetric calibration of two light transmissometers, one Konitest, and two beta radiation attenuation instruments in a coal-fired effluent duct from Schnitzler et al[1189].

Figure 14 is a comparison of the calibration curves for each of the three operating conditions for the Konitest and the two light transmission instruments. Notice that the three Konitest calibration curves fall nearly on top of each other, indicating little effect on the mass correlation due to the changes in plant operating conditions. The two light transmission instruments show considerably different curves for each of the three operating conditions.

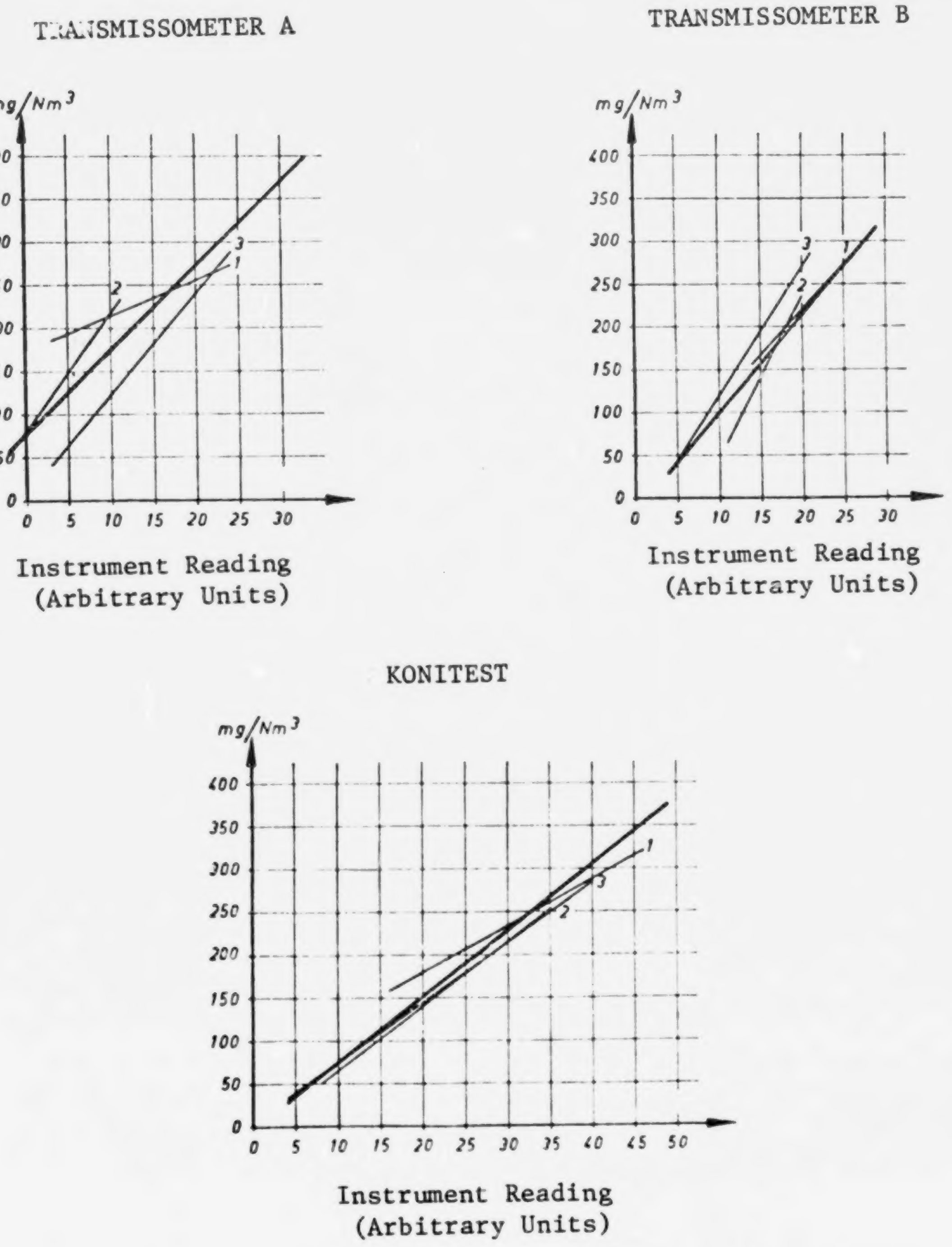

Figure 14. Gravimetric calibration of two light transmissometers and one Konitest in a coal-fired effluent duct under plant operating conditions of: 1) with soot blowing, 2) without soot blowing, and 3) with minimum load from Schnitzler et al[1189].

Application To Mass Emission Measurement In Stacks

From data such as Figures 12 - 14, one is lead to believe that the Konitest responds quite well to particle mass. The literature give no hint of a theoretical reason for this. A possible reason is that the force driving particles toward the steatite tube is centrifugal force, which depends on particle mass. This force also regulates the number of collisions and the intensity of the collisons of particles with the wall.

The concentration range of the instrument is reportedly from less than 100 $\mu gm/m^3$ to greater than 1 gm/m^3. This certainly covers the entire range normally experienced downstream of a collector in a coal- or oil-fired combustion facility.

The response of the Konitest is essentially instantaneous. The electrical signal can be monitored with its natural, fast response or it can be damped electrically yielding a more steady concentration value.

The major problems with the Konitest for measuring particulate emissions from coal- or oil-fired combustion facilities are:[659]

a) Long-term contamination of the exciter tube, primarily by submicron particles,

b) Rapid changes in the instrument indication, caused by large fluctuations in submicron particle concentration, which do not represent real changes in particle mass loading, and

c) The measured parameter is not true particle mass, although on-site calibrations can make resonable correlation possible.

d) Changes in particle composition can change the calibration drastically, even causing the readout current to reverse polarity.

Although we do not fully understand why they occur, the good mass correlation reported from several test programs are impressive. The investigators report no major operational problems with the Konitest. The device requires calibration in each different installation, but its fast, nearly instantaneous, response and its good calibrated mass correlation recommend it for some monitoring applications. More information should be obtained from people with operating experience and, if their recommendations warrant it, considerable work appears jusitifed to develop both the theory and the hardware for this technique. The problems listed above could limit the use of the Konitest in coal-fired stacks quite severely.

Until recently, the Konitest was commercially manufactured by J. C. Eckardt, Stuttgart-Bad Cannstatt, West Germany. However, the company no longer manufactures them.

Probe-In-Nozzle Technique

Schutz[659,684,922,1036] describes another contact charge transfer instrument which consists of a conical metal probe in the throat of a venturi as shown in Figure 15. Particles passing through the nozzle hit the probe because of their high inertia caused by flow velocities above 100 m/sec. When the particles hit the probe, a charge transfer occurs, similar to the charge transfer in the Konitest instrument. The current draining from the probe is an indication of dust concentration. The current signal can be amplified, linearly or logarithmically, and recorded by a strip chart recorder. As with the Konitest, the particle parameter which is being sensed, i.e., area, mass, etc., is not clearly defined but experimentally appears to be related to particle surface area.

Cheng, et al,[20] and Soo, et al,[5, 104] describe measurements made with a device apparently using similar principles.

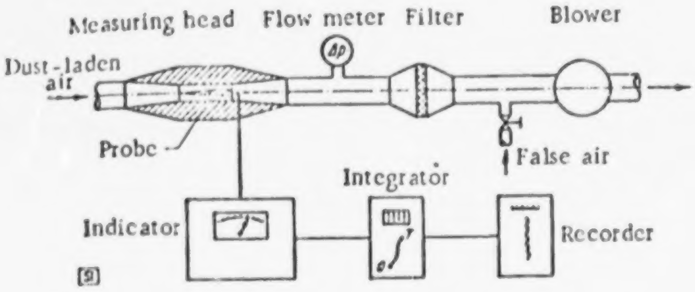

Fig. 15. Probe-in-nozzle design from Schutz.[659]

Application To Mass Emissions Measurement in Stacks

Several problems make the instrument questionable for mass emissions measurement from coal- and oil-fired combustion sources.

A reasonable portion of the particles striking the probe must be large, i.e., greater than 10 μm, in order to keep the probe clean. If all particles are less than 10 μm with a significant portion below 1 μm, the probe will become dirty and change the calibration of the instrument. Also, because all submicron particles do not strike the probe, the instrument may not detect such particles reproducibly.

The current levels measured from the prototype instruments was in the range of 10^{-8} to 10^{-13} amperes. Such low current levels require careful instrument design. The particles must be dry to prevent current leaks and also to prevent excessive contamination of the probe. Schutz reports the maximum temperature at which the instrument can operate is 70°C, considerably below the 175°C normally encountered in power plant stacks. To cool the gas stream to 70°C without vapor condensation requires dilution. The maximum temperature and dilution requirement eliminates the possibility of mounting the sensing head directly in a stack, one of the primary features of this technique.

No instruments of this type have been commercially marketed.

Because of the rather major problems with this technique and because the technique has no real advantage over other electrostatic techniques, we recommend that further development emphasize the other electrostatic techniques rather than this one.

Particle Bounce Technique

Coenen[226] describes a unique particle concentration measurement technique whereby particles bounce between plates of a high voltage, electric condenser, carrying electric charges with them. Figure 16 illustrates the principle. When a particle enters the air gap between the plates, the electric field accelerates it toward one side or the other, depending on its initial charge. When it strikes a plate, it exchanges its charge and is repelled toward the other plate. This process continues until the particle is carried out from the condenser by the air flow. With each bounce, the particle carries charge from one condenser plate to the other, causing a net current to flow between the plates. The current level, measured by an electrometer, is an indication of the concentration of the particles. The indicated current can be amplified, and then recorded by a strip charge recorder, as shown in Figure 17. The charge per particle is related roughly to particle surface area. The technique works best with large particles (>100μm) but reportedly works well for some particles as small as 1μm.

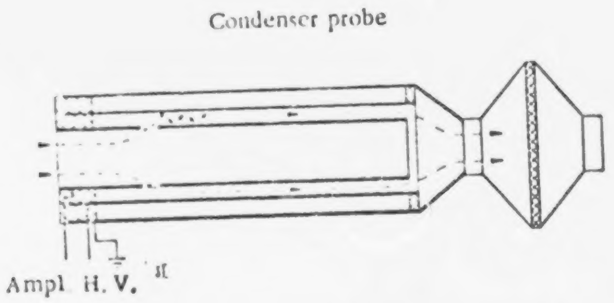

Fig. 16. Illustration of particle bounce technique from Coenen.[226]

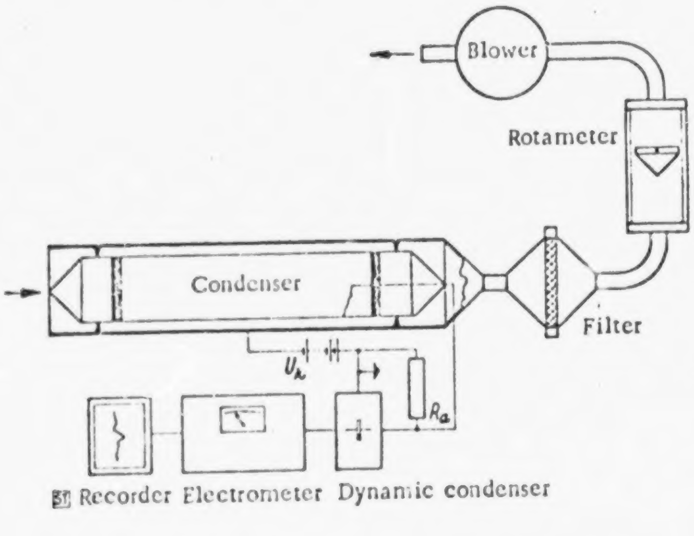

Fig. 17. Particle bounce instrument design from Coenen.[226]

Application To Mass Emissions Measurement in Stacks

This technique has most of the same problems as the Konitest discussed earlier. In addition, the particles should be primarily above 10μm, above the range of sizes in coal- or oil-emissions stacks.

No commercial units exist. No further development for stack monitoring is recommended at this time.

CONCLUSIONS

Several electrostatic techniques show considerable promise for measurement of effluent particle flow rates. One correlates well with mass concentration and two measure particle surface area. These techniques are:

1. Konitest,
2. Ion capture, and
3. Ion current attenuation.

The Konitest, developed and tested in Germany, shows surprisingly good experimental correlation with manually-obtained gravimetric measurements in several different studies of effluent from coal-fired power plants. Although theory is not developed for the device, the centrifugal force on the particles in the cyclone may account for the good mass correlation. On the other hand, several other people report poorly-documented operational problems with the instrument. Further work on the development of theory and hardware appears justified because of the potential advantages of the instrument.

A number of new designs are suggested for both the ion current attenuation and the ion capture instruments. These instruments would probably respond to particle surface area (D_p^2) with field charging or $D_p^{1.2}$ with diffusion charging. An interesting suction technique, useful only on low pressure drop devices such as these, makes the instrument respond to particle flow rate rather than particle concentration. The instantaneous readout of a wide variety of particle concentration levels is a positive feature of these instruments. Further development work appears justified on these electrostatic techniques.

REFERENCES

20 Cheng, L., Tung, S. K., and Soo, L. S., "Electrical Measurement of Flow Rate of Pulverized Coal Suspension", ASME Paper No. 69-WA/Pwr-1, 14. p. (1969).

226 Coenen, W., "A New Principle of Recorded Dust Measurement and Its Technical Application in a Battery-Powered Instrument", Staub-Reinhalt der Luft (Engl. Trans.), V. 27, no. 12, p. 32-40 (Oct 1967).

245 Coenen, W., "Registrierende Staubmessung nach der Methode der Kleinionenanlagerung", Staub-Reinhalt der Luft, V. 24, no. 9, p. 350-353 (Sep 1964).

284 Coenen, W., "Staubmonitor zur betrieblichen Staububerwachung", Staub-Reinhalt der Luft, V. 23, no. 2, p. 119-123 (Feb 1963).

1040 Coenen, W., "Dust Measurement and Recording by the Method of Small Ion Accumulation", Staub-Reinhalt der Luft, V. 24, no. 9, p. 350-353 (Sep 1964).

225 Duwel, L., "Latest State of Development of Control Instruments for the Continuous Monitoring of Dust Emissions", Staub-Reinhalt der Luft (Engl. Trans.), V. 28, no. 3, p. 42-53 (Mar 1968).

122 Grindell, D. H., "An Electrostatic Dust Monitor", IEE Proc., Series A (34), V. 107, p. 353 (1960).

552 Grindell, D. H., "Atmospheric Pollution by Solid Particles, Measuring Significant Particle Surface Area by Charge Transfer", Engineering, V. 187, p. 1350-1351 (Mar 1959).

554 Grindell, D. H., "Monitoring Smoke and Flue-Dust Emission", AEI Eng., V. 2, no. 5 (1962).

242 Hasenclever, D., and Siegmann, H., "Neue Methode der Staubmessung mittels Kleinioneanlagerung", Staub-Reinhalt der Luft, V. 20, no. 7, p. 212-218 (Jul 1960).

241 Konig, W., and Rock, H., "Untersuchungen am elektrostatischen Staubgehaltsmessgerate Konitest", Staub-Reinhalt der Luft, V. 21, no. 8, p. 355-356 (Aug 1961).

581 Mohnen, V. A., and Holtz, P., "The SUNYA-ASRC Aerosol Detector", APCA Journal, V. 18, p. 667-668 (Oct 1968).

923 Prochazka, R., "Recording Dust Measurement With The Konitest", Staub-Reinhalt der Luft (Engl. Trans.), V. 26, no. 5, p. 22-28 (May 1966).

659 Schutz, A., "Possibilities for Recorded Dust Measurement and Dust Control", Staub-Reinhalt der Luft (Engl. Trans.), V. 26, no. 10, p. 1-8 (Oct 1966).

684 Schutz, A., "Eine Anordung zur Registrierenden Kontaktelektrischen Staubmessung", Staub-Reinhalt der Luft, V. 24, p. 359-363 (1964).

922 Schutz, A., "A Recording Dust-Measuring Instrument Based on Electric Contact, with Logarithmic Indication", Staub-Reinhalt der Luft (Engl. Trans.), V. 26, no. 5, p. 18-21 (May 1966).

1036 Schutz, A., "An Arrangement for Continuous Recording Dust Measurements by the Contact-Electrification Method", Staub-Reinhalt der Luft, V. 24, no. 9, p. 359-363 (Sep 1964).

1189 Schnitzler, H., "Messtand fur die Prufung und Kalibrierung von Registrierenden Staub - und Gasmessgeraten in einem Steinkohlengefeuerten Kraftwerk", SchrReihe Ver. Wass. - Boden Lufthyg. Berlin-Dahlem, V. 33, Stuttgart (1970).

302 Slone, T. J., Lagarias, J. S., and Schlaffer, G. C., "Stack Effluent Monitoring for Power Stations", Reprint No. 285, American Inst. Co., Inc., Silver Spring, Md.

5 Soo, S. L., Stukel, J. J., and Hughes, J. M., "Measurement of Mass Flow and Density of Aerosols in Transport", Environmental Science and Technology, V. 3, no. 4, p. 386-392 (Apr 1969).

104 Soo, S. L., Trezek, G. J., Dimick, R. C., and Hohnstreiter, G. F., "Concentration and Mass Flow Distributions in a Gas-Solid Suspension", Industrial & Engineering Chemistry Fundamentals, V. 3, p. 98-106 (1964).

8 Whitby, K. T., and McFarland, A. R., "Electrical Measurement of the Mass Concentration of a Self-Preserving Aerosol Size Distribution", APCA Journal, V. 18, no. 11, p. 760-764 (Nov 1968).

68 Whitby, K. T., and Clark, W. E., "Electric Aerosol Particle Counting and Size Distribution Measuring System for the 0.015 to 1 μ Size Range", Tellus, V. 18, p. 573-586 (1966).

1211 Whitby, K. T., and Liu, B.Y.H., Chapter 3, Aerosol Science, Davies, C. N., editor, Academic Press, New York, (1966).

LIGHT TRANSMISSION

by: B.Y.H. Liu and K. T. Whitby

INTRODUCTION

When light, or other electromagnetic radiation, passes through an aerosol, its intensity reduces because of scattering and absorption by the particles. The transmission or attenuation of light through an aerosol, therefore, can be used as a measure of aerosol concentration.

Figure 1, according to Hodkinson,[1211] shows the basic requirements of an instrument for measuring light transmission through aerosols. Pin-hole apertures are needed in order to prevent scattered light from reaching the photocell.

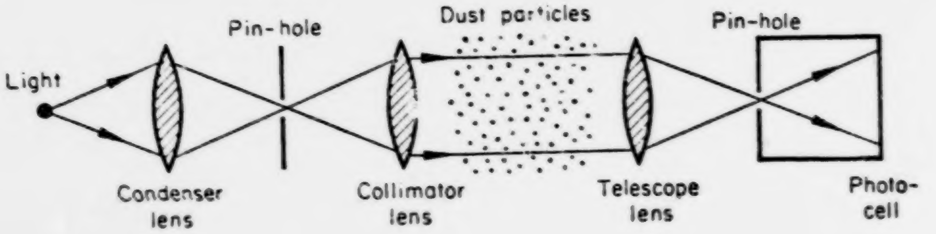

Fig. 1. Basic requirements of instrument for light extinction measurement according to Hodkinson.[1211]

Since the scattering and absorption of light by a particle is dependent upon the geometrical and optical properties of the particles, light transmission measurement alone generally does not provide sufficient information to determine the aerosol mass concentration. In order to measure mass concentration by the transmission of light through an aerosol, the density, the refractive index, the shape and the size distribution of the particles must remain constant. For such aerosols the relationship between mass concentration and light transmission usually must be established by calibration.

Despite this rather severe limitation in terms of mass concentration measurement, light transmission has remained one of the most widely used principles for the continuous monitoring of smoke emission from stacks. The method is relatively simple, and the apparatus involved can be comparatively inexpensive. Further, the light beam is usually projected across a portion of the stack so that a reading is obtained of the average particle concentration in that portion of the stack, and the measured parameter relates closely to the visual appearance of the stack effluent, one of the principal concerns in the monitoring and control of emission from stacks.

When combined with a suitable particle size classification device, light transmission measurement can also be used to determine the particle size distribution. One such device, the photosedimentometer, combines light transmission measurement wtih a liquid sedimentation cell to determine the size distribution of powder particles dispersed in a liquid. Similar principles can be considered for possible application to size distribution measurements in stacks.

Although light transmission measurement is relatively simple to make, its results are often difficult to interpret because the particle size is often of the same order of magnitude as the wavelength of light used, and the scattering of light by particles whose size is comparable to the wavelength of light is a rather complex phenomenon. Therefore, in the following sections we shall briefly review the fundamental light scattering properties of small particles from the standpoint of stack monitoring by light transmission measurement.

BASIC PRINCIPLES

Consider a parallel light beam passing through a fluid medium containing suspended particles. The transmittance, T, of the medium, i.e., the ratio of transmitted light intensity to incident light intensity, is given by the Bouguer, or the Beer-Lambert, law,[1211]

$$T = \exp\,(-k\ell) \tag{1}$$

where k is the extinction coefficient, or turbidity, and ℓ is the thickness of the medium. Sometimes, the measured transmittance is expressed in terms of optical density defined as

$$\mathrm{O.D.} = \mathrm{Log}\,(\ell/T) \tag{2}$$

instead of the transmittance or the turbidity. Consequently, instruments and methods for aerosol measurement based upon light transmission principles have been referred to variously under such names as transmissometer, smoke density meter, photo-extinction measurement, turbidimetric measurement, etc.

The extinction (scattering and absorption) of light by a particle is usually described in terms of a particle extinction coefficient, K, defined as the ratio of the flux scattered and absorbed by the particle to the flux geometrically incident upon the particle. If A_p is the projected area of a particle against the light beam, then the product

$$A_e = K\,A_p \tag{3}$$

defines a cross-section, A_e, for total light extinction by the particle. The transmittance of a medium of thickness ℓ is thus given by

$$T = \exp\,(-\ell\,\Sigma\,A_e) = \exp\,(-\ell\,\Sigma\,K\,A_p) \tag{4}$$

where the sum, Σ, is to be performed over all particles within a unit volume. The turbidity, k, of the medium,

$$k = \Sigma A_e = \Sigma K A_p \tag{5}$$

is thus seen to provide a measure of the total extinction cross-section of the particles in a unit volume.

The particle extinction coefficient, K, is a complicated function of the size, shape and refractive index of the particle. It is also dependent upon the spectral energy distribution of the light beam and the spectral sensitivity of the photodetector if it is to be related to the transmittance measured by the light source-photodetector combination. However, in the geometrical scattering region where the particle size is large compared to the wavelengths of radiation, the extinction coefficient, K, assumes the constant value of 2. Under such conditions, equation (5) shows that the turbidity is a measure of the total projected area of the particles in a unit volume. For particles which are reasonably convex in shape and orientated at random, their projected area is approximately equal to 1/4 their total surface area according to Cauchy's Theorem.[1211] Thus

$$k = (1/2)\Sigma A = (1/2)(\rho \Sigma V) \frac{1}{\rho D_{vs}} \tag{6}$$

where A is the external surface area of a particle, V is the particle volume, $(\rho \Sigma V)$ is the mass concentration of the aerosol and

$$D_{vs} = \Sigma V/\Sigma A \tag{7}$$

is the volume-surface, or the mean Sauter, diameter of the particles. Thus, we see from equation (6) that, in the geometrical scattering regime, the turbidity of the medium is directly proportional to the mass concentration of the aerosol only when the volume-surface mean diameter of the aerosol remains constant. On the other hand, for the same mass concentration, the turbidity, or the optical density of an aerosol, is inversely proportional to the mean volume-surface diameter. Figure 2, showing the results of a study by Lucas and Snowsill[485] on the response characteristics of a smoke density meter, seems to confirm this conclusion.

Theoretically, the particle extinction coefficient, K, will approach the constant value of 2 only in the limit when the particle size parameter $\alpha = \pi D/\lambda \to \infty$, where D is the particle diameter and λ is the wavelength of light. From a practical point of view, K will have reached the value of 2 to within about ± 20% when α exceeds a certain critical value. Table 1 shows an estimate of this critical α value and the corresponding minimum particle size for $\lambda = 0.5$ μm for various types of particles. These are rough estimates based upon our present knowledge of the light scattering properites of particles. More accurate estimates on some of the values can be obtained by further calculation.

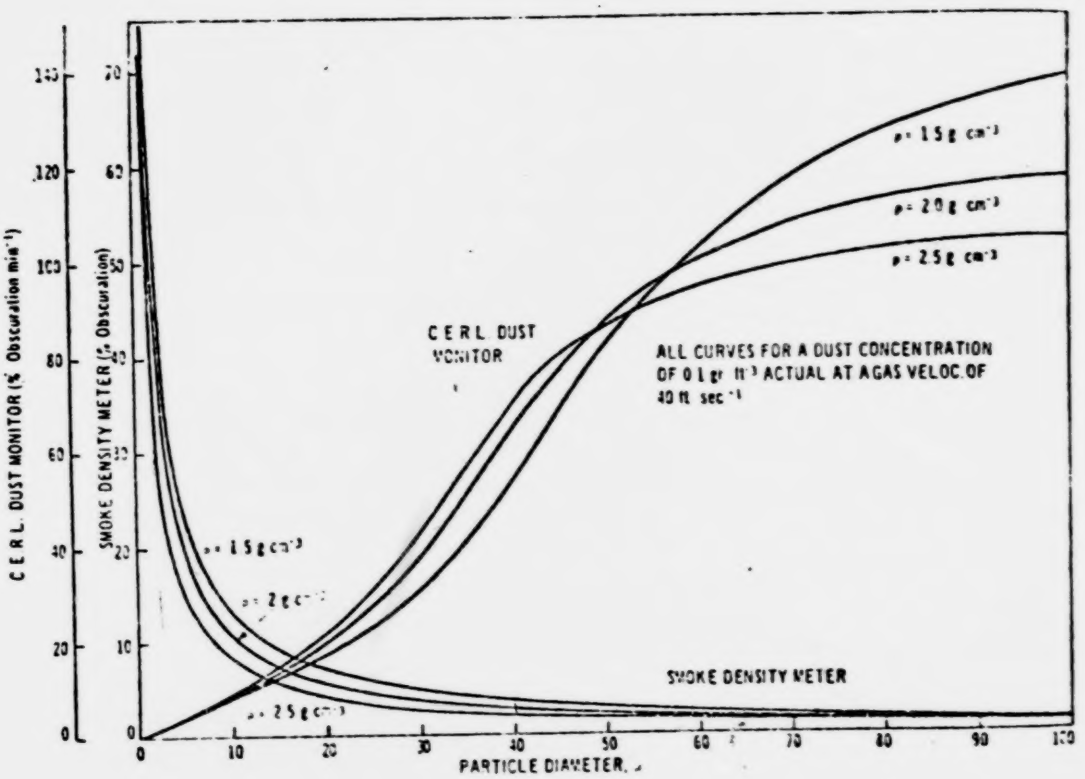

Fig. 2. Response of smoke density meter to dust particles of different sizes according to Lucas and Snowsill.[485]

Table 1

Estimated minimum value for $\alpha = \frac{\pi D}{\lambda}$ and D in order that the particle extinction coefficient, K, is within $\pm$ 20% of the constant value, 2.

Aerosols	α_{min}	D_{min} (λ = 0.5 μm)
Monodisperse spheres		
m = 1.33 (water)	9	1.5 μm
m = 2.0 (many mineral particles)	20	3.3 μm
m = ∞ (totally reflecting particle)	1	0.17 μm
m = 1.55 - 0.66 i (highly absorbing particles such as carbon black)	2.5	0.42 μm
Irregularly shaped particles and polydisperse aerosols		
m = 1.5	5	0.84 μm
m = 2.0	10	1.7 μm

It is interesting to note in Table 1 that for light transmission measurement in stacks where the aerosol is undoubtedly quite polydisperse, transmissometers or smoke density photometers will operate essentailly in the geometrical scattering regime for particles larger than 1 to 2 μm diameter. For highly absorbing particles such as carbon black the geometrical scattering regime can be reached for particles as small as 0.5 μm. This is a particularly significant conclusion since in the geometrical scattering regime the particle extinction coefficient, K, is independent of the wavelength of the radiation. Thus, the turbidity and the optical density of the aerosol will not depend on the wavelength for particles larger than 0.5 to 2 μm. Hence, no information on the size distribution of the particles can be obtained by varying the wavelength of the radiation within the limited range of the optical spectrum and in the near infrared if the particles in the stack are predominantly larger than these minimum sizes. This point is discussed more fully in the section entitled "Multi-Wavelength Light Transmission".

Below the geometrical scattering regime, the light scattering properties of the particles become quite complicated. The following paragraphs review briefly the scattering properties of small particles.

A. Dielectric and Absorbing Spheres

For spherical particles, the particle extinction coefficient, K, is a function of two parameters: m, the refractive index of the particle relative to the suspending medium, and $\alpha = \pi D/\lambda$, a dimensionless particle size parameter, defined as the ratio of the particle circumference, πD, to the wavelength of the incident radiation λ. The complete theory for the calculation of K from electromagnetic theory for this case was first formulated by Mie,[147] and treated in several well known texts and papers including Stratton,[1250] Van de Hulst,[1201] Kerker,[1214] Kratohvil,[843] Born and Wolf,[1212] Newton,[1199] and Kerker.[1215] The calculation, requiring the summation of many terms in an infinite series, has been performed by many authors for various values of m and α. Published values of K derived from Mie theory calculations are available in the literature. Summaries of the available calculation results have been given by Van de Hulst[1201] (p. 166, 273), Hodkinson[1211] (p. 303), and more recently by Kerker[1215] (Table 3.2, p. 78).

Figure 3 shows the extinction coefficient, K, for scattering by non-absorbing dielectric spheres with refractive indices of 1.4, 1.44, 1.486, 1.5 and 2.0 according to the calculations of Penndorf.[846,847,848,1181] All curves show the characteristic feature of a damped oscillation, with the value of K reaching a peak at the first maximum and eventually tending to the constant value of 2 as $\alpha \to \infty$. Superimposed on this damped oscillation are minor ripples, which may be ignored for all practical purposes. A table giving the smoothed values of K for $0.8 \leq m \leq 2.0$ and $0.2 \leq \alpha \leq 20$ is given by Penndorf.[1200]

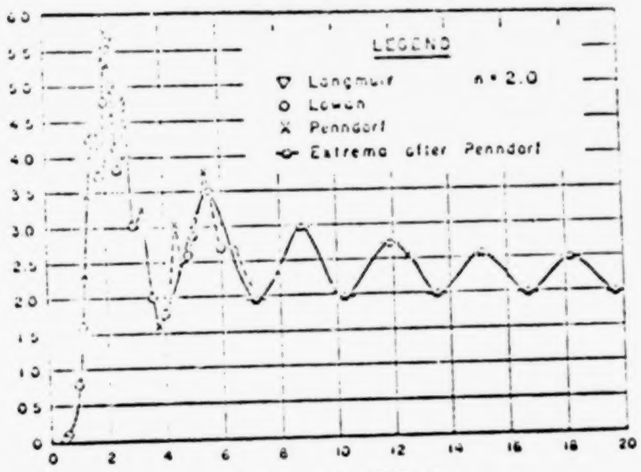

Total Mie scattering coefficients K as functions of the size parameter α for the refractive index $n = 2.00$.

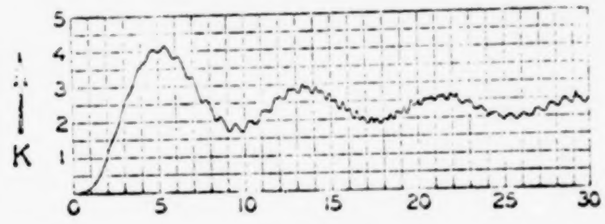

Total Mie scattering coefficient K for $n = 1.40$ as function of the size parameter α.

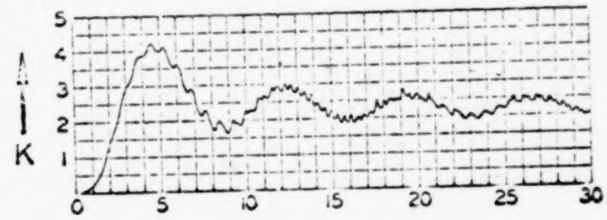

Total Mie scattering coefficient K for $n = 1.44$ as function of the size parameter α.

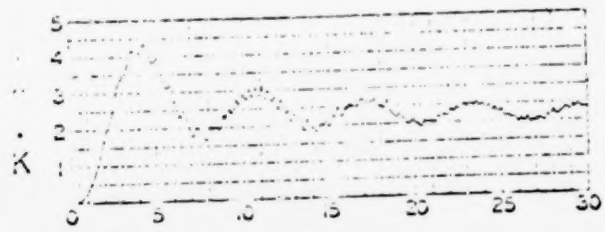

Total Mie scattering coefficient K for $n = 1.50$ as function of the size parameter α.

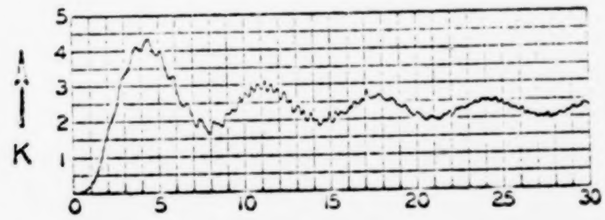

Total Mie scattering coefficient K for $n = 1.486$ as function of the size parameter α.

Fig. 3. Scattering coefficient for dielectric particles according to Penndorf.[846,847,848,1181]

Figure 4 shows the value of K plotted against the phase shift parameter, $\rho = 2\alpha(m - 1)$, as presented by Kerker[1215](p. 105). It shows that the scattering curves are similar in shape and the maxima and minima are nearly equally spaced on this K vs ρ plot, with the maximum located at approximately $\rho_{max} = (n - 1/4)2\pi$ and the minima at $\rho_{min} = (n + 1/6)2\pi$, where n is an integer. The peak scattering coefficient, which occurs at the first maximum, extends from approximately 3.2 for m = 1, to 6 for m = 2. For the case of anomalous diffraction when m = 1 the scattering coefficient is given by the Van de Hulst equation[1201](p. 176)

$$K = 2 - 4\,\frac{\sin\rho}{\rho} + 4\,\frac{(1 - \cos\rho)}{\rho}. \qquad (8)$$

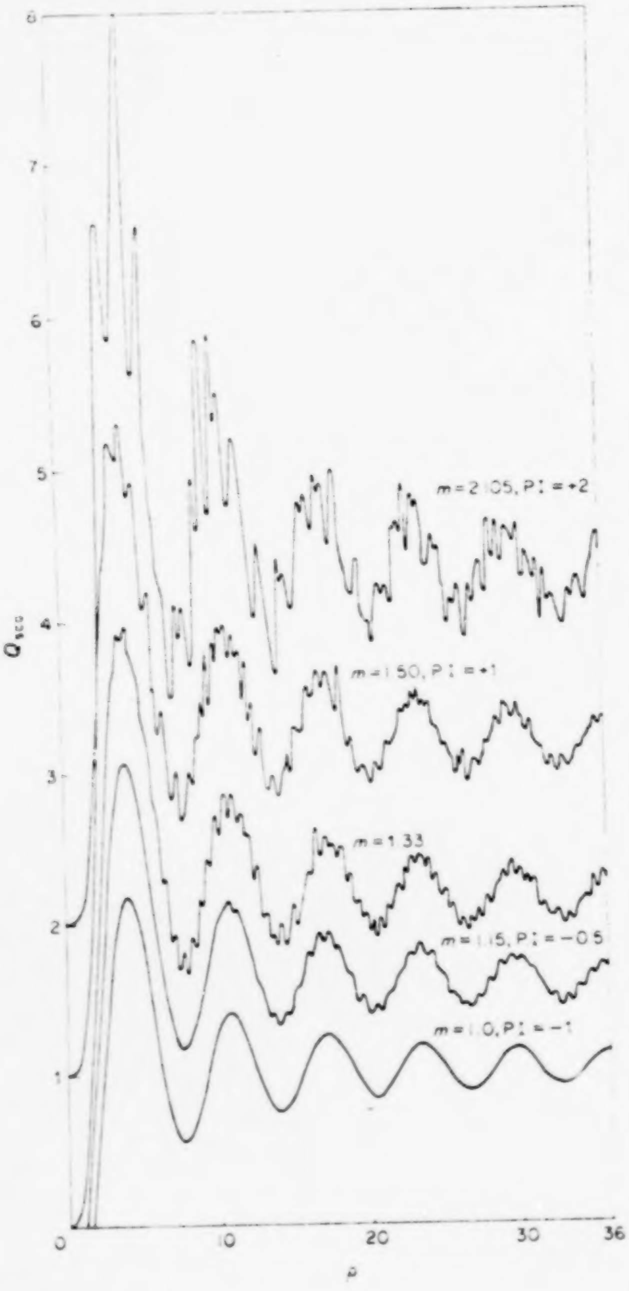

Fig. 4. Scattering coefficient of dielectric spheres plotted against the phase shift parameter $\rho = 2\ \alpha(m - 1)$ according to Kerker.[1215] P.I. designates the plotting increment.

For absorbing spheres the oscillation in the extinction curve becomes less pronounced. Curve C of Figure 5, according to Hodkinson[1211] (p. 289), shows that for an absorbing particle with the complex refractive index $m = 1.55 - 0.66\ i$, which would be appropriate for carbon particles in water, the oscillation has

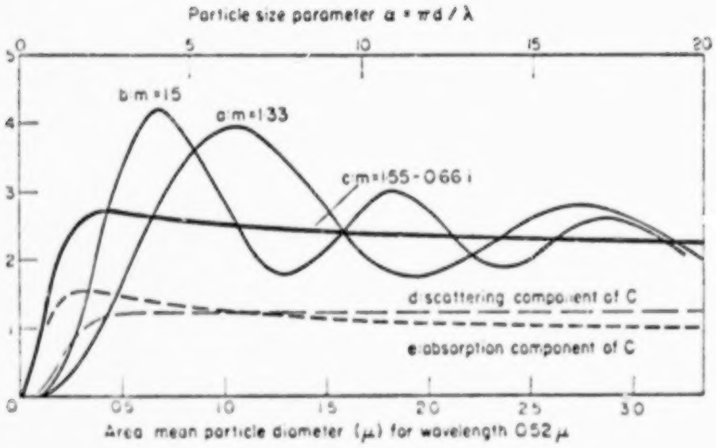

Fig. 5. Extinction coefficient for absorbing and dielectric spherical particles according to Hodkinson[1211] (p. 289).

completely damped out. The effect of absorption in a particle can be more clearly seen in Figure 6 given by Allen,[33] calculated according to the following equation given by Van de Hulst[1201] (p. 179)

$$K = 2 - \exp(-\rho \tan \beta) \left(\frac{\cos\beta}{\rho}\right)^2 \sin (\rho - \beta)$$
$$- \exp(-\rho \tan \beta) \left(\frac{\cos\beta}{\rho}\right)^2 \cos (\rho - \beta) + 4 \left(\frac{\cos\beta}{\rho}\right)^2 \cos 2\beta. \tag{9}$$

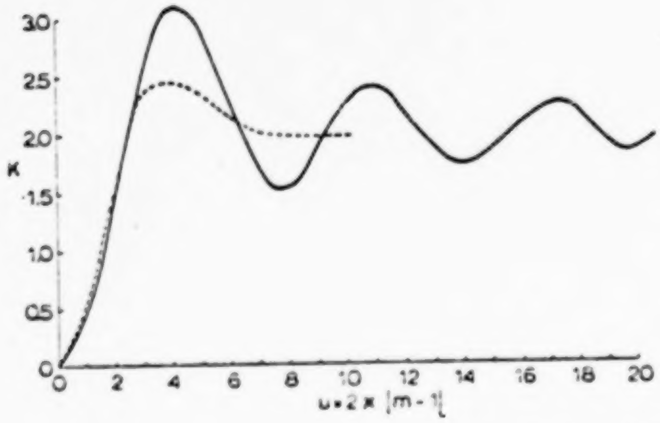

Fig. 6. Extinction coefficient for absorbing (broken line) and dielectric (full line) spheres calculated by Allen[33] according to the equation of Van de Hulst[1201] (p. 179).

Here the complex refractive index of the particle material is $m = m' + m'' i$ and the loss angle β is defined as

$$\tan \beta = m'/(m' - 1). \tag{10}$$

Equation (9) is valid when $|m - 1| << 1$. Figure 6 shows that the oscillation in the extinction curve is quickly damped out for finite values of β.

Figure 7 shows that for the case of the totally reflecting sphere ($m = \infty$) whose extinction coefficient can be represented by the empirical equation[1201]

$$K = 2 + 0.07\ \alpha^{-2/3} + 0.42\ \alpha^{-1} \qquad (11)$$

over the range, $6 < \alpha < 90$, the oscillation in the extinction curve is also not very pronounced.

NOT REPRODUCIBLE

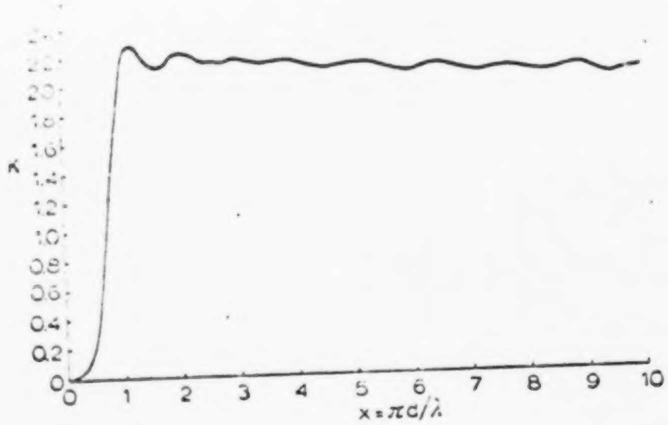

Fig. 7. Extinction coefficient for a totally reflecting sphere ($m = \infty$), with monochromatic light, according to the calculation of Allen[33] using the empirical equation given by Van de Hulst[1207] (p. 162).

B. Effect Of Using White Light And Photocells With Sensitivities That Are Wavelength Dependent

For light transmission measurement in stacks, a tungsten light source and a photo detector are generally used. Since the light from the tungsten source is no longer monochromatic and the sensitivity of the detector is usually wavelength dependent, the extinction coefficient, K, must now be averaged over the wavelength range of the source-detector combination. Figure 8 shows how the extinction coefficient is changed when it is thus averaged over the wavelength range for a tungsten source operated at 2700°K and for a selenium photocell. Although the oscillation in the extinction curve is smoothed out somewhat, as expected, it does not differ appreciably from the extinction curve for monochromatic radiation.

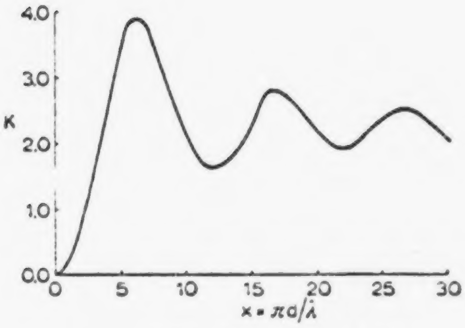

Monochromatic light

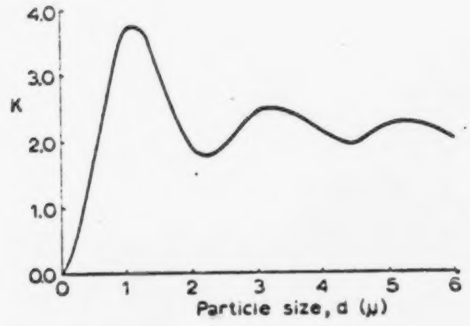

White light

Fig. 8. Smoothing of the extinction curve (m = 1.33) produced by white light from a tungsten source at 2700°K and a selenium photodetector.[33]

C. Irregular Particles

Figure 9 and Figure 10 show the scattering curves for various irregularly shaped particles dispersed in a liquid as measured experimentally by Hodkinson.[1211,1213] As expected, the oscillation in the scattering curves are nearly completely damped out due to the random orientation of the irregular particles. The approach to the geometrical scattering regime (where K = 2) is much more rapid as compared to spherical particles of the same refractive index.

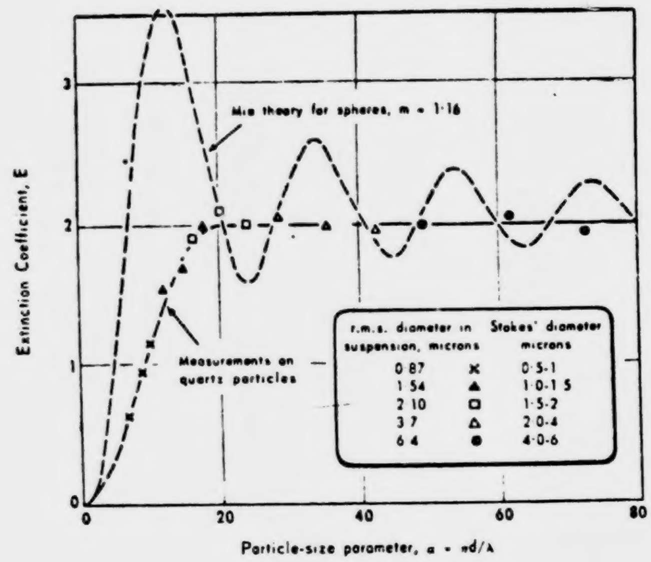

(a) Quartz particles in water

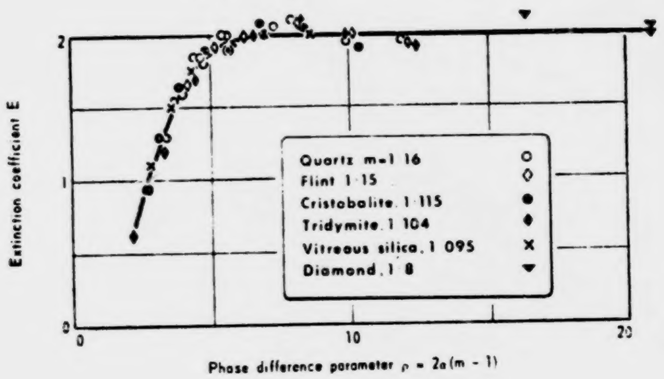

(b) Various minerals in water

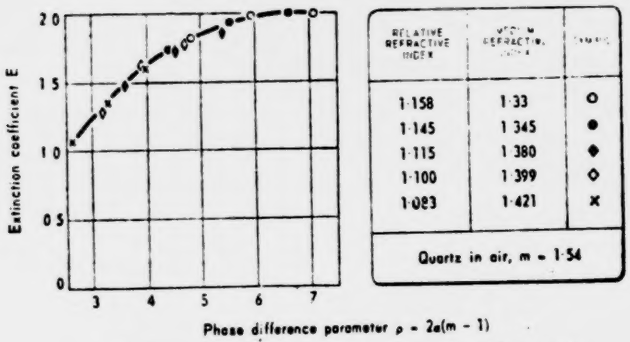

NOT REPRODUCIBLE

(c) Quartz in various sugar solutions, m = 1·083 to 1·158

Fig. 9. Scattering coefficient for irregularly shaped particles according to Hodkinson.[1213]

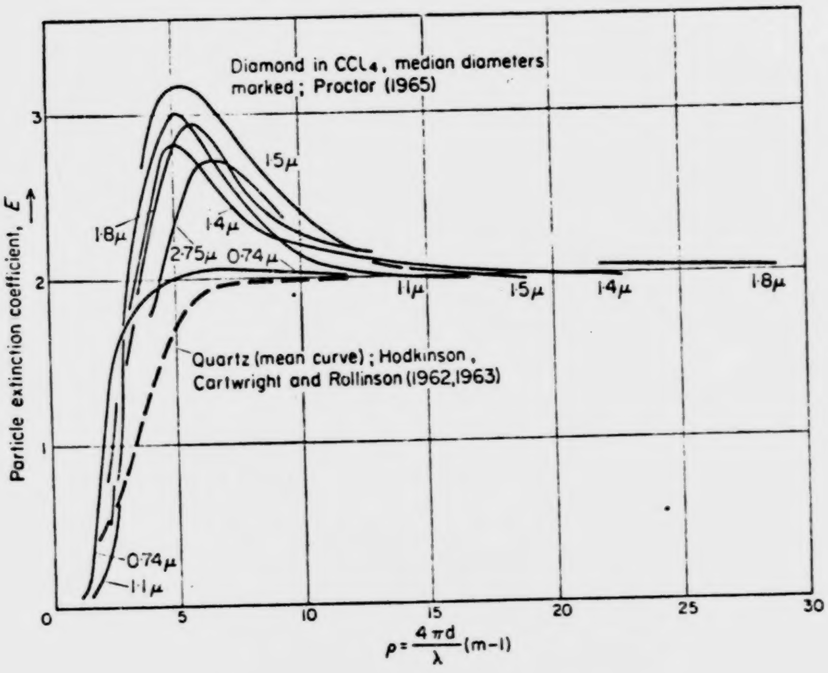

Fig. 10. Scattering coefficient for irregularly shaped particles according to Hodkinson.[1211]

APPLICATION TO MASS CONCENTRATION MEASUREMENT IN STACKS

Light transmission instruments are widely used for the continuous monitoring of smoke emission from stacks. Such instruments are generally referred to as smoke density meters. Their readings are usually expressed in smoke density units, as defined in equation (2), or simply in units of percent transmittance. Sometimes the readings are also expressed in equivalent Ringelmann numbers, where Ringelmann 5 would be equivalent to 0% transmittance, Ringelmann 4, 20% transmittance, etc. A list of domestic manufacturers of smoke density meters and alarms is given below:

Airflow Developments (Canada) Ltd.
Bailey Meter Co.
Cleveland Controls, Inc.
Combustion Equipment Associates, Inc.
Electronics Corporation of America
Infra-Red Industrial Systems Div.
Intertech Corporation
Leeds & Northrup Co.
Mac Leod & Stewart Co., Inc.
Nebetco Engineering
Photobell Co., Inc.
Photomation, Inc.
Reliance Instrument Manufacturing Corp.
Sentry Controls, Inc.
Robert M. Wager Company, Inc.

Many of the early publications on smoke density meters such as the papers by Littlewood,[950] Storey,[963] Lambie,[850] Collins and Steele,[851] and Kolbow and Thieme[193] deal with details of instrument design. A tungsten light source and a photocell detector, such as a cadmium sulfide cell, are generally used. However, an instrument described by Hicks[1033] uses a bolometer detector.

Since in these instruments a light beam must be projected through windows on the sides of the stack, these windows must be kept clean to insure reliable operation. According to Crosse, et al,[487] some of the early attempts at keeping the windows clean by blanketing them with clean air have not been particularly successful, and they have therefore developed the "Everclean Window". The principle of this "Everclean Window" can be seen more clearly in Figure 11 presented by Lucas.[13] The air drawn in from the outside through the small holes by duct suction keeps the coarse dust from accumulating in the large tube, while the thin-walled honeycomb, which is cemented to the window, acts as a vapor trap to keep the vapor from condensing on the window.

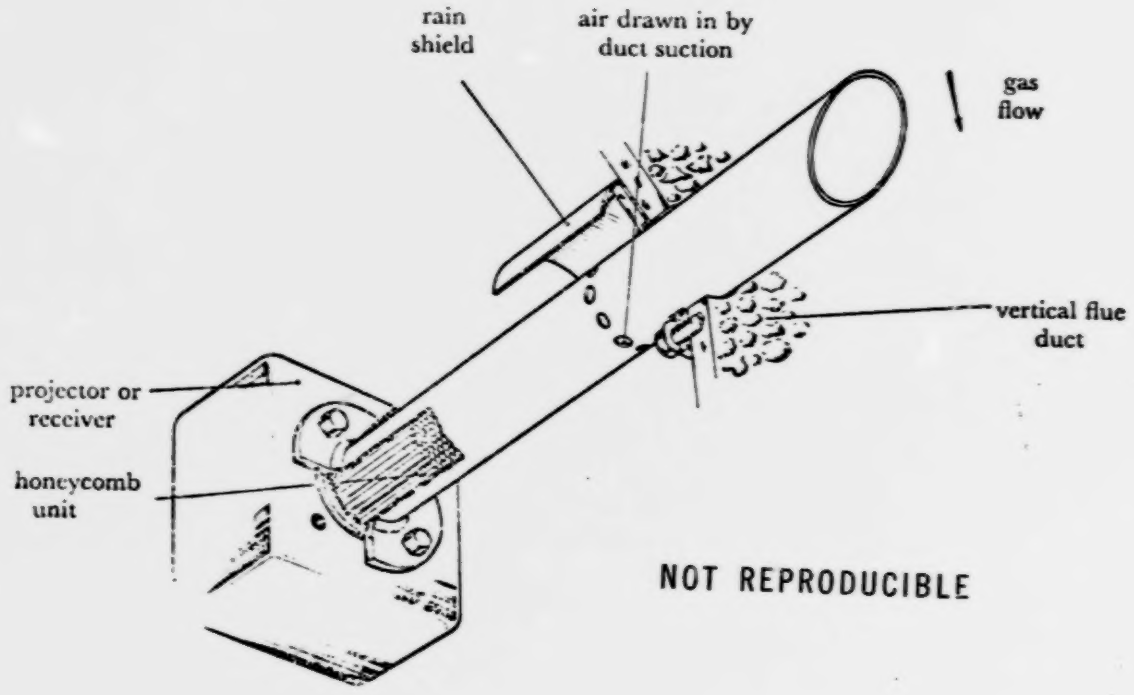

NOT REPRODUCIBLE

Fig. 11. The Everclean window described by Crosse, et al,[487] and by Lucas.[13]

The relationship between the optical density of the aerosol as measured by a smoke density meter and the mass concentration of the particles is quite complex, as discussed earlier. The relationship is dependent on the density, shape, refractive index, and size distribution of the particles. A direct relationship between optical density and mass concentration can be found only when these variables remain constant. In general, the optical density is a measure of the total scattering cross section of the particles. However, in the geometrical scattering regime the optical density is directly proportional to the total surface area of the particles, and for a given mass concentration it is inversely proportional to the mean volume-surface diameter. There have been only a few experimental studies made on the relationship between the optical density of the aerosol in stacks and the properties of the particles.[718,964,485] The results presented by Lucas and Snowsill[485] as shown in Figure 2 appear to be in agreement with the conclusion that, for a given mass concentration, the optical density is inversely proportional to the mean volume-surface diameter.

Schnitzler et al[1189] experimentally calibrated two smoke density meters in terms of particulate mass concentration in a coal-fired effluent duct. They took 5-minute gravimetric filter samples at the center of the effluent duct and compared the measurements with the corresponding 5-minute average smoke density measurement. The results are shown in Table 1 and Figures 13 and 14 and the accompanying discussion of the section entitled "Electrostatic Measurement Methods". Transmissometer A had trouble with window contamination and thus correlated poorly with mass concentration. Transmissometer B correlated reasonably well with mass concentration on the average. However, both transmissometers showed different calibration curves for each of the 3 plant operating conditions in the test. These results show that, although transmissometers may be constructed to yield reasonable mass correlation under normal plant operating conditions, the correlation deteriorates during such operating conditions as soot blowing and partial load. Perhaps most disturbing is that the operator often does not know whether the mass calibration is valid at a given time.

In order to measure correctly the true transmittance of the aerosol, the smoke density meter must have pin-hole apertures as shown in Figure 1 to prevent scattered light from reaching the photocell. Many smoke density meters described in the literature and available commercially do not have pin-hole apertures, and they generally accept a substantial amount of scattered light in the forward direction. The response characteristics of these instruments are much more complicated. Thus, two instruments of identical design will generally respond differently to the same aerosol if they are installed in stacks that are different in size and have different optical path length. Also, the Bouguer, or Beer-Lambert, law will no longer hold for these instruments. Thus a complicating factor is introduced which is best avoided by the use of pin-hole apertures.

The question of the desirability of using pin-hole apertures has also arisen in a related field. In the design of photo sedimentometers for measuring the size distribution of powder particles by sedimentation and by light extinction measurement, the question has arisen as to whether one should use a narrow-angle instrument, in which pin-hole apertures are used to limit the amount of scattered light received by the photocell, or a wide-angle instrument, in which the photocell is deliberately placed very close to the liquid suspension so that practically all the scattered light due to diffraction around the particles is received by the photocell. The question is somewhat controversial, with Hodkinson[1211] favoring a narrow-angle instrument and Allen[34] favoring a wide-angle instrument. The advantage of the wide-angle instrument, according to Allen, is that the instrument will operate in the regime of geometrical scattering over a wider range of particle sizes than the narrow-angle instrument. From the standpoint of instrument design for stack monitoring, aside from the question of relative merit of the wide-angle and the narrow-angle instruments, it is difficult to conceive how a truly wide-angle smoke density meter can be built, since the aperture size in a wide-angle instrument is of the same order of magnitude as the thickness of the medium. Thus, the photocell or the collecting lens aperture must be as large as the thickness of the aerosol illuminated by the light beam and this would appear to be prohibitively large for an instrument designed for aerosol monitoring in stacks. The same question of aperture size is considered from a somewhat different point of view in the section on Angular Light Scattering.

Crosse, et al,[637] and Lucas and Snowsill[485] described an instrument to measure and record the likelihood that dust emitted from a chimney would cause nuisance and complaint at ground level. Since only large particles are involved in causing such nuisance and complaint, they designed an instrument to measure these large particles. The large particles in the stack gas enter a small opening on the side of a vertical tube by inertia and settle to the bottom of the tube. The tube is closed at the upper and lower ends by two glass plates and the amount of dust settled to the bottom glass plate is measured by light extinction. The instrument response is rather complicated, being dependent not only on the optical properties of the particles but also on the somewhat uncertain characteristics of the particle collection device.

CONCLUSIONS

Smoke density meters based upon the principle of light transmission or extincation are likely to continue as an important method for the continuous monitoring of aerosols in stacks. A properly designed smoke density meter with pin-hole apertures will provide a measure of the turbidity of the aerosol which is equal to the total light extinction cross section of the particles. In the geometrical scattering regime, the turbidity is also proportional to the total surface area of the particles. Thus, in the geometrical scattering regime the instrument provides a measure of the aerosol mass concentration only when the volume-surface diameter and the density of the aerosol remain constant and, for a given mass concentration, the aerosol turbidity is inversely proportional to the mean volume-surface diameter. The section of this report entitled "Stack Emissions Properties and Instrument Specifications" shows that particle size distribution and specific density do not remain constant in fossil fuel effluent streams, making correlation of mass concentration with light extinction impossible. From a study of the light scattering properties of small particles, it is concluded that, for aerosol measurement in stacks, a smoke density meter using a tungsten light source will operate essentially in the geometrical scattering regime when the particles are larger than 0.5 to 2 μm diameter, the exact limit being dependent upon the design of the instrument as well as the properties of the particles.

REFERENCES

26 Adams, J. M., "Light Extinction Photometer for Measurement of Particle Sizes in Polydispersions", Review of Scientific Instruments, V. 39, no. 11, p. 1748-1751 (Nov 1968).

33 Allen, T., "Determination of the Size Distribution and Specific Surface of Fine Powders by Photo-extinction Methods. I. Theoretical Estimate of Variation in Extinction Coefficient with Particle Size Using a White Light Source", Powder Technology, V. 2, p. 133-140 (1968-69).

34 Allen, T., "Determination of the Size Distribution and Specific Surface of Fine Powders by Photo-extinction Methods. II. Comparison between Wide-Angle and Narrow-Angle Photosedimentometers and Experimental Determination of Extinction Coefficients", Powder Technology, V. 2, p. 141-153 (1968-69).

106 Anon, "Particle Size Determination Simplified", Chemical & Eng. News, (Feb 1969).

1212 Born, M., and Wolf, E., Principles of Optics, Pergamon Press (1964).

851 Collins, K. E., and Steele, D. J., "High-Sensitivity Recording Optical Density Meter", Journal of Scientific Instruments, V. 38, p. 186-190 (May 1961).

487 Crosse, P. A. E., Lucas, D. H., and Snowsill, W. L., "Design of an "Everclean Window" for the Observation of the Optical Density of Flue Gas", Journal Inst. of Fuel, V. 34, no. 250, p. 503-505 (1961).

637 Crosse, P. A. E., Lucas, D.H., and Snowsill, W. L.,"Instrument for Recording the Dust Nuisance by Chimneys", Journal of Scientific Instruments, V. 38, p. 12-17 (Jan 1961).

46 Harris, G. W., "A Laboratory Instrument for Measuring the Turbidity of a Suspension of Dust Particles", Powder Technology, V. 3, p. 107-111, (1969-70).

1033 Hicks, C. E., "Sensor Measures Stack Effluents--Accurately", Petro/Chem. Engr., V. 39, no. 5, p. 33-34 (1967).

1213 Hodkinson, J. R., "The Physical Basis of Dust Measurement by Light Scattering", Aerosols: Physical Chemistry and Application, p. 181-194, Publishing House of the Czechoslovak Academy of Sciences, K. Spurny, Ed. (1965).

1211 Hodkinson, J. R., "The Optical Measurement of Aerosols", in Aerosol Science, C. N. Davies (Ed), Chap. 10, Academic Press (1966).

718 Hurley, T. F., and Bailey, D. L. R., "The Correlation of Optical Density with the Concentration and Composition of the Smoke Emitted from a Lancashire Boiler", Journal Inst. of Fuel, V. 31, p. 534-550 (Dec 1958).

1214 Kerker, M. Electromagnetic Scattering, Pergamon Press (1963).

1215 Kerker, M., The Scattering of Light and Other Electromagnetic Radiation, Academic Press (1969).

193 Kolbow, P., and Thieme, R., "Smoke-Density Meter for Supervising the Percentage of Dust Contained in the Flue Gases of Industrial Plants", Siemens Rev., V. 38, no. 8, p. 276-278 (Aug 1965).

843 Kratohvil, J. P., "Light Scattering", Analytical Chemistry, V. 36, no. 5, p. 458R-472R (Apr 1964).

850 Lambie, R., "Improved Smoke Density Recorder", Journal of Scientific Instruments, V. 37, p. 144-146 (Apr 1960).

950 Littlewood, A., "Measurement of the Optical Density of Smoke in a Chimney", Journal of Scientific Instruments, V. 33, p. 495-499 (Dec 1956).

485 Lucas, D. H., and Snowsill, W. L., "Some Developments in Dust Pollution Measurement", Atmospheric Environment, V. 1, p. 619-636 (1967).

13 Lucas, D. H., "I. Air Pollution Measurements", Phil. Trans. Royal Society of London, V. A257, p. 143-151 (1969).

147 Mie, G., "Beitrage zur Optik truber medien, speziell kolloidaler Metallosungen", Annalen der Physik, V. 25, no. 3, p. 377-445 (1908).

754 Musgrave, J. R., and Harner, H. R., "Turbimetric Particle Size Analysis", Eagle Picher Research Laboratories, Joplin, Mo., Research Technique & Technology, no. 1, 47 p. (1947).

1199 Newton, R. G., Scattering Theory of Waves and Particles, McGraw Hill (1966).

895 Orr, Clyde, Jr., "Automatic Particle Size Analysis in the Subsieve Range", Paper 6-1, U. S. - Japan Particulate Technology Seminar, Kyoto, Japan (6-11 Oct 1969).

846 Penndorf, R. B., "Total Mie Scattering Coefficients for Spherical Particles of Refractive Index n=2", Journal of the Optical Society of America, V. 46, p. 1001 (Nov 1956).

848 Penndorf, R. B., "New Tables of Total Mie Scattering Coefficients for Spherical Particles of Real Refractive Indexes ($1.33<n<1.5$)", Journal of the Optical Society of America, V. 47, no. 11, p. 1010-1015 (Nov 1957).

847 Penndorf, R. B., "Total Mie Scattering Coefficient for Spherical Particles of Refractive Index n=1", Journal of the Optical Society of America, V. 47, no. 7, p. 603-605 (Jul 1957).

1200 Penndorf, R. B., "New Tables of Mie Scattering Functions for Spherical Particles, Part 6: Total Mie Scattering Coefficients for Real Refractive Indexes", Geophysical Research Paper No. 45, Air Force Cambridge Research Center, Bedford, Mass. (1957).

1181 Penndorf, R. B., "An Approximation Method to the Mie Theory for Collodial Spheres", J. Phys. Chem., V. 62, p. 1537-1542 (Dec 1958).

1189 Schnitzler, H., Maier, O., and Jander, K., "Messtand fur die Prufung and Kalibrierung von Registrierenden Staub - und Gasmessgeraten in einem Steinkohlengefeuerten Kraftwerk", SchrReihe Ver. Wass. - Boden Lufthyg. Berlin-Dahlem, V. 33, Stuttgart (1970).

964 Stoecker, W. F., "Smoke-Density Measurement. Correlation of Solids Content in Gas with Photoelectric Smoke-Meter Readings", Mechanical Engineering, V. 72, no. 10, p. 793-798 (1950).

963 Storey, R. M., "Smoke Density Integrator", Journal of Applied Physics, V. 11, p. 509-512 (Nov 1960).

1250 Stratton, J. A., Electromagnetic Theory, McGraw Hill (1941).

973 Traxler, R. N., and Baum, L. A. H., "Measurement of Particle Size Distribution by Optical Methods", American Society for Testing Materials, V. 35, p. 457-470 (1935).

1201 Van de Hulst, H. C., Light Scattering by Small Particles, Wiley (1957).

MULTI-WAVELENGTH LIGHT TRANSMISSION

by: B.Y.H. Liu and K. T. Whitby

INTRODUCTION

The transmission of light or other electromagnetic radiation through a particulate suspension is dependent upon the wavelength of light used. This fact can be utilized for the measurement of particulate suspensions, including aerosols. By observing the change in the attenuation of light through a particulate suspension with wavelength, certain physical properties of the suspension can be inferred.

Multi-wavelength light transmission, or spectral attenuation, measurement is a powerful tool in the study of colloids and aerosols, where few other methods are as simple and as easy to use. Further, within the limits of its useful size range, the method can provide a measure of the volumetric concentration and the size distribution of the particulate phase. Thus, if the particle density is known or remains fixed, the aerosol mass concentration can be determined.

The transmittance of an aerosol can be measured by means of a transmissometer, which is dicussed in the chapter entitled "Light Transmission". Therefore, the details are not repeated here. In order to reduce the amount of scattered light reaching the optical sensor and to measure the true transmittance, the angular apertures of the instrument must be limited. Because of the reduced light intensity due to the use of monochromatic light, a photomultiplier, instead of a photocell, may have to be used.

To measure the transmittance as a function of wavelength, the wavelength must be varied. This can be accomplished either with monochromatic filters or with a monochromator. In principle, one can also use a tungsten source and vary its temperature to vary the mean effective wavelength, but this approach does not appear to have been tried.

BASIC PRINCIPLE

There are three possible methods whereby the same general principle can be utilized for size and concentration measurements. These are usually referred to as the first maximum method, the dispersion quotient and turbidity ratio method, and the wavelength exponent method. These methods have been reviewed and discussed in some detail in the recent book by Kerker[1215] (pp. 334-343).

The general principle underlying these methods can be seen by referring to Figure 1. This figure shows the typical relationship between the particle extinction coefficient $K(m,\alpha)$ and the dimensionless particle size parameter

$$\alpha = \pi D/\lambda \qquad (1)$$

calculated from the Mie theory. Here m is the refractive index of the particle, D is the particle diameter (assuming a sphere) and K, the particle extinction coefficient, is defined as the ratio of the flux scattered and absorbed by the particle to the flux geometrically incident upon the particle. It is seen that for particles of a specific size varying the wavelength, λ, varies the dimensionless size parameter, α, and causes a similar change in the extinction coefficient, K. The corresponding change in light attenuation through the suspension is the basis of the methods considered in this section.

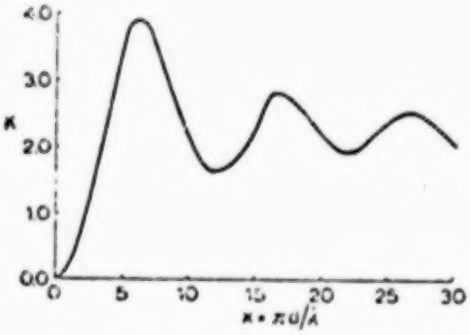

Fig. 1. Typical particle extinction curve.

The first-maximum method was first applied to monodisperse particulate suspensions by La Mer and Sinclair[1203] and later used by many others for measuring the size and the concentration of particulate suspensions[1186,1182,1172,1202]. In applying this method to monodisperse systems, the dimensionless particle size parameter, α, is varied by varying the wavelength until it reaches a point corresponding to the first maximum in the particle extinction curve. At this point, the turbidity, k, of the suspension, which is related to the experimentally measured transmittance, T, as follows

$$T = \exp(-k\,\ell), \qquad (2)$$

should also show a maximum. Here, ℓ is the path length of the light beam through the suspension. Knowing the value of α at the first maximum from theory and the wavelength λ at which the maximum is observed, the particle diameter can then be determined by means of equation (1). To calculate the concentration of the particles in the suspension, the following relationship between turbidity, k, and concentration is used:

$$k = (1/4)\ \pi D^2\ K\ C_n \tag{3}$$

where C_n is the number concentration of the particles. Since the volumetric concentration of the particles, C_v, is related to the number concentration C_n, as

$$C_v = (1/6)\ \pi D^3\ C_n, \tag{4}$$

equation (3) is equivalent to

$$k = \frac{3\ K\ C_v}{2\ D}. \tag{5}$$

Thus, knowing the value of K from theory and the value of k and D from experiment, the volumetric concentration C_v can be calculated by means of equation (5).

For a polydisperse system of spherical particles, equations (3) and (4) must be integrated over the appropriate size distribution. Dobbins and Jizmagian[603] have shown that equation (5) continues to apply provided K is replaced by the mean extinction coefficient, $\bar{K}$, defined as

$$\bar{K} = \frac{\int K\ D^2\ f(D)\ dD}{\int D^2\ f(D)\ dD} \tag{6}$$

and D is replaced by the volume-surface, or the mean Sauter, diameter, D_{vs}, defined as

$$D_{vs} = \frac{\int D^3\ f(D)\ dD}{\int D^2\ f(D)\ dD}. \tag{7}$$

Thus, for a polydisperse system,

$$k = \frac{3\ \bar{K}\ C_V}{2\ D_{vs}}. \tag{8}$$

Dobbins and Jizmagian have also shown that the values of $\overline{K}$ obtained by integrating over a rectangular, a parabolic and an upper limit distribution function are essentially the same and that there is a universal function relating $\overline{K}$ and the phase shift parameter

$$\rho_{vs} = 2(m - 1)\alpha_{vs} \tag{9}$$

where the dimensionless particle size parameter, α_{vs}, is based on the volume-surface or mean Sauter diameter of the suspension. Table 1, reproduced from the paper of Dobbins and Jizmagian, shows the relationship between $\overline{K}$ and α_{vs} with the refractive index, m, as a parameter. On the basis of these results it can be concluded that the first maximum method should continue to apply to polydisperse systems.

Table 1

Data from Dobbins & Jizmagian[603] showing the mean particle extinction coefficient K as a function of the phase-shift parameter, $\rho_{vs} = 2\ (m - 1)\alpha_{vs}$ with the refractive index, m, of the particle as a parameter.

				m			
ρ_{32}	1.20	1.33	1.40	1.50	1.65	1.75	1.85
0.5	(0.0840)*	0.04924	0.03601	0.02336	0.01297	0.00910	0.00658
1.0	(0.500)	0.3986	0.3500	0.2821	0.1957	0.1504	0.1150
1.5	(1.122)	1.043	0.9987	0.9176	0.7688	0.6584	0.5495
2.0	1.820	1.781	1.768	1.726	1.621	1.523	1.412
2.5	2.399	2.446	2.469	2.479	2.475	2.413	2.332
3.0	2.824	2.931	2.986	3.041	3.150	3.135	3.083
3.5	3.057	3.200	3.275	3.360	3.562	3.590	2.566
4.0	3.114	3.272	3.356	3.458	3.717	3.775	3.776
5.0	2.904	3.066	3.147	3.249	3.521	3.605	3.635
6.0	2.618	2.773	2.842	2.930	3.152	3.233	3.273
7.0	2.442	2.589	2.649	2.725	2.904	2.978	3.021
8.0	2.349	2.490	2.544	2.612	2.766	2.835	2.881
9.0	2.293	2.427	2.476	2.538	2.675	2.739	2.787
10.0	2.255	2.383	2.428	2.486	2.610	2.670	2.718
12.0	2.209	2.327	2.368	2.420	2.522	2.577	2.623
14.0	2.181	2.287	2.327	2.363	2.460	2.510	2.553
16.0	2.159	2.255	2.296	2.330	2.412	2.457	2.497
18.0	2.142	2.300	2.270	2.302	2.373	2.414	2.452
20.0	2.129	2.208	2.246	2.279	2.341	2.378	2.413
30.0	2.087	2.147	2.168	2.195	2.234	2.262	2.289
50.0	2.032	2.087	2.099	2.117	2.173	2.179	2.182
100.0	2.024	2.042	2.049	2.059	2.075	2.085	2.093

* Values in parentheses obtained by extrapolation.

NOT REPRODUCIBLE

The question of how the first maximum in the particle extinction curve is affected by the polydispersity of the suspension was also studied by Hilbig.[905] The author used a log-normal and a Maxwellian distribution, and described a procedure for determining the parameters in these distributions from a knowledge of the volumetric concentration of the suspension and the location of the first maximum as determined by spectral attenuation measurements.

The first maximum method was applied to irregularly shaped particles by DeVore and Pflund.[1255] The authors measured the spectral attenuation of particulate suspensions consisting of uniform sized but irregularly shaped particles over the wavelength range from 0.8 to 3.0 μm and found typical turbidity maxima similar to those observed for spherical particles. The measured particle sizes based on the first maximum method were in excellent agreement with those found by light microscopy.

Since the particle extinction coefficient is also a function of the refractive index of the particle, to use the first maximum method for size and volumetric concentration measurements the particle refractive index must also be known. Additionally, to measure the mass concentration of the suspension, the particle density must be known. Both of these parameters, if unknown, presumably can be determined by an independent procedure. Thus, in actual practice, it is only necessary that these parameters remain unchanged.

The particle size range of the first-maximum method is dependent upon the refractive index of the particles and the range of wavelength that is available. From Table 1 we see the first maximum in the particle extinction curve occurs at approximately the point $\rho_{vs} = 2\,\alpha_{vs}(m - 1) = 4$. For example, if $m = 2$, then $\alpha_{vs} = \pi D_{vs}/\lambda = 2$. Thus if λ can be varied within the range from 0.35 to 2 μm, then the corresponding range in D_{vs} is from 0.22 to 1.27 μm. Thus, the size range of the method is quite limited. However, within its useful size range the method does provide a measure of the particle mass.

The turbidity ratio method and the dispersion quotient method are similar in principle and both require that the turbidity, k, of the suspension be measured at two preselected wavelengths, λ_1 and λ_2. Figure 2 shows the turbidity ratio as a function of the particle size calculated from Mie theory for a particle refractive index of 1.2 and $\lambda_1 = 0.365$ and $\lambda_2 = 1.01$ μm. Using this method, Dobbins and Jizmagian[602] measured the volume-surface mean diameters and the volumetric concentrations of several latex suspensions. The results are in satisfactory agreement with the corresponding values measured by electron microscopy and by a gravimetric method, the maximum error in the volume-surface mean diameter and the volumetric concentration being on the order of 10% and 13% respectively. The same method was also applied by Dobbins[757,567] to the measurement of aluminum oxide particles in the exhaust of a small rocket motor.

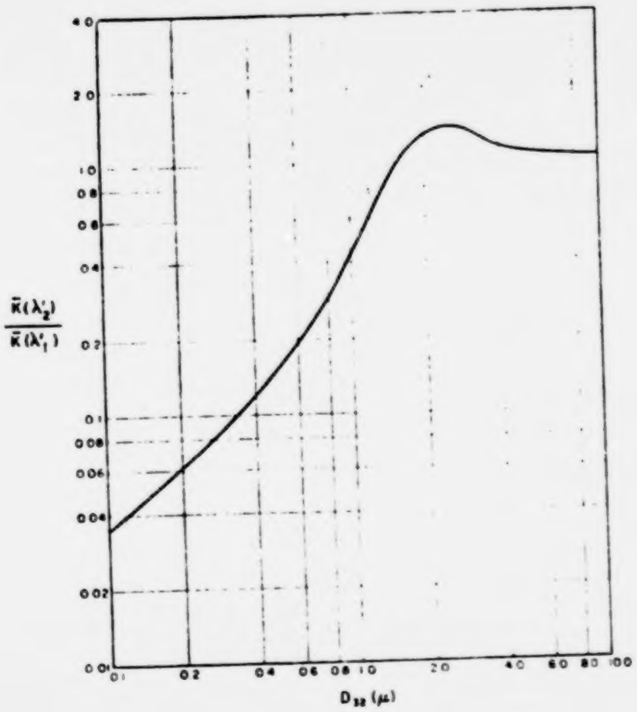

Fig. 2. Turbidity ratio for m = 1.2 and λ_1 = 0.365 and λ_2 = 1.01 μm.[602]

In the dispersion quotient method, first suggested by Teorell nearly 40 years ago, the dispersion coefficient defined as

$$DQ = \frac{k_1 \lambda_2^2}{k_2 \lambda_1^2} \tag{10}$$

is determined experimentally by measuring k_1 and k_2 at the wavelengths λ_1 and λ_2. By referring to a theoretical curve for the dispersion quotient as a function of particle size, the particle size is determined. Figure 3 shows the comparison of the theoretical and the experimental dispersion coefficients for m = 1.214 and 1.200 and λ_1 = 0.405 and λ_2 = 0.546.

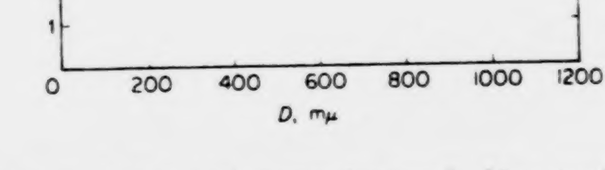

Fig. 3. Theoretical and experimental dispersion coefficient.[1185]

The wavelength exponent method was applied to polystyrene latex suspensions by Heller, et al,[144] and Bateman, et al,[1172] and studied in considerable detail theoretically by Heller, et al,[1184] and by Heller.[1183] The method is based on the observation that for a specific suspension, if the variation of the turbidity, k, with the wavelength is written as follows,

$$k = (\text{const})\lambda^{-g} \qquad (11)$$

the wavelength exponent, g, is a function of the dimensionless particle size parameter, α. The exponent, g, is equal to 4 for Rayleigh scattering and decreases steadily to zero with increasing particle size or decreasing wavelength and eventually goes negative. Thus, knowing the wavelength exponent, g, and the wavelength, the particle size can be determined. The wavelength exponent, g, is usually determined by measuring the turbidity at two slightly different wavelengths. Figure 4 shows the wavelength exponent calculated from Mie theory.

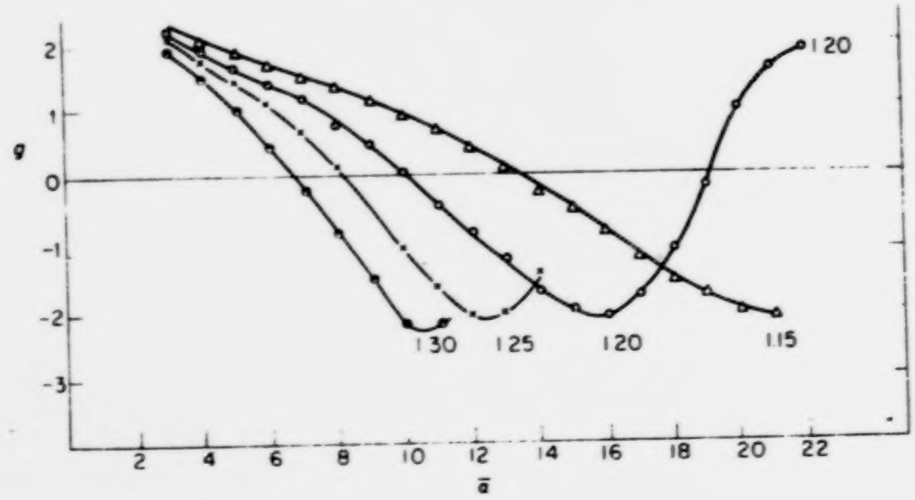

Fig. 4. The wavelength exponent, g, for a slightly polydisperse system.[1184]

The size distribution of particulate suspensions can sometimes be inferred from spectral attenuation measurements. The process of deriving the size distribution from spectral attenuation measurements is a complicated one and many procedures have been devised. The procedures generally fall into two classes. In one, the spectral attenuation curves are calculated for various size distribution functions. The curve that appears to fit the experimental data the best is selected and the corresponding distribution function is taken to represent that of the suspension. In the second procedure, the basic equation for calculating the turbidity

$$k(\lambda) = \int D^2 K(\lambda) \; C_n \, f(D) \, dD \qquad (12)$$

is regarded as an integral equation and solved numerically on a computer to obtain the size distribution. These procedures have been discussed in considerable detail by Kerker[12][15] and by Yamamoto and Tanaka.[22] We shall not discuss them in further detail here since the possibility of applying them to general stack monitoring appears to be quite limited.

For making spectral attenuation measurements, various investigators have generally used the general purpose laboratory spectrophotometer, for which there are many manufacturers. However, an instrument specially designed for measuring flue gases is available from the DuPont Co. (Model 400 photometric analyzer, Instrument and Equipment Division, Wilmington, Delaware 19898). In this instrument the wavelength can be varied between the limits of 210 and 1000 nm.

APPLICATION TO MASS CONCENTRATION AND SIZE DISTRIBUTION MEASUREMENTS IN STACKS

Spectral attenuation measurement can be considered as a natural extension of the usual smoke density meter in which white light from a tungsten source is generally used. As such, it possesses all the advantages of the smoke density meter including the relative simplicity and the relative low cost of the instrument as well as the ability to integrate the reading along the path of the light beam. The fact that the instrument does not have to be in actual physical contact with the flue gas, except for the window through which to project the light beam, is of course, another advantage. The added requirement of changing the wavelength does not necessarily mean that the instrument is considerably more complex than the usual smoke density meter, since the wavelength can be simply changed by turning a wheel on which a series of filters has been mounted.

Any one of the three methods discussed in the preceeding section can be used to measure the mean volume-surface diameter of the particles and the mass concentration of the aerosol. The equipment required is essentially the same, the difference being primarily in the method of data interpretation and reduction. In order for the instrument to measure the true aerosol mass, the refractive index and the density of the particles must remain constant with time so that, once the values of these parameters are determined for a specific emission source, they can be used subsequently for the same source and similar sources with similar particle characteristics. This requirement may turn out to be a major limiting factor in the application of these methods. Unfortunately, the size ranges of these methods are quite limited. The mean volume-surface diameter of the aerosol covered by this method extends at most over a decade, because of the limit in the wavelength range that is available for such measurements. However, if the technical problem of making the measurement, say up to a wavelength of 5 μm, can be solved, then upper size limit can be extended considerably beyond 2 μm which we regard as the upper limit based on existing technology. Some further research on the application of these methods to stack monitoring definitely appears worthwhile. Even if the upper size limit cannot be pushed further, the method as it exists should be useful for such sources as oil-fired furnaces and incinerators where the mean particle size may be small and be within the range of these methods.

Although in principle it should be possible to infer the particle size distribution from spectral attenuation measurements, the data reduction process does not lend itself to the type of automatic operation required for stack monitoring. In addition, the method works the best only on relatively narrow size distributions and the variation in these narrow size distributions that can be detected by the method appears to be of little interest from the standpoint of stack monitoring.

REFERENCES

1186 Barnes, M. D., and LaMer, V. K., "Monodispersed Hydrophobic Colloidal Dispersions and Light Scattering Properties, II. Total Scattering from Transmittance as a Basis for the Calculation of Particle Size and Concentration", J. Coll. Sci., V. 1, p. 79-91 (1946).

1172 Bateman, J. B., Weneck, E. J., and Eshler, D. C., "Determination of Particle Size and Concentration from Spectrophotometric Transmission:, J. Coll. Sci., V. 14, p. 308-329 (Jun 1959).

1255 DeVore, J. R., and Pflund, A. H., "Optical Scattering by Dielectric Powders of Uniform Particle Size", J. Optical Society America, V. 56, p. 1351 (1947).

1185 Dezelic, G., Dezelic, N., and Tezak, B., "A Simple Method for Particle Size Determination by Turbidity Measurement", J. Coll. Sci., V. 18, p. 888-892 (1963).

601 Dobbins, R. A., "Measurement of Mean Particle Size in a Gas-Particle Flow", AIAA Journal, V. 1, p. 1940-1942 (1963).

757 Dobbins, R. A., "An Emission-Scattering Photometer for Particle Size Measurement", Brown University, Providence, R. I., Report on Research for Jet Propulsion Lab., Padadena, Calif., Contract No. JPL 950573, (Aug 1964).

603 Dobbins, R. A., and Jizmagian, G., "Optical Scattering Cross Sections for Polydispersions of Dielectric Spheres", Optical Society of America Journal, V. 56, p. 1345 (1966).

602 Dobbins, R. A., and Jizmagian, G., "Particle Size Measurements Based on Use of Mean Scattering Cross Sections", Optical Society of America Journal, V. 56, p. 1351 (1966).

567 Dobbins, R. A., "Remote Size Measurements of Particulate Products of Heterogeneous Combustion", 11th International Symp. on Combustion, Combustion Inst., Pittsburgh, Pa. (1967).

759 Dobbins, R. A., and Strand, L. D., "A Comparison of Two Methods of Measuring Particles Size of Al_2O_3 produced by a Small Rocket Motor", Brown University, Providence, R.I.

1184 Heller, W., Bhatnagar, H. L., and Nakagaki, M., "Theoretical Investigations on the Light-Scattering of Spheres. XIII. The Wavelength Exponent of Differential Turbidity Spectra", *J. Chem. Phys.*, V. 36, p. 1163-1170 (1962).

1183 Heller, W., "Theoretical Investigations on the Light Scattering of Spheres. XV. The Wavelength Exponents of Small α Values", *J. Chem. Phys.*, V. 40, p. 2700-2705 (1964).

905 Hilbig, G., "Particle Size Distributions of Polydisperse Systems by Means of the First Maximum Methods", *Staub-Reinhalt der Luft (Engl. Trans.)*, V. 29, no. 5, p. 1-5 (May 1969).

1211 Hodkinson, J. R., "The Optical Measurement of Aerosols", in *Aerosol Science*, C. N. Davies (Ed.), Chap. 10, Academic Press (1966).

1182 Johnson, I., and LaMer, V. K., "The Determination of the Particle Size of Monodispersed Systems by the Scattering of Light", *Amer. Chem. Soc. J.*, V. 69, p. 1184-1192 (1947).

1202 Kenyon, A. S., "Higher Order Tyndall Spectra in Monodispersed Sulfur Sols", *Trans. N.Y. Acad. Sci.* (1962).

1215 Kerker, M., *The Scattering of Light and Other Electromagnetic Radiation*, Academic Press (1969).

1203 LaMer, V.K., and Sinclair, D., "Verification of the Mie Theory", OSRD Rep. No. 1857 and 944, Office of Publ. Board, U. S. Dept. of Comm., Washington, D. C. (1943).

22 Yamamoto, G., and Tanaka, M., "Determination of Aerosol Size Distribution from Spectral Attenuation Measurements", *Applied Optics*, V. 8, No. 2 p. 447-454 (Feb 1969).

Reviewed But Not Cited in Test

1204 Cole, J. E., III, Dobbins, R. A., and Semerjian, H., "Time-Resolved Measurement of Droplet Size and Concentration in Cloud Chambers", to appear in *J. Appl. Met.* (1970).

792 Conner, W. D., and Hodkinson, J. R., "Optical Properties and Visual Effects of Smoke-Stack Plumes", National Center for Air Pollution Control, Cincinnati, Ohio, Clearinghouse No. PB 174 705 (1967).

836 Hodkinson, J. R., "Some Observations on Light Extinction by Spherical Particles", *British Journal of Applied Physics*, V. 14, p. 931-932 (Dec 1963).

735 Lanzo, C. D., and Ragsdale, R. G., "Experimental Determination of Spectral and Total Transmissivities of Clouds of Small Particles", Lewis Research Center, Cleveland, Ohio, Clearinghouse No. N 62 16012 (Sep 1962).

631 Marteney, P. J., "Experimental Investigations of the Opacity of Small Particles", United Aircraft Corp., East Hartford, Conn., Clearinghouse No. N 65 20983 (1965).

170 Takahashi, K., "Determination of Number Concentration of Polydispersed Small Aerosol Particles by Turbidity Measurement", Journal of Colloid & Interface Science, V. 24, no. 2, p. 159-163 (1967).

137 Wallach, M. L., Heller, W., and Stevenson, A. F., "Theoretical Investigations on the Light Scattering of Colloidal Spheres. XII: The Determination of Size Distribution Curves from Turbidity Spectra", Journal of Chemical Physics, V. 34, p. 1796-1802 (1961).

LIGHT SCATTERING: POLARIZATION RATIO METHODS

by: N. Barsic, B.Y.H. Liu and K. T. Whitby

INTRODUCTION

When unpolarized incident light is scattered by an object, the scattered light intensity can be described by two plane polarized components, i_1, perpendicular to, and i_2, parallel to the plane of observation. There is a relationship between the intensity of scattered light and the wavelength of incident light, object size, shape, size distribution, index of refraction, and observation angle. Most light scattering studies utilize the sum of the two intensity components to determine the particle size and distribution of an aerosol, as in the conventional optical counter and aerosol photometer. However, in the polarization ratio method considered in this section, the ratio, i_1/i_2, is used as a measure of the particle size.

BASIC PRINCIPLE

If the light scattering theory is applied to a monodisperse aerosol system, a unique relationship is found to exist between the polarization ratio, i_1/i_2, and particle size for right angle scattering with $\alpha < 2.5$. Here $\alpha = \pi d/\lambda$ is the dimensionless particle size parameter that occurs in light scattering theories, d is the particle diameter and λ is the wavelength. The device commonly used to perform these experiments is illustrated in Figure 1. The eyepiece is fitted with a split field polarizer disk, one half having its direction of vibration parallel to

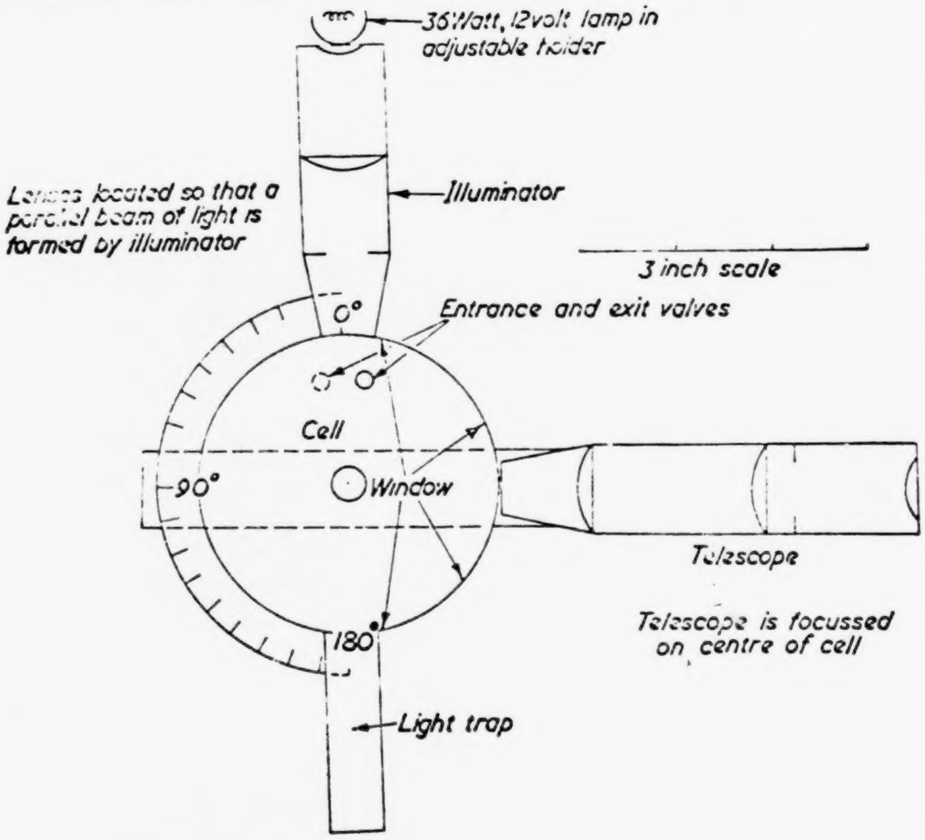
36 Watt, 12volt lamp in adjustable holder
Lenses located so that a parallel beam of light is formed by illuminator
Illuminator
3 inch scale
0°
Entrance and exit valves
Cell
90°
Window
Telescope
Telescope is focussed on centre of cell
180
Light trap

Fig. 1. Instrument for determining angular distribution of spectral colours and polarization - the Owl.[1216]

a dividing line and the other half perpendicular to it. The dividing line is usually parallel to the plane of observation. A filter is placed in the optical system between the polarizer and the observer to yield nearly monochromatic light. The polarizer is rotated until both halves of the field are equal in brightness. This angle, ϕ, is related to the polarization ratio by the following equation:

$$\tan^2 \phi = i_1/i_2 = \rho(\theta)$$

The system can then be calibrated with different sized aerosols and indices of refraction. The data are summarized in a series of curves as shown by Figure 2 from Green and Lane.[1216]

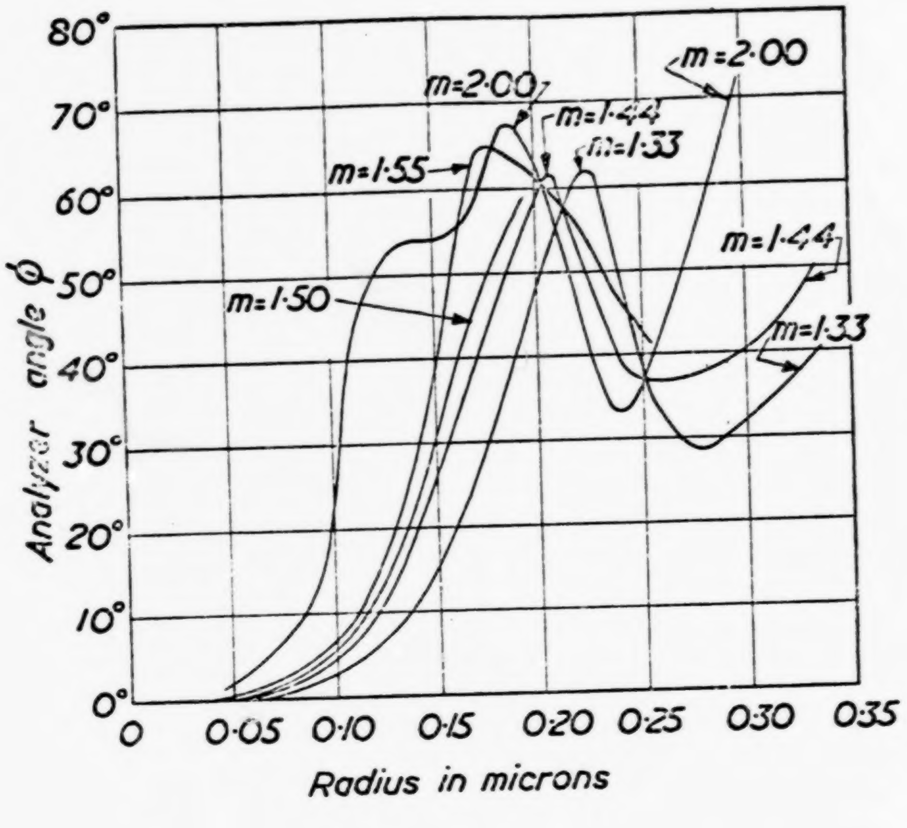

Fig. 2. Analyzer angle ϕ as a function of radius of particle.[1216]

Because the measurement obtained by this method is a ratio, no instrument constant is necessary, which greatly simplifies the application of the method.[144]

The polarization ratio method is easily applicable to studying both monodisperse and polydisperse aerosols. The polarization ratio increases monotonically from its value of $\cos^2 \theta$ for small particles up to a maximum at approximately $\alpha = 2.5$.[909] If some knowledge about the aerosol system is available, a single measurement of $\rho(\theta)$ at one angle can provide a measure of particle size for a monodisperse aerosol. For polydisperse aerosols the polarization ratio is defined in terms of a size distribution function as presented in the equation below:

$$\rho(\theta) = I_2(\theta)/I_1(\theta) = \frac{\int f\ (\alpha) i_2(\theta,\alpha) d\alpha}{\int f\ (\alpha) i_1(\theta,\alpha) d\alpha}$$

where

$f(\alpha)$ is the size distribution function

θ is the scattering angle

α is $\pi d/\lambda$

d is particle size

λ is light wavelength.

Analysis of an aerosol is then reduced to determining the distribution function corresponding to measured values of $\rho(\theta)$ by comparison with theoretical calculations. Theoretical values of $\rho(\theta)$ have been computed for many cases.[1215] Heller and Wallach[140] and Takahashi and Iwai[58] present detailed approaches to this problem. The exact procedure is complex and time consuming; therefore, initial studies indicate that this method is appropriate for research applications only.

The effect of varying the spread (increasing the standard deviation, σ) of the distribution function is illustrated in Figure 3.

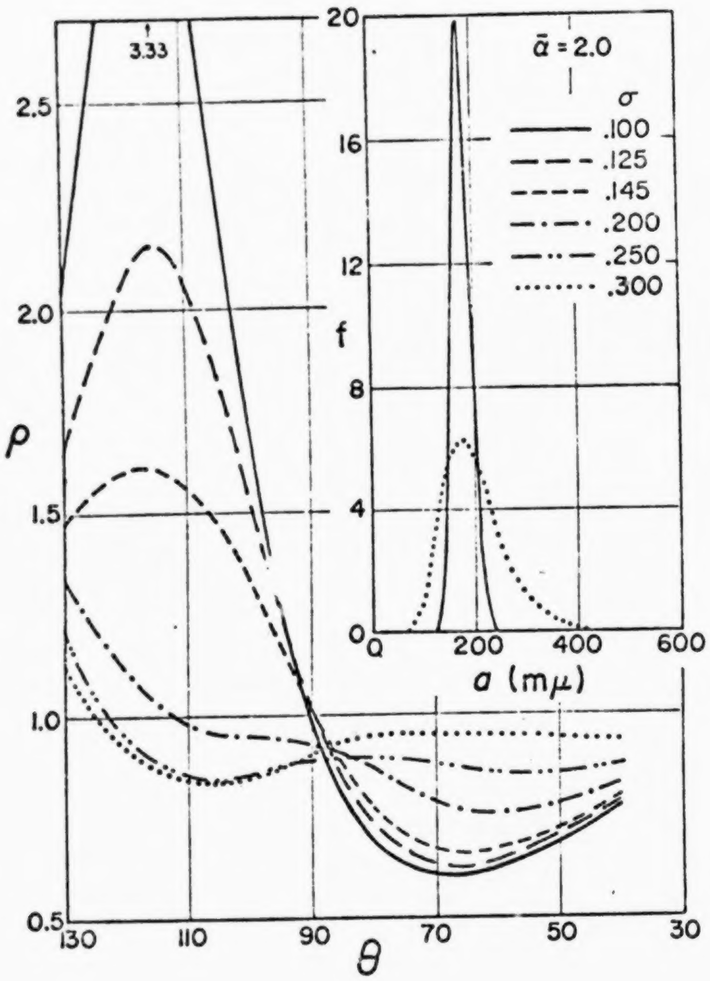

Fig. 3. Plot of $\rho(\theta)$ versus θ for $\bar{\alpha}$ = 2.0 and σ = 0.100, 0.125, 0.145, 0.200, 0.250, and 0.300. The insert shows the corresponding extreme distribution curves. a = radius in mμ.[71]

Figures 3 and 4 illustrate the increase in oscillation evident as α increases. Also obvious in these two figures is the tendency of the oscillation amplitude to decrease as σ (standard devivation) increases. These graphs indicate that a more precise determination of size distribution is possible for narrower distributions, and that σ = 0.3 is the upper limit of this method.

Note that as σ changes, the extreme of these curves remains at the same angular position. This tendency provided an earlier method of determining particle size using single particle scattering functions.[71]

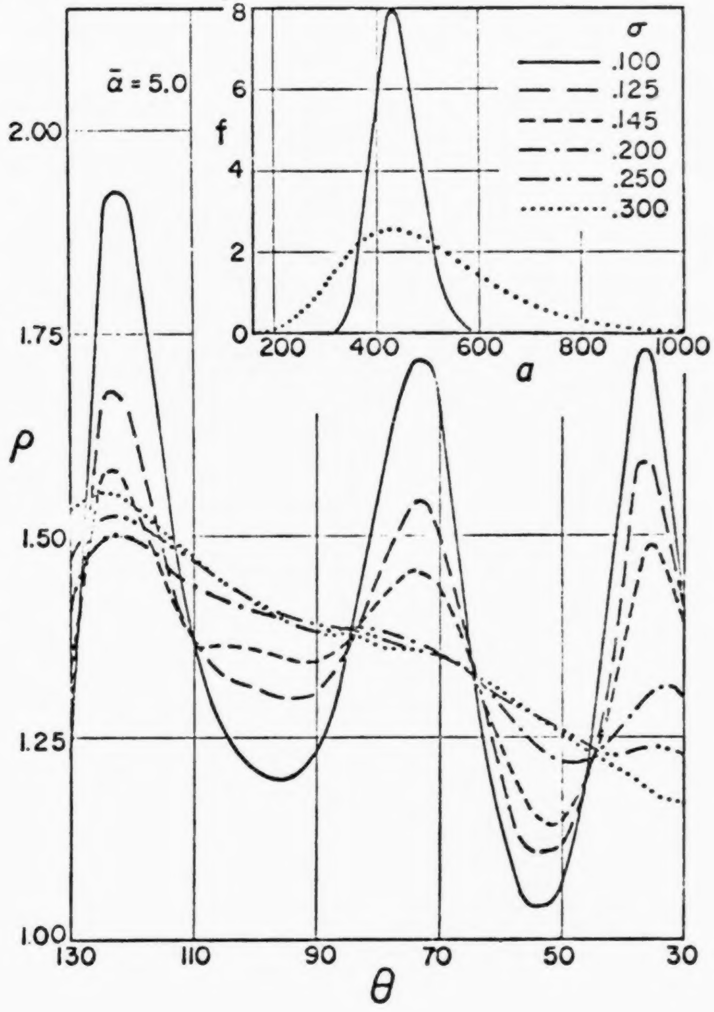

Fig. 4. Plot of $\rho(\theta)$ versus θ for $\bar{\alpha} = 5.0$ and $\sigma = 0.100$, 0.125, 0.145, 0.200, 0.250 and 0.300. The insert shows the corresponding extreme distribution curves. a = radius in mμ.[71]

The effect of refractive index on polarization ratio measurements is illustrated in Figure 5 from Takahashi and Iwai.[58] This figure presents the dissymmetry factor (a form of polarization ratio) as a function of log σ_g for several values of α and refractive index.

Although the polarization ratio method has not been treated as

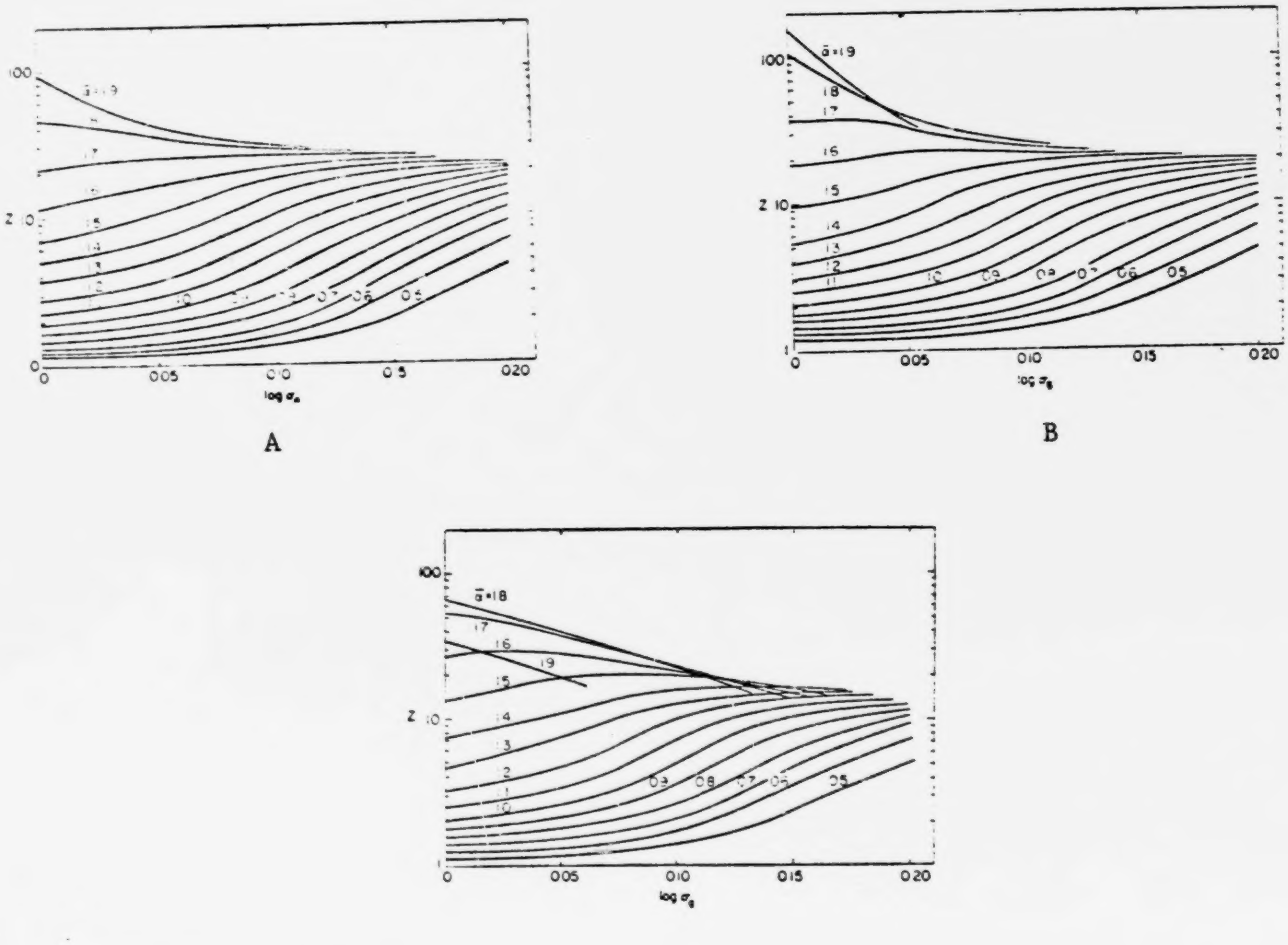

A

B

C

Fig. 5. Dissymmetry factor vs. particle size distribution: (A) m = 1.33, (B) m = 1.44, and (C) m = 1.55.

extensively as direct light intensity measurements, it does offer advantages provided the size parameter, α, is less than 2.5, the size distribution standard deviation is less than 0.3 and refractive index is relatively uniform. Within these limits, polarization ratio measurements provide a useful research tool for determining the size distribution of an aerosol.

APPLICATION TO MASS EMISSIONS MEASUREMENT IN STACKS

Measurements of the polarization ratio of scattered light intensity is useful to determine mass concentration only if aerosol characteristics such as density and particle shape are available. Such information is necessary because this method; like all optical techniques, is sensitive to particle geometry and not mass; therefore direct mass concentration data cannot be obtained.

REFERENCES

1216 Green, H. L., and Lane, W. R., Particulate Clouds: Dusts, Smokes and Mists, E. and F. N. Spon Ltd., London (1964).

144 Heller, W., and Wallach, M. L., "Experimental Investigations on the Light Scattering of Colloidal Spheres. V: Determination of Size Distribution Curves by Means of Spectra of the Scattering Ratio", Journal of Physical Chemistry, V. 67, p. 2577-2583 (1963).

1211 Hodkinson, J. R., "The Optical Measurement of Aerosols", in Aerosol Science, C. N. Davies (Ed.) Chapter 10, Academic Press (1966).

1215 Kerker, M., The Scattering of Light and Other Electromagnetic Radiation, Academic Press (1969).

71 Kerker, M., Matijevic, E., Espenscheid, W. F., Farone, W. A., and Kitani, S., "Aerosol Studies by Light Scattering. I. Particle Size Distribution by Polarization Ratio Method", Journal of Colloid Science, V. 19, p. 213-222 (Mar 1964).

147 Mie, G., "Beitrage zur Optik truber medien, speziell kolloidaler Metallosungen", Annalen der Physik, V. 25, no. 3, p. 377-445 (1908).

580 Ogle, H. M., "Particle Counting Techniques Available for Aerosol Research", APCA Journal, V. 18, p. 657-659 (Oct 1968).

140 Stevenson, A. F., Heller,W.,& Wallach, M. L.,"Theoretical Investigations on the Light Scattering of Colloidal Spheres. XI: Determination of Size Distribution Curves from Spectra of the Scattering Ratio or from Depolarization Spectra", Journal of Chemical Physics, V. 34, p. 1789-1795 (1961).

909 Sinclair, D. and LaMer, V.K., "Light Scattering as a Measure of Particle Size in Aerosols", Chemical Reviews, V. 44, p. 245-267 (1949).

58 Takahashi, K., and Iwai, S., "Estimation of Size Distribution of Small Aerosol Particles by Light-Scattering Measurements", Journal of Colloid & Interface Science, V. 23,p. 113-119 (1967).

1201 Van de Hulst, H. C., Light Scattering by Small Particles, Wiley (1957).

ANGULAR LIGHT SCATTERING

by: N. Barsic, B.Y.H. Liu and K. T. Whitby

INTRODUCTION

Light scattering refers to the redirection of illumination that is incident upon an object. Light is scattered by a combination of transmission, reflection, and diffraction; and depends upon characteristics of the object, the surrounding medium, and the incident radiation. Important parameters which influence light scattering are the light wavelength, particle size and shape, the refractive index of the particle with respect to the medium, and the angle at which an observer is located in relation to the incident light.

The nature of light scattered at various angles from the direction of illumination provides an effective means of studying aerosols. The light intensity as a function of observation angle provides information that describes particle size if the index of refraction and light wavelength are known and the particle is spherical. Such information can yield an estimate of particle mass concentration if particle density is known.

CHARACTERISTICS OF ANGULAR LIGHT SCATTERING

A. Basic Theory

Analytical studies by Mie[147] provide the most comprehensive theory of light scattering. However, simplifications are applicable for particles that are much larger than the wavelength of incident light (geometric optics) and particles much smaller than the wavelength of incident light (Rayleigh scattering). The net result of this theory is a relationship between the intensity of scattered light as a function of viewing angle, θ, the light wavelength, λ, particle diameter, d, index of refraction, m, and viewing distance, R:

$$I(\theta) = f\ (\theta, \lambda, d, m, R). \tag{1}$$

A different functional relationship exists for the three major scattering regions: Rayleigh, Mie, and geometric scattering. The exact nature of the equations is presented by Van de Hulst,[1201] Hodkinson,[1211] Call,et al,[702] Kerker,[1215] and Sinclair and La Mer.[909] Solving the scattering equations is usually difficult and expensive, even with a modern digital computer. Therefore, mathematical simplifications for special cases are extremely valuable.

Important simplications are possible if either the refractive index or particle size parameter ($\alpha = \pi d/\lambda$) is very close to 0 or ∞. Van de Hulst[1201] presents a figure and an accompanying table to summarize the regions of refractive index and particle size parameter where particular solutions are applicable (Fig. 1 and Table I). There are six boundary regions (1 to 6) where one of the parameters may have an arbitrary value from near 0 to infinity. The applicable computational methods are indicated in Table I. The corner regions: 61, 12, 23, 34, 45, and 56 are characterized by even simpler theories as indicated in Table I. The simplest mathematical reductions and the clearest physical interpretations of scattering theory are obtained in regions of the m - ∝ domain that are far from dividing lines.

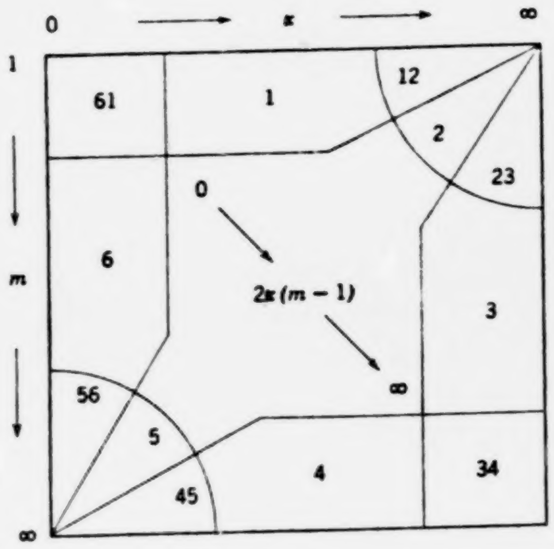

Fig. 1. Survey of limiting cases in the m - ∝ domain[1201]

Table I. Boundary Regions of the m - ∝ domain[1201]

Region	x	$m-1$	$x(m-1)$	Chapter or Section	Extinction Formula
61	s	s	s		$Q = (32/27)(m-1)^2x^4$
1	arb	s	s	7.2 (Rayleigh-Gans)	
12	l	s	s		$Q = 2(m-1)^2x^2$
2	l	s	arb	11 (anomalous diffraction)	
23	l	s	l		$Q = 2$
3	l	arb	l	12 (large spheres)	
34	l	l	l		$Q = 2$
4	arb	l	l	10.6 (total reflector)	
45	s	l	l		$Q = (10/3)x^4$
5	s	l	arb	10.5 (optical resonance)	
56	s	l	s		$Q = (8/3)x^4$
6	s	arb	s	6.3 (Rayleigh scattering)	

B. Intensity Diagrams

The net result of calculations outlined by the intensity equations is a relationship between the resulting light intensity at a given angle for different values of particle diameter and light wavelength. Most theoretical work completed thus far concerns spherical particles. For example, the Rayleigh scattering intensity function is composed of two components: $I_1(\theta)$ is independent of θ and therefore gives a circular pattern meaning equal scattering in all directions, and $I_2(\theta)$ is proportional to $\cos^2 \theta$ and therefore gives a figure 8 pattern. These results are summarized in the upper left of Figure 2 where scattered light intensity per particle is presented as a function of scattering angle in addition to the corresponding polar diagram. This polar diagram shape is representative of all Rayleigh scatterers since the basic form of the intensity equation is a simple function of $\sin^2 \theta$.

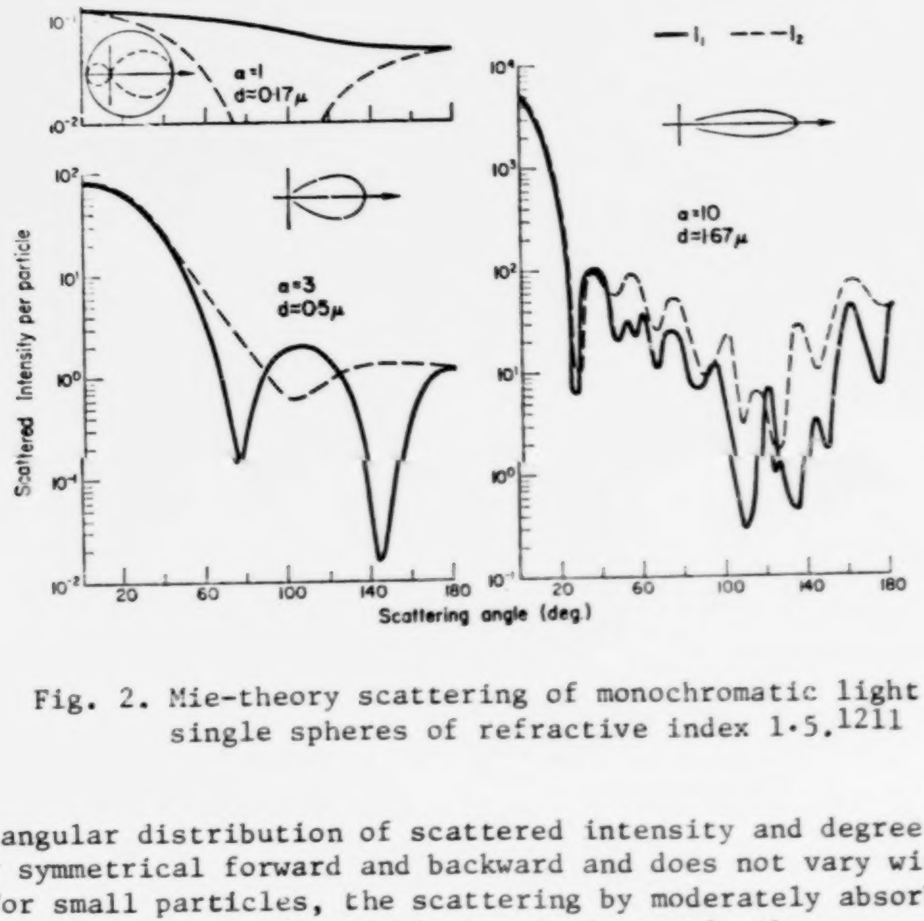

Fig. 2. Mie-theory scattering of monochromatic light by single spheres of refractive index 1·5.[1211]

The relative angular distribution of scattered intensity and degree of polarization is completely symmetrical forward and backward and does not vary with particle size and shape. For small particles, the scattering by moderately absorbing particles of complex refractive index $m(1 - i k)$, $k < 1$, is nearly the same as that by non-absorbing particles with the same real component of refractive index.

The scattering diagrams of larger particles might be expected to differ from particles in the Rayleigh region because the governing intensity functions are noticeably different.[702] This is indeed true and is demonstrated in the two lower illustrations of Figure 2. In addition, the general shape of Mie region scattering patterns varies as a function of particle size, unlike Rayleigh scatterers. For increasing particle size, the Mie scattering pattern becomes more forward directed and develops an array of angular maxima and minima in addition to the principal forward maximum evident in Figure 2. Polar diagrams of scattered light for size parameters of 1, 10, and 30 in Figure 3 clearly illustrate this phenomenon.[1233] In general, the number of minima in the pattern between $\theta = 0^\circ$ and 180° is approximately α.

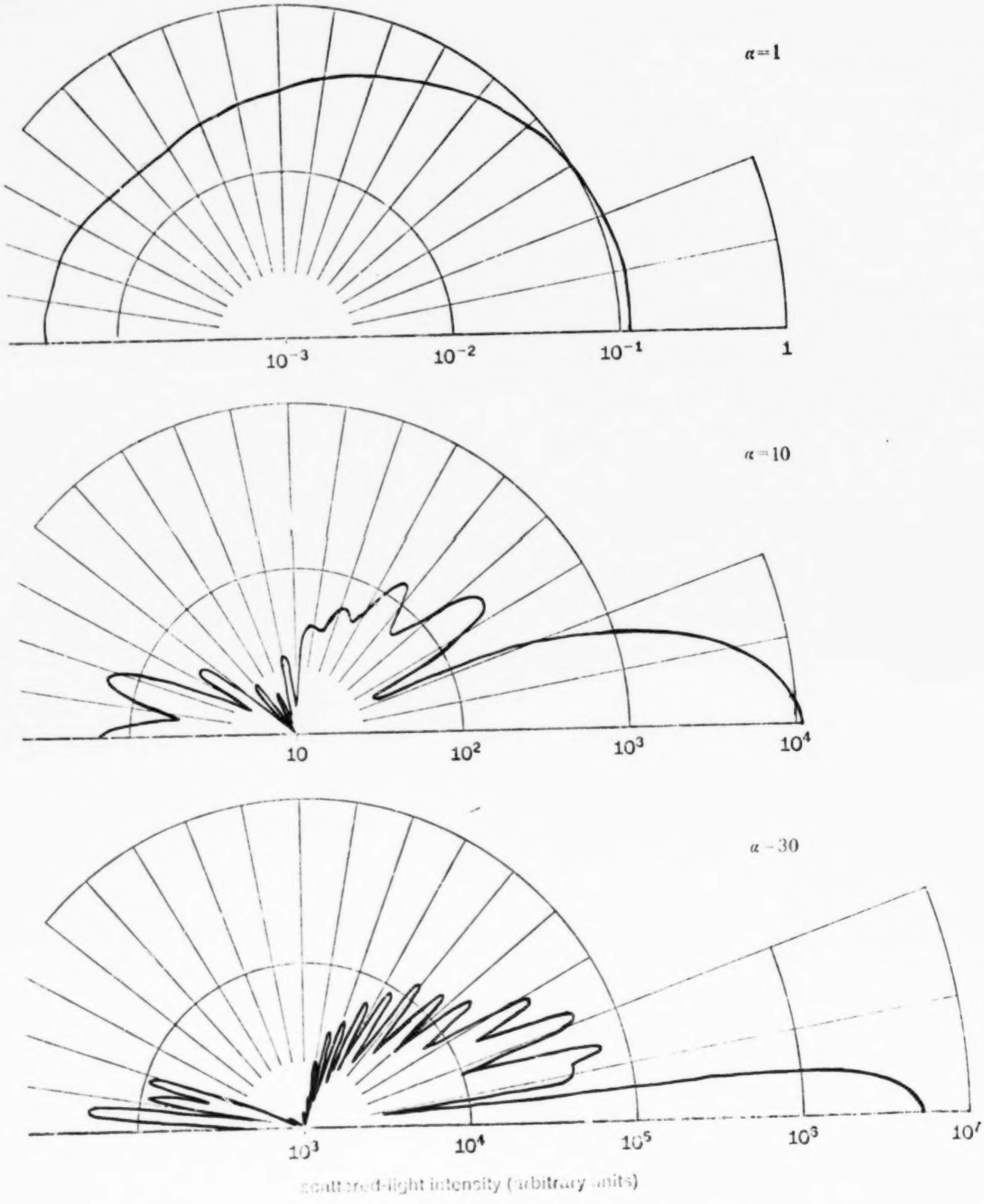

Fig. 3. Polar diagrams of scattered light for three different Mie parameters (refractive index of the particle material n = 1.50).[1233]

For spheres that are significantly larger than the wavelength, the diffracted radiation is concentrated very close to the forward direction. Van de Hulst[1201] has considered this situation in detail and determined that the exact scattering theory can be replaced by geometric ray optics for dielectrics with α = 10 to 20 except in the neighborhood of the rainbow angle where it will fail regardless of the value of α.[1215] A comparison of exact theory and geometric optics is presented in Figure 4.

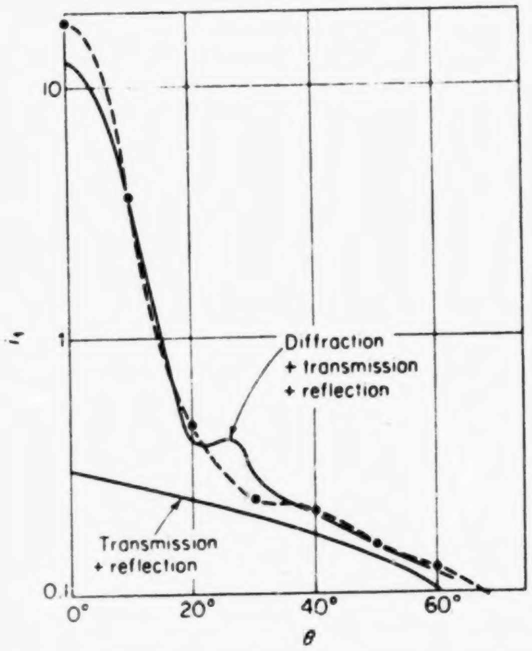

Fig. 4. Angular distribution function calculated as the sum of contributions from diffraction, reflection, and refraction compared with the exact values (dashed line) for m = 2.105. A size distribution over the range α = 10 to 15 is assumed for which the frequency of particles is proportional to α^{-2} (Hodkinson and Greenleaves, 1963).[1215]

Since the light intensity observed at different angles is a function of particle size, light intensity measurements provide a means of determining particle size. Kerker, et al,[70] describes a method of finding particle size data by observing the minima and maxima in the angular scattering pattern. Intensity measurements are often made at a fixed angle and compared with theoretical intensity values or experimentally determined values from a standard aerosol. Kratohvil and Smart[842] describe the calibration of an angular light scattering system using Dow polystyrene latex spheres as a reference.

Many investigators have calculated values of the scattering function for a variety of conditions. In the past, investigators first tried to seek tables of scattering functions that had been compiled previously, such as the tables presented by Shahroken and Wolf,[474] and McCormick and Lawrence,[805] and in Table II from Hodkinson.[85] Perhaps the most complete table of such authors is presented by

Hodkinson.[85] Because of the voluminous nature of these tables and the lack of an exhaustive set of tables, many investigators have found it just as convenient to calculate the desired intensity functions. The availability of digital computers makes direct calculation more feasible than table use, especially if additional calculations are to be performed with intensity values.

Table II. Principal published Mie theory computations of the angular distribution of scattered intensity for medium and large transparent and moderately absorbing spheres.[85]

			Range and increments of	
Authors	Refractive index m	Absorption coefficient k	Scattering angle θ	Particle size parameter $\alpha = \pi d/\lambda$
N. Mori and H. Kikuchi, Bull. Electrotech. Lab. (Tokyo) **21**, 561; **22**, 209 (1957).	1.33	—	0°(5°) to 180° 0°(2.5°) to 180°	5.5 (5) to 10 10 to 18.5 (23 values)
R. O. Gumprecht, N. L. Sung, J. H. Chin, and C. M. Sliepcevich, J. Opt. Soc. Am. **42**, 226 (1952).	1.33	--	0°(1°) to 10° 10°(10°) to 180°	6, 8, 10(5) to 40
L. E. Ashley and C. M. Cobb, J. Opt. Soc. Am. **48**, 261 (1958).	1.20	—	0°(1°) to 10° 10°(10°) to 180°	1, 2, 3, 5, 8, 10, 15, 20, 30, 35.
M. Kerker and E. Matijević, J. Opt. Soc. Am. **51**, 87 (1961).	2.105	—	0°(10°) to 180°	0.2(0.4) to 5.8, 6.0(2) to 15.0
R. H. Giese, Z. Astrophys. **51**, 119 (1961).	1.33, 1.55	—	0°(2°) to 180°	1(1) to 40
R. B. Penndorf, U. S. Air Force Geophysics Research Directorate, Bedford, Mass., (1961) Tech. Rept. RAD-TR-61-32, (1962) Tech. Rept. RAD-TR-63-9, (1963) Tech. Rept. RAD-TR 63-26.	1.1, 1.2, 1.33 1.4, 1.44, 1.5	—	0°(5°) to 180°	0.1 (0.5) to 10
J. Olaf and K. Robock, Staub **21**, 495 (1961).	1.5	--	0°(1°) to 180°	1, 2(2) to 30
D. Deirmendjian, R. Clasen, and W. Viezee, J. Opt. Soc. Am. **51**, 620 (1961).	1.29, 1.315 1.34	--	0° to 180°	0.5 to 30, 0.5 to 40 0.5 to 70
R. H. Giese, E. deBary, K. Bullrich, and C. D. Vinnemann, Abhandl. Deut. Akad. Wiss. Berlin, Kl. Math. Phys. Tech. **1961**, No. 6 (1961).	1.5	--	0°(1°)10°(10°) 180°	0.2 (0.2) to 159
L. Rémy-Battiau, Mem. Roy. Soc. (Liége) Ser. (4) **2**, No. 7 (1962).	1.25	—	0°(2°) 10°(10°) 170°(2°) 180°	0.1(1) 10(1) 20(3) to 50
R. H. Giese, Z. Astrophys. **51**, 119 (1961).	1.27, 1.33	1.08, 0.038 0.38, 1.0 2.25	0°(2°) to 180°	1(1) to 40
J. Olaf and K. Robock, Staub **21**, 495 (1961).	1.75, 2.0	0.05, 0.125 0.25	0°(1°) to 180°	1, 2(2) to 30
D. Deirmendjian, R. Clasen, and W. Viezee, J. Opt. Soc. Am. **51**, 620 (1961).	1.29 to 1.525	0.05, to 0.045	0° to 180°	0.5 to 15 or 25
W. J. Pangonis and W. Heller, *Angular Scattering Functions for Spherical Particles* (Wayne University Press, Detroit, 1960).	1.05 (0.05) to 1.30	—	0°(5°) to 180°	0.2(0.2) to 7.0

ANGULAR INTENSITY MEASUREMENTS

Figure 5 illustrates the basic optical system used in most light scattering instruments. Hodkinson[1211] discusses several instrument designs and Block[787] discusses one design incorporating a laser as a light source.

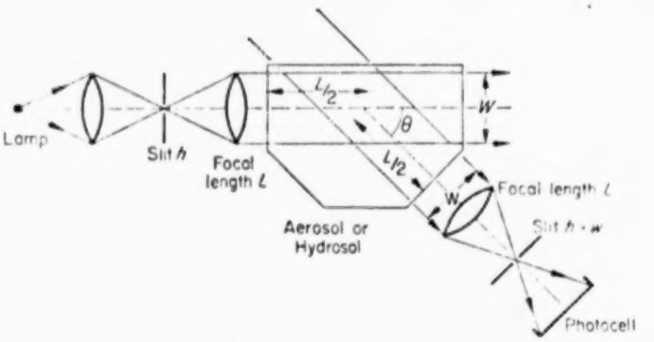

Fig. 5. Idealized optical system for absolute light-scattering measurements.[1211]

Measurement of particle size by studying the effect of observation angle on light scattering is possible only in the Mie region. Rayleigh scattering patterns all have the same angular configuration regardless of particle size. Geometrical scattering patterns demonstrate a correlation with particle size only for very specialized conditions.[1211] Therefore, for practical purposes, there is no noticeable particle size effect due to geometrical scattering.

Within the Mie range three common methods are available for correlating angular intensity variations with particle size. The first method correlates particle size parameter, α, with the number of minima observed in a scattering pattern such as Figure 2 or 3. The number of minima observed is approximately equal to α for a monodisperse aerosol of spherical particles as reported by Johnson and Le Mer[1234] and Barnes, et al.[1051]

The angular location of the first intensity minimum yields a correlation with particle size as described by Maron and Elder[1235] and Kerker.[70] For a refractive index near unity and Mie scattering ($\alpha > 0.1$) the light intensity decreases with increasing angle of observation, θ, and eventually passes through a minimum at values of θ that are dependent on α. The following equation describes the relationship discussed by Maron and Elder[1235]:

$$\frac{d}{\lambda} \sin \left(\frac{\theta_1}{2}\right) = K_1 \qquad (2)$$

where:

θ_1 is the first angular minimum,

d is the particle diameter,

λ is the wavelength of incident light, and

K_1 is a constant that depends on the relative refractive index of particle and medium.

Maron, Pierce and Elder[1236] described an extension of the above method for the first two maxima and minima of the intensity pattern. The same governing equation is used with subscript "i" corresponding to one of the four cases investigated here:

$$\frac{d}{\lambda} \sin \left(\frac{\theta_i}{2}\right) = K_i \tag{3}$$

For monodisperse aerosols the diameter obtained is essentially the same for all maxima and minima observed by Maron, Pierce, and Elder.

For polydisperse aerosols Maron and Elder[1235] found a correlation between the weight average diameter and the intensity extrema. The diameter obtained at the different maxima and minima is essentially the same as the weight average diameter obtained from electron microscopy for incident light of low wavelength (λ = 2711 Å). The size range covered was 0.18 μm to 7.7 μm.

The third major method of studying the angular dependence of scattered light intensity is the Sloan-Arrington treatment.[1237,1238] These authors plotted log $I\theta^2$ vs. log θ and observed that a monodisperse aerosol yielded a single maximum on such a graph while polydisperse aerosols produced as many maxima as there were dominant particle sizes, as illustrated in Figure 6.

The presence of steep slopes indicates a uniform particle size, while broader peaks indicate the existence of a wider size distribution. A constant intensity region in which the scattering curve has a constant slope of -2 indicates that no particles are present in that size range. The vertical height of a peak is related to the fraction of particles of this size range.

Livesey and Billmeyer[38] discuss the Sloan-Arrington plots extensively and conclude that although the method has not yet been fully established on a theoretical basis and is less accurate than results obtained from other absolute methods, it is most useful because reasonable size approximations can be obtained readily with a minimum of computation for both monodisperse and polydisperse aerosols. The method is quite versatile because there are no particle shape and concentration limits. In addition, the Sloan-Arrington method is applicable over a wide range of particle sizes and refractive indicies.

APPLICATION TO STACKS

Current light scattering equipment appears to be unsuited for stack monitoring to determine particle size distribution or mass concentration for three reasons. First, the measurement procedure is essentially manual and does not lend itself to the type of automatic operation required for stack monitoring. Second, the data reduction procedure can be complicated and it has not been demonstrated that results of adequate accuracy can be obtained on stack aerosols. Finally, available equipment has been developed primarily for research use in the laboratory. Considerably more theoretical and experimental work needs to be done before the problems and the advantages of this method for stack monitoring can be more thoroughly assessed. Therefore, angular light scattering is not recommended as an immediate candidate for stack monitoring.

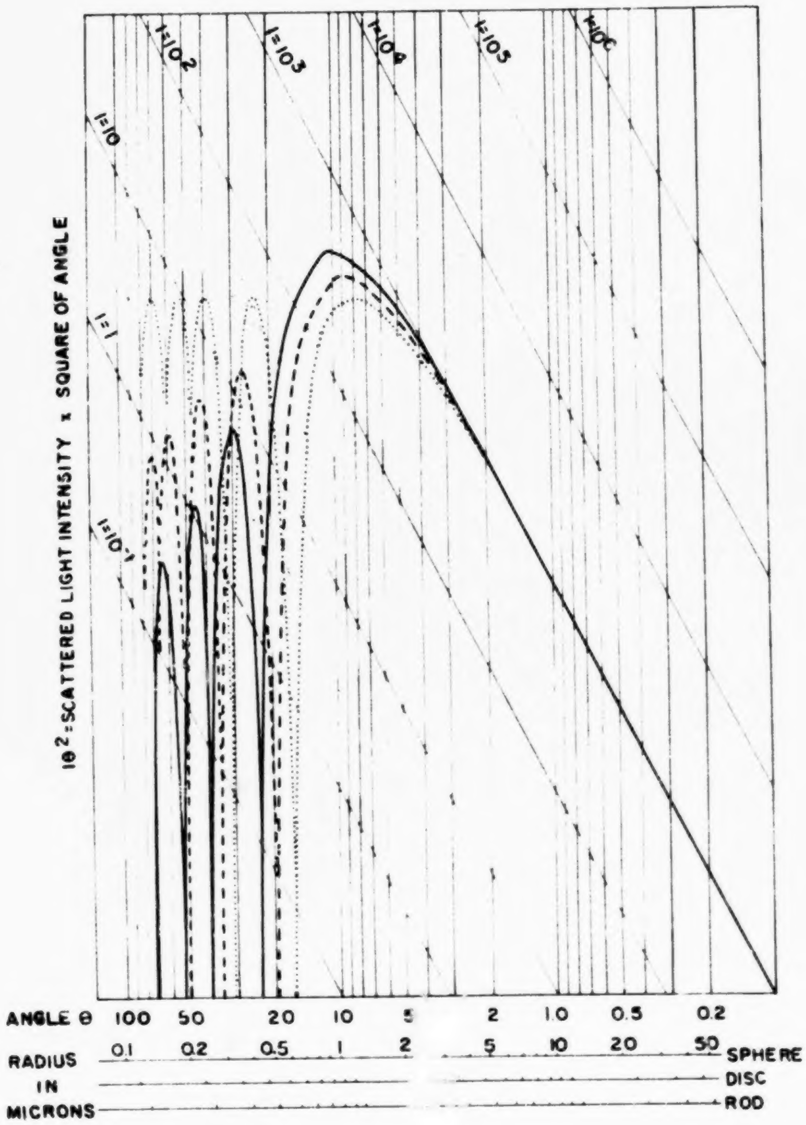

Fig. 6. Sloan plot of the scattered light intensity from spheres (——), discs (---), and rods (···) according to Livesey and Billmeyer.[38]

REFERENCES

1232 Barnes, M. D., Kenyon, A. S., Zaiser, E. M., and LaMer, V. K., "Monodispersed Sulfur Sols. IV. Comparison of the Particle Radius Determined by Transmittance and by the Angular Positions of Higher Order Tyndall Spectra from the Mie Theory", Journal of Colloid Sciences, V. 2, p. 349-359 (1947).

787 Block, A. M., "Scattering of Laser Light by Uniform Spherical Particles", Rutgers State Univ., New Brunswick, N. J., Univ. Microfilms order no. 68-4527 (1967).

1233 Bol, J., Gebhart, J., Roth, C., and Wurzbacher, G., Battelle Institut, Frankfurt (1969).

702 Call, R. W., Palmer, E. P., and Grow, R. W., "Measurement of Atmospheric Aerosols by Polarized Laser Light Scattering", Utah University, Salt Lake City, Utah, Clearinghouse No. PB 175 688 (Jun 1967).

1211 Hodkinson, J. R., "The Optical Measurement of Aerosols", in Aerosol Science, C. N. Davies (Ed.) Chap. 10 Academic Press (1966).

85 Hodkinson, J. R., "Particle Sizing by Means of the Forward Scattering Lobe", Applied Optics, V. 5, no. 5, p. 839-844 (May 1966).

1234 Johnson, I., and LaMer, V. K. "Particle Size of Colloidal Sulfur by Light Scattering", Journal of the American Chemical Society, V. 69, p. 1184-1192 (1947).

70 Kerker, M., Farone, W. A., Smith, L. B., and Matijevic, E., "Determination of Particle Size by the Minima and Maxima in the Angular Dependence of the Scattered Light, Range of Validity of the Method", Journal of Colloid Science, V. 19, p. 193-200 (Mar 1964).

1215 Kerker, M., The Scattering of Light and Other Electromagnetic Radiation, Academic Press (1969).

842 Kratohvil, J. P., and Smart, C., "Calibration of Light-Scattering Instruments, III. Absolute Angular Intensity Measurements of Mie Scatters", Journal of Colloid Science, V. 20, no. 8, p. 875-892 (1965).

38 Livesey, P. J., and Billmeyer, F. W., Jr., "Particle-Size Determination by Low-Angle Light Scattering: New Instrumentation and a Rapid Method of Interpreting Data", Journal of Colloid and Interface Science, V. 30, no. 4, p. 447-472 (Aug 1969).

1235 Maron, S. H., and Elder, M. E., "Determination of Latex Particle Size by Light Scattering, I. Minimum Intensity Method", Journal of Colloid Science, V. 18, p. 107-118 (1963).

1236 Maron, S. H., Pierce, P. W., and Elder, M. E., "Determination of Latex Particle Size by Light Scattering, III. Minima and Maxima in Angular Dependence of Intensity", Journal of Colloid Science, V. 18, p. 391-399 (1963).

805 McCormick, M. P., and Lawrence, J. D., Jr., "Tables of Mie Scattering Functions for Particles with Refractive Index 1.5", Langley Research Center, Langley Station, Hampton, Va., Clearinghouse No. N 69-20905, NASA TN D-5110 (Mar 1969).

147 Mie, "Beitrage zur Optik truber medien, speziell kolloidaler Metallosungen", Annalen der Physik, V. 25, no. 3, p. 377-445 (1908).

474 Shahrokhi, F., and Wolf, P., "Mie-Scattering Function", University of Tennessee, Tullahoma, Clearinghouse No. N 68-21227 (Apr 1968).

909 Sinclair, D., and LaMer, V. K., "Light Scattering as a Measure of Particle Size in Aerosols", Chemical Reviews, V. 44, p. 245-267 (1949).

1237 Sloan, C. K., "Angular Dependence Light Scattering, Characterization of Disperse Systems Containing Particles 0.1 to 100 Microns in Radius", Paper presented at 125th Meeting of American Chemical Society, St. Louis, (Mar 24 - Apr 1 1954).

1238 Sloan, C. K., "Angular Dependence of Light-Scattering Studies of the Aging of Precipitators", Journal of Physical Chemistry, V. 59, p. 834-840 (1955).

1201 Vande Hulst, H. C., Light Scattering by Small Particles, Wiley (1957).

SOILING POTENTIAL

by: N. Barsic, B.Y.H. Liu and K. T. Whitby

INTRODUCTION

Interest in the effects of sub-micron, nonsettling particles in the atmosphere has led to the development of instruments that yield "soiling index" or "soiling potential" data. Increased industrial activity and automotive traffic result in airborne particles from incomplete combustion. These small particles are not removed due to gravity forces and therefore remain in the atmosphere until they settle on buildings and create a dirt nuisance. In addition, the physiological effects of small particles are more harmful since they can reach the lungs and remain there rather than being removed by the upper respiratory tract as are the larger (greater than 5 μm) particles. Effective means of abating the small particle problem requires a method of detecting their presence.

Most instruments which measure the soiling index basically consist of an air flow system and a filter. Air passes through the filter for a specified length of time and the soiled filter is then viewed optically to determine the amount of material that was deposited. This technique has been adopted by the AISI (American Iron and Steel Institute) as a means of determining pollution levels for the steel industry.[519]

PRINCIPLES OF OPERATION

The most common instruments utilize a strip of filter paper that is indexed automatically and evaluated optically at a later time. Figure 1 is a schematic of the sampler.[396] The original development of this method was pioneered by Hemeon.[831] The established unit of measurement, called the Coh (coefficient of haze) Unit, is defined as that quantity of light-scattering solids producing an optical density of 0.01 when measured by light transmission. Optical density is $\log_{10} (I_o/I)$, where I_o is the light intensity for 100% reflectance or transmittance and I is the observed reflectance or transmittance.

An alternate unit system, Ruds (reflectance unit of dirt), specifies the stain potential caused by light reflection rather than transmission. This approach emphasizes the soiling of light colored surfaces which is noticeable due to light reflectance. The Rud value is that quantity of light-scattering solids producing an optical density of 0.01 when measured by light reflection.

Both Rud and Coh values are further standardized to a unit volume of air filtered through a unit area of filter. The soiling index of the atmosphere is then defined as Ruds or Cohs per 1000 linear feet of air or 1000 cubic feet of air flowing through one square foot of filter area.

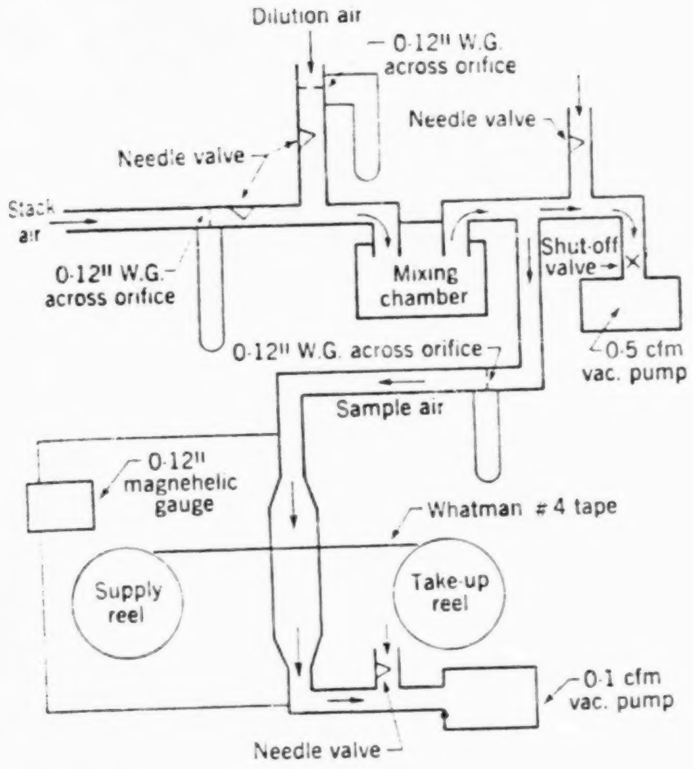
Dilution air
0·12" W.G. across orifice
Needle valve
Needle valve
Stack air
0·12" W.G. across orifice
Mixing chamber
Shut-off valve
0·12" W.G. across orifice
0·5 cfm vac. pump
Sample air
0·12" magnehelic gauge
Whatman #4 tape
Supply reel
Take-up reel
0·1 cfm vac. pump
Needle valve

Fig. 1. Schematic diagram of soiling potential Sampler (Model #4).[396]

Tests conducted by Gruber and Schumann[396] utilized the instrument in Figure 1 with a reflectance meter to evaluate the soiled spots. During these tests a typical value of soiling potential per cubic foot of stack gases was 1.10 Ruds-ft^2/ft^3. This is equivalent to 134 Rud-ft^2/lb coal.

The soiling potential correlation with Ringelmann number appears in Figure 2 where both parameters are reported as a function of time. This figure demonstrates that the soiling potential method is useful as a means of determining smoke opacity in addition to its original intended use as an atmospheric dirt measurement method.

Although the soiling index method yields good quantitative results, the method in its present form is not capable of determining size or mass distribution data. The method is strictly empirical and is intended to measure the overall visual effect of atmospheric pollutants and not specific characteristics of an aerosol such as size or mass distribution.

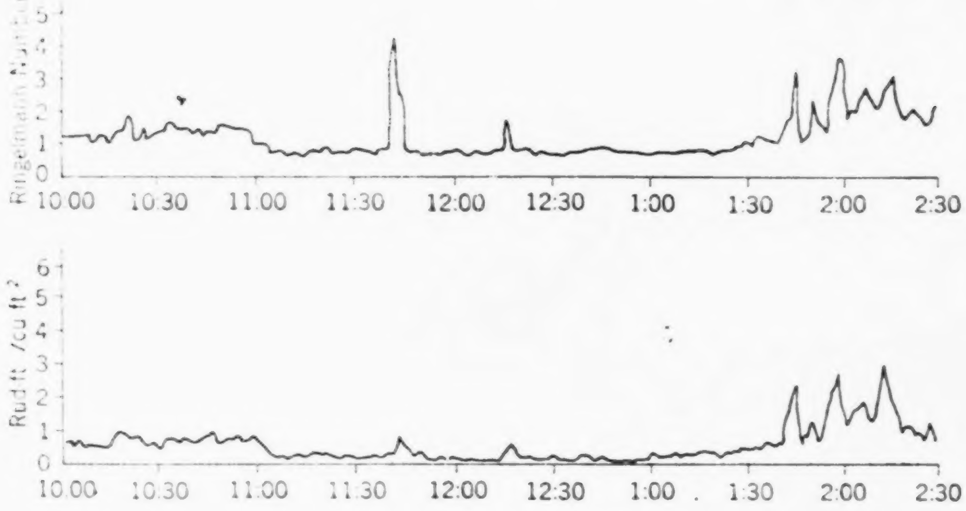

Fig. 2. Soiling potential vs. recorded and observed smoke.[396]
Plant #9 - 85,000 lb boiler with spreader stoker.

APPLICATION TO STACKS

The possiblity of obtaining either mass or size distribution data from the soiling potential recorder is remote since the method was not intended for this purpose. A correlation between Cohs or Ruds and aerosol mass concentration may exist. But the relationship is undoubtedly dependent upon the size distribution of the particles and such particle properties as density and refractive index. Therefore the method is not considered suitable for either mass concentration or size distribution measurement in stacks.

REFERENCES

519 Gruber, C. W., and Alpaugh, E. L., "The Automatic Filter Paper Sampler in an Air Pollution Measurement Program", APCA Annual Meeting Paper No. 54-5, Chattanooga, Tenn., May 3-6, 1954.

396 Gruber, C. W., and Schumann, C. E., "Soiling Potential - A New Method for Measuring Smoke Emission", APCA Journal, V. 16, p. 272-275 (1966).

831 Hemeon, W. C. L., "Instruments for Air Pollution Measurement", Meteorological Monographs, V. 1, no. 4, p. 20-23 (Nov 1951).

305 Schumann, C. E., and Gruber, C. W., "A Recommended Method for Soiling Index Surveys by Automatic Filter Paper Sampler", Paper 60-37 presented at 53rd Annual Meeting of Air Pollution Control Assoc., Cincinnati, Ohio (May 22-26, 1960).

OPTICAL COUNTERS AND PHOTOMETERS

by: B.Y.H. Liu and K.T. Whitby

INTRODUCTION

Optical counters and photometers are widely used as experimental tools in the study of aerosols. Because of their high sensitivity and their commercial availability they are now used routinely in such applications as the monitoring of clean rooms, testing of filters, air pollution studies, as well as numerous other applications involving aerosols in the laboratory and the atmosphere.

For the purpose of the present discussion optical counters refer to those instruments that measure the individual aerosol particles by light scattering or extinction. As such they are useful for size distribution and concentration measurements. They are also referred to as single particle optical counters, aerosol counters, particle counters or dust counters. In the context of the present discussion, photometers refer to those instruments that perform their measurement on a cloud of aerosol particles by light scattering. As such they are useful primarily for concentration measurements. These instruments are also referred to variously under such names as nephelometers, light scattering photometers or simply as aerosol photometers.

BASIC PRINCIPLE

The principle of the optical counter can be seen by referring to Figure 1 which shows the optical system of a typical counter available commercially (Royco Model PC 200). In the counter, aerosol particles are drawn in by suction through a small tube. As each particle passes through the small illuminated viewing volume, which is on the order of 1 mm^3 in size, it scatters a pulse of light which is detected by the photomultiplier tube. The output of the photomultiplier tube, in the form of a voltage pulse, provides an electrical signal whose amplitude is a measure of the particle size. By measuring the amplitudes of the individual pulses by means of a pulse-height analyzer, the size distribution of the aerosol can be determined.

The history of the aerosol counter dates back to World War II. As a result of the pioneering studies of Gucker and his co-workers[145,146,1192,1193,1194] and similar later studies by O'Konski and associates,[1180,559,1253] and Fisher, et al,[288] numerous counters have been developed and are now commercially available. Table 1 is a list of the manufacturers of aerosol counters known to the authors. The counters manufactured by the Royco Instrument Co. have been described by Zinky,[370], and Ogle,[580]; those manufactured by the Bausch & Lomb Instrument Co. are described by Randall & Keller,[1210] Martens and Keller,[756] Martens and Fuss,[670] and Martens.[578] The instrument manufactured by

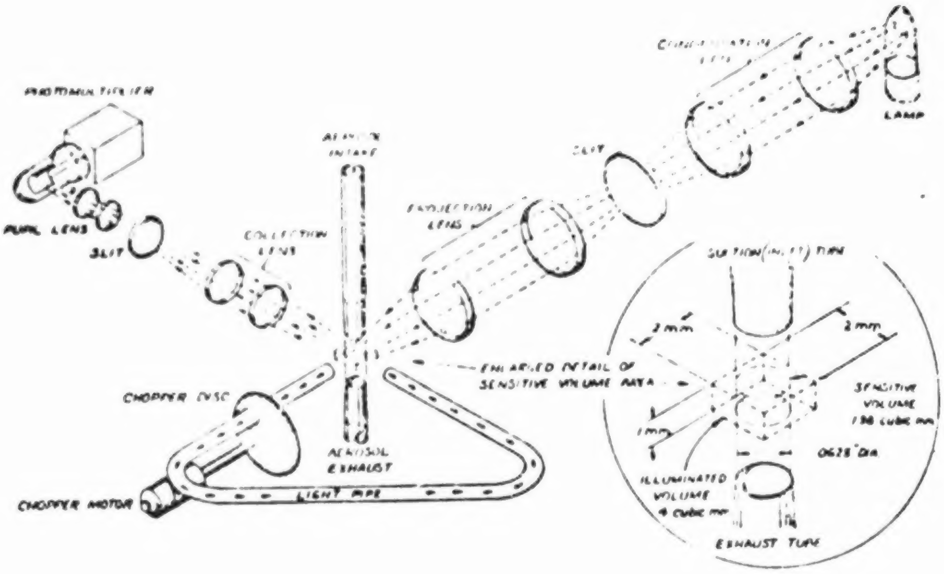
PHOTOMULTIPLIER
PUPIL LENS
SLIT
COLLECTION LENS
AEROSOL INTAKE
PROJECTION LENS
SLIT
LAMP
SUCTION (INLET) TUBE
2 mm
2 mm
ENLARGED DETAIL OF SENSITIVE VOLUME AREA
SENSITIVE VOLUME 1.38 cubic mm
1 mm
.0625" DIA
ILLUMINATED VOLUME 4 cubic mm
EXHAUST TUBE
CHOPPER DISC
AEROSOL EXHAUST
CHOPPER MOTOR
LIGHT PIPE

Fig. 1. Optical system of a typical aerosol counter available commercially.

the Phoenix Precision Instrument Co. is described by Sinclair.[615] In addition several special purpose counters have been built and described. These include the special battery-operated portable counter described by Thomas, et al,[120] and Moroz, et al,[1128] the high volume (10 to 50 cfm) counter described by Whitfield and Mashburn,[949] and by Neitzel,[824] and the counters described by Nelson,[276] and Mumma.[598] A counter built in Russia has been described by Kiktenko, et al.[1066]

Table 1. List of aerosol counter manufacturers.

1. Bausch & Lomb, 635 St. Paul St., Rochester, New York 14602
2. Climet Instruments, Inc., 1240 Birchwood Drive, Sunnyvale, Calif. 94086
3. Dynac Corp., Thomson's Point, Portland, Maine 04120
4. Envirco, P.O. Box 6098, Albuquerque, New Mexico 87107
5. High Accuracy Products Corp., 141 Spring St., Claremont, Calif. 91711
6. Phoenix Precision Instrument Co., 3803-05 North Fifth St., Philadelphia, Pa.19140
7. Royco Instruments, Inc., 141 Jefferson Drive, Menlo Park, Calif. 94025

Although most counters make use of an optical system in which only part of the scattered light is collected by the photomultiplier tube, a counter has been described by Jacobi, et al,[822] in which practically all the scattered light is collected through a novel lensless optical system using laser illumination and light collection by a plastic light pipe. Also, it should be mentioned that the instrument manufactured by the High Accuracy Products Corp. is based on light extinction principles rather than on light scattering principles. Another instrument of a different principle is described by Knollenberg.[876,1082] The instrument makes use of a novel arrangement of an optical array consisting of many small fiber-optical light detecting elements. The size of the particle is determined by the size of the "shadow" cast by the particle on these elements. The number of light detecting elements in the shadow area of the particle provides a measure of the particle size.

The response characteristics of an aerosol counter are generally dependent upon its optical design. For counters of a specific optical design, the response of the counter to particles of a specific size is in turn dependent upon the refractive index of the particle, the geometrical shape of the particle and the orientation with which the particle enters the optical viewing volume. The response characteristics of optical counters have been the subject of experimental studies by several investigators, including Hosey, et al,[993] Channell and Hanna,[988] Lewis,[731] Whitby and Vomela,[171] and Preining,[32] and they have generally confirmed the facts stated above. Thus, the effect of the particle refractive index is such that the size of absorbing carbon black particles can be underestimated by as much as a factor of five by a counter whose calibration is established in the usual manner by the use of transparent polystyrene latex spheres. The effect of particle shape is such that a monodisperse aerosol of irregularly shaped particles will be detected by the optical counter as a polydisperse aerosol because of the dependence of light scattering on particle shape and orientation. Also, a high concentration of small particles below the size range of the instrument could scatter sufficient light to give a false reading[680]. Thus, the response of an optical counter to a specific aerosol is somewhat empirical and must be established by calibration.

Despite these limitations aerosol counters are widely used because there is no comparable instrument operating over the range of the optical counter, approximately 0.3 to 10 μm, that can detect single individual particles. Thus, the optical counter is specified in Federal Standard 209 for clean room monitoring (see also Magill[711]) and it has been studied[732,731] for possible applications to the monitoring of the cabin atmosphere in manned space crafts.

Several theoretical studies[143,515,362,813] have been made on the design of optical counters. Hodkinson and Greenfield[143] have concluded that, with proper design, an optical counter using forward scattered light can have the effect of the particle refractive index minimized.

In order to avoid loss of particle count due to coincidence, i.e., due to the presence of more than one particle in the sensor viewing volume, the aerosol concentration must be sufficiently low. Therefore, aerosol with high number concentrations must be first diluted by clean air before being fed to the counter. The theoretical basis for calculating the coincidence loss in particle counters has been thoroughly explored by Bennert and Hilbig.[625]

The light scattering aerosol photometer differs from the aerosol counter only in the size of the illuminated viewing volume and in the fact that the aerosol photometer provides a dc electrical signal instead of a pulsed signal as in the aerosol counter. Because the viewing volume in the aerosol photometer is considerably larger than that in the aerosol counter, many particles are present simultaneously in the viewing volume. Thus, the dc output signal of the photometer provides a measure of the light scattered collectively by all the particles in the viewing volume. As such, the instrument is useful only for concentration measurements. A schematic diagram of the commercially available Sinclair-Phoenix instrument is shown in Figure 2.

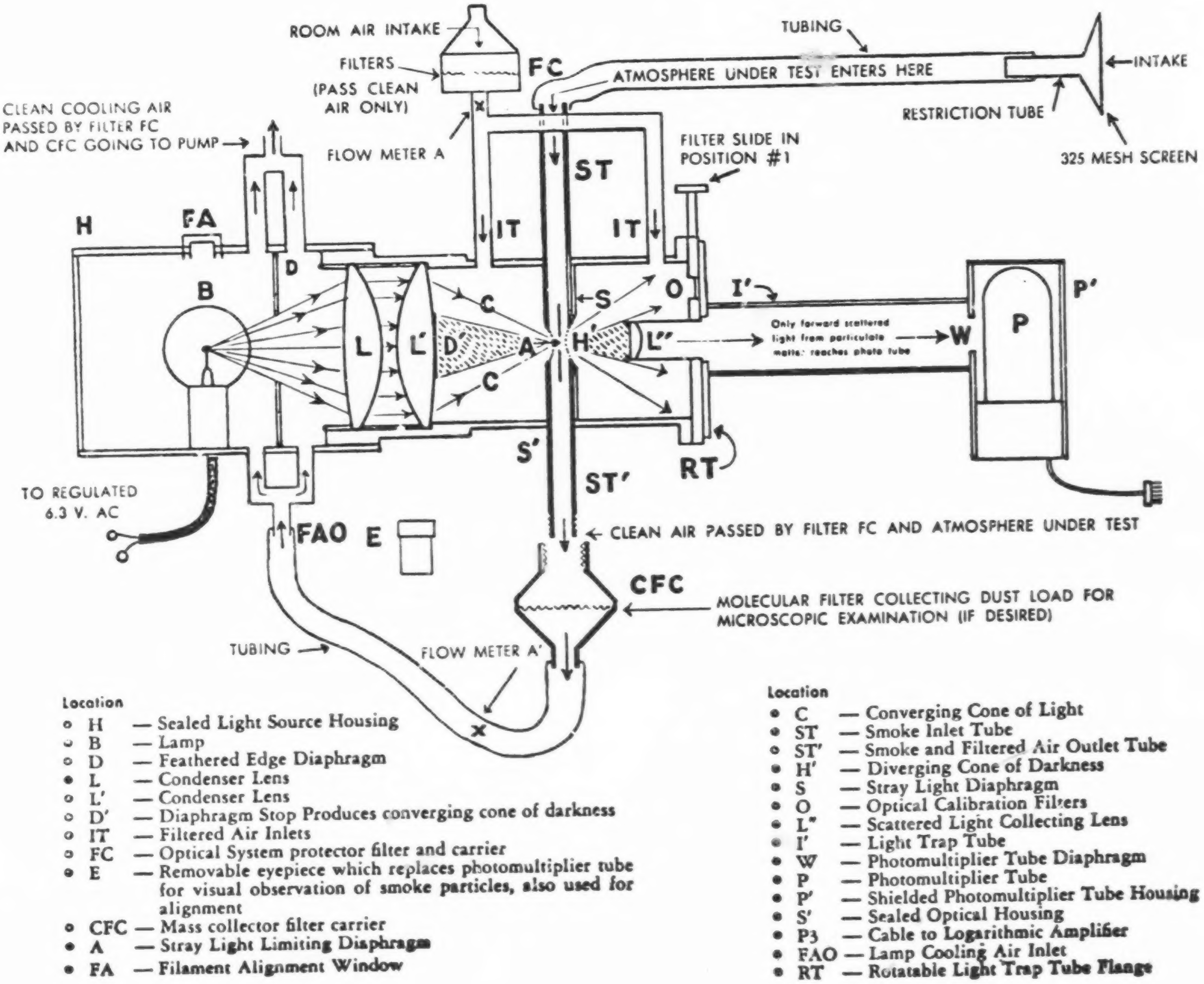
ROOM AIR INTAKE
FILTERS
(PASS CLEAN AIR ONLY)
FC
TUBING
ATMOSPHERE UNDER TEST ENTERS HERE
INTAKE
RESTRICTION TUBE
325 MESH SCREEN
CLEAN COOLING AIR PASSED BY FILTER FC AND CFC GOING TO PUMP
FLOW METER A
FILTER SLIDE IN POSITION #1
ST
H
FA
IT
IT
D
B
C
S
O
I'
P'
L
L'
D'
A
H'
L"
Only forward scattered light from particulate matter reaches photo tube
W
P
C
S'
ST'
RT
TO REGULATED 6.3 V. AC
FAO
E
CLEAN AIR PASSED BY FILTER FC AND ATMOSPHERE UNDER TEST
CFC
MOLECULAR FILTER COLLECTING DUST LOAD FOR MICROSCOPIC EXAMINATION (IF DESIRED)
TUBING
FLOW METER A'

Location
○ H — Sealed Light Source Housing
○ B — Lamp
○ D — Feathered Edge Diaphragm
● L — Condenser Lens
○ L' — Condenser Lens
○ D' — Diaphragm Stop Produces converging cone of darkness
○ IT — Filtered Air Inlets
○ FC — Optical System protector filter and carrier
● E — Removable eyepiece which replaces photomultiplier tube for visual observation of smoke particles, also used for alignment
○ CFC — Mass collector filter carrier
● A — Stray Light Limiting Diaphragm
● FA — Filament Alignment Window

Location
● C — Converging Cone of Light
● ST — Smoke Inlet Tube
○ ST' — Smoke and Filtered Air Outlet Tube
● H' — Diverging Cone of Darkness
● S — Stray Light Diaphragm
● O — Optical Calibration Filters
● L" — Scattered Light Collecting Lens
● I' — Light Trap Tube
● W — Photomultiplier Tube Diaphragm
● P — Photomultiplier Tube
● P' — Shielded Photomultiplier Tube Housing
● S' — Sealed Optical Housing
● P3 — Cable to Logarithmic Amplifier
● FAO — Lamp Cooling Air Inlet
● RT — Rotatable Light Trap Tube Flange

Fig. 2. Schematic diagram of the Sinclair-Phoenix aerosol photometer.

THERMO-SYSTEMS INC.

The basic design requirements of the aerosol photometer suitable for laboratory use are described in considerable detail in the Naval Research Laboratory report by Knudson and White.[840] Further studies of the aerosol photometer have been described by Mueller and Givens[374] and by Doyle and Wiederhorn.[285] The response characteristics of the aerosol photometer as a function of particle size for a photometer of Soviet design have been described by Kogen and Pankratova.[1083] The design and the application of a total scattering aerosol photometer, called the integrating nephelometer, to the measurement of the meteorological range and atmospheric aerosol concentration have been described in a series of papers by Charlson and his coworkers.[928,69,919]

The response characteristics of the aerosol photometer are complicated due to their dependence on the size, the shape, and the optical design of the instruments. Generally, for a specific instrument the dc signal provides a measure of the aerosol mass concentration only when the characteristics of the particles, including the refractive index, the density and the size distribution, remain unchanged. For application to stacks where all of these parameters can and do vary, the instrument cannot provide a measure of aerosol mass.

Although the aerosol photometer can also be used to determine the size distribution by combining its operation with an impactor as Thompson[124] has done, the data is difficult to convert to either the number distribution or the mass distribution because of the complicated nature of the relation between particle size and light scattering.

APPLICATION TO MASS CONCENTRATION MEASUREMENT IN STACKS

Single particle optical counters are unsuitable for continuous mass concentration measurement in stacks for several reasons. The instruments measure the size distribution of particles, making the readout quite difficult to handle. Most practical instruments have a rather narrow size range. An instrument designed for large particles has a large sensing zone which makes it insensitive to small particles. In order to relate the measured number concentration to particle mass concentration, the specific density of the particles must be assumed. Specific particle density changes drastically in effluents. The size classification depends strongly on the refractive index of the particles. Nearly all present commercial instruments are designed for clean room atmospheres. Design for aerosols as concentrated as stack effluents would require very high dilution (e.g., 1,000 - 10,000 X dilution) with clean air to prevent coincidence counting errors.

Aerosol photometers are also unsuitable for continuous mass concentration measurement in stacks. They share many of the problems of transmissometers for mass concentration measurements. The sensitivity of photometers is higher than transmissometers, a feature not necessary for stack effluents. The greatest disadvantage of a photometer compared to a transmissometer is that a photometer requires an extracted sample, introducing another large measurement uncertainty.

SUMMARY AND CONCLUSIONS

Optical counters and aerosol photometers have been used as experimental tools in numerous aerosol studies. The optical counter measures the size of a particle by detecting the amount of light scattered by the particle in passing through the small illuminated sensing volume whereas the aerosol photometer measures the light scattered collectively by all the particles present in the illuminated viewing volume. The optical counter can be used for size distribution measurements whereas the aerosol photometer is suitable primarily for concentration measurements. Optical counters are unsuitable for mass concentration measurement in stacks because of their sensitivity to the refractive index of the particles, the limit in the aerosol concentration, their inability to sense particle density, their inconvenient data readout and several other reasons. Aerosol photometers are unlikely candidates for stack mass monitoring because they have no specific advantage, but do have a large disadvantage, over the transmissometer.

REFERENCES

625 Bennert, W., and Hilbig, G., "The Theory of the Coincidence Error for Digital Particle Size Analysis", Staub-Reinhalt der Luft (Engl. Trans.), V. 27, p. 24-29 (Apr 1967).

346 Brown, P. M., "A Modification of the Bausch and Lomb Aerosol Dust Counting System to Automatically Measure Aerosol Size Distribution", Environmental Science & Technology, V. 3, no. 8, p. 768-769 (Aug 1969).

732 Burgess, W., and Reist, P. C., "Study of Space Cabin Atmospheres", Harvard School of Public Health, Clearinghouse No. N 67 12641 (Sep 1966).

988 Channell, J. K., and Hanna, R. J., "Experience with Light Scattering Particle Counters", Archives of Environmental Health, V. 6, p. 92 - 106 (1963).

919 Charlson, R. J., Ahlquist, N. C., Horvath, H., "On the Generality of Correlation of Atmospheric Aerosol Mass Concentration and Light Scatter", Atmospheric Environment, V. 2, p. 455-464 (1968).

69 Charlson, R. J., "Atmospheric Visibility Related to Aerosol Mass Concentration, A Review", Environmental Science & Technology, V. 3, no. 10, p. 913-918 (Oct 1969).

928 Charlson, R. J., Ahlquist, N. C., Selvidge, H., and MacCready, P. B.,Jr., "Monitoring of Atmospheric Aerosol Parameters with the Integrating Nephelometer", APCA Journal, V. 19, no. 12, p. 937-942 (Dec 1969).

285 Doyle, A. W., and Weiderhorn, N. M., "The Use of a Light-Scattering Photometer in Air Pollution Studies", paper presented at 3rd Annual Meeting, New England Section, Air Pollution Control Assoc., May 14,1959.

813 Dunn, J. F., Jr., Foster, A. R., Lautman, D. A., Nardone, L. J., Swanson, J. L., and Zelinski, J. J., "On the Design of an Instrument to Use Forward-Scattered Light to Detect Small Particles", Northeastern Univ., Boston, Mass., Clearinghouse No. AD 693 557 (Aug 1969).

225 Duwel, L., "Latest State of Development of Control Instruments for the Continuous Monitoring of Dust Emissions", Staub-Reinhalt der Luft (Engl. Trans.), V. 28, no. 3, p. 42-53 (Mar 1968).

288 Fisher, M. A., Katz, S., Lieberman, A., and Alexander, N. E., "The Aerosoloscope; An Instrument for the Automatic Counting and Sizing of Aerosol Particles", Proc. 3rd National Air Pollution Symposium, Pasadena, Calif., p. 112-119 (Apr 18-20 1955).

145 Gucker, F. T., Jr., O'Konski, C. T., Pickard, H. B., and Pitts, J. N.,Jr., "A Photoelectric Counter for Colloidal Particles", American Chemical Society Journal, V. 69, no. 10, p. 2422-2431 (1947).

146 Gucker, F. T., Jr., and O'Konski, C. T., "An Improved Photoelectric Counter for Colloidal Particles, Suitable for Size-Distribution Studies", Journal of Colloid Science, V. 4, p. 541 (1949).

1192 Gucker, F. T., and Rose, D. G., J. Appl. Phys. Suppl. 3, (1954).

1193 Gucker, F. T., and Rose, D. G., Proc. Third Natl. Air Pollution Symp. (1955).

1194 Gucker, F. T., Proc. Ind. Instr. Conf., p. 284 (1956).

515 Gucker, F. T., and Tuma, J., "Influence of the Collecting Lens Aperature on the Light-Scattering Diagrams from Single Aerosol Particles", Contribution No. 0000 from the Chemical Laboratory of Indiana University, Bloomington, Indiana, 47401.

1110 Gucker, F. T., "Instrumental Methods of Measuring Mass Concentration and Particulate Concentration in Aerosols", Proc. U. S. Technical Conference on Air Poll., Chap. 75.

752 Harris, F. S., Jr., Sherman, G. C., and Morse, F. L., "Experimental Comparison of Scattering of Coherent and Incoherent Light", IEEE Trans. on Antennas and Propagation, V. AP-15, no. 1, p. 141-147 (Jan 1967).

143 Hodkinson, J. R., and Greenfield, J. R., "Response Calculations for Light-Scattering Aerosol Counters and Photometers", Applied Optics, V. 4, p. 1463-1474 (1965).

993 Hosey, A. D., Jones, H. H., and Ayer, H. E., "Evaluation of an Aerosol Photometer for Dust Counting and Sizing", American Industrial Hygiene Assoc. Journal, V. 21, p. 491-501 (Dec 1960).

822 Jacobi, W., Eichlers, J., and Stolterfoht, N., "Particle Size Spectrometry of Aerosols Through Light Scattering in a Laser Beam", Sandia Lab., Albuquerque, N. M., Clearinghouse No. PB 187 705T (Nov 1969).

307 Kay, K., "Analytical Methods Used in Air Pollution Study", Industrial and Engineering Chemistry, V. 44, p. 1383-1388 (1952).

1066 Kiktenko, V. S., Safronov, Y.P., Kudryautsev, S. I., Fedorov, B. F., Pushchin, N. I., and Fedorovich, A. A., "Photoelectric Count of the Number of Aerosol Particles of Organic and Inorganic Origin", Engl. Trans. from: Gigiyenai Sanitariya, Moscow, V. 26, no. 2, p. 47-53, Feb. 1961, Clearinghouse No. JPRS-8334 (May 1961).

876 Knollenberg, R. G., "An Optical-Electrical Particle Size Discriminator", University Corp. for Atmospheric Research, Clearinghouse No. PB 179 645 (Apr 1968).

1082 Knollenberg, R. G., "The Optical Array: An Alternative to Scattering or Extinction for Airborne Particle Size Determination", Journal of Applied Meteorology, V. 9, no. 1, p. 86-103 (Feb 1970).

840 Knudson, H. W., and White, L., "Development of Smoke Penetration Meters", U. S. Naval Research Laboratory, Washington, D. C., NRL Report P-2642 (1945).

1083 Kogan, Y. I., and Pankratova, M. E., "Dependence of Light Scattering on Particle Size in Aerosol Nephelometers with Viewing Angles of 90 and 135 Deg.", Colloid Journal, USSR (Engl. Trans.), V. 31, no. 4, p. 496-500 (Jul-Aug 1969).

731 Lewis, T. W., "Evaluation of an Automatic Aerosol Particle Counter for Measuring the Airborne Contamination Level in a Controlled Environment", George C. Marshall Space Flight Center, Huntsville, Ala., Clearinghouse No. 66 29075 (Mar 1966).

711 Magill, P. L., "Instrument Measurement of Contamination in Clean Rooms for Proposed Federal Standard No. 209", Proc. National Analytical Inst. Symp., 10th, San Francisco, Calif., p. 287-297 (1964).

578 Martens, A. E., "Errors in Measurement and Counting of Particles Using Light Scattering", APCA Journal, V. 18, p. 661-663 (Oct 1968).

670 Martens, A. E., and Fuss, K. H., "An Optical Counter for Dust Particles", Staub-Reinhalt der Luft, V. 28, no. 6, p. 14-18 (Jun 1968).

756 Martens, A. E., and Keller, J. D., "An Instrument for Sizing and Counting Airborne Particles", American Industrial Hygiene Assoc. Journal, V. 29, p. 257-267 (May - Jun 1968).

1128 Moroz, W. J., Withstandley, V. D., and Anderson, G. W., "A Portable Counter and Size Analyzer for Airborne Dust", Review of Scientific Instruments, V. 41, no. 7, p. 978-983 (Jul 1970).

374 Mueller, P. K., and Givens, R. G., "Dynamic Calibration and Data Interpretation of a Light-Scattering Instrument", APCA Journal, V. 11, no. 12, p. 576-580, 584 (Dec 1961).

598 Mumma, V. K., Thomas, A. L.,Jr., and Collins, R. H., III, "A Particle Size Analyzer for Aerosols", Army Biological Labs., Frederick, Md., Clearinghouse No. AD 636 858 (1962).

969 Nader, J. S., Ortman, G. C., and Massey, M. T., "Light-Scatter Instrumentation for Measurement of Atmospheric Particulates", American Industrial Hygiene Ass'n. Journal, V. 22, no. 1, p. 42-48 (Feb 1961).

824 Neitzel, W. E., "A High-Volume, Real-Time Aerosol Monitor", Sandia Lab., Albuquerque, N. M., Clearinghouse No. SC-DR-69-56 (Jun 1969).

276 Nelson, M. B., "Fabrication of Particle Counters for Clean Rooms", IIT Research Institute, Chicago, Ill., NASA Tech. Brief 67-10076. (Jul 1966).

580 Ogle, H. M., "Particle Counting Techniques Available for Aerosol Research", APCA Journal, V. 18, p. 657-699 (Oct 1968).

1180 O'Konski, C. T., and Doyle, J., "Light-Scattering Studies in Aerosols With a New Counter-Photometer", Analytical Chemistry, V. 27, p. 694-701 (May 1965).

559 O'Konski, C. T., Bitron, M. D., and Higuchi, W. I., "Light-Scattering Instrumentation for Particle Size Distribution Measurements", American Society of Testing Materials, Spec. Tech. Pub. No. 250, p. 2-28 (1959).

1253 O'Konski, C. T., Bitron, M. D., and Higuchi, W. I., ASTM Spec. Tech. Publ., No. 234, (1958).

32 Preining, O., "The Cross Sensitivities of the Royco Aerosol Photometer PC200", *Staub-Reinhalt der Luft (Engl. Trans.)*, no. 1, p. 29-32 (Jan 1968).

1210 Randall, L. M., and Keller, J. D., "Electro-Optical Aerosol Counter Inst.,", AIHA Conf., Houston, Texas (1955).

340 Setzer, D. E., "Comparison of Measured and Predicted Aerosol Scattering Functions", *Applied Optics*, V. 8, no. 3, p. 905-911 (May 1969).

615 Sinclair, D., "A New Photometer for Aerosol Particle Size Analysis", *APCA Journal*, V. 17, no. 2, p. 105-108 (1967).

287 Anon, "Reference Manual for the Southern Research Institute Particle Size Analyzer", Southern Research Institute, Birmingham, Alabama (Oct 1959).

120 Thomas, A. L., Jr., Bird, A. N., Jr., Collins, R. H., III, and Rice, P.C., "A Portable Photometer and Particle Size Analyzer", *ISA Journal*, V. 8, p. 52-56 (Jul 1961).

124 Thompson, J. K., "Determination of Aerosol Size Distributions by Jet Impactor-Light Scattering Technique", *Analytical Chemistry*, V. 29, p. 1847-50 (1957).

362 Welch, E. C., "Design of an Optical System for Counting and Sizing Airborne Particles", *ISA - Nat. Symposium on Instrumental Methods of Analysis, 8th - Proc.*, p. 173-178 (1962).

171 Whitby, K. T., and Vomela, R. A., "Response of Single Particle Optical Counters to Nonideal Particles", *Environmental Science & Technology*, V. 1, no. 10, p. 801-814 (1967).

680 Whitby, K. T., and Liu, B. Y. H., "Generation of Countable Pulses by High Concentrations of Subcountable Sized Particles in the Sensing Volume of Optical Counters", *Journal of Colloid & Interface Science*, V. 25, no. 4, p. 537-546 (1967).

949 Whitfield, W. J., and Mashburn, J. C., "Development of an Increased Sampling Rate Monitoring System", Sandia Lab., Albuquerque, N. M., Clearinghouse No. SC-RR-66-585 (Oct 1966).

370 Zinky, W. R., "A New Tool for Air Pollution Control, the Aerosol Particle Counter", *APCA Journal*, V. 12, no. 12, p. 578-583 (Dec 1962).

LIDAR

by: N. Barsic, B.Y.H. Liu, and K.T. Whitby

INTRODUCTION

Lidar is a relatively new technique that detects particles of dust and other materials in the atmosphere. This method of particle detection is sensitive enough to pinpoint atmospheric debris in what appears to be clean air. Lidar has already provided valuable information in many types of atmospheric investigations.

"LIDAR" is the optical analogue of radar, and the word is formed in the same way: from light detection and ranging. This technique uses light energy from lasers rather than radio waves as with radar.

BASIC OPERATIONAL PRINCIPLES

A. Objective

The goal of atmospheric studies using lidar is to determine the presence of particulate contaminants, establish their concentration, and determine the cloud boundaries. Successful results are reported in numerous instances.[280,221,569,514] Mostapplications involve the study of cloud or pollution formation at distances of 100 m to 100 km from the lidar unit.

The basic concept of lidar operation, like radar, involves sending energy pulses toward an object, and detecting the reflected energy. Energy generated by large, Q-switched lasers used in atmospheric studies is concentrated in very short duration (30 x 10^{-9} sec), monochromatic, high power pulses (45 megawatts). These energy pulse beams are directed by either reflecting or refracting telescopes. Energy returned by the atmosphere is collected by a similar telescope and sensed by a photomultiplier.

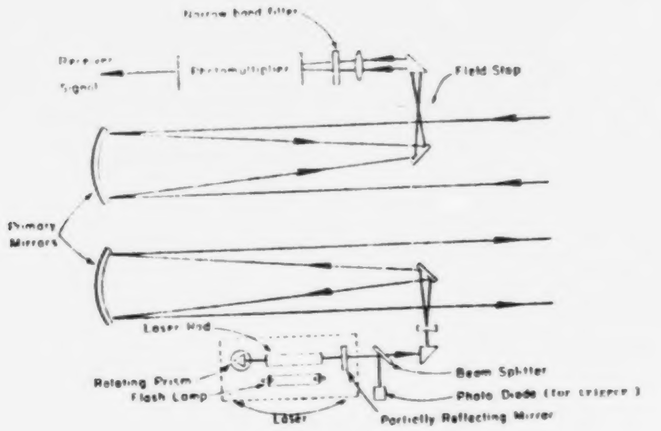
Narrow band filter
Receiver Signal
Photomultiplier
Field Stop
Primary Mirrors
Laser Rod
Rotating Prism
Flash Lamp
Laser
Beam Splitter
Photo Diode (for trigger)
Partially Reflecting Mirror

Fig. 1. A typical lidar system

B. Theory of Operation

A typical lidar system is shown in Figure 1, from Collis (1969). The primary equipment consists of a laser, sending telescope, receiving telescope, and signal detector. Most lidar units are constructed in this manner.[286,802,221]

The laser is generally a 0.6943 μm wavelength ruby laser or a 1.06 μm wavelength neodymium-glass laser. Other laser types have been used successfully, however, more data are available from experiments conducted with these two types. A lidar signal is affected by particles that are larger than one-tenth of the laser light wavelength.[66] Consequently, a ruby lidar is sensitive to particles greater than 0.07 μm diameter, the neodymium lidar to particles greater than 0.1 μm diameter. Since most of the mass of atmospheric aerosols is associated with particles larger than these two limits, either laser appears suitable. However, if small particles must be sensed, the advantage of the ruby lidar is obvious. The neodymium laser is operationally safer because it operates at wavelengths above the visible range.

The sending telescope and receiving telescope are usually of the same construction. A cassegrain telescope is most commonly used. In addition to telescopes, a simple optical system is necessary to direct the laser beam to the telescope, and to direct the return signal to the photomultiplier. Part of the return optical system must include a narrow band filter to eliminate solar noise.

The governing equation for lidar detection of atmospheric targets appears below:

$$P_r = P_t \, (c \, \delta/2) \, \beta \, A/r^2 \exp \left[-2 \int_o^n \sigma(r)dr\right]$$

where

P_r is received power,

P_t is transmitted power,

c is the velocity of light,

δ is pulse duration,

r is range,

β is the volume backscattering coefficient of the atmosphere at range r (dimensions: area/unit volume/steradian),

A is the effective receiver aperture, and

σ is the volume attenuation coefficient.

All values in the above equation are either known or can be calculated except the volume backscattering coefficient, β, and the volume attenuation coefficient, σ. Both of these coefficients are functions of the number concentration, size distribution, and optical properties of the atmospheric aerosol. If the size distribution and optical properties are measured or assumed, then the aerosol mass concentration can be evaluated from a lidar return. The greatest difficulty concerning most lidar users is to determine the size distribution and optical properties of an aerosol. The best method is to use some other independent means of obtaining this information. However, the cost of the project then grows rapidly. Many investigators have estimated the size distribution and optical properties from the literature,but this approach obviously results in some error.

Once the optical properties and size distribution are established, a relationship between the backscattering coefficient, β, and the attenuation coefficient, σ, is necessary. Several methods of determining the functional relationship between σ and β are presented in the literature.[221] The single lidar equation can then be solved for the one remaining unknown, β.

The method of calculating mass concentration as a function of the scattering coefficient, β, is discussed by Barrett and Ben-Dov.[149] In addition to mass concentration, the author also defines turbidity and visibility from lidar returns.

A lidar observation consists of evaluating a received signal, P_r, as a function of range and direction. The minimum detectable signal is limited by the system noise, solar energy noise, and detector sensitivity.

The data signal is generally displayed on an oscilloscope or some permanent record. Typical signals are shown in Figure 2.

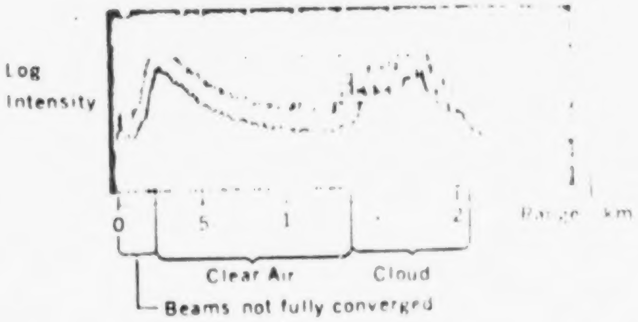

Fig. 2. Typical lidar signal.

Most current lidar units are designed to monitor pollution level from distances of 100 m to 100 km. Two investigators, Cooper and Byers,[89] monitored a laboratory aerosol confined to a 3/8 inch diameter stream. They used a Ne-He gas laser and measured the backscattered light from salt particles. Concentrations measured were about 10^4 μg/m^3 and the mass median diameters ranged from 0.22 μm to 0.70 μm. Although current use of lidar (backscattering) concerns monitoring pollution from a distance of several hundred meters, this investigation demonstrates the possibility of using lidar for short range operation as well. The limiting condition for short range operation is a function of the speed of light and minimum laser pulse duration, which is currently in the nanosecond region. For short range operation, the lidar unit must be located far enough from the source so that the light pulse terminates before the initial radiation reaches the target. Current designs therefore require a minimum lidar-to-target distance of a few hundred centimeters.

Resolution limits of lidar studies concern both particle size and concentration. There is probably no reasonable limit to the maximum concentration that can be detected by lidar. Some of the higher concentrations reports are 50,000 μg/m^3 by Cooper and Byers.[89] The lower resolution limit and the ability to detect concentration gradients are more difficult to define. Lower resolution limits are a function of the lidar system quality and are subject to change due to technical advances. Barrett and Ben-Dov[149] reported detecting concentrations as low as 5 μg/m^3 and variations as small as 2 μg/m^3.

The particle size resolution limit is determined by the laser wavelength since Mie scattering is considered to be the governing mechanism. Particles with a diameter that is greater than one tenth of the laser light wavelength can be detected.[66] Since most lidar units operate at 0.6943 μm or 1.06 μm, the lower limit of particle size resolution should be about 0.07 μm. Experiments conducted with laboratory aerosols have demonstrated the ability of lidar to detect particles of 0.22 μm mass median diameter.[89] Studies made on atmospheric aerosols indicate that particles of smog, haze, and smokes can be detected by lidar.[221]

In addition, Collis indicates that it may even be possible to detect gaseous molecules with lidar. An obvious qualification for the ability to detect gaseous molecules is that the foreign gas be considerably different from the environment through which the lidar signal travels.

APPLICATION TO STACKS

Lidar can be used as a means of evaluating the mass concentration of an aerosol, however, some knowledge of the particle size distribution is necessary. Consequently, either additional effort must be expended to determine the size distribution, or an estimate of size distribution must be made, and particle density must be known.

Lidar has been used to measure the concentration of a laboratory aerosol, so it appears feasible to use this method in a stack. Slight instrument modifications are necessary, such as using the shortest possible laser pulse rate, and locating the lidar unit far enough away from the stack to prevent the signal from being backscattered before the entire forward signal has been sent.

Although lidar seems to be an excellent means of defining atmospheric contamination, three factors make lidar unsuitable for "in-stack" monitoring. The first factor is cost. Virtually all lidar units are best described as research devices. Therefore, cost information is not readily available, but is somewhat higher than the cost of a high quality Q-switched ruby laser. The second prohibitive feature of lidar is reliability. Although it has been used successfully, lidar is still a research device, and probably not well-suited to continuous monitoring on a daily basis. Finally, current lidar units are designed to study atmospheric contaminants from a distance of at least 100 m. A limited amount of research has been conducted with close range lidar. Therefore, additional studies are needed before lidar can be considered for stack monitoring. In any case, lidar cannot measure the particulate mass concentration directly. It requires additional information about particle size distribution and density to correct its basic measurement for particle mass.

REFERENCES

149 Barrett, E. W., and Ben-Dov, O., "Application of the Lidar to Air Pollution Measurements", Journal of Applied Meteorology, V. 6, p. 500-515 (1967).

280 Barrett, E. W., "Lidar Measurements of Particulate Concentration Profiles", Paper 67-128 presented at 60th Annual Meeting of Air Pollution Control Assoc., Cleveland, Ohio, June 11-16,1967.

569 Collis, R. T. H., "Lidar: A New Atmospheric Probe", Royal Meteorological Society, Quarterly Journal, V. 92, p. 220-230 (1966).

221 Collis, R. T. H., "Lidar for Routine Meteorological Observations", American Meteorological Society Bul., V. 50, no. 9, p. 688-694 (Sep 1969).

89 Cooper, D. W., and Byers, R. L., "Laser Light Backscattering from Laboratory Aerosols", APCA Journal, V. 20, no. 1, p. 43-47 (Jan 1970).

66 Johnson, W. B., "Lidar Applications in Air Pollution Research and Control", APCA Journal, V. 19, no. 3, p. 176-180 (Mar 1969).

802 Landry, M. J., "GB-60A Light Detecting and Ranging System (LIDAR)", Sandia Laboratories, Albuquerque, N. M., Clearinghouse No. SC-DR-67-115 (Dec 1967).

286 Northend, C. A., Honey, R. C., and Evans, W. E., "Laser Radar (Lidar) for Meteorological Observations", Review of Scientific Instruments, V. 37, no. 4, p. 393-400 (1966).

514 Proctor, T. D., "A Laser Technique for the Measurement of Aerosols", Journal of Scientific Instruments (Journal of Physics E.), Ser. 2, V. 1, no. 6, p. 631-635 (Jun 1968).

HOLOGRAPHY

by: N. Barsic, B.Y.H. Liu, and K.T. Whitby

INTRODUCTION

Holography is an interferometric technique by which three dimensional information can be recorded on a two-dimensional photograph. This is a step process consisting of first photographing the interference pattern that exists when a diffracted or object field (Fresnel or Fraunhofer diffraction pattern of the object) is allowed to interfere with a reference field or background wave. Holography has received considerable attention recently due to the availability of high power, monochromatic lasers as an illumination source.

Holography can be used in several ways to measure small particles. The first is the photography of individual particles by holography for subsequent viewing for size distribution or shape analysis. The second is the photography of clouds of particles in three-dimensions. Analysis of the intensity of the reconstructed image can yield some information regarding the particle concentration. The third is the photography of light scattered by the particles, either individually or as a cloud. Analysis of the intensity of light scattered by individual particles can yield size information of particles as small as 1 - 10 μm. Analysis of the cloud intensity can yield three-dimensional particle concentration information.

As a means of measuring the particle size and number distribution, holography has two advantages. First, this method enables a size distribution analysis to be made without disturbing the medium under consideration. Secondly, a complete description of the three dimensional sample volume is possible, rather than sampling at a particular point in space.

Problems include the cost and complexity of the necessary apparatus, the difficulty in detecting individual particles as small as 1 - 10 μm across stack-like dimensions, and the lack of ability to detect individual submicron particles. Holography is a complex science in an infant state of development. Future developments will undoubtedly improve present performance and reduce the cost and complexity of the equipment.

Holography is presently being developed for use in effluent stacks and steam-plant boilers.[1279,1257] Results to date demonstrate that holography can be used in such environments. Although the method is costly and data reduction is time consuming, holography offers an excellent method of aerosol classification for research work where accuracy is necessary and the flow field cannot be disturbed. Little application is seen for holography as a continuous monitor.

PRINCIPLES OF OPERATION

A. Objective

Holography can be used as a means of determining the size and number distribution of an aerosol that passes through a given volume. The reconstructed holograms can be displayed on a TV monitor and can then be photographed for observation or data reduction. The Stat Volt Company[1198] also reports the availability of an electronic scanner that yields a digital output of a number and size distribution on a screen or printed on paper.

Another more direct method of analyzing holograms for either particle size or concentration as a function of location within the viewing volume is to use a photocell or photomultiplier with a small aperture. The photo detector can be moved around in the reconstructed viewing volume, scanning the volume for particles or for changes in light intensity.[1257] Once the light amplitudes are converted to electrical signals, a variety of data analysis possibilities exist. The result could be a size-number distribution of the entire volume or any portion of the volume or a three-dimensional spatial distribution of the light-scattering intensity of a cloud.

B. Theory of Operation

1. Introduction

Two types of holograms are the Fresnel or near-field and the Fraunhofer or far-field. The distinction between Fraunhofer and Fresnel holograms lies in the nature of the diffracted radiation from the object. A Fraunhofer diffraction pattern is always formed when the point of observation is infinitely distant from the object, while a Fresnel pattern if formed when the observation point is near the object. The original holograms were photographic records of interference patterns between Fresnel diffraction and a reference beam. One unfortunate consequence of a Fresnel hologram is the existence of a conjugate image (located near the hologram) that degrades the reconstructed image. Fraunhofer holograms produce a clearer reconstructed image since the conjugate image is essentially located at infinity.

A hologram is formed by allowing a laser beam to fall upon a reflecting surface and an object so that both the reflected and diffracted beams intersect at a plane in space that can be photographed. One possible arrangement is shown in Figure 1. Other arrangements of the object, reflecting surface, and photographic plate are possible.[128,148,483] The essential feature is that a reference beam and a diffracted beam intersect in a plane where a photograph can be taken.

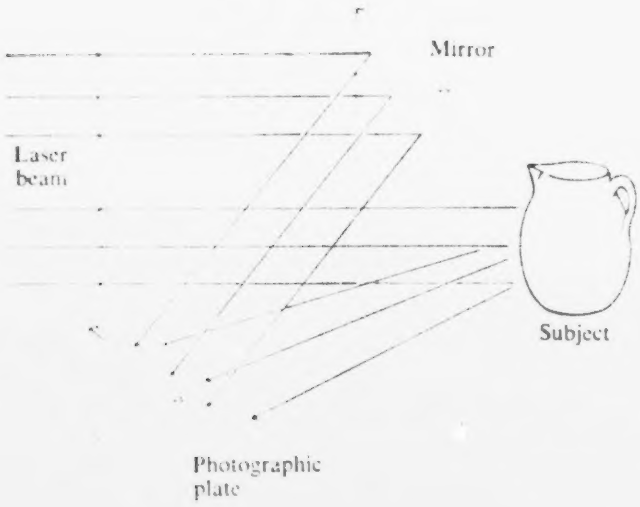

Fig. 1. Arrangement for producing a hologram from G. R. Fowles.[1195]

2. Hologram Formation

The basic experimental schematic for a Fraunhofer hologram is illustrated in Figure 2, from Thompson, et al.[150]

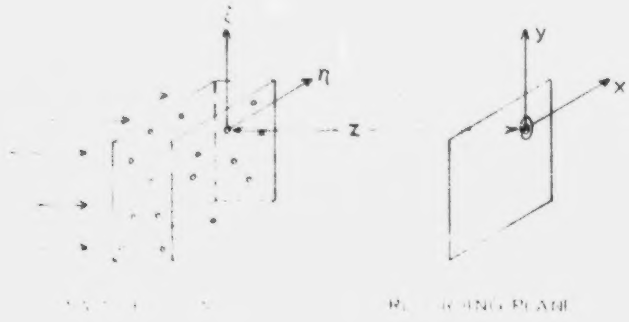

Fig. 2. The basic principle of the disdrometer. Partially coherent, quasi-monochromatic radiation illuminates the sample volume of particles. The hologram of a particular particle is recorded on film placed in the x, y plane a distance z from the particle.

Quasi-monchromatic radiation illuminates the sample volume which is located at a distance Z from the recording plane. The distance Z must satisfy the following equation in order to produce a Fraunhofer diffraction pattern[682,253]

$$Z > \frac{(\xi^2 + n^2)\ \mathrm{max}}{\lambda} \tag{1}$$

where λ is the mean wavelength of illuminating radiation and $(\xi^2 + n^2)$ max is the maximum cross sectional dimension of the object.

$$Z > \frac{4\ a^2}{\lambda} \qquad (2)$$

for spherical objects of diameter $4\ a^2 = (\xi^2 + n^2)^{1/2}$.

Holography is a two-step imaging process utilizing diffraction techniques by means of partially coherent radiation. The theoretical basis for holography depends upon the solution of a simultaneous pair of wave equations with appropriate boundary conditions. The measureable quantity described in this wave equation is related to the illumination intensity. Details of the wave equation, boundary conditions, and solution are discussed by Belz[682] and Reynolds and DeVelis.[126] The results of this solution are presented in the following equation which defines the intensity distribution for a particle of diameter 2r:

$$I\ (\rho) = 1 - \frac{2\ k\ a^2}{Z_1}\ \frac{J_1\left(\frac{k\ a\rho}{Z_1}\right)}{\left(\frac{k\ a\rho}{Z_1}\right)}\ \sin\left(\frac{k\ \rho^2}{2\ Z_1}\right) + \frac{k^2\ a^2}{Z_1{}^2}\left[\frac{J_1\left(\frac{k\ a\rho}{Z_1}\right)}{\left(\frac{k\ a\rho}{Z_1}\right)}\right]^2 \qquad (3)$$

where

a is the particle radius in the diffracting plane,

ρ is the particle radius coordinate in the observation plane (hologram) and $0 \leq \rho \leq \rho_{max}$, where ρ_{max} corresponds to radius a,

k is $2\ \pi/\lambda$,

λ is the wavelength of the illuminating radiation,

Z_1 is the distance from the observation plane to the diffracting plane (recording distance), and

J_1 is the Bessel function of the first kind.

The first term is simply a constant normalized intensity about which the diffraction pattern is formed. The second term dominates and represents the interference between the Fourier transform of the particle geometry and the coherent background. The third term is the intensity distribution in the Fraunhofer diffraction pattern of an aperture having the same cross sectional dimensions as the particle. This term is small and is frequently omitted.

The above description of the important equations and parameters provides the basis for completing step one (hologram formation) of this two-step imaging process. Thus far, only a film record (hologram) of a diffraction pattern has been formed. The second and final step, reconstruction, yields a three-dimensional image of the particles.

3. Reconstruction

Holographic recording stores information about an object in the form of an interference pattern which appears to consist of a seemingly meaningless array of lines. Reconstruction is a procedure that obtains a three-dimensional image of the object from the interference pattern.

This is accomplished by illuminating the film record obtained during the hologram formation step with a coherent beam of quasi-monochromatic light as illustrated in Figure 3.

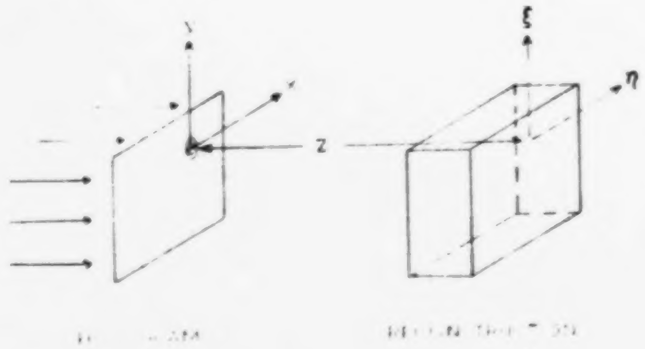

Fig. 3. The basic principle of the readout. The hologram located in the x, y plane is illuminated by partially coherent quasi-monochromatic light. The hologram of a particular particle reconstructs a real image of the particle at a distance z. The distance z, size and shape of the real image and its location in the ξ-η plane are uniquely determined by the hologram.

This light beam is generally collimated, but can be either converging or diverging.[150] For a quasi-monochromatic collimated beam of the same wavelength as the beam forming the diffraction pattern, the reconstructed image is located at a distance Z_2 from the hologram. Under these conditions the magnification is unity. If light of a different wavelength is used, then the reconstructed image lies in a different plane, but the magnification is still unity.

The intensity distribution of the reconstructed image is obtained by solving a pair of wave equations similar to those solved in step one (hologram formation). Equation 4 describes the solution for a particle of radius a.

$$I(r) = 1 + \frac{\gamma}{2} D(r) \quad \cos\left(\frac{k\rho^2_{max}}{2\ Z_2}\right) + \frac{\gamma^2}{4} [D(r)]^2 \qquad (4)$$

where

r is the particle radius coordinate in the image plane and $0 \leq r \leq a$, where a corresponds to ρ_{max},

P_{max} is the particle radius in the hologram plane,

k is $2\ \pi/\lambda$,

λ is the wavelength of illuminating radiation,

Z_2 is the distance from the image plane to the hologram plane (generally $Z_1 = Z_2$),

$D(r)$ is related to the cross sectional geometry of the particle, and

γ is the photographic gamma, Reynolds and DeVelis.[126]

This equation indicates that the cross sectional geometry of the original object is recovered.

4. Discussion

Analysis of a hologram at a single random location within the viewing volume is not representative of the aerosol. Instead, several locations within a hologram are necessary to completely classify an aerosol. The number of separate locations that must be analyzed across a viewing volume depends on the aerosol type, velocity profile, and concentration profile. To obtain a meaningful statistical analysis of an aerosol, the reconstruction analyzer is usually located on a movable carriage that allows continuously spaced successive planes to be in focus on the analyzer. The analyzer can be a camera, a CCTV camera, or a photodetector.

For each recording distance Z_1 there is a minimum resolvable particle diameter resulting in a hologram contrast that is low enough to recede into the background noise level of the film, and not be recorded properly. The noise level is a constant that depends on the film and the quality of the optical system. This fact is especially important if a long sample volume must be transversed or if the recording distance must be long due to the nature of the experiment. The recording distance requirement is summarized in Figure 4 which illustrates the minimum resolved particle diameter as a function of recording (far-field) distance.

If the far-field distance can be controlled in favor of small particles, the resolution limit for present techniques is about 2 μm.[1197] This limitation is set by an approximation made in the derivation of Eq. 3, namely that the dimensions of the diffracting object be larger than the radiation wavelength. For a ruby laser this limit must be much larger than 0.6943 μm.

Ultraviolet pulsed gas lasers are available that produce sufficient power to be used as a light source. With a nitrogen plasma laser and a suitable filtering system, a strong line at 3371 Å can be obtained. This reduction in wavelength allows 1 μm diameter particles to be observed, however, the far-field distance must be increased accordingly (Eq. 2).

Lensless holography, i.e., with no lens between the viewing volume and the photographic film plate, has a magnification of 1 and has a maximum resolution of 15 - 25 μm, depending on the quality of the film. The depth of field of lensless holography can be 30 ft. or more, enough to cross most stacks. However, the resolution as seen in Figure 4 deteriorates at such distances.

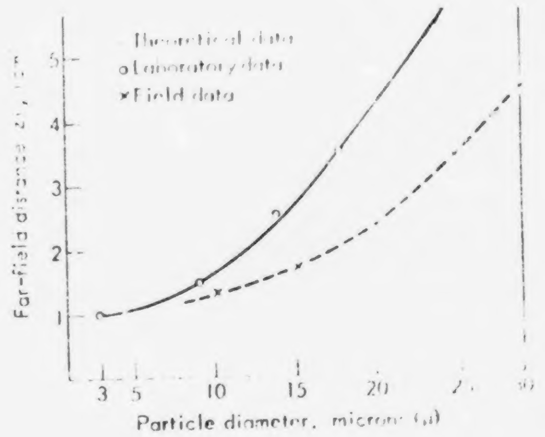

Fig. 4. Comparison of experimental and theoretical results for particle size resolution (using the contrast criterion) versus far-field recording distance. All particles falling below the curve are within the recording range.[150,132]

Lens holography, with a high quality microscope as a lens, can make 1 μm particles visible, but the depth of field and viewing angle suffer greatly.

Using forward-scattered light with a lensless system, investigators have detected individual submicron particles.[1257] Presumably, the intensity of the speck of light in the reconstructed image is proportional to the size of the particle. Work is presently being carried out in this field.

APPLICATIONS TO STACKS

Very recently, holography has been applied to coal-fired combustion chamber environments.[1279,1257] The apparatus used, shown in Figure 5, is a 3-beam forward-scattered light system. The 3-beam system allows holograms to be made even though the scene beam intensity has been strongly attenuated while passing through the stack. This system, or one similar to it, successfully detected the cloud density of the particles in the combustion chamber. The reconstruction apparatus shown in Figure 6 permitted the reconstructed image to be scanned by a photocell which measured the relative cloud intensity at any point in the viewing volume. The 3-beam technique allowed the absolute intensity information to be carried on the hologram. Stack vibrations were no problem because the laser pulse time is very short.

Holography for the analysis of single particles in stacks is more difficult because of the lack of resolution with the necessary recording distances. Development remains to be done in this area.

CONCLUSIONS

For use in stacks, the primary application of holography appears to be as a specialized tool in studying the spatial density of clouds of particles without disturbing the effluent stream in any way. The use of holography for analysis of individual particles is limited, with present technology, by the lack of resolution across normal stack distances. Holography will probably remain expensive and complex for routine monitoring of stack effluents.

The field of holography is developing very rapidly. Statements made here are based on a brief review of present technology. Developments being made even as this is written will undoubtedly make large improvements in the applicability of holography to the measurement of aerosols.

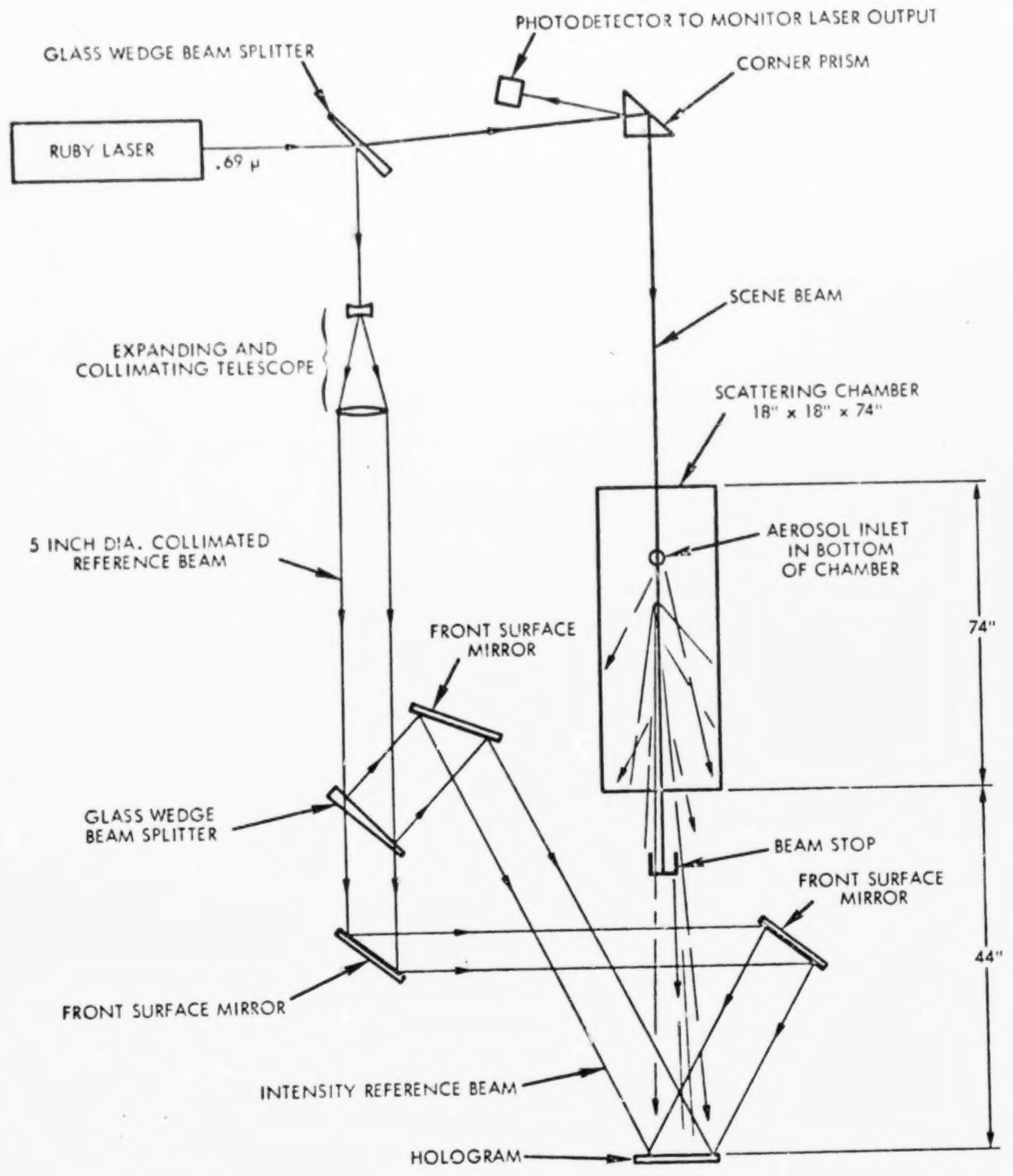
PHOTODETECTOR TO MONITOR LASER OUTPUT
GLASS WEDGE BEAM SPLITTER
CORNER PRISM
RUBY LASER
.69 μ
SCENE BEAM
EXPANDING AND COLLIMATING TELESCOPE
SCATTERING CHAMBER 18" × 18" × 74"
5 INCH DIA. COLLIMATED REFERENCE BEAM
AEROSOL INLET IN BOTTOM OF CHAMBER
FRONT SURFACE MIRROR
74"
GLASS WEDGE BEAM SPLITTER
BEAM STOP
FRONT SURFACE MIRROR
44"
FRONT SURFACE MIRROR
INTENSITY REFERENCE BEAM
HOLOGRAM

Fig. 5. Schematic diagram of scattered light three-beam transmission holocamera test setup.[1257]

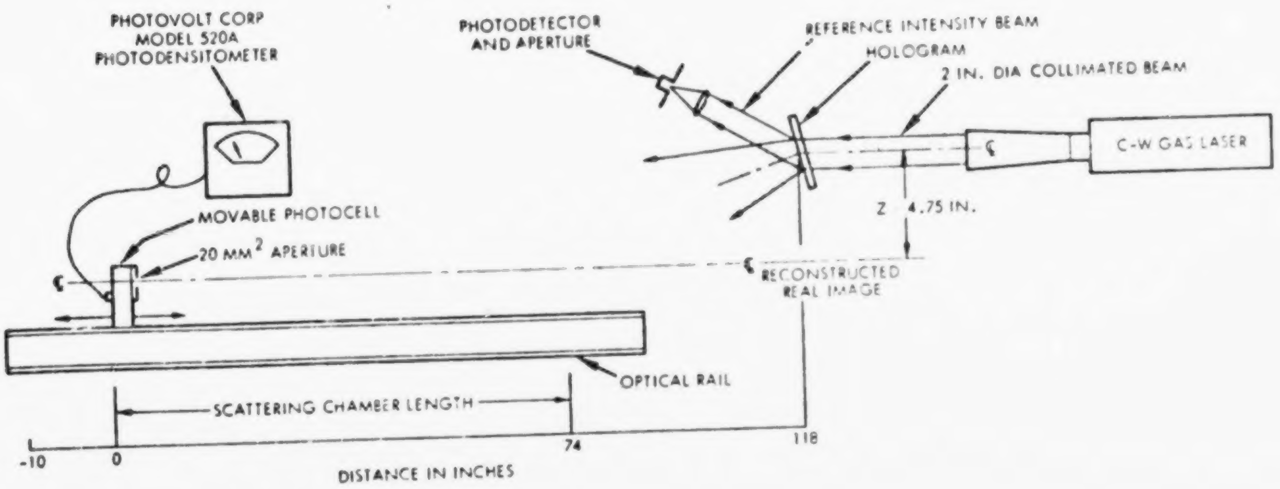
PHOTOVOLT CORP
MODEL 520A
PHOTODENSITOMETER
PHOTODETECTOR
AND APERTURE
REFERENCE INTENSITY BEAM
HOLOGRAM
2 IN. DIA COLLIMATED BEAM
C-W GAS LASER
Z 4.75 IN.
MOVABLE PHOTOCELL
20 MM² APERTURE
RECONSTRUCTED
REAL IMAGE
OPTICAL RAIL
SCATTERING CHAMBER LENGTH
-10
0
74
118
DISTANCE IN INCHES

Fig. 6. Schematic diagram of method used to reconstruct and measure hologram real image light intensity variations as a function of scattering chamber length.[1257]

REFERENCES

682 Belz, R. A., "Analysis of the Techniques for Measuring Particle Size and Distribution from Fraunhofer Diffraction Patterns", ARO, Inc., Clearinghouse No. AD 674 741 (Sep 1968).

132 DeVelis, J. B., Parrent, G. B., Jr., and Thompson, B. J., "Image Reconstruction with Fraunhofer Holograms", Optical Society of America Journal, V. 56, p. 423-427 (1966).

1195 Fowles, F. R., Introduction to Modern Optics, Holt, Rinehart, and Winston, Inc., New York (1968).

1279 Matthews, B.J., and Kemp, R. F., "Holographic Determination of Injected Limestone Distribution in Unit 10 of the Shawnee Power Plant", TRW Systems Group, Redondo Beach, Calif., TRW Report No. 14103-6001-R0-00 under NAPCA Contract CPA 70-4 (Jun 1970).

1257 Matthews, B. J., and Kemp, R. F., "Investigation of Scattered Light Holography of Aerosols and Data Reduction Techniques", TRW Systems Group, Redondo Beach, Calif., TRW Report No. 14103-6002-RO-00 under NAPCA Contract CPA 70-4 (Nov 1970).

218 Meier, R. W., "Magnification and Third-Order Abberations in Holography", Optical Society of America Journal, V. 55, p. 987-992 (1965).

1196 Anon., "Model 177 Holographic Camera", Optics Technology, Inc., 901 California Ave., Palo Alto, Calif. 94304

1197 Reynolds, G. O., and DeVelis, J. B., *Theory and Application of Holography*, Addison-Wesley, Reading, Mass. (1967).

126 Reynolds, G. O., and DeVelis, J. B., "Hologram Coherence Effects", *IEEE Trans.*, V. AP-15, p. 41-48 (1967).

148 Silverman, B. A., Thompson, B.J., and Ward, J. H., "A Laser Fog Disdrometer", *Journal of Applied Meteorology*, V. 3, p. 792-801 (1964).

1198 Anon., Stat Volt Company, "Holographic Particle Determination Literature", 1130 Channel Drive, Santa Barbara, Calif.

150 Thompson, B. J., Parrent, G. B., Ward, J. H., and Justh, B., "A Readout Technique for the Laser Fog Disdrometer", *Journal of Applied Meteorology*, V. 5, p. 343-347 (1966).

483 Ward, J., "Laser Fog Disdrometer System", Technical Operations, Inc., Burlington, Mass., Clearinghouse No. AD 656 487 (Jun 1967).

253 Zinky, W. R., "Hologram Camera and Reconstruction System for Assessment of Explosively Generated Aerosols", Technical Operations Research, Burlington, Mass., Clearinghouse No. AD 474 534 (Oct 1965).

ACOUSTICAL ATTENUATION AND DISPERSION

by: John Borgos

INTRODUCTION

Acoustical attenuation is the decrease in amplitude of an acoustical wave traveling through a media due to such effects as wall losses, viscous losses due to interaction with particles, etc. The coefficient of attenuation, α, is defined for a particulate medium such that the ratio of the sound intensity at a distance ℓ from the source to the intensity at the source is given by $\exp[-\alpha\,\ell]$. Acoustical dispersion is related to the decrease in sound velocity due to the presence of particulate matter in the conducting medium. The dispersion coefficient, β, is defined as

$$\beta = (a_o/a)^2 - 1,$$

where a and a_o are the sonic velocities in the gas with and without particles, respectively[103].

There are several attractive characteristics of the use of acoustic measurements of aerosol concentration which other measurement techniques can seldom duplicate. However, the acoustic method requires a knowledge of particulate density and the gas properties. One characteristic of the acoustical method which makes it appear much less promising is that it is not nearly as sensitive as other techniques to aerosol mass concentration. This is a serious limitation.

The most comprehensive work on the subject of acoustical measurements of aerosol size and concentration has been done by Temkin and Dobbins[103,138,139]. They have outlined a theory which explains the phenonema of acoustical attenuation and dispersion using the mechanisms of the thermal and dynamic relaxation processes, and they have produced considerable experimental data to verify their conclusion. Much of their work is based on previous work, the earliest notable being that of Knudson et al[605], who made measurements of the rate of decay of sound in a medium with and without particles present. Later, Epstein and Carhart[616] included the effects of thermal attenuation of their theory, which agreed fairly well with Knudson's data. Zink and Delsasso[604] also reported a theory that agreed quite well with their experimental results. The work of Temkin and Dobbins, while similar to much of the previous work, presented more accurate results over a wide range of conditions.

ANALYSIS OF BASIC PRINCIPLES

When a pure gas is exposed to acoustic waves, the waves experience practically no attenuation, except that caused by the presence of discontinuities such as confining walls. If the same gas contains an aerosol of sufficient concentration, an acoustic wave will experience measureable attenuation while propagating through the gas, and its propagation velocity will be less than it was in the particle-free gas. The attenuation is measured in terms of the attenuation coefficient, α, and the change in propagation velocity is measured in terms of the dispersion coefficient, β.

Consider a particle immersed in a gas that is isolated from any other particle in the gas. If an acoustic field is applied, the motion of the particle will be affected by the motion of the gas molecules as the sound wave propagates through the medium. If the particle is extremely large, it will remain nearly motionless because of its inertia. As the particle size decreases, the particle tends to oscillate more closely with the sound field. This follows from the fact that the inertia, which resists particle motion, changes as D^3; on the other hand, surface area, which is proportional to the viscous drag forces, only changes as D^2. Thus, for an extremely small particle, the amplitude of the particle oscillating motion approximates that of the gas molecules. For a range of intermediate size particles, the particle motion is somewhat less than the motion of the gas.

Dobbins and Temkin[138] have verified experimentally that this is indeed what happens in the case of a plane wave and nearly spherical particles. In fact, the intermediate particles not only vibrate with smaller amplitudes, but they lag behind the motion of the gas molecules. The important parameters in the determination of particle lag for a particular particle size are $\omega\tau_d$ and $\omega\tau_t$, where ω is the circular frequency of the sound field and τ_d and τ_t are the dynamic and thermal relaxation times, respectively, of the particle in the medium.

Two mechanisms account for practically all of the acoustic attenuation caused by particles. The most important is the viscous attenuation caused by the lagging motion of the particles, which causes viscous energy loss due to the relative motion of the particle and gas. The dynamic relaxation time, τ_d, is a measure of this contribution to the attenuation. The other mechanism is the thermal attenuation, which is a result of the irreversible flow of heat between the suspended particle and the gas during the rarefactions and compressions of the sound wave. Though usually smaller than the viscous contribution,[139] it is usually of the same order of magnitude. The thermal relaxation time, τ_t, provides a measure of the thermal attenuation for a given frequency and particle size.

The dispersion, or velocity change, of a sound wave due to the presence of particles in a gas is simply the result of the combined effects of the increase in heat capacity and increase in density of the gas particle mixture. The increase in heat capacities results in a lower ratio of specific heats. Because the acoustic velocity is proportional to the square root of the specific heat ratio and inversely proportional to the square root of density, the presence of particles in a gas can only decrease the sound velocity in the medium.[604] The dispersion can also be shown to be a function of $\omega\tau_t$ and $\omega\tau_d$.[138,139]

The equipment used by Dobbins and Temkin[138,139] in obtaining experimental data, usually referred to as an acoustical interferometer, consisted of a hollow cylinder, one end of which was plugged by a rigid cap, while the other end contained an acoustical driver. The acoustical driver was used to set up a standing wave pattern in the tube, and the resulting pressure field was explored with a capillary tube attached to a microphone. The dispersion of a sound wave due to the presence of particles was found by measuring the change in wave length of a sound wave of a particular frequency when particles were added. The attenuation was determined by measuring the decrease in amplitude of the fluctuating pressure when particles were added.

The aerosol mass concentrations used in the experiments were on the order of one part per hundred. Interaction with the walls of the tube can be neglected at such high concentrations, so the attenuation measured was due almost entirely to the particles in the tube. Acoustic frequencies varied from 1 KHz to about 10 KHz, and the mean particle size varied from 0.8 to 4.7μ.

Data shows that for $\omega\tau_d \simeq 1$, maximum attenuation occurs. If either the frequency or mean particle size increases or decreases, the attenuation drops sharply. The magnitude of the maximum attenuation is weakly dependent on the particulate mass concentration for $C_m > 0.01$, where C_m is the ratio of the total mass of particles to the mass of gas in a given volume of the mixture. For $C_m < 0.01$, the maximum attenuation is not dependent on C_m (Fig. 1). The data also shows that as $\omega\tau_d \to 0$, a maximum dispersion occurs. This maximum is also dependent on mass concentration for $C_m > 0.01$, and independent of mass concentration for $C_m < 0.01$. As $\omega\tau_d \to \infty$, the dispersion tends to zero (Fig. 2).

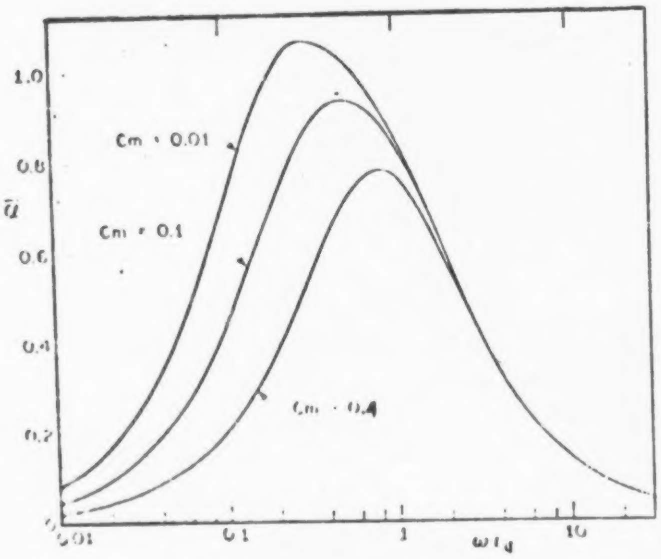

Fig. 1: Attenuation by Water Droplets in Air.

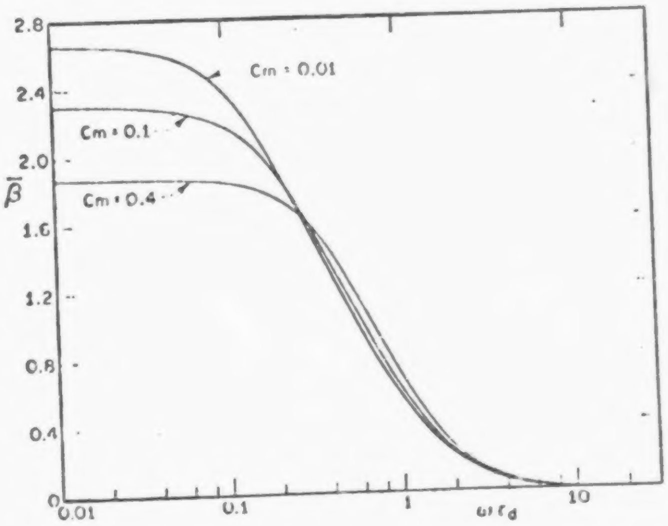

Fig. 2: Dispersion by Water Droplets in Air.

The measurement of a mean particle diameter appears possible if a measurement of mass concentration is obtained separately. This mean diameter is the same diameter that is measured by an optical-scattering photometer; namely, the volume-surface mean diameter.[138]

The measurements of mean diameter and mass concentration of particles has been shown theoretically to be nearly independent of the particle size distribution function,[138] and although the range of the data is limited, it seems to confirm this.

APPLICATION TO MASS CONCENTRATION MEASUREMENT IN STACKS

There are several problems connected with using an acoustic interferometer for monitoring particulate mass concentration in stacks that do not appear to have immediate solutions. The outstanding problem is the lack of sensitivity. The mass concentration of particles used in most of the experiments thus far has been on the order of one part per hundred, which is about three orders of magnitude greater than the lower limit of concentration encountered in stacks. Furthermore, even at such high mass concentrations, the instrument is still insensitive to higher concentration. Even in a stack, the instrument would need to measure a sound velocity change of 0.01% in order to detect any particles at all, and would have to measure velocity within 10^{-4}% to accurately measure a change in concentration. Both appear unfeasible.

In addition to this, there are problems involved in the use of the sensing tube in a stack. Contamination of the acoustic driver, the need for a discontinuous isokinetic sampling system (the air should be at rest in the sensing tube when measurements are made, so the sampling system would have to be able to fill the tube, empty it, fill it, etc.), settling of particles in the sampling tube, and the effect of temperature all need to be carefully examined.

CONCLUSIONS

Because of the extreme sensitivity requirement, which is impossible to attain even in a laboratory environment, the acoustic technique cannot be considered for mass concentration measurements in stacks. If a satisfactory technique is developed which makes it possible to increase the particle mass concentration by three orders of magnitude in a given sample, it may be feasible to make measurements in the concentrated samples which give meaningful data. Otherwise no apparent use can be made of the technique.

RECOMMENDATIONS

Since the overwhelming problem with the acoustic technique lies in the required sensitivity for the normal range of mass concentration values, an instrument is needed which will concentrate the particles. Such an instrument might be a version of a cyclone, designed such that the particles were not separated from the air but remained in suspension.

REFERENCES

943 Anon, "Applications of Ultrasonic Energy, Ultrasonic Instrumentation for Nuclear Applications", Aeroprojects, Inc., West Chester, Pa., Clearinghouse No. NYO-9585 (Oct 1961).

600 Blair, D. W., "Particle Damping of a Plane Acoustic Wave in Solid Propellant Combustion Gases", AIAA Journal, V. 1, p. 2625-2626 (1963).

314 Dobbins, R. A., and Temkin, S., "Measurements of Particulate Acoustic Attenuation", AIAA Journal, V. 2, no. 6, p. 1106-1111 (Jun 1964).

103 Dobbins, R. A., and Temkin, S., "Acoustical Measurements of Aerosol Particle Size and Concentration", Journal of Colloid & Interface Science, V. 25, no. 3, p. 329-333 (Nov 1967).

616 Epstein, P. S., and Carhart, R. R., "The Absorption of Sound in Suspensions and Emulsions", Journal of the Acoustical Society of America, V. 25, p. 553-565 (1953).

557 Gucker, F. T., Jr., "Determination of Concentration and Size of Particulate Matter by Light Scattering and Sonic Techniques", Proc. National Air Pollution Symposium, 1949, V. 1, 14-26 (1951).

605 Knudson, V. O., Wilson, J. V., and Anderson, N. S., "The Attenuation of Audible Sound in Fog and Smoke", Journal of the Acoustical Society of America, V. 20, p. 849-857 (1948).

139 Temkin, S., and Dobbins, R. A., "Attenuation and Dispersion of Sound by Particulate - Relaxation Processes", Journal of the Acoustical Society of America, V. 40, no. 2, p. 317-334 (Aug 1966).

138 Temkin, S., and Dobbins, R. A., "Measurements of Attenuation and Dispersion of Sound by an Aerosol", Journal of the Acoustical Society of America, V. 40, no. 5, p. 1016-29 (Nov 1966).

604 Zink, J. W., and Delsasso, L. P., "Attenuation and Dispersion of Sound by Solid Particles Suspended in a Gas", Journal of the Acoustial Society of America, V. 30, p. 765-771 (1958).

HOT-WIRE ANEMOMETRY

by: John Borgos

INTRODUCTION

A hot-wire anemometer placed in an airstream with liquid aerosol will display voltage output fluctuations due mainly to two phenomena: the transient cooling effect due to the turbulence level in the airstream and the impaction on the sensor of the liquid droplets. If the thermodynamic properties of the liquid and airstream are known, the two effects can be discriminated, and measurements can be made of each of the two by a single system.[10]

As a monitor of mass concentration, the hot wire anemometer has several advantages which are important in a large number of applications. The main advantage is that it does not disturb the flow significantly in most cases. This is especially important when concentration at a point must be measured. An extraction probe which removes a sample is often the only substitute, a method which usually results in some particle loss in the probe. Also, if the flow is turbulent and the mean velocity is small, an extraction probe may not be ideal because the local velocity may change direction too frequently for the probe to follow.

Most of the experimental work done thus far with a hot wire anemometer has been done by Goldschmidt.[10,14] His hot wire was quite small (4.5 μm diameter). Most of the droplets he measured had diameters larger than the wire. Most of his experiments were on dibutylphthalate droplets, although he also experimented with water, Sinco-Prime 70, and safflower oil.

PRINCIPLES OF OPERATION

A hot wire anemometer can be operated either by maintaining constant current or constant temperature in the wire. In either case, a local velocity fluctuation or deposition of a droplet on the wire will result in a transient voltage change across the wire. These voltage fluctuations can be discriminated through a set of electronic filters, and the particles can be counted by sending the filtered signals through a high-frequency electronic counter.

With the experimental apparatus used by Goldschmidt,[10] the droplet sizes which could be sensed ranged from a minimum of roughtly 3 μm to approximately 200 μm, the minimum being fixed by the noise level of the system, and the aerosol and wire properties. Since the wire diameter was 4.5 μm, the mechanisms of inertial impaction and interception were both important in causing particles to hit the wire.[79] Thus, Goldschmidt determined the droplet collection efficiency of the wire experimentally to avoid errors associated with various theories.

He also assumed that a droplet which came in contact with the wire would wet the wire and quickly vaporize. Photographs later showed that this was almost always the case, with the exception of collisions where the particle only touched the side of the wire. In these cases, the droplet did not seem to vaporize completely, thus producing a smaller cooling effect than a droplet intersecting the wire near the stagnation point.

As stated, the impingement of a droplet on the wire causes a voltage fluctuation. This is because the droplet is cooler than the wire and requires a large amount of heat to vaporize. A quantitative measurement can be made of this heat by observing the magnitude of the voltage fluctuation and correlating it with power output. The magnitude of the voltage fluctuation is primarily a function of the temperature difference between the wire and the droplet, the size of the droplet, and the specific heat of the droplet, with surface tension of the droplet and wire tension producing lesser effects.

If the hot wire is exposed to a droplet-laden airstream, the output can be filtered (to eliminate turbulence - generated fluctuations) and examined on an oscilloscope. With a knowledge of the droplet's specific heat and temperature and of the wire temperature, the system can be calibrated to measure particle size. Goldschmidt and Householder[10] have shown that for droplets smaller than 200 μm in airstreams of moderate velocity ($V<300$ cm/sec), the peak value of the voltage fluctuation is linearly proportional to particle diameter. Droplets smaller than about 3 μm are difficult to detect because of the noise level of the electronics.

CONCLUSIONS

The hot wire anemometer is not applicable to the measurement of particulate mass concentration in stacks. Its main disadvantage is its inability to measure solid particles. A solid particle does not vaporize on contact with the wire, but instead coats the wire and actually decreases the heat transfer. Thus, solid and liquid particles yield completely different output signals. The signal caused by solid particles cannot easily be interpreted, making the hot-wire anemometer a poor candidate for stack monitoring of particle concentration or size distribution.

REFERENCES

10 Goldschmidt, V. W., and Householder, M. K., "The Hot Wire Anemometer as an Aerosol Droplet Size Sampler", Atmospheric Environment, V. 3, p. 643-651 (1969).

14 Goldschmidt, V. W., "Measurement of Aerosol Concentrations with a Hot Wire Anemometer", Journal of Colloid Science, V. 20, p. 617-634 (1965).

79 Golovin, M. N., and Putnam, A. A., "Inertial Impaction on Single Elements", Indust. & Eng. Chem. Fundamentals, V. 1, no. 4, p. 264-273 (Nov 1962).

224 Vonnegut, B., "Means for Measuring Individual Aerosol Particles", U. S. Patent No. 2,702, 471 (Feb 1955).

PRESSURE DROP IN NOZZLES

by: John Borgos

INTRODUCTION

The use of nozzles and venturi meters as instruments for measuring particulate mass flow in particle-laden gas streams has been confined mainly to applications where the transportation of the particles was of primary interest. The technique has not received much recognition in the pollution control field because it is suited for the monitoring of particle concentrations that are much higher than those normally found even in heavily polluted air.

ANALYSIS OF BASIC PRINCIPLES

If a gas stream if passed through a venturi nozzle, the flow rate can be calculated using the well-known relationships between pressure drop and velocity. The presence of particles affects these relationships by a mechanism that is not defined quantitatively.[1031] The principle involved is that the particles do not instantly follow the velocity change of the gas in the constriction of the nozzle, but lag behind. In the diffusor section, on the other hand, the particles decelerate slower than the carrier gas.

Barth and Weber[225] have designed a venturi such that the pressure differential between the throat and the diffusor inlet is linearly related to the dust quantity passing the nozzle per unit time. The relationship is dependent on the size distribution of the particles, which limits its use to applications where the size distribution is constant.

RECENT APPLICATIONS

The instrument designed by Barth and Weber has been used to measure the dust content of industrial emission sources. Because its design limits it to specific dust contents of 500 g/m^3 or more, it had to be modified to accommodate normal emissions dust contents of about 500 mg/m^3. This was done by a cyclone used as an amplifier to enrich the concentration. The experiment was not entirely satisfactory because the periodic nature of the separation mechanism of the cyclone caused severe pressure fluctuations[225].

A nozzle has been used in conjunction with an orifice plate to successfully measure both the velocity of carrier gas and mass flux of particles in a stream laden with coal dust.[1031] The orifice is insensitive to the presence of particles, so a measure of velocity can be obtained by its pressure drop. With this data, the pressure drop across the nozzle can be used to measure particle concentration. Errors as low as ± 5% have been claimed for coal-air ratios between 0.5 to 1.4 lb. coal per lb. of air.

CONCLUSIONS

The pressure drop method, as has been stated, cannot be directly applied to airstreams whose dust content is below approximately 500 g/m^3. Since no satisfactory method is available that can be used to increase concentration of normal stack gases to that level, the pressure drop method cannot be made sensitive enough to be useful for mass concentration measurements in stacks.

RECOMMENDATIONS

The decisive problem that inhibits further development of this method lies in its inability to detect particle mass concentrations as low as those found in stack gases. Therefore, the discovery of a highly efficient separator that operates continuously and provides a particle-enriched airstream would constitute a major breakthrough.

REFERENCES

1067 Barth, W., Nagel, R., and Waveren, K., "New Method for the Instantaneous Determination of Material Quantities Moved in Air Stream of Pneumatic Conveyers", Chemie-Ing. Techn., V. 29, no. 9, p. 599-602 (1957).

1031 Beck, M. S., and Wainwright, N., "Current Industrial Methods of Solids Flow Detection and Measurement", Powder Technology, V. 2, p. 189-197 (1968).

225 Duwel, L., "Latest State of Development of Control Instruments for the Continuous Monitoring of Dust Emissions", Staub-Reinhalt der Luft (Engl. Trans.), V. 28, no. 3, p. 42-53 (Mar 1968).

1029 Gast, T. H., "Determination of Solids in Hot Waste Gases Using Electrical Micro-Balance", Chemie-Ing. Techn., V. 29, p. 262-266 (Apr 1957).